Université catholique de Louvain
Secteur des sciences de la santé
Institut de Neuroscience
Ecole doctorale en sciences biomédicales

THE RHYTHMS OF PAIN: UNCOVERING THE FUNCTIONAL RELATIONSHIP BETWEEN PAIN PERCEPTION AND THE MODULATION OF ONGOING OSCILLATIONS

Chiara Leu

2025

Thèse de doctorat présentée en vue de l'obtention du grade de
Docteur en Sciences biomédicales et pharmaceutiques

Cover page illustration: Abstract drawing of a brain and its oscillatory response to a heat stimulus provided by a lighter. Image generated by OpenAI's DALL·E 2 (January 2025).

Jury

Prof. Giulia Liberati, Université catholique de Louvain (*promotrice*)

Prof. Valéry Legrain, Université catholique de Louvain (*président*)

Prof. Sylvie Nozaradan, Université catholique de Louvain (*secrétaire*)

Prof. Paolo Belardinelli, Università di Trento

Prof. Valérie Goffaux, Université catholique de Louvain

Prof. André Mouraux, Université catholique de Louvain

Prof. Markus Ploner, Technische Universität München

This thesis was supported by a *FRIA* grant of the Fonds National de la Recherche Scientifique (F.R.S.-FNRS) of the French-speaking community of Belgium.

TABLE OF CONTENTS

Abbreviations

ACC:	anterior cingulate cortex
ECG:	electrocorticography
EEG:	electroencephalography
ERD:	event-related desynchronization
ERP:	event-related potential
EMG:	electromyography
ERS:	event-related synchronization
FFT:	Fast Fourier Transform
fMRI:	functional magnetic resonance imaging
FT:	frequency-tagging
FT-OO:	frequency-tagging of ongoing oscillations
FOS:	frequency of stimulation
FOI:	frequency of interest
iEEG:	intracerebral electroencephalography
LEP:	laser-evoked potential
LFP:	local field potential
LMM:	Linear Mixed Model
MRI:	magnetic resonance imaging
PET:	positron emission tomography
s:	second
S1:	somatosensory cortex 1
S2:	somatosensory cortex 2
SSEP:	steady-state evoked potential
SNR:	signal-to-noise ratio
TCS:	Thermal Cutaneous Stimulator
TMS:	Transcranial magnetic stimulation
VAS:	Visual Analog Scale

Outline

The aim of this doctoral thesis was to identify cortical correlates of pain perception using electroencephalography (EEG), specifically targeting the modulation of ongoing neural oscillations. To this date, the specific mechanisms through which the perception of pain arises from neural activity are not fully elucidated. Ongoing oscillations have been shown to be flexible and dynamic in nature, integrating and coordinating information across the human brain. It is therefore plausible that they play an integral role in the translation of nociceptive stimuli into the perception of pain. To this end, a "frequency-tagging" paradigm was used in all experiments, meaning that all stimuli were delivered in a slow sustained periodic manner, eliciting a periodic neural response which can be detected precisely at the frequency of stimulation. This paradigm allows the differentiation between neural activity related to the stimulus and other irrelevant activity, and therefore enables us to be more precise in the evaluation of ongoing neural activity. I will further elaborate on this technique and other relevant background information for the understanding of the different studies presented in this thesis in chapter 1.

The fundamental hypothesis underlying all experiments of this thesis is that – if the modulation of ongoing oscillations is indeed functionally related to pain perception – changes in pain perception will be mirrored by a concomitant change in the modulation of ongoing neural oscillations. Thus, in chapter 2, we assessed whether an arithmetic distraction task that reduces the perceived intensity of thermonociceptive and innocuous vibrotactile stimulation could lead to a reduction in the modulation of ongoing oscillations. Similarly, chapter 3 describes how the expectation of

a stimulus' intensity can be manipulated to change its perception, and whether this manipulation induces changes in ongoing oscillations. Chapter 4 uses a different approach to modulate perception, by applying an oddball paradigm using different stimulation intensities. Here, participants had to rate their perception on a continuous scale, allowing for a precise temporal comparison between perception and modulation of ongoing oscillations. Finally, while scalp EEG was used in all previous chapters, we investigated human brain activity in deeper structures in chapter 5, by assessing oscillatory activity in the insular cortex using intracerebral EEG (iEEG). The paradigm of chapter 2 was re-used; we aimed to distract the patients from the stimuli with the arithmetic distraction, evaluating responses in the anterior and posterior insula, brain regions which have been frequently implied in the perception of pain. Chapter 6 discusses the implications of the selection of harmonics of interest in frequency-tagging investigations by re-examining data of chapter 5. All findings and their potential implications are subsequently discussed in chapter 7 of this doctoral thesis.

CHAPTER 1. General introduction

Overview

In healthy humans, the sensation of pain is a warning signal from the body, alerting us to a potentially harmful physical threat (Eccleston & Crombez, 1999). However, not every stimulus that activates peripheral nerve afferents sensitive to nociception elicits the sensation of pain (Cervero, 2012). Conversely, in many chronic pain conditions, even non-nociceptive stimuli can be perceived as painful, and in many cases, the underlying pathophysiology is not fully elucidated (Jensen & Finnerup, 2014). Thus, the aim of this doctoral thesis it to better understand the cortical links between nociception and pain in healthy humans, with the long-term aim to deepen the understanding of the neurophysiological system and inform the development of treatments for chronic pain conditions.

In this first part of this chapter, I will briefly discuss the nociceptive fiber pathways and the cortical integration of the nociceptive information in humans. Then, the modulation of pain perception through top-down and bottom-up modulation is introduced and current literature on the assessment of the neural response to nociceptive stimuli is discussed. In the following section, the role of ongoing oscillations as a flexible and dynamic system for cortical integration and coherence is reviewed, specifically its (potential) involvement in the perception of pain. Consecutively, the specific analysis technique - which has been used in all experiments performed as part of this thesis - to assess the modulation of these ongoing oscillations called “frequency-tagging” is presented. The final section of this introductory chapter will focus on the insular cortex, a centrally located brain region that is considered to be strongly involved in pain perception (Apkarian et al., 2005), which has been probed in the last experiment of this thesis.

Pain and nociception

Importantly, the activation of the nociceptive system does not necessarily lead to the sensation of "pain" (Cervero, 2012) and vice versa, the sensation of pain is not always elicited by an external nociceptive stimulus (Jensen & Finnerup, 2014). The International Association for the Study of Pain (IASP) defined pain as "An unpleasant sensory and emotional experience associated with, or resembling that associated with, actual or potential tissue damage" (Raja et al., 2020). This updated definition highlights the involvement of psychological and social factors in the experience of pain and underlines its differentiation from the mere activation of the nociceptive system. Given this potential dissociation between the experience of pain and the activation of the nociceptive system (particularly in cases of pathological adaptations leading to chronic pain conditions), it is imperative that we understand how the brain shapes the experience of pain beyond the activation of nociceptive fibers and transmission of this signal to cortical regions.

To better understand how a nociceptive stimulus can lead the perception of pain, the involved fiber pathways and brain regions need to be considered. A painful stimulus, such as a hot drop of oil jumping out of a frying pan, gets in contact with the skin. This activates peripheral afferent nerve fiber endings in the skin that are sensitive to nociception, so called nociceptors. Two types of fibers relay this nociceptor input to the spinal cord: myelinated Aδ-fibers, which are activated at around 47°C and are responsible for the first "sharp" sensation of pain, and unmyelinated C-fibers, which are much slower and activated at lower temperatures of around 40°C, eliciting a more diffuse second wave of burning pain (Churyukanov et al., 2012). From the primary afferent neurons, the nociceptive information enters the spinal cord at the dorsal horn and elicits activity within second order neurons, crosses over to the other side

and ascends via the contralateral spinothalamic tract through supraspinal structures to the thalamus (Figure 1).

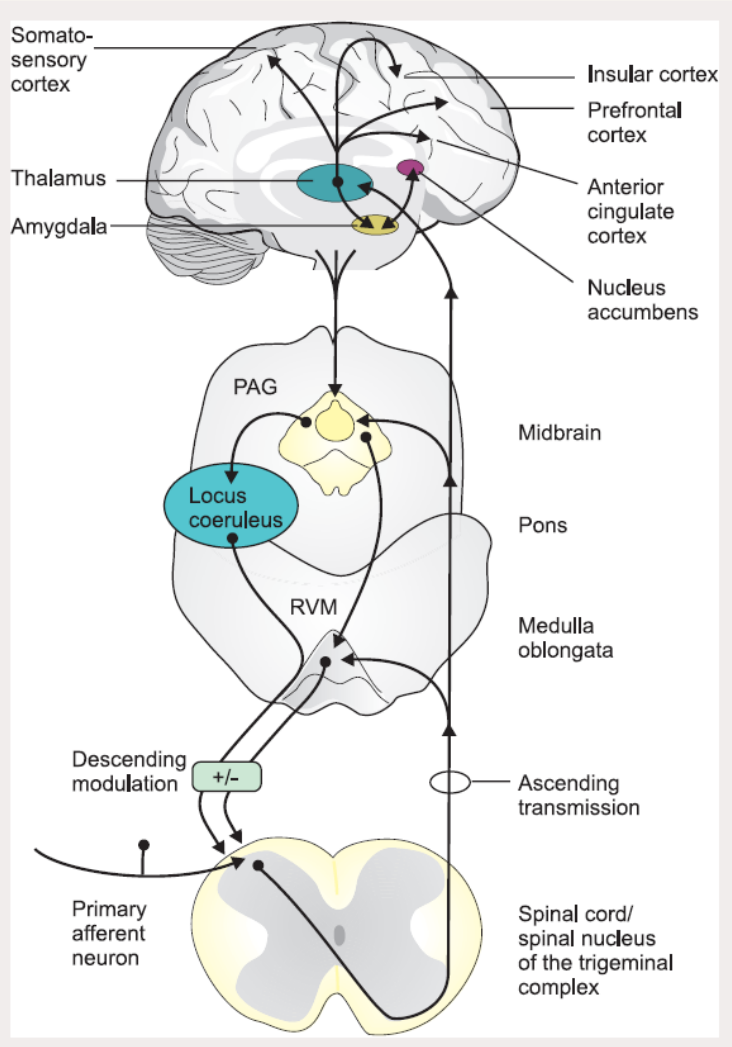

Figure 1. Pathways for ascending transmission following activation of nociceptors and for descending pain modulation as well as brain regions involved in nociception. Adapted from Brodin et al. (2016).

The medulla and brainstem receive information from the spinoreticular and spinomesencephalic tracts, enabling the integration of nociceptive information not only for homeostatic control and autonomic processes, but also projection to forebrain regions (Dostrovsky & Craig, 2006). Reaching the cortex through the thalamus, the ascending signals are

processed in multiple cortical areas (see Figure 2), such as the primary and secondary somatosensory cortices (SI, SII), the insula, the anterior cingulate cortex (ACC) and the prefrontal cortex (PFC). While the former are thought to primarily integrate the sensory component, the latter might be more involved in the affective component of pain perception (Apkarian et al., 2005; Schnitzler & Ploner, 2000; Treede et al., 1999).

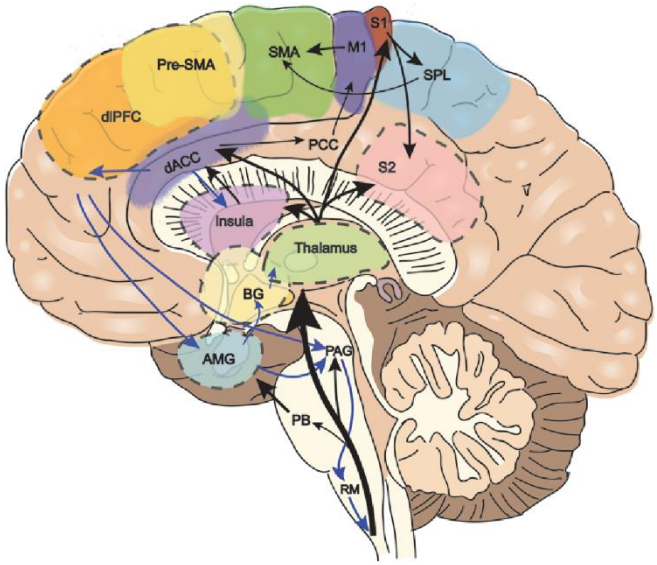

Figure 2. Illustration of the brain regions involved in the perception of a painful stimulation. Their interactions with another are indicated either in black (ascending) or blue (descending). dACC = dorsal anterior cingulate cortex, dlPFC = dorsolateral prefrontal cortex, amygdala (AMG), BG = basal ganglia; M1 = primary motor cortex; PB = parabrachial nuclei; PCC = posterior cingulate cortex; RM = rostral medulla; S1 = primary somatosensory cortex; S2 = secondary somatosensory cortex; SMA = supplementary motor area; SPL = superior parietal lobule. Adapted from Russo and Sheth (2015).

For many years, it was believed that these regions form a so-called “pain matrix”, a rigid activation pattern *specific* to pain. Yet, this claim has been challenged by multiple investigation in the past decade, showing that the brain regions activated in the “pain matrix” also respond to sufficiently salient innocuous sensory stimuli (Iannetti et al., 2008; Legrain, Iannetti, et al., 2011; Mouraux, Diukova, et al., 2011). Thus, the quest for a “signature” of

pain in the human brain continued. Increased computational power and novel neuroimaging techniques led to the development of concepts such as pain "signature" (Wager et al., 2013) or "connectome" (Kucyi & Davis, 2015), but one should remain cautious in assuming that these frameworks are truly *specific* to the experience of pain (Mouraux & Iannetti, 2018). Thus, it remains an important mission to further elucidate how pain emerges from human brain activity to develop effective treatments that can decrease the level of pain a person experiences in pathological conditions.

Modulating pain perception

When investigating how nociception leads to pain, it is crucial to consider that this is an integrative phenomenon comprising sensory, cognitive, and affective components, where individual as well as contextual factors have to be taken into account. In order to consider all these factors, the integrative processes need to be highly flexible to continuously adjust to momentary behavioral demands. This adjustment is evident, for instance, when a stimulus that would generally cause excruciating pain is barely noticed (think about soldiers wounded during a battle (Beecher, 1956)) or when a noxious stimulus does not lead to the same sensation in two different individuals (Ploner et al., 2015). Following this perspective of a dynamic neural system, a noxious stimulus would lead to a perturbation in the neural system and thus lead to the perception of pain through a modulation of this neural activity. Consequently, internal (e.g. top-down attentional control, expectancy) and external (e.g. bottom-up capture of attention) factors would exert a cross-modulation of these features to interact with the processing of the noxious stimulus. Hence, understanding the integrative processes (i.e. its flexibility) could help to understand inter-individual variability of pain perception as well as

different factors such as anxiety, expectancy, or distraction which are known to dramatically modulate the perceptual outcome of forthcoming painful stimuli (Ploner et al., 2015). Thus, to investigate whether neural activity is functionally related to pain perception, we chose to modulate pain perception and observe whether the neural activity would exhibit an equivalent modulation. But first, it is necessary to determine *how* the perception of a painful stimulus can be modulated.

Generally, we can differentiate between bottom-up and top-down modulation (Figure 3). Simplified, bottom-up refers to an external factor (such as higher stimulation intensity) changing the perception of a stimulation, while top-down refers to cognitive factors (such as distraction), that can modulate the perception of a painful stimulus.

Top-down modulation is amongst other mechanisms mediated by descending endogenous pain modulation in the brainstem, through structures such as the periaqueductal grey (PAG), locus coeruleus (LC) and rostral ventromedial medulla (RVM) (see Figure 1) (Tracey & Mantyh, 2007). Interconnected with cortical structures such as the rostral ACC (rACC), amygdala, hippocampus, prefrontal cortex and insula, these structures are able to both up- and down-regulate the sensation of pain following e.g. tissue damage (Bingel & Tracey, 2008), mediated by the endogenous opioid system (μ-opioid receptors in cortical and subcortical structures) (Petrovic et al., 2002) and other neurotransmitters such as cannabinoids (Benedetti et al., 2011) and dopamine (Peciña & Zubieta, 2015). Crucially, it seems that cortico-cortical modulations in brain regions receiving the ascending input from the nociceptive fibers (such as SI, SII, ACC and insula) are mainly involved in top-down modulation, especially related to attentional processes. This has been evidenced in a series of experiments using laser-evoked potentials (LEPs) (reviewed by Legrain et al. (2012)), which demonstrated that all components of the LEPs exhibit a similar

change in response to varying cognitive demands, suggesting they are equally involved in the top-down modulation.

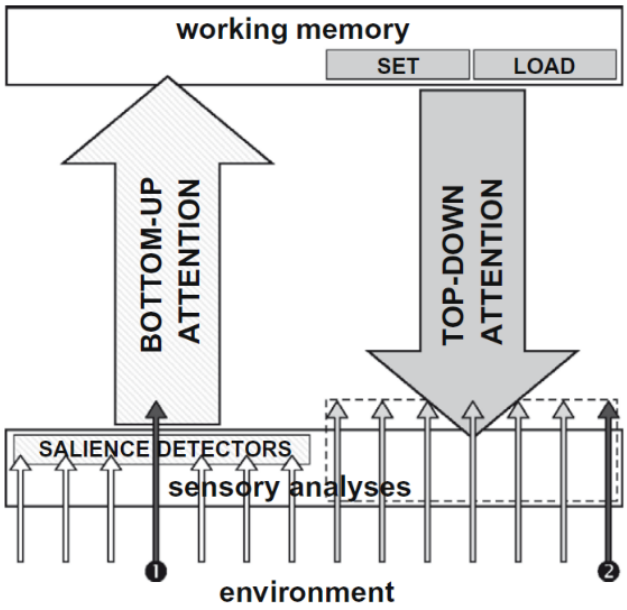

Figure 3: The brain constantly selects sensory signals that are most relevant for behavior, giving them priority access to working memory for conscious processing. This selection can occur in two ways: Bottom-up selection, driven by attention captured by salient sensory stimuli (black arrow #1), and top-down selection, directed by cognitive goals. Goals determine task-relevant features and control attentional focus (grey arrows for relevant signals, white arrows for irrelevant ones). When shifting attention from pain, a painful stimulus can still capture attention if it is highly salient (black arrow #1) or shares features defined by the attentional set (black arrow #2). Adapted from Valéry Legrain et al. (2009).

Attentional control is one of the most prominent examples of top-down modulation (Wiech et al., 2008). In experimental settings, a decrease in pain perception is often achieved by having the subject complete a demanding cognitive task to divert attention away (i.e. distract) from the painful stimulation. The effectiveness of such tasks has been proven in many studies (e.g. (Bantick et al., 2002; Buhle et al., 2012; Dowman et al., 2008; Plaghki et al., 1994; Veldhuijzen et al., 2006). One of the first explanations for this effect was the “limited capacity” theory (Kahneman, 1973). The underlying hypothesis was that the brain has only a limited

capacity to process information and will allocate its processing to the task that seems more important. More recently, the inherent saliency (i.e. the ability of a stimulus to capture attention) of painful stimuli has been taken into account and the necessity of inhibiting the capacity of the nociceptive stimulus to attract attention to create a successful distraction task (Eccleston & Crombez, 1999) became evident. Subsequently, Legrain et al. (2002) proposed the "sensory gain control hypothesis", suggesting that attention can regulate the response levels in cortical regions that receive and process nociceptive input, therefore controlling the "gain" of these areas. Consequently, very demanding cognitive tasks such as working memory tasks are more effective at diverting attention away from pain. Functional imaging investigations have shown that the decrease in pain perception during distraction is matched by a decrease in activity in relevant cortical and brainstem structures, such as the ACC, insula, thalamus and SI/SII (Bantick et al., 2002; Tracey et al., 2002; Valet et al., 2004). We made use of the effect of distraction on the perception of painful stimuli in chapter 2 of this thesis, to probe the functional relationship between the changes in stimulus perception and the modulation of ongoing oscillations.

Expectation is another powerful cognitive factor that can modulate the perception of painful stimuli. Broadly speaking, effects of expectation can be differentiated into placebo analgesia, nocebo hyperalgesia and stimulus expectancies, each having unique effects on pain intensity processing (Atlas & Wager, 2012). While placebo and nocebo effects rely on the application of an inert cream (or similar), stimulus expectancies are shaped by visual or verbal information and an associative learning paradigm, during which subjects learn to associate certain cues with certain stimulus intensities, which consequently changes their perception of the painful stimulus (e.g. (Atlas et al., 2010; Keltner et al., 2006; Koyama

et al., 2005; Lorenz et al., 2005). This modulation is likely generated when a mismatch between presented cue and stimulus intensity is created (Wiech, 2016). This cue-based expectation effect is arguably stronger than placebo/nocebo modulations (Atlas & Wager, 2012), mediated by brain regions such as the somatosensory cortices (Koyama et al., 2005), ACC, insula and thalamus (Atlas et al., 2010). Notably, pre-stimulus expectations seem to be shaped by the orbitofrontal cortex and ventral striatum, highlighting the top-down modulation involved in the modulation of pain perception by a cue-based expectation paradigm. The cue-based expectation modulation paradigm presented in Atlas et al. (2010) was used in chapter 3 of this thesis.

The **saliency** of a stimulus is a classic example of bottom-up modulation; the more a stimulus stands out from its environment (e.g. through intensity), the more likely it is to capture attention, even involuntarily and when task-irrelevant (Egeth & Yantis, 1997). In relationship to pain, this behavior comes down to the evolutionary task of pain as a warning signal of a potential imminent physical threat, which makes any painful stimulus a salient one (Eccleston & Crombez, 1999). Brain regions that respond to salient sensory stimulation form a multimodal network, including the prefrontal cortex, anterior insula, temporoparietal junction and ACC (Downar et al., 2000; Downar et al., 2003). Following painful salient stimulation, a network of brain regions is activated (Legrain, Iannetti, et al., 2011), highlighting the global effects of saliency. This far-reaching change in cortical activity / excitability following brief painful stimulation has also been demonstrated using EEG (M. Ploner et al., 2006). Generally, it has been shown that the saliency of a painful stimulation elicits activity that is closely related to the allocation of attention to a potentially damaging event (Valéry Legrain et al., 2009) and drives the neural response (i.e. event-related potentials (ERPs)) to a larger extent than pain perception (Iannetti

et al., 2008). An oddball paradigm using periodic salient stimulation has been used in chapter 4, to probe the relationship between the modulation of ongoing oscillations and the saliency vs intensity of a painful stimulation.

While the understanding of these top-down and bottom-up processes is relevant, they are not the main focus of this doctoral thesis. These processes are used to actively modulate the pain perception of the participants in a predetermined direction, to then assess whether we can detect modulations of ongoing oscillations that are congruent with the change in perception.

Assessing pain

Since the goal of this PhD thesis is to identify potentially pain-related neural activity which could be used in the future for the development of a biomarker or as target for neuromodulation, it first needs to be discussed how the neural response to a nociceptive (and potentially painful) stimulation can be measured.

The most straightforward method is to simply ask a person “how much pain did you feel on a scale from 0 to 10, while 0 represents no pain and 10 represents the most intense pain you can imagine”. However, rating perceived pain on an arbitrary numerical scale is incredibly subjective, and depends heavily on a person’s current mental state, their previous pain experiences, the gender of the experimenter and many other influencing factors (McGrath, 1994). Nevertheless, they are considered the “gold standard” to identify a painful sensation (Katz & Melzack, 1999). These subjective reports will be used in all chapters to verify whether the

nociceptive stimulations used were perceived as painful, and to get an idea of the magnitude of the perceived intensity of the stimulation.

Different techniques exist to help us understand how the sensation of pain emerges from brain activity: Functional magnetic resonance imaging (fMRI) is an imaging technique which has been used in many of the investigations that laid the foundation to our understanding of brain areas involved in pain perception (e.g. (Treede et al., 1999)). While fMRI has a very high spatial accuracy, its resolution on the time scale is not ideal to investigate the temporal dynamics of pain perception. And while it is important to understand the *"where"* in pain perception (as a snapshot of activity in time*)*, it does not allow to capture the dynamic complexities of pain perception. Thus, we want to focus on *how* the brain acts and interacts to create the perception of pain through flexible and dynamic neural communication. EEG is not able to determine exactly the source of the recorded electrical activity but provides an excellent temporal resolution on the millisecond scale. The technique is based on the recording of differences in electrical potentials on the scalp, largely generated by synchronous changes in excitatory or inhibitory postsynaptic potentials (EPSP/IPSP) of relatively large cortical neuronal populations of pyramidal neurons. Importantly, a positive or negative charge on the extracellular membrane creates a dipole, i.e. a charge of the opposite polarity. Only if those dipoles are oriented perpendicular to the cortex, the EEG electrodes are able to pick up the EPSPs. Action potentials, which transmit signal within the neuron, are technically also charged, yet too brief to contribute to the signal recorded by scalp EEG electrodes. Additionally, the cerebrospinal fluid, skull and scalp are in between the electrodes and the actual potential at the postsynaptic membrane, distorting the signal (i.e. volume conduction). Thus, the closer (and more perpendicular) these EPSPs are to the surface of the scalp, the stronger

the recorded signal. This implies that it is rather difficult to assess the activity of deep brain structures such as the thalamus or the insula using scalp EEG (see Barlow (1983) for a comprehensive introduction to EEG).

Nevertheless, EEG has been used successfully for many years to record responses to brief somatosensory (and nociceptive) stimulation in so called event-related potentials (ERPs), a characteristically shaped biphasic response often found at the scalp vertex. While the components of this response are relatively well understood, they are less meaningful when using longer (tonic) stimulation. Yet, to gain a better understanding of the cortical processes involved in sustained pain (to approximate processes underlying chronic pain conditions), less focus should be put on brief (thermo-)nociceptive stimuli, which are prone to reflect the saliency of the stimulus more than the pain-related processes (Legrain, Crombez, et al., 2011). Rather, long-lasting thermonociceptive stimuli generating sustained activity in slowly-adapting thermonociceptors should be investigated to improve the approximation of the processes during persistent pain (Schepers & Ringkamp, 2010). While they are not a model for chronic pain conditions per se, they can guide the understanding of processes during sustained pain in a healthy system. Furthermore, to better understand the fluctuating and dynamic nature of pain, a neural correlate should be investigated that is able to integrate and modulate information across cortical regions: ongoing neural oscillations. The next chapter will illustrate the neural substrates for this activity and how it could be leveraged to increase our understanding of neural activity related to pain perception.

Ongoing oscillations

Ongoing neural oscillations arise from ongoing and spontaneous fluctuation of brain activity, which cycle and interact at different frequencies and spatial scales (Buzsáki & Draguhn, 2004; Schnitzler & Gross, 2005; Singer, 1999) and have first been characterized around a century ago (Berger, 1929). Further early research in this area showed that these neural oscillations are indeed always "ongoing", fluctuating naturally in a sort-of resting-state (Adrian & Matthews, 1934).

One of the key functions of this oscillatory activity might be the integration of neural activity across the brain, allowing for flexible processes in a fixed anatomical space. One of the predominant models for this neuronal communication is "communication through coherence", a term coined by Fries (2005) and updated a decade later (Fries, 2015). This model underlines that, for communication between neuronal populations to be effective, the sending as well as the receiving group need to be in the same state of excitability, thus exhibiting a *coherent* (i.e., *phase-locked*) rhythmic reoccurring behavior in certain time frames (Fries, 2005) (Figure 4). Coherence between neuronal groups is only possible due to the predictable regular oscillations that occur naturally in neural oscillations (Fries et al., 2002; Gray et al., 1992) as well as the equally consistent conduction velocity along the axons (Innocenti et al., 1994). This physiological coherence allows for phase synchronization, the association between the temporal structure of the signal which happens regardless of signal amplitude and enables the brain to connect different anatomical and functional regions of the brain (Varela et al., 2001; Womelsdorf et al., 2007). The amplitude on the other hand is a correlate for the number of neurons that were active within the population (Elul, 1972). Thus, the higher the frequency of the oscillation, the lower the amplitude of the signal generally is.

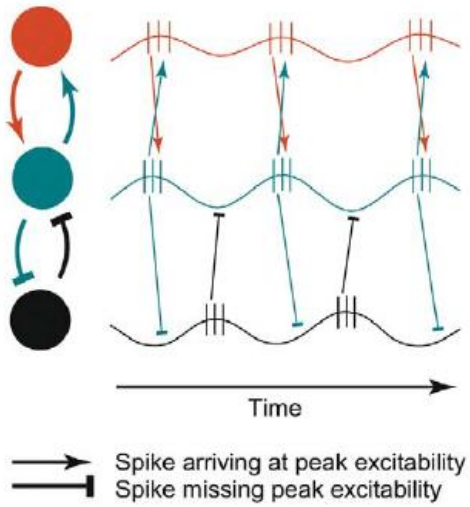

Figure 4. Schematic representation of coherence between oscillating neurons. Adapted from Fries (2005).

How can we assess changes in neural oscillatory activity? While ERPs reflect changes in afferent activity and the cortical response to it ("evoked" activity), oscillations are characterized by transient changes in the modulation of local neurotransmitters, dynamic processes at the membrane level and the connectivity between different neural networks ("induced" activity) (Pfurtscheller & Lopes da Silva, 1999). Shifts in the oscillatory activity that are time-locked but phase-independent can be identified as either event-related synchronization (ERS, increase in power in the specific frequency band (Pfurtscheller, 1992)) or event-related desynchronization (ERD, decrease in power in the specific frequency band (Pfurtscheller & Aranibar, 1977)), which reflect different neural processes than ERPs (Mouraux & Iannetti, 2008) and relate to cortical excitability (Pfurtscheller & Lopes da Silva, 1999). These responses are usually illustrated using time-frequency maps, and can be differentiated in their components such as latency, magnitude and scalp distribution (which are also used for ERPs) as well as frequency, phase, neural generator and phase coupling (which are specific to ongoing oscillations) (Peng & Tang, 2016). Each of these components could be involved in the generation of pain perception, either by itself or in mediation with other factors. For example, using ultra-slow nociceptive stimuli for neural entrainment showed that both power and phase correlated with pain sensitivity on a group level (Guo et al., 2020).

Frequency bands

The spectrum of neural oscillatory activity can be decomposed into multiple different frequency bands. Berger (1929) already characterized the oscillatory neural rhythms within the alpha and beta frequency bands. The exact range for each band vary within few Hz in many publications, and only recently a “best practice” recommendation has been published to reach a homogenous definition of the frequency band widths in future publications (Pernet et al., 2020). Thus, the frequency bands are being defined as theta (4 to < 8 Hz), alpha (8 to < 13 Hz), beta (13 to 30 Hz) and gamma (>30 Hz).

Crucially, different functional implications have been associated with different frequency bands; for instance low-frequency oscillations in the theta and alpha range have been linked to long-distance area-to-area interactions, possibly involved in the attentional selection through which contextual information modulates perception (Lőrincz et al., 2009; Sauseng et al., 2005). Contrarily, high-frequency gamma-band oscillations have been related to the neuronal activity required for conscious perception and within-area interactions (Ploner et al., 2017). Additionally, in cats, corticocortical synchronization in lower frequency bands has been related to top-down control, while synchronization in higher frequency bands seems to be more closely related to the saliency of a stimulus (von Stein et al., 2000). Similar results were also found in humans (Tiemann et al., 2015), underlining the importance of understanding the contribution of each frequency band to the perception of pain.

In the following section, each frequency band will be briefly described and its (potential) role in pain perception will be discussed (see also Ploner et al. (2017) and Kim and Davis (2021) for extensive reviews).

Theta frequency band (4 to < 8 Hz)

Theta band oscillations are considered to be the strongest and most stable amongst the frequency bands (Kowalczyk et al., 2013). Originating largely from the hippocampus, theta band oscillations seem to be predominantly involved in the formation and retrieval of memories (Jensen & Tesche, 2002; Klimesch et al., 2008) as well as fear conditioning and emotional arousal (Knyazev, 2007). In relationship to pain, ongoing theta band oscillations were found to be modulated by sustained nociceptive stimuli (Chang et al., 2001; Chang et al., 2002; Chen & Rappelsberger, 1994; Chen et al., 1998; Ferracuti et al., 1994; Huber et al., 2006; Huishi Zhang et al., 2016). Oscillations in this frequency band appear more prominently if pain turns pathological: alterations in ongoing theta band oscillations, measured during resting state EEG, were reported in a variety of chronic pain conditions (Drewes et al., 2008; Sarnthein & Jeanmonod, 2008; Sarnthein et al., 2005; Walton et al., 2010). Conversely, these oscillations could be modulated to change pain perception. Aiming to develop a neurofeedback brain-computer-interface (BCI) intervention, Rustamov et al. (2021) searched for EEG markers of recovery after a painful stimulus. Especially in the left lateral cortical regions such as the insula, dorsolateral prefrontal cortex (DLPFC), S1 and cingulate cortex, a “rebound” (i.e. over-recovery) of theta power was found following painful stimuli, indicating a potential relationship with the reduction in pain perception. Based on this previous investigation, a BCI intervention trying to increase frontal theta power was developed, and achieved a reduction in pain severity in a small group of chronic pain patients (Demarest et al., 2024). Additionally, a recent meta-analysis evaluating the efficacy of sensory neural entrainment (e.g. through visual or auditory stimuli) on pain perception indicated that – while results are still quite heterogenous and studies are few – they are potentially an effective option to alleviate chronic pain through theta

entrainment (Maddison et al., 2023). However, despite this clinical evidence, the involvement of oscillations in the theta frequency band in (experimentally induced) pain perception remains inconclusive (Kim & Davis, 2021). Still, data from intracerebral recordings of electrode contacts located in the human posterior insula suggested at least a potential involvement of the theta frequency band in pain perception, since a preferential modulation of the theta (and alpha) frequency band was found following thermonociceptive, but not non-nociceptive vibrotactile stimulation (Liberati et al., 2019).

Alpha frequency band (8 to < 13 Hz)

The alpha band was the first frequency band to be described in the literature (hence its name) (Berger, 1929). Activity within the alpha frequency band is most likely generated by the thalamus (Goldman et al., 2002; Pfurtscheller, 2003). The μ-rhythm, a sub-category of the alpha rhythm centered at 10 Hz correlating with sensory-motor activity, seems to originate from the somatosensory cortex (Jones et al., 2009). On a functional level, the alpha frequency band is involved in many basic cognitive processes; its largest contribution is likely towards attentional processes (Klimesch, 2012). ERS (increase in amplitude) and ERD (decrease in amplitude) in the alpha frequency band are linked to inhibition and disinhibition, respectively, demonstrated in working memory and visual attention tasks (Jensen & Mazaheri, 2010; Pfurtscheller, 1992, 2003). During a task, inhibitory alpha activity (i.e. a large amplitude) can downregulate activity in cortical regions not involved in the completion of the task while small amplitudes have the opposite effect. This can be observed even during the memorization of a painful stimulus, where the increase of alpha activity might reflect the effort of the brain to filter out potentially disrupting inputs during the time of retention (Caldichoury et al., 2024). Recently, alpha activity has also been proposed to be involved in the

processing of salient unattended stimuli (i.e. stimuli that capture one's attention) (Jensen et al., 2012; Liang et al., 2020).

More importantly, oscillations in the alpha frequency band are the most prominently indicated frequency band in nociception and pain perception. Several EEG studies demonstrated that tonic painful stimuli could modulate alpha band activity (Chang et al., 2001; Egsgaard et al., 2009; Hu et al., 2013; Huber et al., 2006; Huishi Zhang et al., 2016; Le Pera et al., 2000; Mulders et al., 2020; Nir et al., 2012; Schulz et al., 2015). More specifically, a decrease in power (i.e. ERD) in this frequency band has been found in a range of investigations following painful stimuli, which has been correlated to the perceived pain intensity (Giehl et al., 2014; Huishi Zhang et al., 2016; Nir et al., 2012; Peng et al., 2014; Shao et al., 2012; H. Wang et al., 2022). In an interesting experimental design using 3 different stimulus durations and 2 different intensities, H. Wang et al. (2022) revealed that alpha ERD duration and amplitude originating from the sensorimotor cortex mediate the effect of stimulus duration on pain perception. Alterations in functional connectivity measured by EEG during tonic experimental pain (10min) were also found by Nickel et al. (2020), who identified an increased connectivity between sensorimotor and prefrontal areas in addition to the commonly observed decrease in alpha power during experimental pain. Similar changes in EEG connectivity were found in an investigation employing a long-term pain model of 24h by the sensitization of the skin with capsaicin cream, observing a decrease in resting-state functional connectivity in the alpha frequency band as well as decreased projections to medial prefrontal cortex and right angular gyrus (Alhajri et al., 2023). Yet, given the general decrease in alpha activity during mental tasks, these observed relationships are not necessarily pain *specific*. Supporting this thought, Schulz et al. (2015) and (Bott et al., 2023) demonstrated that the observed decrease in oscillatory power in the alpha

frequency band might be more closely related to the objective stimulus intensity rather than the perceived intensity of the stimulus, specifically in regions such as S1, ACC, prefrontal cortex and parietal operculum (Bott et al., 2023).

The modulation of ongoing oscillations before a stimulus is even applied could reveal more about the underlying functions of changes in oscillatory activity in specific frequency bands. Concretely, the expectation of painful stimuli can lead to alterations in functional connectivity in the alpha frequency band between the prefrontal cortex and S1 (Bott et al., 2023) as well as modulations of alpha band oscillations (Babiloni et al., 2005; Franciotti et al., 2009). These findings have been suggested to reflect cortical activation or disinhibition related to the alerting function (i.e. saliency) of pain (Hu et al., 2013; Peng et al., 2014; Peng & Tang, 2016; Pfurtscheller & Lopes da Silva, 1999).

In recent years, a novel candidate for "a cortical biomarker of pain" emerged: peak alpha frequency (PAF, i.e. the frequency at which the alpha band magnitude is maximal (Klimesch, 1997)). And indeed, the "speed" (i.e. frequency) of PAF over sensorimotor areas appeared to correlate negatively with pain sensitivity (Furman et al., 2018), consistent across minutes as well as weeks (Furman et al., 2019) and days (Nahian S. Chowdhury et al., 2023) induced by long-lasting pain models (capsaicin cream or injection of nerve growth factor, which induces muscle pain). Despite this encouraging evidence, a recent systematic review concluded that there is to date little evidence of effective interventions using non-invasive neuromodulation techniques to "speed up" PAF and reduce pain sensitivity (Millard et al., 2024). This result is supported by other investigations, demonstrating that the slowing of PAF during prolonged pain did not differ between high- or low-pain sensitive groups (De Martino et al., 2021). Moreover, the individual alpha frequency has been shown to

have no causal relationship with acute pain perception in healthy volunteers (Valentini et al., 2022). This result has been further corroborated by a large-scale experiment in 159 participants, demonstrating that PAF did not appear to be predictive for the perceived pain following brief nociceptive stimuli using a multiverse analysis approach (May et al., 2024 Preprint). These results suggest that while PAF might have some clinical utility as a prospective cortical biomarker of prolonged / chronic pain, it is not a "one fits all" solution for the understanding of how the brain shapes pain perception.

Changes in evoked oscillatory activity induced by experimental pain can also be probed directly using transcranial magnetic stimulation (TMS) together with EEG, eliciting TMS-evoked potentials (TEPs), which are considered a correlate for cortical excitability (Rogasch & Fitzgerald, 2013). De Martino et al. (2024) demonstrated that TEPs elicited by TMS pulses delivered over M1 during acute pain induced a local reduction in alpha band power, which correlated with cold and heat pain thresholds. Moreover, phase synchronization locally as well as with remote occipital-parietal clusters was decreased, also correlating with pain sensitivity. These results fall in line with a recent investigation of (Nahian S Chowdhury et al., 2023), and suggest that cortical excitability, which is inherently linked to oscillatory activity, could be a potential marker of pain sensitivity. But this promising body of work on the relationship of cortical excitability and pain perception is still in its infancy, as the reliable use of TMS-EEG has only been made possible in recent years due to technological advances in both hardware and software (Ilmoniemi & Kičić, 2010).

Beta frequency band (13 to 30 Hz)

Activity in the beta frequency band seems to be generated from two distinct brain regions; while lower beta appears to originate from the somatosensory cortex, higher beta activity is probably generated by the

hippocampus (Pfurtscheller, 1981). Beta band activity has long been thought to mostly reflect sensorimotor activity (Pfurtscheller et al., 1996), but a summary of more recent evidence by Engel and Fries (2010) suggests that beta band activity is mainly maintaining a certain (predicted or intended) internal state through top-down modulation, in both cognitive function as well as motor control.

Similarly to the alpha band, the modulation of oscillations within the beta band has been associated with acute as well as tonic painful stimuli, exhibiting decreased amplitudes (Alhajri et al., 2023; Mouraux et al., 2003; Mulders et al., 2020; Nickel et al., 2020; M. Ploner et al., 2006; Schulz et al., 2015). Interestingly, the intensity of the applied stimulus (i.e. objective intensity) seems to be one of the driving factors behind this modulation (Bott et al., 2023; Hauck et al., 2015; Nickel et al., 2017; Strube et al., 2021a). Not attending a painful stimulus reduced amplitudes in the beta frequency band, highlighting its potential involvement in top-down modulation (Diers et al., 2020). Tonic pain has also been shown to increase the connectivity between alpha and beta band oscillations in sensorimotor areas contralateral to the site of the painful stimulation (Nickel et al., 2020), highlighting that the interplay between these oscillations could be crucial in our understanding of how the brain shapes pain perception.

Gamma frequency band (>30 Hz)

Gamma band activity are the fastest oscillations of the recognized frequency bands, enabling it to react in milliseconds to internal or external changes (Buzsáki & Chrobak, 1995). These oscillations are not specific to one brain region and appear throughout the cortex, reacting to a variety of sensory stimuli (Fries, 2009). Furthermore, gamma band synchronization has been implied in selective attention, motor planning and processing, and memory (Kaiser & Lutzenberger, 2003). On a more cognitive level, gamma band activity is thought to mediate the “prediction

error" in the brain, i.e. the mismatch between what is expected and what is actually happening (Rao & Ballard, 1999; Spratling, 2017). Thus, gamma band activity has been observed to increase in unexpected trials compared to a decrease in predictable trials of experimental investigations (Bauer et al., 2014; Brodski et al., 2015). Moreover, this high frequency oscillatory activity has been shown to mediate long-range communication in the cortex through ERD (Rodriguez et al., 1999).

The relationship between gamma band activity and nociception/ pain perception has also been debated. Some investigations found a consistent activation of gamma band oscillations in the medial prefrontal cortex following tonic painful stimuli, which has also been correlated to pain intensity perception (Li et al., 2016; Nickel et al., 2017; Peng et al., 2014; Schulz et al., 2015). Conversely, in rats, it has been shown that nociceptive-induced gamma band oscillations seem to originate largely from the spiking of superficial interneurons in S1 contralateral to the side of stimulation (Yue et al., 2020). Interestingly, gamma band activity following acute experimental pain has been shown to be prominent over sensorimotor areas (Gross et al., 2007; Hauck, Lorenz, & Engel, 2007; Linde et al., 2023; Zhang et al., 2012), highlighting the fact that the duration of pain elicits distinct neural responses and appears to shift from brain regions involved in "objective" processing to regions thought to be more emotionally driven with a longer duration of the stimulus (Ploner et al., 2017). Using brief triplet stimulations (i.e. 3 consecutive brief stimuli with a fixed interstimulus interval) to disentangle effects of stimulus saliency and pain intensity, it has been shown that gamma band oscillations indeed predict perceived pain levels (Zhang et al., 2012). However, in a similar triplet study design, Liberati et al. (2017) was not able to replicate these findings in insular responses recorded using iEEG, since the gamma band oscillations clearly habituated across the triplets while pain perception did

not. This comparison suggests that the gamma band oscillations observed in those studies originate from different sources, potentially muscular artifacts in case of the scalp EEG study. Nevertheless, Heid et al. (2020) found that nociceptive but not tactile stimuli elicited an increase in high-frequency gamma band oscillations over the contralateral S1 shortly after stimulus onset and similar results were found in the insula (using iEEG), comparing transient thermonociceptive to non-painful thermal and mechanical spinothalamic stimulation (Liberati et al., 2020). Comparing nociceptive to saliency-matched non-nociceptive modalities, a reliable correlation between gamma band ERS and pain sensitivity within- and between subject has been found at central electrodes which seemed to be preferential for nociceptive stimuli (Hu & Iannetti, 2019). Summarizing these findings, a recent systematic review and meta-analysis concluded that there might indeed be a relationship between the magnitude of gamma band oscillations and pain perception, but also that the "type" of pain was a crucial factor for the induced activity. While phasic pain led to higher frequency (~66 Hz) activity at the sensorimotor cortex, tonic and chronic pain induced activity at slightly lower frequencies (~55 Hz), prominent over prefrontal areas (Li et al., 2023).

However, gamma band activity has also been proven to be difficult to assess, given its high frequency it has a comparatively low amplitude. Additionally, muscular activity can easily be mistaken for gamma band neural activity (Fries et al., 2008). Moreover, investigations using both scalp EEG and iEEG in the insula have shown that gamma band oscillations do not always correlate with perceived pain intensity and can therefore not be utilized as a direct marker for pain perception (Liberati et al., 2018; Liberati et al., 2017; Tiemann et al., 2015). The large interindividual differences in pain-induced gamma band oscillations are also problematic, and results

should be considered to be potentially driven by a sub-group of the sample with large gamma band activity (Valentini et al., 2023).

Despite all this evidence, the literature on pain-related neural oscillations remains inconclusive (Huishi Zhang et al., 2016; Kim & Davis, 2021; Mathew et al., 2024; Ploner et al., 2017). Yet, their dynamic nature makes them an apparently ideal substrate for the flexibility observed in the pain perception and its modulation. They are therefore of utmost interest to identify an objective readout for an individual's perception of pain and potential target for therapeutic approaches in the treatment of chronic pain conditions. The next sections of this chapter will further elucidate how we can assess and perturbate/modulate the activity of this ongoing neural activity and investigate their relationship to the perception of pain.

Frequency-tagging

Ongoing oscillations can be analyzed in a multitude of ways, most often in the form of time-frequency maps. While these allow us to analyze differences over time, we cannot clearly distinguish whether the activity that is observed is actually related to our stimulus, as ongoing oscillations are naturally fluctuating over time in a dynamic manner and are not phase-locked to a stimulus.

To isolate activity related to our stimulus and differentiate it from other ongoing neural activity, a so-called "frequency-tagging" approach (Regan, 1989) can be applied to steady-state evoked responses (SSEP). This approach is based on the assumption that a periodic sensory stimulation will elicit a periodic response in higher-order neurons, which in turn generates peaks in the EEG frequency spectrum at the frequency of stimulation and its harmonics (Figure 5, left side). This leads to a unique

combination of objectivity in the analysis and sensitivity to signal fluctuation, making it an ideal tool to assess the activity of ongoing neural oscillations. While this approach has been used for years in other sensory domains such as auditory (Geisler, 1960; Pantev et al., 1996), vision (Norcia et al., 2015; Rossion, 2014; Rossion et al., 2020; Rossion et al., 2015) or rhythm perception (Nozaradan, 2014; Nozaradan et al., 2011), it can also be extended to tactile and crucially, nociceptive stimuli (Colon, Legrain, et al., 2012; Colon, Nozaradan, et al., 2012; Mouraux, Iannetti, et al., 2011).

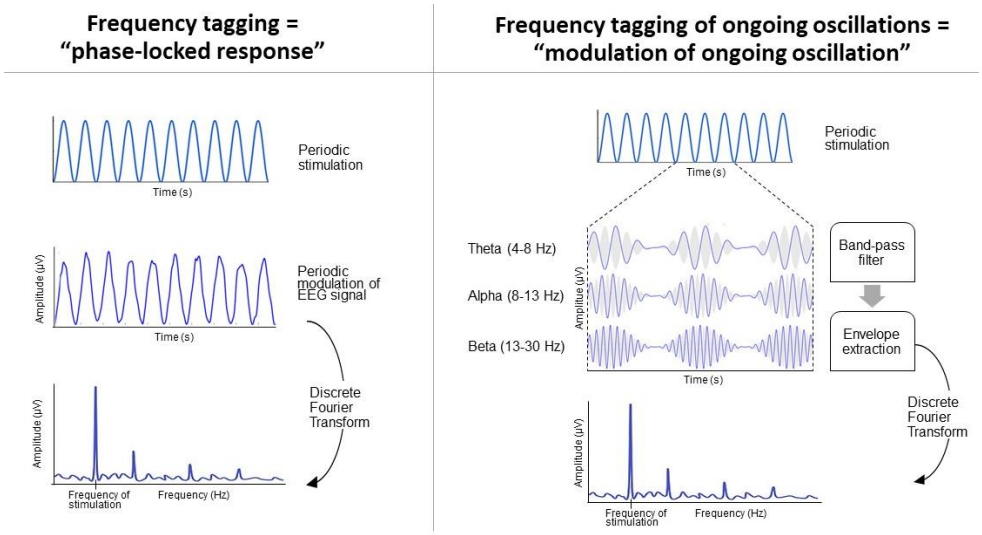

Figure 5. Illustration of the frequency-tagging method as well as its extension for the frequency-tagging of ongoing oscillations. Frequency-band ranges were defined following the COBIDAS guidelines (Pernet et al., 2020).

At first, the same fast-paced stimuli (6-7 Hz) as in the other sensory domains were used to deliver sustained periodic thermonociceptive stimuli with a CO_2 laser (Colon, Legrain, et al., 2012; Colon et al., 2014; Mouraux, Iannetti, et al., 2011), but it became apparent that a much slower sinusoidal thermonociceptive stimulation applied at 0.2 Hz would lead to an improved signal-to-noise ratio (Colon et al., 2017) (Figure 6). Additionally, due to the slow rise and fall of the stimulation temperature, this type of stimulation predominantly activates unmyelinated C-fiber

thermonociceptors, as shown by the application of an Aδ-fiber block (Colon et al., 2017). This makes it an ideal paradigm to gain a better understanding of neural processes during sustained / tonic pain (Campbell & Meyer, 1983; Wooten et al., 2014)).

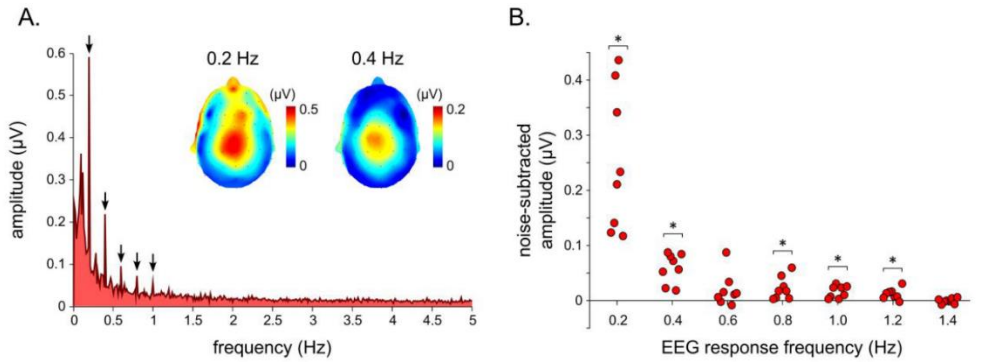

Figure 6: Periodic neural response to slow sustained periodic sinusoidal thermonociceptive stimulation delivered at a frequency of 0.2 Hz for 75s per trial, cycling between 35°C and 50°C. A: Group average frequency spectrum as well as topographic representation of the measured signal at the scalp vertex (Cz). B: Individual EEG responses (averaged across all channels) at the frequency of the stimulation and its harmonics. * p <.05 (Wilcoxon signed ranked test against zero). Adapted from Colon et al. (2017)

The largest periodic response to these ultra-slow stimuli was found at the scalp vertex, likely reflecting activity of the ACC as well as left and right operculo-insular cortices (Mouraux, Iannetti, et al., 2011; Owen et al., 2010; Peyron et al., 2000). Consistent topographies have been found in other SSEP investigations (Courtin & Mouraux, 2024 Preprint; Leu et al., 2023; Leu et al., 2024; Mulders et al., 2020), and together with the observed time-frequency activity it appears that these responses could reflect similar processes as “classical” ERPs elicited by brief sensory stimulation (Courtin & Mouraux, 2024 Preprint), but related to activity of C-fibers instead of Aδ-fibers.

Frequency-tagging of ongoing oscillations

In addition to the "phase-locked" response, Colon et al. (2017) showed that the frequency-tagging approach can be extended to assess the modulation of ongoing oscillations (FT-OO) in different frequency bands (Figure 5, right side), an approach which has since been used in multiple investigations from our lab (Courtin & Mouraux, 2024 Preprint; Leu et al., 2023; Leu et al., 2024; Liberati et al., 2019; Mulders et al., 2020). First, a Butterworth filter is applied to differentiate the different frequency bands (e.g. 4-8 Hz for the theta frequency band). Then, the envelope of the filtered signal is estimated using a Hilbert transform before a discrete Fourier transform is applied to transform the signal into the frequency spectrum. Finally, baseline noise has to be accounted for (e.g. due to non-event-related activity and artifacts) which is inherently present in all brain in the frequency domain (Regan, 1989). A widely used baseline correction is used to remove the mean amplitude of the neighboring frequency bins on each side of the main frequency of interest (Mouraux, Diukova, et al., 2011; Norcia et al., 2015; Regan, 1989). Once removed, the frequency-domain signal amplitude is represented in the same unit as in the time-domain, making them comparable.

Typically, the responses in the alpha and beta frequency band are the largest at electrodes over central and parietal regions contralateral to the stimulated limb, likely reflecting activity of the somatosensory cortices (Becerra et al., 1999; Dowman et al., 2008; Freund et al., 2009; Owen et al., 2010). An analysis of these modulations in the time domain revealed a decrease in power (Mulders et al., 2020), which matches ERD previously observed in the alpha and beta band during both sustained as well as transient nociceptive stimulation (Dowman et al., 2008; Giehl et al., 2014; Hu et al., 2013; Huishi Zhang et al., 2016; Nir et al., 2012; Peng et al., 2014; Schulz et al., 2015). While positive gamma band modulations were

observed in other tonic heat experiments (Dowman et al., 2008; Schulz et al., 2015), no consistent periodic response has been observed in this frequency band using the FT-OO approach (Colon et al., 2017; Mulders et al., 2020). Finally, the modulation of the theta frequency band remains less clearly defined. Colon et al. (2017) found a significant periodic modulation in this band, maximal at centro-parietal electrodes. While Mulders et al. (2020) did find a similar pattern in the scalp topography, the peaks at the frequency of stimulation were not consistently modulated.

Furthermore, while previous iEEG investigations from our lab used a CO_2 laser with temperature feedback, Mulders et al. (2020) showed that comparable neural responses can be obtained using a thermal cutaneous stimulator (TCS) (QST.lab, Strassbourg, France). The use of the TCS also allowed the comparison of sustained periodic warm and cold stimuli and different application surfaces, revealing that heat stimuli elicited much larger responses compared to cool stimuli and that a variable stimulation surface can attenuate habituation to a certain extent. More importantly, ratings of stimulus perception and EEG responses showed a similar degree of habituation, supporting the notion that these EEG responses could reflect stimulus perception (Mulders et al., 2020).

Harmonics

While the frequency-tagging paradigm makes it easy to identify responses related to the applied stimulus, the interpretation of the signal and in particular the harmonics generated at the multiples of the main stimulation frequency (i.e. F: 0.2, F_2: 0.4, F_3: 0.6, ...) is still debated (Retter et al., 2021).

First, it is important to understand what the harmonics represent; they are not part of a different activity compared to the response at the frequency of the stimulation (FOS), nor do they represent a specific response in the

frequency domain. Harmonics appear even when the stimulation consists of a perfect sine wave (which is due to technical limitation rarely possible); while a computer would generate a singular peak at the frequency of stimulation in the frequency spectrum, the human brain is prone to imperfection in this transformation (Heinrich, 2010) and is inherently non-linear in its information transmission (Regan, 1989). Thus, the harmonics are simply a byproduct of the frequency domain representation of the original signal in time domain, making the conversions back and forth in the two domains possible (Sieving et al., 1998). Hence, the sum of the harmonics reconstructs the original signal.

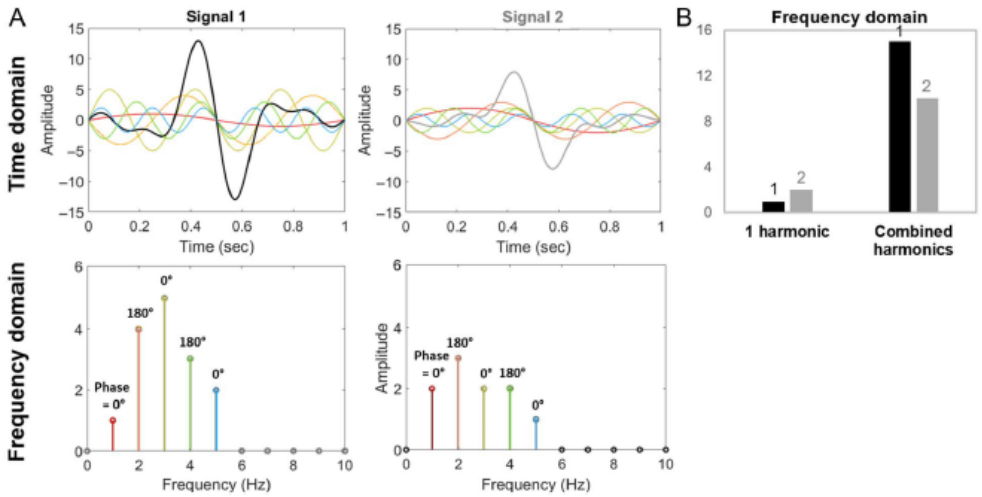

Figure 7. Illustration of the importance of combining higher harmonics in frequency domain analyses. (A) Time (row 1) and frequency domain (row 2) representation of two periodic signals (thick lines). Colored lines represent the harmonics of the main signal. (B) Comparison of the signal in the frequency domain if either only 1 harmonic (left) or all harmonics are combined (i.e. summed up, right). With the summation it is clear that signal 1 is larger than signal 2, a disparity which was not clear without the summation. Adapted from Retter et al. (2021)

In the past, harmonics have often been disregarded in the analysis of responses evoked by a sensory stimulus (Retter et al., 2021), but by doing so an important part of the evoked response is lost. To avoid this, harmonics should be summed up to take the full neural response in the

frequency spectrum into account and accurately reflect the original time-domain potentials (Figure 7). Yet, how many of the harmonics should be summed up and what constitutes a “functionally relevant” harmonic is still debated. Some authors argue that the harmonics of the entire spectrum should be summed up, and that potential noise would be cancelled out in the process (Courtin & Mouraux, 2024 Preprint). Others chose a partial of the harmonics based on different criteria such as significance threshold (based on amplitude, signal-to-noise ratio or power) (Retter & Rossion, 2016; Rossion et al., 2015)), harmonic series number (Appelbaum et al., 2006) or the relationship of the harmonics to other stimulation frequencies (Milton et al., 2020). Importantly, depending on the FOS, the weight of the harmonics is distributed differently: the lower the FOS, the larger the amplitude of higher frequency harmonics relative to the FOS (Retter et al., 2021), making the summation of harmonics a crucial part of the analysis in the investigations presented in this thesis, as they all use a 0.2 Hz stimulation frequency.

The insula

While many brain regions are involved in pain perception, the human insular cortex (i.e., insula) serves as a “hub” for multimodal integration of sensory information as well as playing a crucial role in interoception and emotional regulation (Gogolla, 2017; Kurth et al., 2010; Zhang et al., 2024) and could thus also be chiefly involved in the perception of pain. To better understand the many physiological functions the insula has in the human brain and why they are still not fully decoded, its anatomy should first be examined: from a surface level view, the insula is not visible, as it is hidden deep in the brain by parts of the parietal, frontal and temporal lobes (i.e., the opercula), forming the bottom of the lateral sulcus (i.e., Sylvian fissure).

Given its location, assessing the activity of the insula is not trivial; scalp EEG can hardly record insular activity since the overlaying structures are "overpowering" in the recordings. While iEEG provides a highly accurate spatial and temporal solution, it relays on the invasive technique of implanting depth electrodes in the human brain. Often, these implantations are done as part of the treatment of epilepsy patients who have seizures which cannot be controlled with pharmaceutical methods, and the activity recorded by the depth electrodes aides in the identification of the ictal zone of these seizures. Obviously, there are not many hospitals doing these implantations, and thus, the number of patients that can be recruited for experimental investigations is rather limited. Nevertheless, given its superior temporal resolution compared to fMRI and positron emission tomography (PET) scans, iEEG is a highly valuable research tool to examine the functional processes in the insula.

The insula is divided into two functionally distinct parts by the central sulcus (Rolandic fissure), forming the anterior insula and the posterior insula (Figure 8). The former consists of three short gyri (anterior, middle and posterior) whereas the latter is formed by two long gyri (Naidich et al., 2004; Nieuwenhuys, 2012). The gyri are separated by pre- and post-central sulci. On a cytoarchitectural level, the insula can be differentiated in 6 different layers (Morel et al., 2013), classified as granular, dysgranular and agranular subdivisions. Interestingly, a gradient from granular to agranular (relating to the disappearance of layer 4) can be traced from the posterior to the anterior insula (Mesulam & Mufson, 1985), suggesting that there might also be a gradient in the functional connectivity of the insula. A very particular type of neuron can be found in layer 5: the so-called "von Economo neuron", named after its discoverer Constantin von Economo (von Economo, 1927). While the function of these neurons is not fully understood, they are generally only found in animals with complex social

structures. Furthermore, it has been shown that they are predominantly involved in subcortical projections (e.g. to brainstem or spinal cord) and interoceptive functions (Cobos & Seeley, 2013). Functional connectivity analyses of areas with von Economo neurons (predominantly the ACC and anterior insula) suggest that these neurons form networks involved in saliency detection and self-regulation, but also interact with sensory-motor and dorsal attention networks (Cauda et al., 2013).

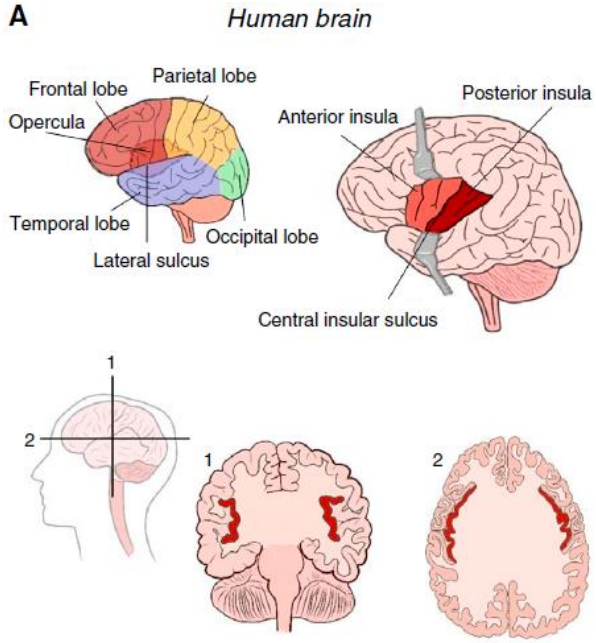

Figure 8. Anatomy of the human brain. Top left: the insula is folded below the lateral sulcus and is hidden by the opercula (shaded area) of the frontal, parietal and temporal lobes. Top right: when temporal and parietal lobes are pushed aside, the underlying insula can be seen; it is separated into an anterior and posterior part by the central insular sulcus. Bottom: coronal (1) and horizontal (2) cross sections of the human brain reveal the position of the insular cortex (red). Adapted from Gogolla (2017).

Given its central location, the insula is connected to many brain regions (see Figure 3). Notably, the insula integrates multisensory inputs, originating from thalamic nuclei (Gauriau & Bernard, 2004; Guldin & Markowitsch, 1983) and SI and SII (Gehrlach et al., 2020; Shi & Cassell, 1998). Connections to the limbic system are established via the amygdala, with bi-directional projections between sub-structures of these two regions (Gehrlach et al., 2020). Furthermore, the prefrontal cortex relays specifically to the anterior insula (Gehrlach et al., 2020), while the cingulate cortex connects to the posterior insula (Bouchatta et al., 2022). Outputs from the insula activate different systems; the anterior insula engages in the

motivation / reward system via the caudate putamen and nucleus accumbens (Jasmin et al., 2004; Q. Wang et al., 2022). Crucially, the insular cortex is also involved in the activation of descending pain modulation through outputs to the PAG, LC and RVM (Almashaikhi et al., 2014).

These particular neuroanatomical structures lay the foundation for the physiological functions of the insula, detailed in a review by Shura et al. (2014) and (Nieuwenhuys, 2012). As mentioned previously, this small "island" of the cerebral cortex is involved in a multitude of essential tasks. Many of them can be summarized as foundations of the understanding of the "self" (Devue et al., 2007) as well as the "overseer" of internal homeostasis, being chiefly involved in interoception through gustation, thermoception and visceral sensation (Craig, 2002, 2009; Craig et al., 2000; Maffei et al., 2012; Saper, 2007). While somatosensory perception seems to be located predominantly in the posterior insula (Baier et al., 2014; Baumgärtner et al., 2010; Cloutman et al., 2012; Hua et al., 2005; Kupers & Kehlet, 2006), viscerosensory and gustatory responses can be found more towards the central part of the insula (Cerliani et al., 2012; Stephani et al., 2011). Additionally, more recent investigations have found the involvement of the insula in the regulation of feelings and emotions, both positive (Craig, 2009) and negative (such as anxiety (Paulus & Stein, 2006) and fear (Klein et al., 2021)), as well as empathy (Singer et al., 2009). These connections are originating predominantly from the anterior insula and integrate into the cognitive control and emotional saliency networks (Cloutman et al., 2012; Uddin et al., 2014), likely mediated by connections to the limbic system (Cerliani et al., 2012) and become more apparent in pathological states where the functioning of the insula is impaired (Ibañez et al., 2010; Namkung et al., 2017).

More importantly in the context of this thesis, the insula has also been shown to be consistently activated during the perception of painful stimuli

in multiple fMRI studies, as reviewed by Apkarian et al. (2005), and serves as an integration site for multiple areas involved in pain perception (Brooks & Tracey, 2007). A comprehensive review on the role of the insula in pain perception in human as well as preclinical studies has recently been published (Labrakakis, 2023). While it has been suggested that, rather than exhibiting a clear cut off between the lateralities, there is a relatively smooth gradient along the posterior-anterior axis in terms of functional connectivity (Cerliani et al., 2012; Geuter et al., 2017; Nieuwenhuys, 2012), distinct structural and resting state connectivity patterns have been found between the anterior and posterior insula and other brain regions involved in pain perception (Wiech et al., 2014). Given the previously discussed structural connectivity and functional partition of the insula, it is not a surprise that the processing of painful stimuli also takes place in distinct parts of the insular cortex. While the anterior insula likely encodes the cognitive and emotional properties of pain perception (Brooks et al., 2002; Geuter et al., 2017; Hein & Singer, 2008; Kong et al., 2006; Sharvit et al., 2018; Singer et al., 2004; Stancak & Fallon, 2013) and its pre-stimulus activity has been shown to predict subsequent perception (Ploner et al., 2010; Wiech et al., 2010), the posterior insula has been shown to be primarily involved in the perception / relay of the physical properties of a painful stimulus (Cerliani et al., 2012; Craig et al., 2000; Frot et al., 2006; Geuter et al., 2017; Andrew R. Segerdahl et al., 2015; Sharvit et al., 2018). In line with this discrimination, a study assessing a large cohort of epileptic patients with implanted depth electrodes for iEEG recording demonstrated that the processing of LEPs seems to follow a posterior to anterior axis (Frot et al., 2014). Investigations in the same patient group but with electrodes that can not only record but also deliver electrical stimulation have demonstrated that the stimulation of the dorsal posterior part of the insula elicit a painful or warm sensation (Stephani et al., 2011). Similar results were found by Ostrowsky et al. (2002), showing a gradual overlap from painful

to non-painful sensations in less dorsal parts of the posterior insula, which also seemed to be somatotopically organized. Finally, Liu et al. (2021) found an increase in pain threshold following stimulation of the anterior insula, joint by attenuated LEPs and changed frequency band power of ongoing oscillations.

Despite this evidence, there is still an ongoing debate surrounding the specific role of the anterior and posterior insula in pain perception. PET and fMRI investigations around the turn of the millennium argued that activity of the anterior insula reflects perceived level of intensity following a nociceptive stimulation (Craig et al., 2000; Davis et al., 1998) and that the posterior insula was primarily involved in the detection of tactile and non-painful stimulation (Davis et al., 1998). Conversely, Baumgärtner et al. (2010) found activation in both the anterior and posterior insula following thermonociceptive stimulation. Comparing stimuli of different intensities, Baliki et al. (2009) found that a sub-portion of the insula translates the nociceptive information into a sensation which corresponds to the signal magnitude. Local field potentials (LFPs, reflecting synchronized activity of small neuronal populations close to the electrode (Buzsáki et al., 2012)) were also found in both the anterior and posterior insula following thermonociceptive and innocuous transient somatosensory stimulation measured using iEEG in refractory epilepsy patients undergoing presurgical evaluation (Liberati et al., 2017; Liberati et al., 2016). While low-frequency phase-locked LFPs did not differ between modalities, gamma-band oscillations (GBO) seemed to exhibit activity preferential for nociception (Liberati et al., 2017). Yet, this activity can be dissociated from the perceived level of pain intensity, underlining that the GBO responses are not a cortical correlate for pain intensity (Liberati et al., 2018). Finally, Isnard et al. (2011) hypothesized that the posterior insula shapes the perception of pain following the assessment of painful epileptic seizures

originating from posterior insula and Wiech et al. (2005) found in a capsaicin-induced hyperalgesia model that the activity in the mid-posterior insula correlated with perceived pain intensity. Moreover, using arterial spin-labeling quantitative perfusion imaging Andrew R. Segerdahl et al. (2015) claimed that the posterior insula reflect pain-*specific* activity, which has been received with criticism (Davis et al., 2015) and further nurtured this ongoing debate (A. R. Segerdahl et al., 2015). In summary, while the posterior insula likely does not reflect activity *specific* to pain, the majority of the recent literature seems to point to a predominantly posterior involvement of the insula in the perception of painful stimuli in heathy participants (Labrakakis, 2023).

Up to date, most investigations used brief (thermo-)nociceptive stimuli to probe the physiological processing of nociceptive stimuli in the insula, activating predominantly quickly-activating mechano-heat nociceptors. Importantly, and as outlined previously in this chapter, to gain a better understanding of potential underlying mechanism of sustained pain, it might be beneficial to use longer sustained or tonic stimulations such as the sustained periodic stimulation paradigm used for the frequency-tagging approach, which also activate slowly-adapting thermonociceptors. Such a shift has recently been demonstrated in a longitudinal study by Hashmi et al. (2013), which followed low back pain patients from acute pain to chronic pain. Interestingly, a shift from posterior to anterior representation of the pain was observed concomitant to the chronification of the symptoms. Following this rationale of adopting a less “phasic” view of pain, Liberati et al. (2019) showed that slow sustained periodic stimuli (see “frequency-tagging” section) lead to a *preferential* modulation of ongoing oscillations in the dorsal posterior insula when comparing thermonociceptive and innocuous vibrotactile stimuli in epilepsy patients with implanted depth electrodes in the insula (Figure 9).

While LFPs elicited by brief nociceptive stimuli have been shown to habituate (Liberati et al., 2018), this was not the case for the "frequency-tagged" response to these slow sustained stimuli, suggesting that the observed responses have different underlying neural mechanisms (Liberati et al., 2019). Additionally, unlike LFPs, the responses elicited by the frequency-tagging are mainly related to C-fiber activity (Colon et al., 2017). These findings support the previously mentioned literature attributing the dorsal posterior insula a key role in the processing of painful stimuli. More importantly, they identified ongoing neural activity which could be preferential for pain. Yet, whether the observed modulations are indeed functionally related to the perception of a painful stimulus remains unclear. The final chapter of this thesis will explore this question further, while employing the same experimental paradigm as used in the scalp EEG investigation of chapter 2, but in epileptic patients and using iEEG in collaboration with the St-Luc university hospital in Brussels.

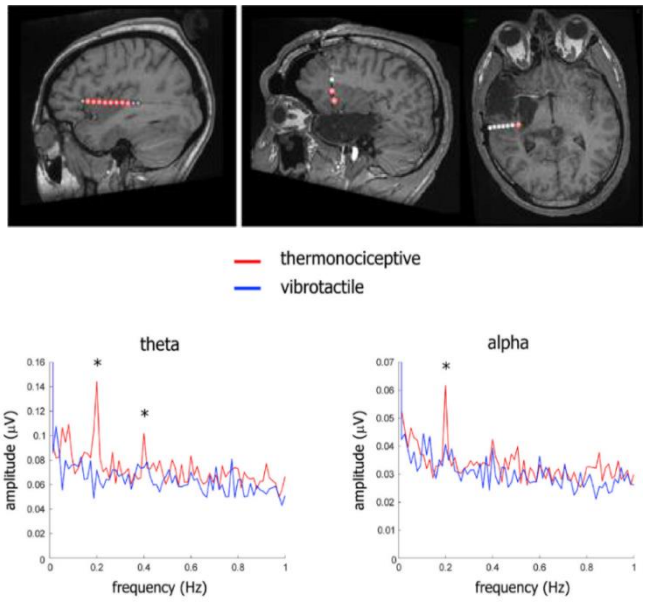

Figure 9. Group-level average frequency spectrum of the intracerebral EEG signal in the theta (4- 8 Hz) and alpha (8-12 Hz) frequency band averaged across all insular contacts. Compared to 0.2 Hz vibrotactile stimulation, 0.2 Hz thermonociceptive stimulation elicited a greater modulation of ongoing oscillations at 0.2 Hz and at 0.4 Hz in the theta frequency band (both $p < .001$), and a greater modulation of ongoing oscillations at 0.2 Hz in the alpha frequency band ($p = .002$). Adapted from Liberati et al. (2019).

CHAPTER 2. The role of ongoing oscillation in pain perception: Absence of modulation by a concomitant arithmetic task [1]

---

[1] Published as: **Leu, C.,** Courtin, A., Cussac, C., & Liberati, G. (2023). *The role of ongoing oscillation in pain perception: Absence of modulation by a concomitant arithmetic task.* Cortex, 168, 114-129. https://doi.org/10.1016/j.cortex.2023.08.005

Abstract

Sustained nociceptive stimuli have been shown to modulate the amplitude of ongoing neural oscillations in the theta, alpha and beta frequency bands at the frequency of stimulation, suggesting a relationship between these ongoing oscillations and pain perception. Yet, whether these ongoing oscillations are actually related to the pain experience remains unclear. If it were the case, then cognitive processes that are known to affect pain intensity should also affect these ongoing oscillations. To this end, we used electroencephalography (EEG) to investigate whether distraction – an attentional state known to affect pain perception – also modulates the amplitude of these neural oscillations. More specifically, we hypothesized that performing an unrelated arithmetic task during sustained nociceptive stimulation would lead to a decrease in the modulations of ongoing oscillations exerted by the stimulation. To assess the selectivity of this modulation for nociception, we compared the modulations of ongoing oscillations exerted by sustained periodic thermonociceptive and non-nociceptive vibrotactile stimulation (0.2 Hz, 75 s), while participants were either asked to solve an unrelated arithmetic task (distraction task) or received no specific instruction (baseline). The intensity of perception was significantly reduced by the arithmetic task in both the thermonociceptive and the vibrotactile modality, and the sustained periodic stimulation elicited a periodic response at the frequency of stimulation in both modalities. However, the distraction task did not show a differential effect for the two stimulation modalities in any of the frequency bands. The fact that, unlike pain perception, these oscillations did not appear to be affected by the task suggests that they are dissociable from pain perception. Whether a different task (leading to a stronger degree of distraction) could lead to different results is unclear.

1. Introduction

Painful thermonociceptive stimuli have been shown to modulate ongoing EEG oscillations within different frequency bands (Dowman et al., 2008; Huishi Zhang et al., 2016). However, whether these modulations actually reflect pain-specific activity is still debated (Huishi Zhang et al., 2016; Ploner et al., 2017). Ongoing neural oscillations arise from fluctuations of brain activity, which cycle and interact at different frequencies and spatial scales (Buzsáki & Draguhn, 2004). One of the key functions of these oscillations might be to strengthen the connectivity between synchronously oscillating neurons (Akam & Kullmann, 2014; Fries, 2015), thus possibly integrating the sensory, cognitive, and affective components of pain. Moreover, it has been suggested that the oscillatory status of key brain areas could be related to pain perception and therefore pinpoint to a crucial role of ongoing oscillations in the experience of pain (Mayhew et al., 2013; Ohara et al., 2008).

Previous scalp electroencephalography (EEG) (Colon et al., 2017; Guo et al., 2020) and intracerebral EEG (Liberati et al., 2019) studies have shown that sustained periodic thermonociceptive stimuli induce a modulation of ongoing EEG oscillations at the frequency of stimulation. More specifically, Colon et al. (2017) reported that ultra-slow (0.2 Hz) and long-lasting (75 s) periodic thermonociceptive stimulation elicited a consistent periodic phase-locked EEG response at the frequency of stimulation and at its harmonics, as well as a periodic modulation of the amplitudes of theta, alpha, and beta band ongoing oscillations. By recording intracerebral EEG activity from the insula of patients undergoing a presurgical evaluation of focal epilepsy and using the same stimulation parameters, Liberati et al. (2019) observed that sustained periodic thermonociceptive stimulation exerted modulations of theta and alpha ongoing oscillations at the frequency of stimulation, which were predominant in the posterior insula.

Importantly, these modulations were not observed in response to sustained periodic non-nociceptive vibrotactile stimuli, suggesting that they may be preferentially related to nociception and/or to the perception of pain within the insula.

If the modulations of ongoing oscillations exerted by nociceptive stimuli are actually related to pain perception and are relatively close to the end of the chain of neural events leading to this perception, a modulation of the perception intensity, caused for example by a cognitive state change, should be accompanied by a congruent change in the modulation of ongoing oscillations. The effects of top-down modulators on pain perception are well known (Bantick et al., 2002; Miron et al., 1989; Shipp, 2004; Torta et al., 2017), and distraction from the nociceptive input (e.g. by a highly attention-demanding task) has been shown to reduce subjective pain perception in a large number of studies (Eccleston, 1995; Eccleston & Crombez, 1999; Torta et al., 2017; Tracey et al., 2002). A similar decrease in amplitude during distraction was observed for event-related potentials (ERPs) (Beydoun et al., 1993; Boyle et al., 2008; Qiu et al., 2002), but whether non-phase locked responses (i.e. event related ongoing oscillation synchronization or desynchronization) are modulated in a similar way is unclear. Additionally, a slow and sustained stimulation paradigm might control for biases related to stimulus saliency and arousal, which normally interfere with ERPs investigations.

To clarify this, we investigated whether the decrease in pain perception caused by an attention-demanding task concomitant to a sustained periodic thermonociceptive stimulation would be matched by a decrease in the modulation of ongoing oscillations exerted by the stimulation. Furthermore, to probe whether there is a preferential relationship between these oscillation modulations and pain perception, we used both sustained non-nociceptive vibrotactile and sustained nociceptive heat

stimulations and compared the results obtained for both modalities. Based on Eccleston (1995) and Torta et al. (2017), we hypothesized that (1) diverting the attention from both nociceptive and vibrotactile stimulation would lead to a decrease in perceived intensity of stimulation. In parallel, based on previous findings from our group (Colon et al., 2017; Liberati et al., 2019), we hypothesized (2) that both the thermonociceptive and vibrotactile stimuli would elicit a periodic EEG activity at the frequency of stimulation and at its harmonics in the different frequency bands. Moreover, we hypothesized (3) that thermonociceptive stimuli would exert a greater modulation of ongoing oscillations in the alpha, beta and theta frequency bands, at the frequency of stimulation and its harmonics, compared to vibrotactile stimuli. Finally, we hypothesized (4) that the distraction condition would lead to a smaller modulation of ongoing oscillations exerted by thermonociceptive and vibrotactile stimuli, as compared to the baseline condition.

2. Methods

We report how we determined our sample size, all data exclusions, all inclusion/exclusion criteria, whether inclusion/exclusion criteria were established prior to data analysis, all manipulations, and all measures in the study. Since this study was submitted as a Registered Report, all analysis steps were defined prior to data collection. The OSF stage I publication can be found under the following link: https://osf.io/4nbsc. All anonymized study raw data, analysis codes and pre-processing pipelines have been uploaded to the public archive of Harvard Dataverse under the following link: https://doi.org/10.7910/DVN/YNRKQH.

2.1 Participants

25 healthy participants (between 18 and 35 years old) were recruited via an established website and remunerated with 20 € for the duration of the experiment (approximately 2h). A detailed description of the sample size calculation can be found in the Supplementary Materials. One participant had to be removed from the data set due to artifacted EEG signals. The remaining participants (n=24) were 23 ± 3.4 (mean ± sd) years old and 7 participants were male.

Exclusion criteria were established prior to data analysis and included any neurological diseases, psychiatric disorders or any recent trauma of the upper limbs on direct questioning. Additionally, the intake of paracetamol, nonsteroidal anti-inflammatory drugs (NAIDs), or acetylsalicylic acid within 12 hours before the assessment led to the exclusion of the participants. Only right-handed participants were included in the investigation. All participants gave written informed consent prior to the beginning of the assessment and were informed that they could withdraw from the experiment at any given time.

All procedures were performed in accordance with the relevant guidelines and regulations. The local Research Ethics Committee approved all experimental procedures (Commission d'Ethique Hospitalo-Facultaire Saint-Luc UCLouvain, B403201316436).

2.2 Thermonociceptive stimulation

A thermal cutaneous stimulator (TCS II, QST.Lab, Strasbourg, France) with the T03 probe, which is set with 15 micro Peltier elements (each ~7.7 mm^2) whose temperature can vary at rates of up to 300°C/s, was used to deliver sustained periodic thermonociceptive stimuli (0.2 Hz) on the right volar forearm (Mulders et al., 2020) (Figure 1). The stimulation probe weights 440 g and has a flat 30-mm diameter surface. The temperature of stimulation

varied between baseline temperature (35°C) and 50°C in a sinusoidal manner over a duration of 5 s per cycle (Figure 1). It has been shown that periodic thermonociceptive stimulation at 0.2 Hz frequency predominantly activates unmyelinated C-fibers, generating a reliable periodic EEG response with a high signal-to-noise ratio (Colon et al., 2017). Previous investigations have shown more inconsistent and weaker responses using a higher frequency of stimulation (Colon, Nozaradan, et al., 2012). Each sustained periodic stimulation comprised 15 stimulation cycles, lasting at total of 75 seconds per stimulus, as in Liberati et al. (2019) and Mulders et al. (2020). Inter-stimulus-intervals were variable and self-paced by the experimenter to allow participants to provide intensity ratings as well as to give responses to an arithmetic task. The thermode was displaced after each trial to avoid habituation or sensitization.

2.3 Vibrotactile stimulation

Sustained periodic vibrotactile stimuli were delivered via a recoil-type vibrotactile transducer driven by a standard audio amplifier (Haptuator, Tactile Labs Inc., Canada), positioned between the fingertips of the index and the thumb of the dominant hand (Figure 1). The vibrations consisted in a 251 Hz sine wave whose amplitude was periodically modulated at a frequency of 0.2 Hz (15 cycles, each lasting 5 s, for a total of 75 s) (Figure 1). We chose this type of stimulation because, despite being non-nociceptive and non-painful, it is generally perceived as highly intense, which makes it a suitable comparison to investigate whether the observed modulations might be preferential for pain perception.

2.4 Experimental tasks

During the distraction task, participants were asked to solve an arithmetic task unrelated to the stimulation, to distract them from the thermonociceptive stimuli. Starting from a 3-digit number (e.g. 754), they

had to subtract the number 7 continuously and report their final value at the end of the trial (Dowman et al., 2008). Answer accuracy was tracked to ensure compliance. The number from which participants had to subtract changed for each trial. The 20 numbers (10 trials for each modality) were generated prior to data gathering using a random numbers generator within the limits of 100 and 999. The numbers were the same for every participant but randomized in their order of appearance during the experiment. In baseline (as opposed to distraction) condition, participants did not receive any specific instructions.

2.5 Experimental procedure

In this within-subject study design protocol, participants were seated comfortably in a chair, and received thermonociceptive and vibrotactile stimulation on their right (dominant) arm. Before the beginning of the experiment, each participant was exposed to a familiarization trial (i.e. 1 periodic heat stimulation and 1 periodic vibrotactile stimulation) on their non-dominant side. The stimulations for each modality were divided into two different blocks (i.e. distraction task and baseline, see 1.6), with a short break in-between the blocks and modalities. The order of the blocks and modalities was randomized across participants. To mask any noise that could be generated by the haptuator, white noise was delivered to the participants during all stimulation sessions.

Rationale for numbers of trials

The EEG recordings of a recent investigation by Mulders et al. (2020) were examined to assess whether a reduced number of trials (compared to the trial set used in said investigation) would still lead to a measurable modification of ongoing neural oscillations. This specific dataset was chosen because the used stimulation paradigm closely resembled the proposed paradigm. Mulders et al. (2020) also investigated periodic neural

responses and the modulation of ongoing oscillations, elicited by very similar sustained stimuli compared to the proposed paradigm. Additionally, the investigation followed a 2 x 2 design, similar to the modality and condition parameters of the proposed paradigm.

The EEG recordings were analyzed using the Letswave7 (http://www.letswave.org/) toolbox in MATLAB (2020b MathWorks). To find the minimal amount of trials necessary to record a reliable modulation of ongoing neural oscillations, the filtered and averaged trials (following the method of Mulders et al. (2020)) were reduced from originally 12 to 6, 8 and 10 trials respectively. For each scenario, the phase-locked response as well as the modulation in the different frequency bands were analyzed. Phase-locked responses were found for all 3 sub-trials at the frequency of the stimulation (0.2 Hz), using a t-test against 0 ($p<0.0001$). Similar results were found for the different frequency bands modulations (theta: 4-8 Hz, alpha: 8-12 Hz, beta: 12-30 Hz, gamma: 30-50 Hz). These results show that a reduction in trials is feasible without loss in the ability to detect the response of interest. Thus, 10 trials were included in each condition, to reduce the number of trials while keeping a safety margin for the assessment (e.g. in case some epochs would have needed to be discarded in the analysis process due to artifacts).

2.6 Behavioral measures

Participants were instructed to rate the average of the perceived intensity of each stimulus on a visual analog scale (VAS) (using a 10 cm ungraduated sliding ruler) at the end of each trial (i.e. after the full 15 cycles). The left extremity of the VAS was labeled ‘no perception’ and the right extremity was labelled ‘the most intense stimulation you can imagine’. Additionally, after each trial they were asked whether they perceived the stimulus as painful.

2.7 EEG recordings

Electroencephalographic (EEG) activity was recorded using an elastic electrode-cap with 64 active, pre-amplified Ag-AgCl electrodes (BioSemi, Netherlands), arranged according to the international 10-10 system, sampled at 1024 Hz and re-referenced to the average activity recorded from all electrodes. The direct-current offset was kept below 30 mV during electrode placement. Eye movements were recorded using two additional electrodes, one pasted to one of the zygomatic processes and the other between the eyebrows. The BioSemi ActiView software was used to store the recorded signal for offline analyses.

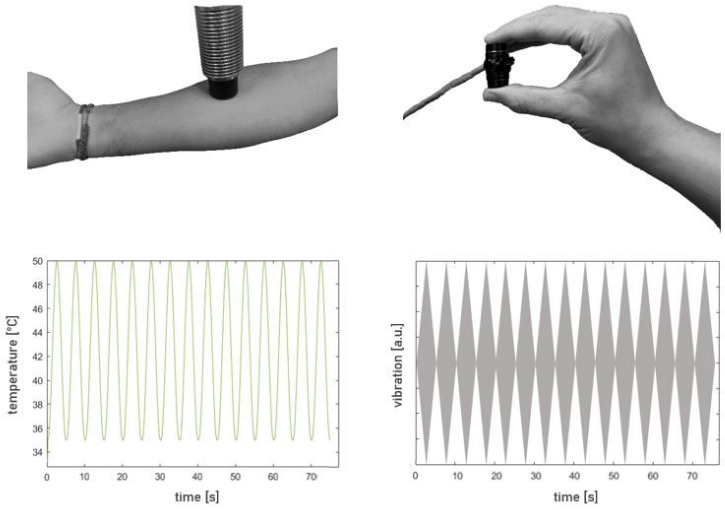

Figure 1: Experimental procedure. Two conditions were applied in two different stimulation modalities (left: thermonociceptive, right: vibrotactile). The stimuli were applied in a sustained periodic manner, at a frequency of 0.2 Hz over a duration of 75 s (i.e. 15 cycles of 5 s) per trial. One representative trial is shown for each modality. 10 trials were applied per condition (i.e. distraction / baseline) and modality. Both modality and condition were randomized across participants. The thermonociceptive stimuli were applied using a thermal cutaneous stimulator (TCS II, QST.Lab, Strasbourg, France), placed on the right volar forearm of the participants. The vibrotactile stimuli were applied using a haptuator (Haptuator, Tactile Labs Inc., Canada), which was held between the fingertips of the index finger and the thumb of the right hand.; a.u., arbitrary amplitude unit.

2.8 EEG analyses

An illustration summarizing the EEG data pre-processing can be found in the supplementary material (Supplementary Figure 1).

2.8.1 Analysis of the phase-locked periodic response

The EEG recordings were analyzed using the Letswave7 (www.letswave.org) toolbox in MATLAB (2020b The MathWorks). To characterize the response to the different stimulation paradigms, a frequency-tagging (Regan, 1989) analysis approach was used. This approach is based on the notion that periodic stimuli elicit a periodic surge in neural activity, leading to a periodic EEG response in the EEG at the frequency of stimulation (Colon, Nozaradan, et al., 2012; Mouraux, Iannetti, et al., 2011). Using the periodicity of the stimulus allows us to differentiate between neural responses related to the applied stimulus and other ongoing activity (Colon, Nozaradan, et al., 2012). A tonic stimulation would not allow to do this as easily.

As in previous investigations performed in our lab (Colon et al., 2014; Colon et al., 2017; Colon, Nozaradan, et al., 2012; Liberati et al., 2019; Mouraux, Iannetti, et al., 2011; Mulders et al., 2020), the assessment of the periodic modulation of the EEG responses was done by obtaining the filtered EEG recordings using a Butterworth high-pass filter (0.05 Hz) to remove slow drift and a 50 Hz notch filter to eliminate power line noise a that frequency. Then, the recordings were segmented into epochs of 0-75s relative to the onset of the stimulation. Artifacts due to eye movements were removed using a validated method based on Independent Component Analysis (Fast ICA algorithm) (Hyvarinen & Oja, 2000).

After pre-processing (including filtering and ocular artefact removal using ICA decomposition), trials with an amplitude change larger than ± 500 µV (Colon et al., 2014) on any of the electrodes were excluded. We defined a

priori that participants with less than 8 remaining trials would be excluded. No participant had to be excluded using this rule.

Then, the segmented waveforms were averaged for each subject and condition. The resulting average waveforms of 75 s were transformed in the frequency domain using a discrete Fourier transform (FFT) (Frigo & Johnson, 1998). Finally, the residual noise was partially removed from the signal amplitude over the entire spectrum by subtracting – at each electrode and at each frequency bin– the average amplitude of the signal measured at 2-5 neighboring frequencies (Mouraux, Iannetti, et al., 2011). The noise-subtracted amplitudes were then used to analyze the EEG data in the frequency domain. The entire electrode set was taken into account. For further analysis, the electrode with the largest amplitude at the frequency of stimulation across conditions was chosen.

2.8.2 Analysis of the modulation of ongoing oscillations

Frequency-tagging of ongoing oscillations (FT-OO) is a novel method to analyze the effect of sustained sinusoidal thermonociceptive stimulation on the modulation of ongoing oscillations assessed by scalp EEG (Colon et al., 2017). This analysis technique allows to isolate neural activity related to the applied stimulus (Colon, Nozaradan, et al., 2012) and has since been successfully used to identify cortical responses to sustained thermonociceptive stimulation generally or in specific frequency bands using scalp EEG (Colon et al., 2014; Colon et al., 2017; Colon, Nozaradan, et al., 2012; Mulders et al., 2020), as well as intracerebral EEG (Liberati et al., 2019).

To assess whether the different conditions would induce a periodic modulation of the amplitude of ongoing neural oscillation within different frequency bands (theta: 4-8 Hz, alpha: 8-12 Hz, and beta: 12-40 Hz), the signal envelopes within these frequency bands had to be estimated. In

order to achieve this, the filtered, segmented and ICA-treated EEG signal described above were additionally filtered using a band-pass 4th order Butterworth filter for each specific frequency band. The estimates of the envelopes of the signal were computed using a Hilbert transform. The next steps correspond to the procedure described above; the envelopes were averaged across trials, and the frequency transforms were computed using a discrete Fourier transform. The entire electrode set was taken into account and for each frequency band, the electrode with the largest amplitude at the frequency of stimulation in the baseline condition was selected for further analysis. The same electrode was used in the distraction condition to have an adequate measure of the change between the conditions.

Electrodes of interest were determined at group level and were likely to vary for the different modalities/frequency bands. Based on previous results, high phase-locked activity was expected in regions of interest such as central-parietal regions (contralateral to stimulated side) for vibrotactile stimulation, e.g. C3 (Colon et al., 2014) and central electrodes for thermonociceptive stimulation, e.g. Cz/ FCz / CPz (Colon et al., 2014; Colon et al., 2017; Mulders et al., 2020). Non-phase locked responses were expected to be located primarily in the central-parietal regions contralateral to the stimulated side for the alpha and beta frequency bands and more centrally for the theta band (Colon et al., 2017; Mulders et al., 2020)).

Potential differences induced by distraction were considered as well. It has been suggested that cortical interactions between the posterior medial frontal cortex (pMFC) and the lateral prefrontal cortex (LPFC) facilitate cognitive control (Ridderinkhof et al., 2004). Specifically, theta phase synchronization between pMFC and LPFC has been linked to the communication between cognitive monitoring and attention-related

brain network, while alpha phase synchronization seems to relay this information to more posterior (sensorimotor) areas (Clayton et al., 2015). Yet, we did not believe that the proposed frequency-tagging approach would be able to capture these responses in higher order regions, since the distraction task is intrinsically non-periodical.

2.9 Statistical analysis

Statistical analyses were done using R Statistical Software (Version 4.1.0, R Core Team 2021) and MATLAB (2020b The MathWorks). The significance level for the behavioral analysis and LMMs was set at $p<0.05$. The LMM was fitted using REML and the significance of the results was tested using a Kenward-Roger approximation, which has been shown to produce adequate type 1 error rates also for smaller sample sizes (Luke, 2017). In case of a non-normal distribution of the data set, a log-transform was applied to the EEG data (i.e. amplitudes at the frequency of interest (FOI, aggregated harmonics at the frequency of stimulation and its harmonics)) to conform the data to the assumption of normality. This is a frequently used linear transformation, aiming at transforming right-skewed data into a more normal (gaussian) form (Bland & Altman, 1996; Healy, 1993). The log transformed values were used in each of the LMM's, since a non-normal distribution was found for all EEG data. The original amplitude values were used to display meaningful amplitudes in the figures.

2.9.1 Behavioral data

To test for differences in task performance during thermonociceptive and vibrotactile stimulation, a paired t-test was used. Potential differences in performance between gender were assessed with a Welch Two Sample t-test for each modality.

To validate hypothesis (1), we assessed the effect of condition and modality (independent variables (IV)) on perceived stimulus intensity (dependent

variable (DV)), by using a linear mixed model (LMM). The factors “condition” (two levels: baseline, distraction) and “modality” (two levels: thermonociceptive, vibrotactile) were included as fixed effects and “subject” as a random effect accounting for the variation of the regression model intercept across participants.

Intensity rating ~ condition + modality + modality:condition + (1|subject)

We expected the intensity rating to be lower for the distraction condition compared to the baseline condition for both stimulation modalities. If this had not been the case, we would have concluded that the task failed to distract the participants.

2.9.2 Phase-locked response

To investigate hypothesis (2), non-parametrical statistical tests were applied to assess (for each condition / modality combination) whether the magnitude of the aggregated amplitudes at the frequency of interest was significantly larger than zero. Aggregation was done by summing up the amplitudes of the signal at the frequency of stimulation and its first 199 harmonics. This specific number was chosen since it includes all the harmonics up to the frequency of 40 Hz, which is the highest frequency analyzed in this investigation. A right tailed multi-sensor cluster-based permutation test using Wilcoxon signed-rank test as statistic was used to evaluate the periodic response against zero, allowing for non-normality of the dataset and controlling type 1 error rate inflation due to the multiple testing (the median being compared to 0 at each of the 64 channels). To account for multiple testing, a Bonferroni correction was applied to the Wilcoxon signed-rank test, reducing the significance level to 0.0125 by dividing alpha by the number of modality/condition pairs. The threshold of the cluster-based permutation was also set to 0.0125, and 2000 permutations of the dataset were computed. The multi-sensor analysis

was set so that each channel has 4 neighbors on average (equals a threshold of 0.161).

Based on the findings of Colon et al. (2017); Mulders et al. (2020) and Liberati et al. (2019), we expected that the amplitude of the EEG signal at the frequency of stimulation would have been significantly greater than zero for both modalities. If we would not have found a periodic modulation of the EEG signal, then the basic assumption of this investigation that sustained periodic stimuli lead to a periodic modulation of the EEG signal at the frequency of stimulation would not be met and hence the data would not be useful for analysis.

To investigate hypothesis (4), we analyzed the periodic response of the obtained noise-subtracted aggregated signal amplitudes (DV), using an LMM analysis; with 2 factors for "modality" (thermonociceptive, vibrotactile) and for "condition" (baseline, distraction) as fixed factors (IV). "Subject" was added as a random factor, to account for the variation of the regression model intercept across participants.

amplitude ~ condition + modality + modality:condition + (1|subject)

We expected to see a similar periodic response for both modalities. We further expected a smaller response for distraction condition than for baseline condition.

2.9.3 Modulation of ongoing oscillations

To assess whether there was a significant periodic modulation of ongoing oscillations in the different frequency bands at the frequency of stimulation (hypothesis 2), the aggregation procedure and statistical test described in the previous section were also applied to the frequency spectrum of the theta, alpha and beta band envelopes. We expected that the amplitude of the EEG signal at the frequency of stimulation would be

modulated for both the thermonociceptive modality and the vibrotactile modality in all frequency bands (Colon et al., 2017; Liberati et al., 2019).

To investigate hypotheses (3) and (4), we assessed the effect of the different modalities and conditions on the modulation of ongoing oscillations in the different frequency bands (DV), by using an LMM; with 2 factors for “modality” (thermonociceptive, vibrotactile) and “condition” (baseline, distraction) as fixed factors (IV). “Subject” was added as a random factor, to account for the variation of the regression model intercept across participants.

For each frequency band of interest (theta, alpha and beta) there was a separate model to account for differences in electrode activation between the frequency bands and to ensure sufficient statistical power.

amp_mod_theta ~ modality + condition + modality:condition + (1|subject)

amp_mod_alpha ~ modality + condition + modality:condition + (1|subject)

amp_mod_beta ~ modality + condition + modality:condition + (1|subject)

Consistently with the findings of (Liberati et al., 2019), we expected a significantly greater modulation in the alpha and theta frequencies exerted by sustained thermonociceptive stimulation compared to vibrotactile stimulation. Furthermore, we expected a greater modulation at the frequency of stimulation for the beta frequency in the thermonociceptive modality (Colon et al., 2017).Moreover, we expected that, for both modalities, the distraction task would lead to a smaller amplitude at the frequency of stimulation compared to baseline.

2.9.4 Outliers

Subjects who failed to complete the experiment would have been excluded from the analysis. However, all participants were able to complete the experiment.

Artifacts due to blinking or eye movements were removed according to the procedure described in 2.9.1. Outliers in the extracted data were assessed using the least-squares method. Therefore, data points that were over 3 standardized residuals away from 0 were removed after fitting the LMM if they violated assumptions (linearity, normality) or influenced the results disproportionally. These data points (participants) were not replaced. The assumption of normality was assessed both visually by QQ-plot as well as using a Shapiro Wilkinson test for a quantitative result. Additionally, the influence of data points identified as potential outliers on the data set was tested using Cook's Distance [D], which is a measure of how much all the fitted values change if one data point is being removed from the data set. The larger the calculated D, the more influential the data point (Cook, 1977). Data points with a D larger than 1 were considered influential and were removed from the data set.

3. Results

3.1 Behavioral response

3.1.1 Task performance

One participant had to be removed from the data set due to an artifact. The median of correct answers during thermonociceptive stimulation was 6 ± 2.25 (median ± interquartile range), while 6 ± 2.25 were correct during vibrotactile stimulation. An illustration of the task performance can be found in the supplementary materials (Supplementary Figure 2).

There was no difference between the modalities or conditions for task performance ($t(23)=-0.569$, $p=0.575$). Despite our best efforts, we were unable to recruit a gender-balanced sample size. Nevertheless, no differences in performance were found based on gender

(thermonociceptive: t(10.475)=-0.672, p=0.516; vibrotactile: t(7.917)=-0.790, p=0.453).

3.1.2 Intensity perception

Participants never perceived the vibrotactile stimuli as painful, while they rated the thermonociceptive stimuli as painful in 70.42% of the baseline condition trials and 57.08% of the trials during the arithmetic task. Ratings of perceived intensity of stimulation for thermonociceptive and vibrotactile stimuli differed significantly (main effect of modality: $F(933,1) = 533.004$, $p < 0.001$). The distraction task led to significantly lower pain ratings in both modalities compared to baseline (Figure 2) (main effect of condition: $F(933,1) = 36.153$, $p<0.001$). A significant effect of interaction between condition and modality was observed, showing that the distraction task led to a stronger reduction in perceived stimulation intensity during vibrotactile stimulation than thermonociceptive stimulation (main effect of interaction: $F(933,1) = 10.114$, $p=0.002$; pairwise comparison, *vibrotactile baseline vs distraction* $p<0.001$, *thermonociceptive baseline vs distraction* $p=0.046$).

3.2 EEG recordings

One participant had to be excluded from the data set because the EEG recordings were contaminated by artifacts. Figures displaying the spectra for each frequency band and condition/modality can be found in the Supplementary Materials (Supplementary Figure 5).

3.2.1 Phase-locked response

A periodic modulation of the EEG signal at the frequency of simulation and its harmonics was recorded in both stimulation modalities and in both conditions. The electrode with the highest Wilcoxon test statistic (W) across conditions for thermonociceptive stimulation was FC2 (W= 4.243).

Pz was the electrode with the largest Wilcoxon test statistic at the FOI for vibrotactile stimulation (W=4.271) (Figure 3).

A significant difference was found between the thermonociceptive and vibrotactile stimulation for the comparison of electrodes FC2 and Pz. The vibrotactile stimuli led to an overall larger modulation at the FOI compared to thermonociceptive stimulation. No differences were found between the conditions (Figure 4, Table 1).

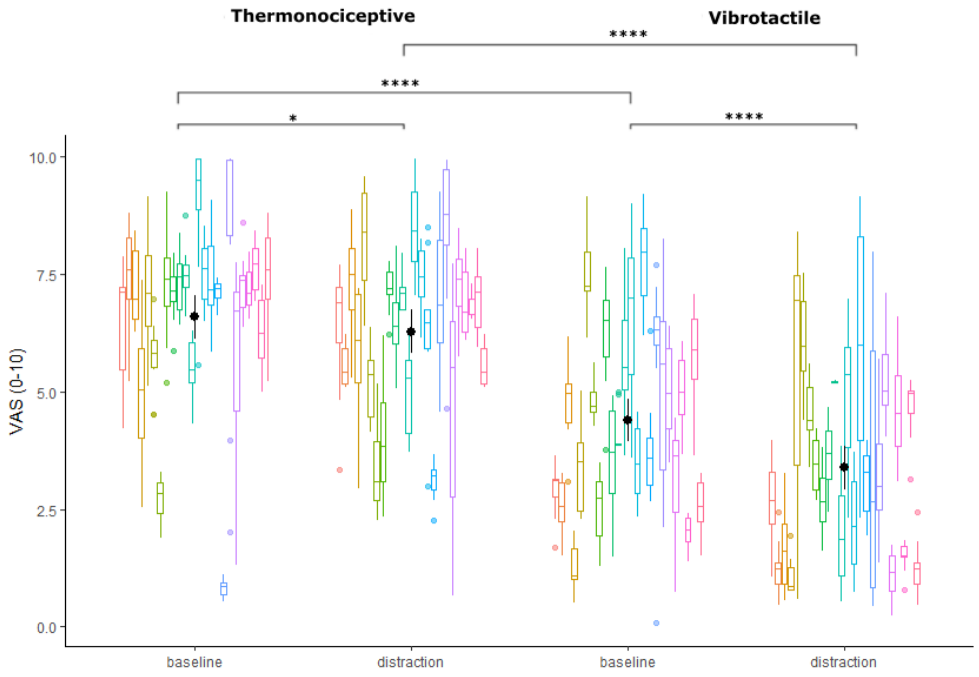

Figure 2: Rating of perceived intensity on a Visual Analog Scale (VAS) for both modalities and conditions. Ratings were collected at the end of each trial. Each color indicates a subject. The black dot represents the model group mean and the vertical lines represent the model .95 confidence interval for each group. The results of the linear mixed model (rating ~ modality + condition + modality : condition + (1|subject)) are represented: p<0.05: *, p<0.0001: ****.

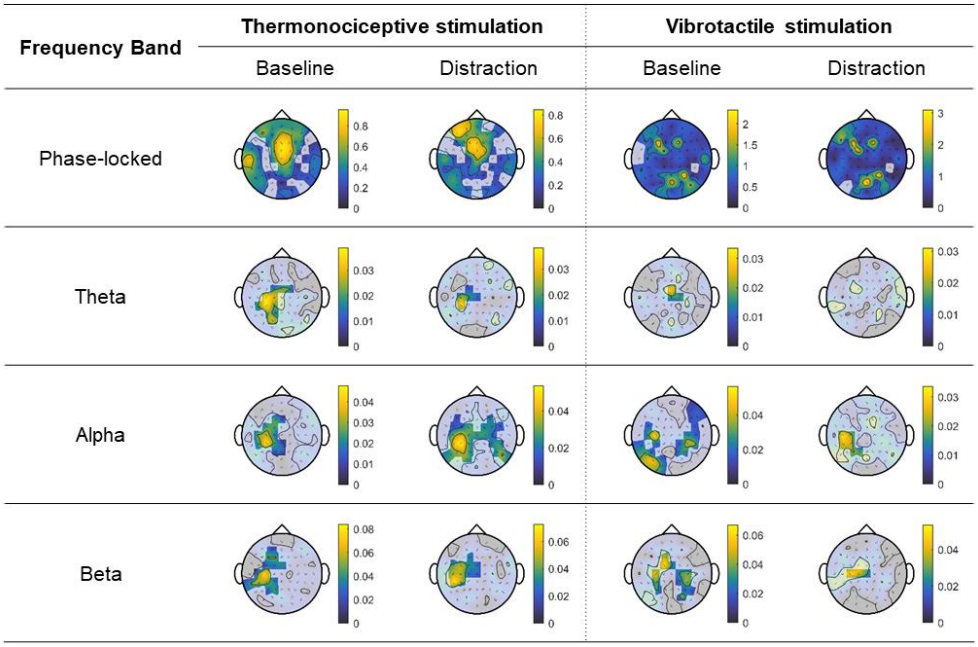

Figure 3: Group-level median topographies of electrode activity at the frequency of interest [µV]. Shaded areas correspond to electrodes which did not show periodic activity at the frequency of stimulation (based on multi-sensor cluster-based permutation Wilcoxon one-sample t-tests).

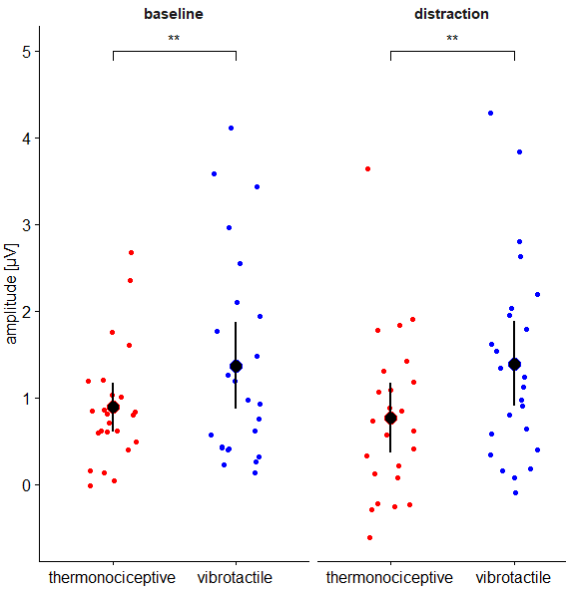

Figure 4: Amplitudes of the aggregated harmonics at the FOI of the respective electrode of interest for the phase-locked response. Electrodes of interest: FC2 for thermonociceptive stimuli, Pz for vibrotactile stimuli. baseline = no task, distraction = arithmetic task during stimulation. Each colored point represents one subject, while the black point represents the mean and the 95% confidence interval for this group. LMM: **: p<0.01.

	Electrode (t, v)	Modality		Condition		Modality : Condition	
		F-value (df)	*p-value*	*F-value (df)*	*p-value*	*F-value (df)*	*p-value*
Phase-locked	FC2, Pz	7.71 (69,1)	**0.007**	0.6144 (69,1)	0.436	0.808 (69,1)	0.372
Theta	C3, C2	4.799 (69,1)	**0.032**	2.048 (69,1)	0.157	0.063 (69,1)	0.802
Alpha	C3, CP4	11.814 (69,1)	**0.001**	0.985 (69,1)	0.324	1.739 (69,1)	0.192
Beta	CP3, F1	12.207 (69,1)	**<0.001**	1.665 (69,1)	0.201	0.389 (69,1)	0.535

Table 1: Result of the LMM following the formula amplitude ~ modality * condition + (1|subject). A Kenward-Roger approximation was used for the significance levels. t = electrode with highest activity identified for thermonociceptive stimulation, v = electrode with highest activity identified for vibrotactile stimulation; df= degrees of freedom.

3.2.2 Modulation of ongoing oscillations

The topographic distribution of the median periodic modulation of EEG at the frequency of interest and of the multi-sensor cluster-based permutation right-tailed Wilcoxon signed-rank test can be seen in Figure 3 for all tested frequency bands. In the theta frequency band, the aggregated harmonics showed a periodic modulation at the FOI larger than zero for both modalities. The electrode with the highest test statistic was C3 (W = 3.44) for thermonociceptive stimulation and C2 (W=2.73) for vibrotactile stimulation. No periodic response was detected for vibrotactile stimulation during the arithmetic task. In the alpha frequency band, the electrode of interest was identified as C3 for thermonociceptive (W = 4.014) and CP4 for vibrotactile stimulation (W = 3.786). A periodic response significantly larger than zero was found for both conditions in both modalities. CP3 was the electrode with the highest activity across the aggregated harmonics for thermonociceptive (W = 4.043) and F1 for

vibrotactile stimulation (W = 3.84) in the beta frequency band. A significant periodic response was found for all conditions and modalities.The LMM showed a significant difference in amplitude of the aggregated harmonics at the FOI between the modalities for the theta, alpha and beta frequency band (Figure 5, Table 1). No differences were detected between baseline condition and the arithmetic task in any of the tested frequency bands (Table 1).

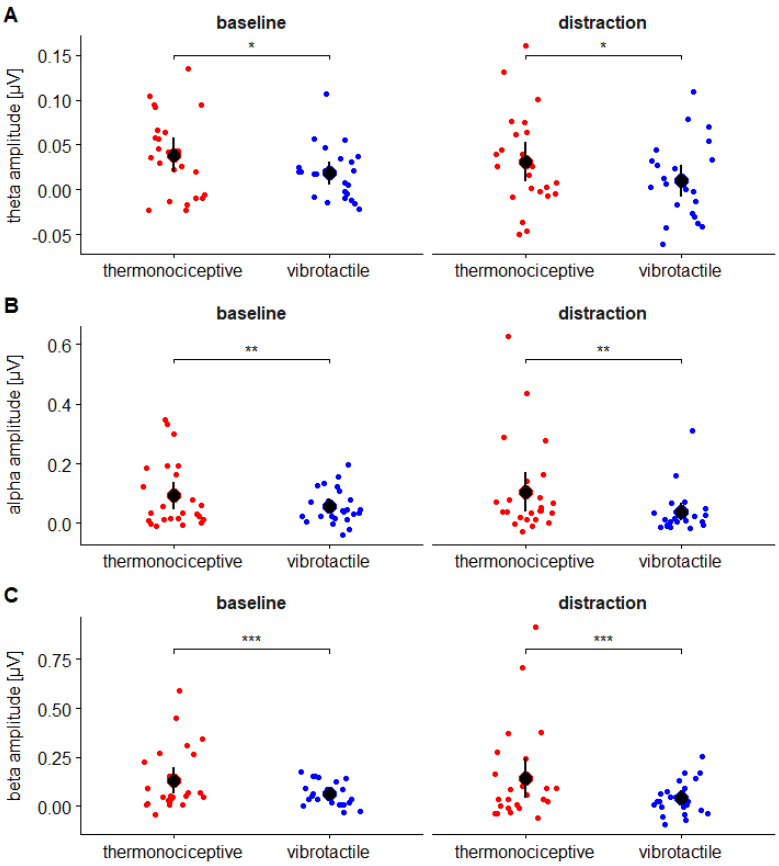

Figure 5: Amplitudes of the aggregated harmonics at the FOI for the respective electrode of interest of each frequency band. A: theta frequency band (4-8 Hz), comparing electrode C3 (thermonociceptive) and C2 (vibrotactile). B: alpha frequency band (8-12Hz), comparing electrodes C3 and CP4. C: beta frequency band (12-40 Hz), comparing electrodes CP3 and F1. baseline = no task, distraction = arithmetic task during stimulation. Each colored point represents one subject, while the black point represents the mean and the 95% confidence interval for this group. LMM: *: p<0.05, **: p<0.01, ***: p<0.001

3.3 Exploratory Analyses

3.3.1 Additional Linear Mixed Models

As the electrodes selected according to the pre-registered methods differed significantly between modalities and as this may lead to comparison of qualitatively different EEG activity for both modalities, we also fitted LMM's using the thermonociceptive baseline electrode with highest activity as electrode of interest for both modalities. These electrodes correspond to the regions of interest which were pre-defined in the stage 1 submission of this registered report. The results of this exploratory analysis also showed a significant difference between the modalities for all tested electrodes, but no effect of condition in any of them (Table 2). One subject had to be removed from the phase-locked analysis as their value was detected as outlier.

Frequency band	Statistical test	Electrode	Difference modalities	Difference conditions
Phase-locked	*Wilcox*	FC2		
	LMM		F(66,1) = 6.501; **p=0.013**	F(66,1) = 0.032; p= 0.860
Theta	*Wilcox*	C3		
	LMM		F(69,1)=5.553; **p=0.021**	F(69,1)=0.495; p=0.484
Alpha	*Wilcox*	C3		
	LMM		F(69,1) = 11.573; **p=0.001**	F(69,1) = 0.512; p=0.477
Beta	*Wilcox*	CP3		
	LMM		F(69,1) = 13.176 ; **p<0.001**	F(69,1)=3.2328; p=0.077

Table 2: Exploratory analysis. Results of the LMM following the formula amplitude ~ modality * condition + (1|subject), for electrodes that corresponded to the pre-selected regions of interest as well as the thermonociceptive baseline results of the Wilcoxon signed-rank test.

3.3.2 Post-hoc power analysis

To investigate whether the failure to show any difference between the conditions in the LMM could be explained by a lack of statistical power, we used the same computational model that was initially used to calculate the sample size based on previous studies ($\alpha = 0.02$) but, this time, using the data of our experiment. Figures illustrating the relationship between power and sample size based on the computational model can be found in the supplementary materials (Supplementary Figure 3). We found that to observe an effect on the phase-locked response, sufficient power ($p>0.9$) could be reached after 10 subjects for the factor modality. In contrast, the power for the factor condition did not change depending on the number of subjects, staying lower than 0.05. Similar results were observed for the different frequency bands, of which only the beta band showed a power level that rose steadily with the number of participants. Nevertheless, more than 400 participants would be necessary to reach a power level of 0.9 for the factor condition in the beta frequency band. Similarly, the power for the interaction between condition and modality would not reach sufficient power until more than 100 participants would be recruited for the phase-locked response. Even though steadily increasing with the number of participants, sufficient power in the theta and beta frequency bands for the interaction effect would have merely been reached after recruiting approximately 400 participants. Only the alpha band had a marginally higher effect and would have needed 200 participants for sufficient statistical power. This suggest that the attention modulation intervention we used leads to inexistent or extremely weak effects which are difficult to capture with our response of interest.

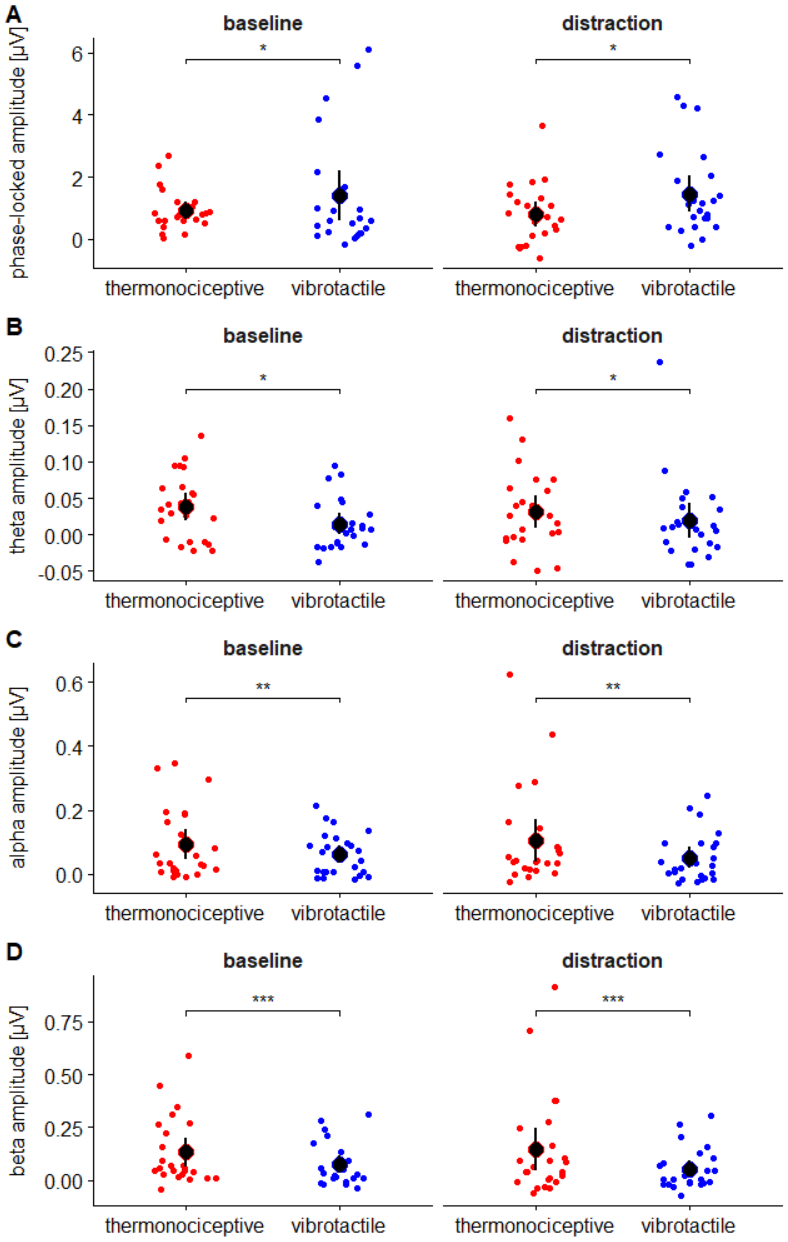

Figure 6: Exploratory analysis. Amplitudes of the aggregated harmonics at the FOI for the respective electrode of interest of each frequency band. A: phase-locked response, electrode FC2. B: theta frequency band (4-8 Hz), electrode C3. C: alpha frequency band (8-12Hz), electrode C3. D: beta frequency band (12-40 Hz), electrode CP3. baseline = no task, distraction = arithmetic task during stimulation. Each colored point represents one subject, while the black point represents the mean and the 95% confidence interval for this group. LMM: *: p<0.05, **: p<0.01, ***: p<0.001

4. Discussion

Regardless of modality, stimuli delivered during the arithmetic task were rated lower than those delivered during the baseline condition blocks. These results confirm our expectations on the effect of the arithmetic task (hypothesis 1) and establish that the positive control for the factor *condition* was met. Interestingly, differences across modalities could be observed, *i.e.* a smaller effect of the arithmetic task on thermonociceptive stimulation ratings compared to vibrotactile stimulation ratings, potentially reflecting differences in the ability of the two modalities to capture attention. Additionally, thermonociceptive stimulation was perceived as significantly more intense than vibrotactile stimulation, regardless of the condition.

A periodic phase-locked response as well as a periodic modulation of oscillatory activity in all frequency bands was elicited by both stimuli, establishing that the positive control for *modality* was met. The LMMs did not show an effect of the arithmetic task on any of the investigated EEG responses for any of the stimulation modalities. It thus appears that both the phase-locked response and the ongoing oscillations amplitude modulation can be dissociated from the intensity of perception. These results diverge from our main hypothesis that the arithmetic task would lead to a reduction of the ongoing oscillation amplitude modulation by the stimuli which would mirror the reduction of the intensity ratings.

Following the procedure in the stage 1 submission of this registered report, we compared electrodes showing the strongest activation for each modality / frequency band combination. This led to comparing signals recorded from different regions that likely corresponded to the activation of (at least partially) different brain generators, making it more difficult to interpret the results. Thus, we decided to add an exploratory analysis, in

which we compared the neural activity at the same electrode for both stimulation modalities. Interestingly, this approach did not change the results, as the same effects were found for the exploratory analyses as in the original analysis.

There are multiple possible explanations for our findings. First, it could be that there is truly no effect of distraction (i.e. diverting attention) on ongoing neural oscillations modulation by thermal and vibrotactile stimuli because they do not reflect processing of these stimuli. Second, ongoing oscillations modulation could be involved in the perception of these stimuli, but at a stage of processing preceding that at which distraction acts. Both these explanations are in conflict with previous evidence that pain-related alpha suppression indexes stimulus intensity / sensation magnitude (Nickel et al., 2022) and is minimized during a distraction task (compared to attention on pain and baseline condition) (Peng et al., 2014). Of note, Schulz et al. (2015) did also not find a relationship between alpha activity and the perception of pain during the application of tonic thermonociceptive stimuli. Finally, it could be that, even though there was an effect of the arithmetic task, its size was too small for it to be picked up by our statistical tests. If we postulate the existence of an effect, based on Peng et al. (2014), our inability to detect it could be related to the specific implementation of the arithmetic task used in this experiment not leading to a large enough effect size, the specific EEG read-outs used in this experiment being too variable (regardless of intervention) to allow detection of small effect sizes, or both.

Importantly, despite promising results in the previously conducted pilot study (detailed in the supplementary materials, Supplementary Figure 4), the arithmetic task led to much smaller thermal stimuli intensity rating changes than expected. Post-hoc power calculations revealed that the effect of the task (i.e. factor *condition*) on these ratings was indeed

extremely small and that a much larger (and unreasonable) sample size would have been necessary to achieve the target statistical power (.9). For most of the EEG signal comparisons, the power level did not even change with increasing sample sizes, indicating that, in our data, the effect of this factor, if existent, is too small to be distinguished from the spontaneous variability of the signal. It is unclear whether a different task (inducing a higher cognitive load / larger effect of distraction) would lead to different results. The results of Peng et al. (2014) seem to suggest it could, despite the fact that their task (counting backwards every 3 seconds from a randomly chosen 4-digit number, for a duration of 5 minutes) was not that different from ours. Similarly, Schulz et al. (2019) found a strong effect of the same counting task as used in the present study on a behavioral level as well as in brain activity measured using fMRI. Yet, it should be considered that the stimuli used in this investigation substantially differ from ours both in duration as well as in stimulus type. Moreover, effects on fMRI signal do not necessarily equate effects measurable in EEG recordings.

Notably, the effect of the arithmetic task was not the same for the two stimulation modalities. While it had a significant but moderate effect on the perception of the thermonociceptive stimuli, the task was much more effective in reducing perception intensity during vibrotactile stimulation. One possible reason for this difference is the intrinsic saliency (i.e., the ability of a stimulus to capture attention) (Yantis, 2008) of painful stimuli. Pain is generally considered to be an alarm signal which alerts us of a potentially harmful event and is therefore a sensation towards which the human brain will always allocate attention (Eccleston & Crombez, 1999). Therefore, vibrotactile and painful stimuli eliciting similar perception magnitude could still be expected to have different saliencies, that of the painful stimulus outweighing that of the vibrotactile stimulus. This

difference in saliency could then lead to differences in the way the perceived intensity of a stimulus is modulated by distraction, painful stimuli being more resistant to it than vibrotactile stimuli. Alternatively, this difference in the effects of the arithmetic task could be related to the absolute magnitude of the perception elicited by the stimuli: stimuli which are perceived more strongly in the baseline condition could be more resistant to distraction, as their absolute magnitude is, in itself, more attention-grabbing. Since the thermal stimuli were rated as significantly more intense than the vibrotactile stimuli, regardless of the condition, it is not possible to differentiate these two possible explanations. This confound also precludes interpretation of the cross-modality difference in the amplitude of oscillatory activity in the various frequency bands investigated in this study. To disentangle the effect of saliency on the modulation of ongoing oscillations, future investigations should be conducted, modulating the saliency of one stimulation modality (e.g., introducing an oddball within the sustained periodic stimulation) and assessing its effect on the modulation of ongoing neural oscillations.

Whereas the phase-locked response evoked by thermal stimulation matched the topography previously observed by others(Colon et al., 2017; Mulders et al., 2020), the phase-locked response to vibrotactile stimuli were less lateralized than expected (Colon, Legrain, et al., 2012; Colon et al., 2014) and instead were rather widespread over the scalp. This discrepancy could stem from the significantly lower stimulation frequency used in this experiment, compared to previous frequency tagging experiments investigating vibrotaction (e.g. 6 Hz and 13 Hz in Colon, Legrain, et al. (2012)).

Liberati et al. (2019) observed that, whereas sustained periodic thermonociceptive stimuli led to a periodic modulation of theta band activity in the insular cortex (using intracerebral EEG), sustained periodic vibrotactile stimuli did not. In the present study, vibrotactile stimuli elicited

a periodic modulation of theta frequency band activity, suggesting that the apparent selectivity of this frequency band for thermonociceptive stimuli in the insula does not generalize to scalp EEG. The observation that vibrotactile stimuli can lead to modulation of scalp EEG theta band activity is also supported by another study from our group (Courtin & Mouraux, 2024 Preprint).

5. Conclusion

The magnitude of the modulation of neural oscillations at the frequency of interest did not differ between the baseline condition and the distraction condition for any of the frequency bands, suggesting that the arithmetic task, which decreased intensity of perception, did not affect the amplitude of the ongoing oscillations modulation by the sensory stimuli. Therefore, subjective intensity of perception and the modulation of pain-related ongoing oscillation measured by scalp EEG appear to be dissociable. These findings, however, should be interpreted with caution. Although the arithmetic task significantly reduced the subjective intensity of perception during the stimulation for both the thermonociceptive and the vibrotactile modalities, the effect was smaller than predicted based on our pilot study. Hence, it cannot be excluded that a task with a stronger distraction effect would lead to effects that could not be captured in the present study.

Significant differences were found in the modulation of ongoing oscillations between thermonociceptive and vibrotactile stimulation. To clarify whether the observed modality differences are mainly an effect of the stimulus saliency or truly a preferential modulation exerted by thermonociceptive stimuli, further investigations should address the effect of stimulus saliency on the periodic modulation of the ongoing oscillations.

Question	Hypothesis	Sampling plan	Analysis plan	Interpretation given different outcomes
Behavioral response				
(1) Does distraction change the level of perceived stimulus intensity during nociceptive stimulation?	Diverting attention from the nociceptive stimulation will lead to a decrease in stimulus intensity perception rating.	See below	LMM: intensity rating ~ modality + condition + modality:condition + (1|subject) DV: *intensity rating* IV: *condition, modality* random coefficient: *subject*	Positive control: If the ratings for perceived intensity are lower during distraction, the arithmetic task has achieved its purpose. If not, we fail to meet the positive control for the task efficacy (i.e. condition).
Time locked, phase locked response				
(2) Does ultra-slow sustained periodic stimulation using different modalities elicit a periodic neural response?	Both thermonociceptive stimuli and vibrotactile stimuli will elicit an increase of EEG power at the frequency of stimulation and at its harmonics.	To reach a statistical power of 0.9 with an alpha of 0.02, 25 participants will be enrolled. Calculations are based on power simulations using the *simr* package in R (Liberati et al., 2019).	Multi-sensor cluster-based permutation Wilcoxon signed-rank test of aggregated and averaged amplitudes at FOIs.	Positive control: A periodic response shows that the stimulation paradigm induces the expected neural activity. If this is not the case, the basic assumption for this investigation is not met.
(4) Does distraction change the modulation of ongoing oscillations in the frequency domain?	Diverting attention from nociceptive stimulation will lead to a smaller modulation of ongoing oscillations as compared to baseline condition.	See above	LMM: amp ~ modality + condition+ modality:condition + (1|subject) DV: *amplitude* IV: *condition, modality* random coefficient: *subject*	A change in modulation of oscillations induced by distraction which corresponds to the change in intensity rating would indicate a connection between perceived pain and ongoing oscillations. A modulation which does not correspond to the intensity ratings would indicate that the processing of perceived pain and oscillations are probably not correlated.

Time locked, non-phase locked response				
(2) Does ultra-slow sustained periodic stimulation using different modalities elicit a periodic neural response in the different frequency bands?	Both modalities will induce a periodic response in the different frequency bands.	See above	Cluster-based permutation and Wilcoxon signed-rank test of aggregated and averaged amplitudes at FOIs in the different frequency bands†.	A modulation at the frequency of stimulation indicates that sustained periodic stimulation leads to a periodic response also in the different frequency bands (Liberati et al., 2019). If the modalities differ from each other, it indicates that thermo-nociceptive stimuli might be processed functionally different than vibrotactile stimuli (based on Dowman et al. (2008).
(3) Does ultra-slow sustained periodic thermonociceptive stimulation differentially affect ongoing oscillations compared to vibrotactile stimulation?	Thermonociceptive stimuli will exert a greater modulation of ongoing oscillations in the alpha, beta and theta frequency bands, at the frequency of stimulation, compared to vibrotactile stimuli.	See above	LMM: amp_mod_frequency_band† ~ modality + condition + modality:condition + (1|subject) DV: *amplitude* IV: condition, *modality* random coefficient: *subject*	A modulation specifically in the alpha and theta frequency band would show that the results of Eccleston and Crombez (1999) are generalizable for scalp EEG (non-insula specific). No difference would indicate that the differential modulation is selective for the insula.
(4) Does distraction change the modulation of ongoing oscillations in the time-frequency domain?	Diverting attention from nociceptive stimulation will lead to a smaller modulation of ongoing oscillations, as compared to baseline.	See above	LMM: amp_mod_frequency_band† ~ modality + condition + modality:condition + (1|subject) DV: *amplitude* IV: *condition, modality* random coefficient: *subject*	A change in modulation of oscillations induced by distraction which corresponds to the change in intensity rating would indicate a connection between perceived pain and ongoing oscillations (in the specific frequency bands). A modulation which does not relate to the intensity ratings would indicate that the processing of perceived pain and oscillations might happen independently from each other.

FOI: frequency of interest; DV: dependent variable; IV: independent variable; LMM: linear mixed model; amp: amplitude of phase-locked neural response; amp_mod_frequency_band: amplitude of non-phase locked neural response for each frequency band (theta, alpha, beta). † One model for each frequency band (theta, alpha, beta)

Table S.1: Hypotheses table defined prior to data collection, detailing hypotheses, analysis plans and interpretations given different outcomes.

I. Sample size rationale

15-20 healthy participants have been shown to be a sufficient number to observe the modulations of neural oscillations exerted using sustained periodic nociceptive stimulation (Colon et al., 2017; Mulders et al., 2020). Importantly, ultra-slow sustained periodic stimulations (i.e., 0.2 Hz) have been shown to elicit responses with a very high signal-to-noise ratio, that can be shown to be significantly different from noise even at individual level (Colon et al., 2017).

All following calculations were done in in R Statistical Software (Version 4.1.0, R Core Team 2021). Power and sample size estimations were conducted using the R package "simr" (Green et al., 2016), which uses simulation to estimate the required sample size to reach sufficient statistical power to detect a specific effect in a linear mixed model (LMM).

To use this method, user-supplied values of intercept, slope, residual variance and random intercept are necessary. The way the input values were selected is described in the following paragraphs. Intercept and slope for modality were based on the time-locked phase-locked EEG data of Mulders et al. (2020), as well as the residual variance. This investigation was chosen because it implemented a similar two by two design using sustained periodic stimulation at 0.2 Hz with the same device as planned in our study design. Noxious heat and innocuous cold stimuli were compared, as well as variable and fixed stimulation surfaces for the thermode and the temperature conditions. Additionally, we expected a similar difference between noxious heat stimuli and vibrotactile stimulation as they observed for noxious heat and innocuous cold stimuli, making it a useful estimate for modality. Furthermore, data was analyzed for phase-locked responses. This data was used for the simulated LMM in a regression model following the syntax: amplitude ~ modality+ location +

modality:location, which closely resembles the one used in this investigation.

The slope for condition was based on Wierda et al. (2010), an ERP study which was chosen to highlight the effect of distraction on EEG responses. The study investigated the Attentional Blink (AB) phenomenon under different circumstances: baseline, control condition and distraction condition. This publication was selected because an LMM was used to investigate the effect of distraction on EEG signal amplitude. The output of this LMM which examined the EEG signal amplitude change in relation to distraction and control condition was used here to estimate the effect of distraction on the slope of the simulated LMM for the power calculation. The intercept of the LMM presented in this investigation was similar to the one from Mulders et al. (2020). Finally, the slope for the interaction between modality and condition was estimated based on the slopes of the main effects.

Therefore, the following LMM and parameters were used in the stimulation:

Equation: y ~ modality + condition + modality:condition + (1|id)

intercept and slopes: 0.296, 0.2,-0.7,-0.14

random intercepts for participants: 0.01

residual variance: 0.09349.

The power to detect a significant interaction effect between modality and condition was tested for different sample sizes. We tested specifically for the interaction term and not the fixed effects since interaction terms are our comparison of interest and usually have a lower effect size and are therefore the most critical for power calculation. The effect of the specified interaction was examined using a Kenward-Roger test. According to this

simulation, enrolling 23 participants would suffice to reach a statistical power of 0.9 with an alpha level of 0.02. As there was a risk that the data of 1 or 2 participant would have to be excluded, 25 participants were recruited to ensure reaching the desired power and significance levels.

II. Task performance

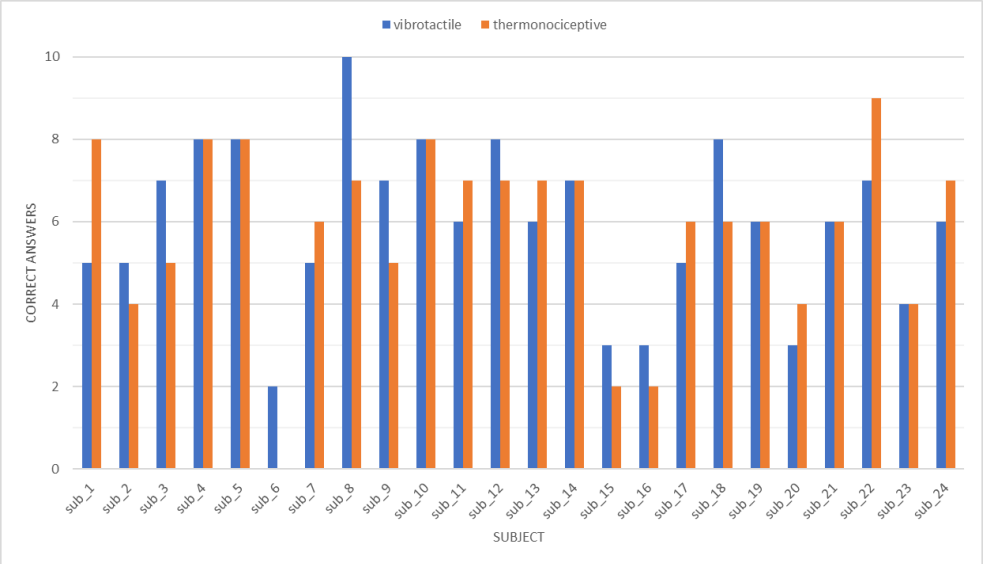

Supplementary Figure S.2: Arithmetic task performance during thermonociceptive (orange) and vibrotactile (blue) stimulation. For each modality, 10 correct answers could be reached. The task consisted of subtracting 7 continuously from a 3-digit starting number, which changed for each trial and was randomized across participants. The calculations had to be carried out throughout the whole stimulation in each trial, and the answers were reported after the end of the trial. Accuracy was defined based on whether the reported number was part of starting number -7*x. No subjects were excluded based on their task performance.

III. Post-hoc power estimation

	Phase-locked response	Theta
Modality	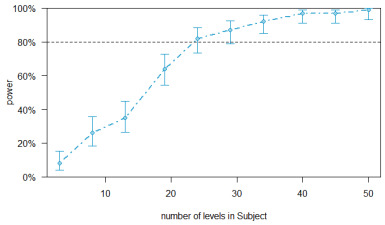	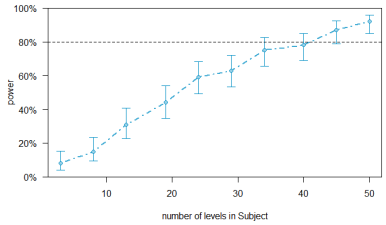
Condition	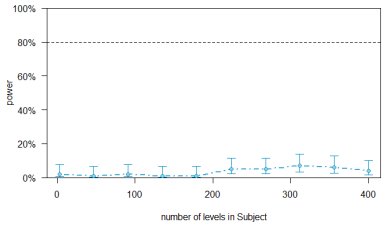	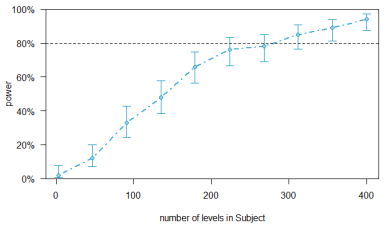
Condition :modality	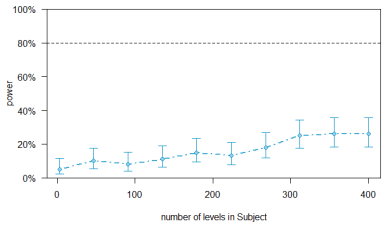	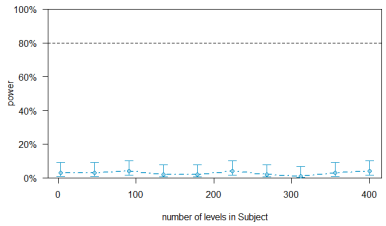

	Alpha	Beta
Modality	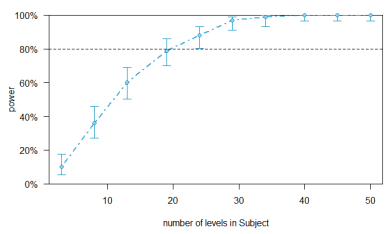	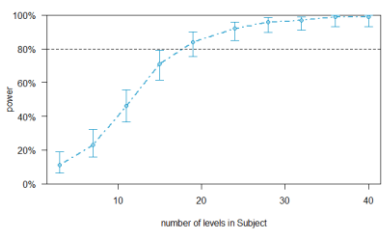
Condition	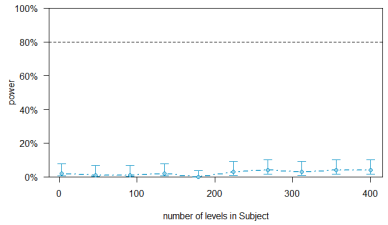	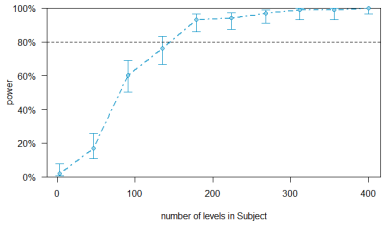
Condition: modality	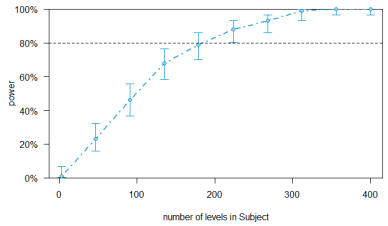	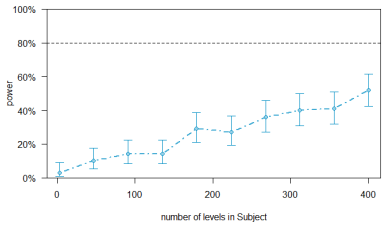

Supplementary Figure S.3: Post-hoc power estimation based on the same sample size simulation which was used to determine the sample size for this experiment, but using the data obtained in this experiment for the linear mixed model (amplitude ~ modality + condition + condition:modality + (1|subject)). Sample sizes over 25 were simulated, to investigate when a sufficient power level could have been reached.

IV. Pilot Study

A pilot study was conducted to determine the behavioural effectiveness of the distraction task in comparison to the baseline condition for the thermonociceptive stimulation. We recruited 21 healthy participants (24.7 ± 2.85 years old, 9 males), and 6 stimuli were applied per condition. A TCS was used to deliver sustained periodic thermonociceptive stimuli (0.2 Hz) on the right volar forearm (as described in 2.3). The thermonociceptive stimulation lasted between 70 and 80 seconds per trial. This range (as opposed to a specific duration like 75s) was chosen for the attention on pain condition which was employed in the pilot but was not used in the actual experiment. In this condition, participants had to count the applied stimulation cycles to focus their attention on the painful stimulation. To ensure that the participants would keep on counting in every trial, the duration of the trials was varied. For coherence, this variable duration was used for all conditions. The distraction and baseline conditions were the same as those described in section 2.5.

Participants were seated comfortably in a chair, with their dominant arm being used for heat stimulation. Each participant was exposed to a brief familiarization stimulus ahead of the experiment on their non-dominant arm. The experiment was divided into three different blocks which were applied in a randomized order with a short break in between. For all blocks, the same thermonociceptive stimulation paradigm was applied. Participants were instructed to rate the perceived painfulness on a numerical rating scale from 0 to 10 (0: no pain, 10: most painful imaginable) at the end of each trial.

Given evidence that the counting of the stimuli could induce a modulation of ongoing neural oscillations at the frequency of the counting (Lu et al., 2019), which would interfere with the effects of the periodic stimulation

that we are interested in, we decided to exclude the attention on pain condition (cycle counting) from the following analysis and final experimental protocol. It is therefore also no longer necessary to vary the duration of the trials in the final experiment.

Statistical analyses were performed using R Statistical Software (Version 4.1.0, R Core Team 2021). LMMs were calculated using the lme4 package (Bates et al., 2015). A linear mixed-effects regression model was applied (pain rating ~ condition + (1|subject)), using “condition” (i.e. baseline / distraction) as factor and “subject” as a random effect to account for the variation of the regression model intercept of the pain ratings across participants. The pain ratings were significantly lower during the distraction condition compared to the baseline condition (beta = -0.90, t(42) = -4.30, p<0.001) (Figure 2), showing that the distraction task succeeded in capturing subject’s attention sufficiently to distract them from the painful stimuli.

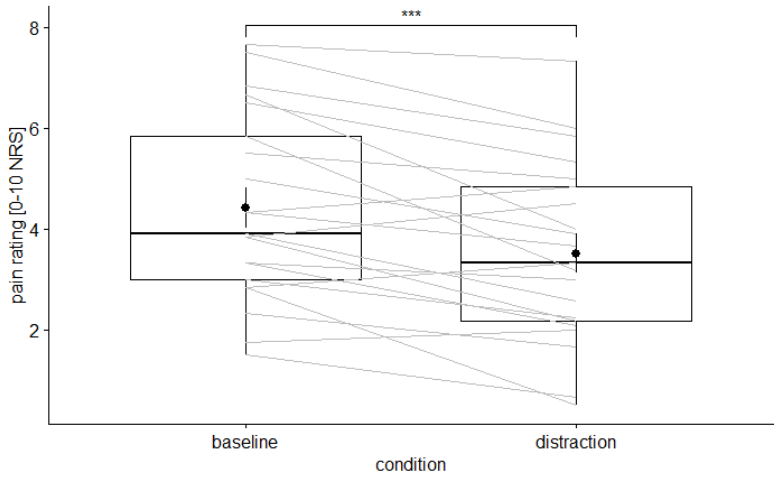

Supplementary Figure S.4: Boxplot showing the average pain rating for each condition. Mean and 95% confidence intervals are represented by the horizontal line in the boxes and the vertical lines, respectively. Each grey line represents one participant. 0: no pain at all; 10: worst pain imaginable. ***: p<0.001.

V. Frequency spectra

	Thermonociceptive stimulation	Vibrotactile stimulation
Phase-locked response		
baseline	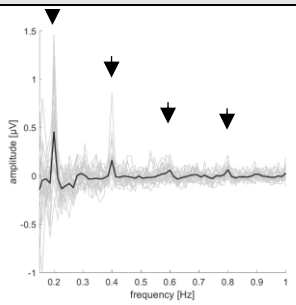	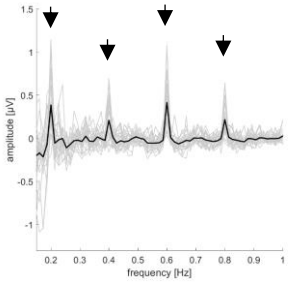
distraction	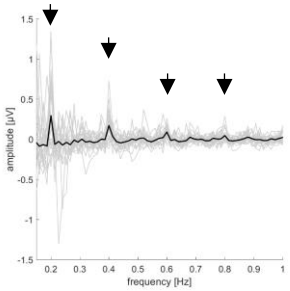	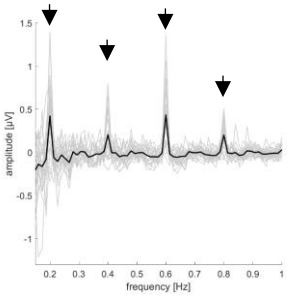
Theta		
baseline	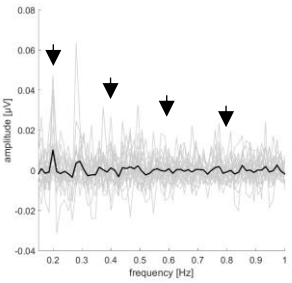	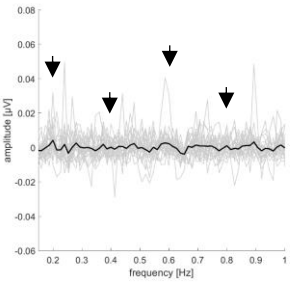
distraction	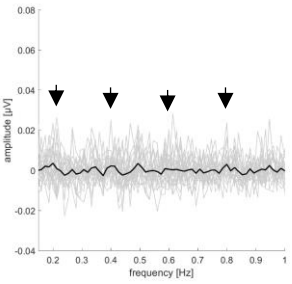	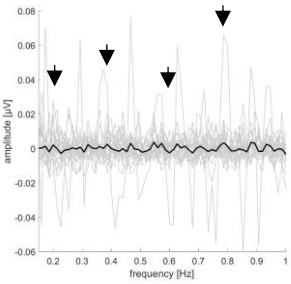

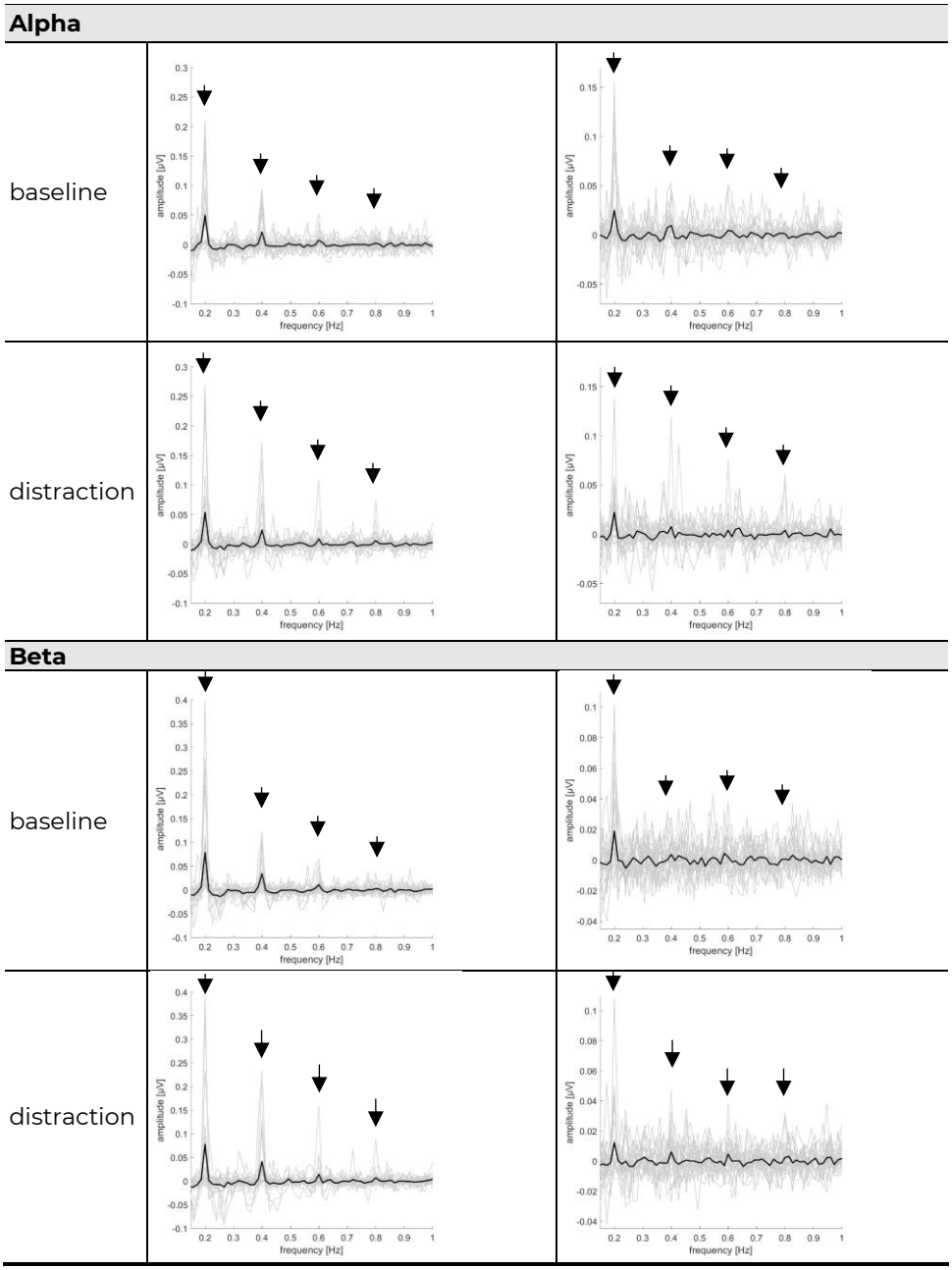

Supplementary Figure S.5: Spectra obtained following either thermonociceptive or vibrotactile sustained periodic stimulation at 0.2 Hz. Data is shown for the phase-locked response, as well as for responses in the theta (4-8 Hz), alpha (8-12 Hz) and beta (12-40 Hz) frequency bands. Grey lines illustrate the neural response of each subject, while the black line illustrates the group average. Vertical arrows mark the harmonics of the frequency of stimulation.

CHAPTER 3. Cue-based modulation of pain stimulus expectation: do ongoing oscillations reflect changes in pain perception? A Registered Report[2]

[2] Published as: **Leu, C.,** Glineur, E., & Liberati, G. (2024). *Cue-based modulation of pain stimulus expectation: do ongoing oscillations reflect changes in pain perception? A registered report*. Royal Society Open Science, 11(6), 240626. https://doi.org/doi:10.1098/rsos.240626

Abstract

A promising stream of investigations is targeting ongoing neural oscillations and whether their modulation could be related to the perception of pain. Using an electroencephalography (EEG) frequency tagging approach, sustained periodic thermonociceptive stimuli perceived as painful have been shown to modulate ongoing oscillations in the theta, alpha and beta bands at the frequency of stimulation. Nonetheless, it remains uncertain whether these modulations are indeed linked to pain perception. To test this relationship, we modulated pain perception using a cue-based expectation modulation paradigm and investigated whether ongoing oscillations in different frequency bands mirror the changes in stimulus perception. 40 healthy participants were instructed that a visual cue can precede either a high or low intensity stimulation. These cues were paired with 3 different levels of sustained periodic thermonociceptive stimuli (low, medium, high). Despite a strong effect of expectation on the perceived stimulus intensity, this effect was not reflected in the modulation of the ongoing oscillations, thus suggesting a potential dissociation of pain perception and these oscillatory activities. Rather, it seems that the intensity of stimulation is the primary generator of the responses collected using an EEG frequency-tagging approach. Importantly, these results need to be confirmed by further investigations that could allow detecting smaller effects than originally estimated.

1. Introduction

The synchronization of information across different brain regions through the flexible activity of ongoing neural oscillations has in recent years been associated with the processing of pain in the human brain (Ploner et al., 2017). Current investigations showcased the benefits of using an EEG frequency-tagging approach paired with the application of slow sustained periodic nociceptive stimuli for the exploration of the characteristic of pain-related ongoing oscillations (Colon et al., 2017; Colon, Nozaradan, et al., 2012; Leu et al., 2023; Mulders et al., 2020). In particular, this approach allows to differentiate between cortical activity related to the applied stimulus and unrelated activity by "tagging" responses at the frequency of stimulation and its harmonics. As such, a periodic modulation was found at the frequency of stimulation in the aforementioned investigations in the alpha, beta and theta frequency bands. Expanding this approach to investigations using intracerebral EEG in patients undergoing a presurgical evaluation of focal epilepsy, Liberati et al. (2019) found a preferential modulation of ongoing oscillations at the frequency of stimulation in the alpha and theta frequency band following thermonociceptive stimulation in comparison to non-nociceptive vibrotactile stimuli. These results suggest that the modulation of ongoing oscillations could be related to nociception and/or the perception of pain. Yet, the functional relationship between ongoing oscillations and the perception of pain remains unclear. If there is in fact a link between these two factors, we expect that a modulation of pain perception should lead to a congruent change in the modulation of ongoing oscillations.

Expectation is a powerful cognitive modulation factor that can strongly influence the subjective experience of pain. While there are numerous ways to influence an individual's expectation towards a painful stimulus, the modulation can be categorized into placebo analgesia, nocebo

hyperalgesia and stimulus expectancies (reviewed by Atlas and Wager (2012)). Importantly, while the former two categories rely on the application of an inert substance or intake of a fake drug, stimulus expectations achieve a modulation of pain perception solely by the association of pain-predictive cues (Atlas et al., 2010; Hauck, Lorenz, Zimmermann, et al., 2007; Jepma et al., 2018; Keltner et al., 2006; Lobanov et al., 2014).

To further understand the modulatory effects of expectation on pain perception, recent investigations studied its effects on ongoing neural oscillations. The application of a placebo analgesic as well as nocebo hyperalgesic intervention both led to an increase in post-treatment resting-state alpha activity (Albu & Meagher, 2016; Huneke et al., 2013). Even before the application of an expected painful stimulus, suppression of alpha frequency band activity has been observed in EEG as well as MEG investigations (Babiloni et al., 2006; Franciotti et al., 2009). Similarly, a visual cue-based expectation modulation paradigm found a cluster of activity between 1-30 Hz when a painful stimulus was expected (Strube et al., 2021b). While similar results were found by Nickel et al. (2022) regarding pre-stimulus activity in a predictive coding paradigm, changes in pain perception induced by expectation did not seem to have an effect on the modulation of ongoing oscillations. Another recent investigation found that while expectations and prediction error did not lead to any changes in local brain activity at the regions of interest (ROI), they did modulate the interregional connectivity within the chosen ROIs in the alpha and gamma frequency band (Bott et al., 2023). As discussed by Nickel and collaborators, it could be possible that commonly used approaches to analyze oscillatory activity are not sufficient to unravel the complexity of pain perception, as higher-order cortical processes such as the contextual modulation of pain might not be rigorously time-locked to the application of a painful stimulus. We aimed to overcome this limitation by using an

EEG frequency tagging approach, which allowed us to more clearly differentiate between activity related to the applied stimulus and other ongoing activity. Moreover, by using long-lasting periodic sustained stimuli, we aimed to capture high-level processes related to stimulus expectation to a larger extent than it is possible in the analysis of relatively brief and sudden stimuli.

We employed a cue-based stimulus expectation modulation paradigm to investigate whether changes in stimulus perception induced by expectation will lead to congruent changes in the modulation of ongoing oscillations at the frequency of stimulation and its harmonics. Based on Atlas et al. (2010) and Keltner et al. (2006), we expect (1) that the information (cue) presented to participants before a nociceptive stimulus can influence the expectations towards that stimulus and consequently (2) alter the perception of this stimulus. Specifically, we hypothesized that if the same medium intensity stimulus is presented with a cue indicating the following stimulus would have a low intensity, the rating of perception would be lower than if the same stimulus is presented with a cue indicating that the stimulus would be highly intense. As demonstrated in previous investigations from our lab (Colon et al., 2017; Leu et al., 2023; Liberati et al., 2019; Mulders et al., 2020), we expected (3) the ultra-slow sustained thermonociceptive stimulation to elicit a periodic response in the different frequency bands at the frequency of stimulation and its harmonics. If the modulation of ongoing oscillations is indeed functionally related to pain perception, we hypothesized (4) that the aggregated amplitudes at the frequency of interest will exhibit a change in modulation congruent to the changes in stimulus perception induced by the cue-based expectation modulation. This would provide evidence that there is an association between the modulation of ongoing oscillations and pain perception.

2. Methods

Stage 1 recommendation and review history can be found on the website of the Peer-Community in Registered Report (PCI RR): https://rr.peercommunityin.org/articles/rec?id=432, as well as the Stage 2 recommendation and review history : https://rr.peercommunityin.org/articles/rec?id=675. All anonymized raw data sets and digital study materials are available in the public archive of Harvard Dataverse (https://doi.org/10.7910/DVN/40ZRQR).

2.1 Participants

We recruited 40 healthy participants. A detailed sample size rationale as well as a discussion of the expected effect sizes can be found in the Supplementary Materials. Participants who have neurological diseases, psychiatric disorders, or recent upper limb trauma upon direct questioning were excluded from the study. In addition, those who have taken paracetamol, nonsteroidal anti-inflammatory drugs (NAIDs), or acetylsalicylic acid within 12 hours before the assessment were also excluded. Before the assessment began, written informed consent was obtained from all participants, who were also informed that they have the option to withdraw from the study at any time. We recruited participants between the ages of 18 and 35 (mean ± std. dev.: 23.65 ± 3.45), with the aim of achieving a gender-balanced sample size (17 males / 23 females). Participants were recruited via an established Facebook group, as well as posters on campus and word-of-mouth.

All procedures were performed in accordance with the relevant guidelines and regulations. The local Research Ethics Committee approved all experimental procedures (Commission d'Ethique Hospitalo-Facultaire Saint-Luc UCLouvain, B403201316436).

2.2 Sample size calculation

Previous investigations in this lab have shown that 15-20 participants are sufficient to observe the modulation of neural oscillations induced by a sustained periodic nociceptive stimulation (Colon et al., 2017; Mulders et al., 2020). This is largely due to the high signal-to-noise ratio in the periodic responses to the ultra-slow 0.2 Hz sustained periodic stimulation, which can even be differentiated from noise at an individual level (Colon et al., 2017). Other investigations using cue-based expectation modulation while acquiring EEG data recruited between 10 and 20 participants per experiment (Albu & Meagher, 2016; Atlas et al., 2010; Hauck, Lorenz, Zimmermann, et al., 2007; Keltner et al., 2006; Koyama et al., 2005) and more recent investigations recruited between 40 and 48 participants (Bott et al., 2023; Nickel et al., 2022).

We thus used a simulation-based approach to calculate appropriate power and sample size estimation to reach sufficient statistical power and detect a specific effect in a linear mixed model (LMM). The calculations were conducted using R Statistical Software (Version 4.1.0, R Core Team 2021) and the R package "simr" (Green & MacLeod, 2016). The regression model used for the simulated LMM was built as follows: *amplitude ~ temperature + cue + temperature:cue + (1|subject),* as detailed in our hypotheses plan and statistical analysis section. The simulated model is based on Mulders et al. (2020). This publication was chosen since the same stimulation and analysis techniques (i.e., frequency tagging of ongoing oscillations) as proposed in this investigation were used to analyze differences in modulation of ongoing oscillations induced by different stimulation surface areas. The LMM interaction between temperature and surface in their investigation had an intermediate effect size of η^2_p=0.060 for the phase-locked response. We simulated the LMM based on the mean and standard deviations obtained for the phase-locked response using a small-

variable surface of the contact-heat thermode probe for the stimulation (equaling our HH condition, mean =0.59 μV, sd = 0.33 μV) and a small-fixed surface of stimulation (equaling our LL condition, mean =0.41 μV, sd = 0.31 μV). The values for the medium intensity conditions (HM (mean = 0.545 μV, sd =0.349 μV) and LM (mean= 0.455 μV, sd = 0.291 μV)) were estimated based on the percentual difference in rating between these conditions that we observed in our behavioral pilot study (18%) (see Supplementary Materials). This percentage is similar to the difference observed in the ratings between HM and LM condition in Atlas et al. (2010). We therefore calculated the mean between our chosen HH and LL values, lowered it by 9% for the condition LM and increased it by 9% for the condition HM. These values reflect our assumption that a stimulus that is expected to be more painful will lead to larger amplitude at the frequency of stimulation and vice versa. The output of this LMM (based on intercept (0.809), slopes for temperature, cue and interaction (-0.228, -0.483, 0.444), residual variance (0.107) and random intercept (0)) was then fed to the LMM-specific sample size simulation.

In the power estimation, we specifically tested for the interaction effect between *temperature* and *cue*, since this is our main comparison of interest. Additionally, interactions usually have a lower effect size compared to main effects and are therefore more critical for the calculation of the adequate sample size. According to the sample size simulation, a sample size of 25 participants would enable us to reach a statistical power of 0.9 while using an alpha level of 0.02. To avoid missing out on any effect and to account for the potential exclusion of participants from the final data analysis (e.g., due to artifacts in the EEG signal), we decided to increase the sample size to 40 participants.

We considered recruiting a sample that would inform us not only about the effect size of interest, but that would also be able to detect the smallest

effect that one could possibly be interested in (Dienes, 2021). The necessary sample size was calculated by obtaining the 80% confidence interval of the LMM and replacing the model estimates with the lower bound estimates of the confidence interval. This updated model was used for the simulation of the power to sample size relationship, resulting in a recommendation to test 150 participants. Unfortunately, limited resources do not allow us to test such a large cohort, and we decided to test only for the more conventional effect size of interest. In consequence, a non-significant result in the LMMs will not necessarily prove the absence of an effect but could also be due to the sample size which might not be large enough to detect effects that are smaller than expected (as noted in the Hypotheses Table).

2.3 Thermonociceptive stimulation

Thermonociceptive stimuli were delivered using a thermal cutaneous stimulator (TCS II, QST.Lab, Strasbourg, France) with the square T11 probe, which is set with 5 micro-Peltier elements (each ~181 mm2) whose temperature can vary at rates of up to 75°C/s and which can be activated individually. The full surface was used in this experiment, covering a rectangular area of 9 cm^2. A sustained periodic stimulation with a frequency of 0.2 Hz was applied and the baseline temperature of stimulation was set to 35°C. The peaks of the stimulation varied from 44°C for the low intensity condition, over 47°C for the medium intensity condition to 50°C for the high intensity condition (illustrated in Figure 1). Each sustained periodic stimulation comprised 10 stimulation cycles, lasting a total of 10x5 seconds per stimulus, similar to Liberati et al. (2019), Mulders et al. (2020) and Leu et al. (2023). Shorter cycle durations were chosen compared to previous investigations to avoid subjecting the participants to a large number of thermonociceptive stimuli. Inter-stimulus-intervals were variable and self-paced by the experimenter to

allow participants to provide intensity ratings. The thermode was placed on the volar forearm of the dominant arm of the participants and was displaced after each trial to avoid habituation or sensitization.

2.4 Experimental procedure

2.4.1 Expectation cue

The visual cues, adapted from Keltner et al. (2006), were displayed on a monitor in front of the participants. The cues consisted of a colored square (blue for low intensity and red for high intensity stimulation), covering the full screen. In the middle of the square, the word “low” or “high”, respectively, was displayed (illustrated in Figure 1). The participants received verbal instructions identifying each cue and which stimulus intensity it is associated with. The cue was presented to the participants prior to the onset of each stimulus and remained visible during the stimulation (illustrated in Figure 2). A pilot study was conducted prior to data collection to ensure that the chosen paradigm would be able to modulate subjects’ pain perception (see Supplementary Materials).

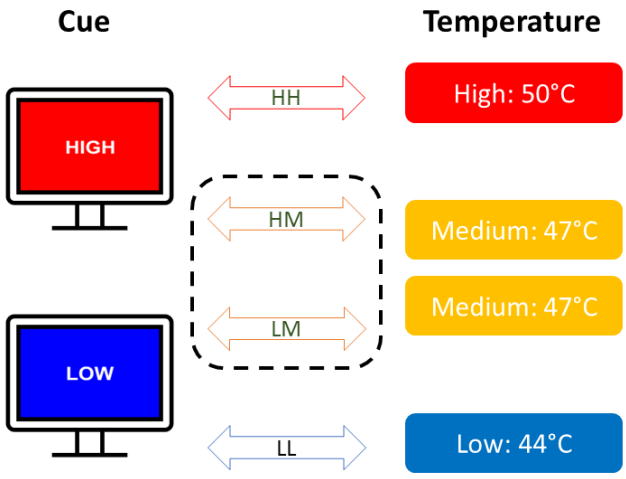

Figure 1: Cue-based expectation modulation paradigm, adapted from Atlas et al. (2010). Cues indicating a high respectively low intensity stimulus were adapted from Keltner et al. (2006).

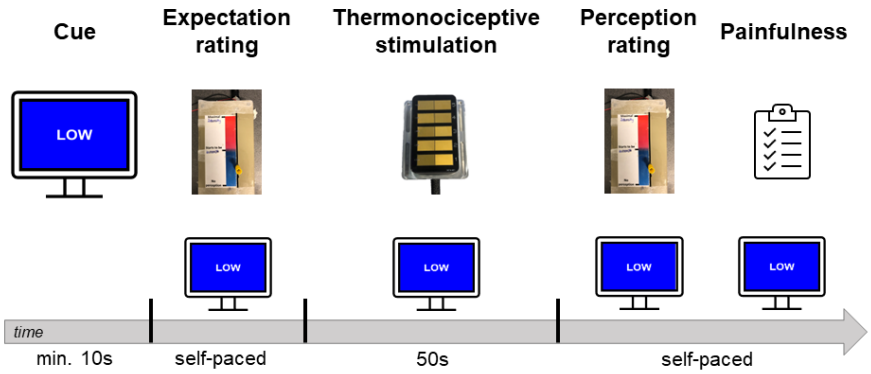

Figure 2: Trial design for one example stimulus, using a cue for a low intensity. VAS ratings were given on a scale from min: "no perception" to a max: "most intense perception imaginable". Participants were asked to evaluate the painfulness of the stimulus with a simple yes/no answer.

2.4.2 Cue-based expectation modulation

Five blocks of stimuli were implemented, each block consisting of 8 trials (each trial consisted of 50 s of sustained periodic stimulation), adapted from Atlas et al. (2010). The first block was used to establish the link between the expectation cue and the stimulation temperature and consisted of only 4 trials, which were not considered for the analysis. Therefore, in this block, the cue for low intensity was always paired with a low intensity stimulus (LL) and the cue for high intensity was always paired with a high intensity stimulus (HH). The second block also started with two trials of matching conditions (LL / HH), followed by a randomized sequence of trials including unmatched cue / temperature combinations. In the unmatched conditions, medium intensity stimuli were paired with either a cue for high intensity (HM) or a cue for low intensity (LM). Blocks 3 to 5 were random in the sequence of conditions. In each block, each condition needed to be presented two times, resulting in a total of 8 trials per condition for the analysis. The experimenters (as well as the participants) were blinded regarding the condition that was be applied; thus neither

knew whether the current stimulus was a matched or unmatched condition.

2.4.3 Behavioral measures

Participants rated the expected intensity of stimulation on a visual analog scale (VAS) using a 10 cm ungraduated sliding ruler right after seeing the cue before the beginning of the stimulation. The lower extremity of the VAS was labeled “no perception” and the higher extremity was labelled “the most intense perception you can imagine”. The time-interval between the rating and the start of the stimulation was variable. During the thermonociceptive stimulation, participants were instructed to sit as still as possible to generate an artifact-free EEG signal. After the stimulation, participants heard a beep sound which indicated the end of the trial. Participants then had to indicate on the VAS how intense they perceived the thermonociceptive stimulation overall, as well as whether they perceived the stimulation as painful or not (as illustrated in Figure 2).

2.5 EEG recordings

EEG was recorded using an elastic electrode-cap with 64 active, pre-amplified Ag-AgCl electrodes (BioSemi, Netherlands), which were arranged according to the international 10-10 system. The sampling rate was set to 1024 Hz. To ensure a clean signal, the direct-current offset was kept below 30 mV. All electrodes were re-referenced offline to the average electrode activity. The recorded signal was stored in the BioSemi ActiView software for offline analyses.

2.6 EEG analysis

The EEG recordings were analyzed using the Letswave7 (www.letswave.org) toolbox in MATLAB (2022a The MathWorks).

2.6.1 *Analysis of the phase-locked response*

To isolate activity related to the applied stimulus, we made use of the frequency tagging analysis approach (Regan, 1989). According to the rationale of this approach, a periodic stimulation elicits a periodic activation of higher order neurons, which in turn leads to a periodic EEG response at the frequency of stimulation and its harmonics (Colon, Nozaradan, et al., 2012; Mouraux, Iannetti, et al., 2011). This approach has been used extensively in our lab over the past years, (Colon et al., 2014; Colon et al., 2017; Colon, Nozaradan, et al., 2012; Leu et al., 2023; Liberati et al., 2019; Mulders et al., 2020), leading to a standardized analysis approach: First, events were created based on the triggers related to the onset of the stimulation. Each trigger received a label according to the condition it preceded (HH, LL, HM, LM). Then, slow drift and high frequency power line noise were removed using a Butterworth band-pass filter between 0.05 Hz and 40 Hz. Epochs were segmented into segments of 0-50s, relative to the onset of the stimulation, creating one file per event code containing all 8 trials of this condition. Electrodes P9, P10 and Iz were removed, since due to their placement on the EEG cap, they frequently only record muscular noise rather than brain activity. All signals were re-referenced to the average of the remaining electrode set. Then, an Independent Component Analysis (Fast ICA algorithm) (Hyvarinen & Oja, 2000) was employed to detect artifacts due to eye movement or other muscular artifacts and remove them. The ICA was computed for each subject separately across all conditions at the same time, using the “runica” algorithm (Bell & Sejnowski, 1995), decomposing the full rank data matrix into 61 independent components. Therefore, the same components were removed in each condition for each subject. Additionally, trials with an amplitude larger than ± 500 µV (Colon et al., 2014) on any of the electrodes were excluded. Any participant with less than 5 trials at this stage would have been removed from the data set, but this did not occur. Finally, the

average signal was calculated for each participant and each condition, and then transformed into the frequency domain using a discrete Fourier transform (FFT) (Frigo & Johnson, 1998). Residual noise was partially removed by subtracting the average amplitude of the signal measures at 2-5 neighboring frequencies, at each electrode and at each frequency bin.

Since the periodic response elicited by the ultra-slow sustained periodic stimulation is not a perfect sinewave, the peaks in the amplitude of the frequency spectrum do not only appear at the frequency of stimulation itself, but also at its harmonics. To account for this, the amplitude at the frequency of stimulation and its harmonics was aggregated and the resulting amplitude at the frequency of interest (FOI) was used for the statistical analysis. To aggregate the harmonics, the signal was cut into chunks of 0.2 Hz length, starting at 0.1 Hz. Therefore, in each chunk, the signal in the middle corresponds to the harmonic of the frequency of stimulation. Then, the chunks were averaged, and the resulting amplitude was multiplied by the number of chunks for which the average has been calculated. The whole electrode set was taken into account for this procedure.

2.6.2 Analysis of the modulation of ongoing oscillations

The analysis of the modulation of ongoing oscillations was almost identical to the previously outlined analysis. To investigate the effect of our stimulation on the periodic modulation of the amplitude of ongoing neural oscillations within different frequency bands (theta: 4-8 Hz, alpha: 8-12 Hz, and beta: 12-40 Hz), the EEG signal was additionally filtered using a 4^{th} order Butterworth filter for each frequency band after calculating the ICA and re-referencing of the electrodes in the remaining signal. Another additional step was the estimation of the envelopes of the signal, which was computed using a Hilbert transform. The following steps were equal to the procedure described for the phase-locked response, including the

aggregation of the signal amplitudes at the frequency of stimulation and its harmonics. The amplitude at the FOI was used for the statistical analysis in each frequency band and the whole electrode set was considered.

2.7 Statistical analysis

Statistical analysis was done using R Statistical Software (Version 4.1.0, R Core Team 2021) and MATLAB (2020b The MathWorks). The significance level of $p<0.05$ was set for the behavioral analysis and LMMs. The LMM was fitted using REML and a Kenward-Roger approximation to produce appropriate type I error rates for smaller sample sizes was used to test the significance of the results. All explicit formulas / equations for the statistical analysis can be found in the hypotheses table.

2.7.1 Behavioral data

To assess whether the cue affected the rating of expected stimulus intensity, an LMM with the independent variable (IV) *cue* and dependent variable (DV) *expectation rating* was used. The factor *subject* accounted for the variation of the regression model intercept across participants and was therefore a random effect in the model. This model was the positive control for the factor *cue*; if the cue would not be effective in influencing the expected stimulus intensity, we had to assume that the cue-based expectation modulation paradigm in this experiment failed.

Further, we employed another LMM to analyze the effect of *cue* (2 levels: low, high) and stimulation *temperature* (2 levels: matched, unmatched) (IV's) on the rating of perceived stimulus intensity perception (DV). We further wanted to assess the interaction between these two factors on the intensity rating. As in the aforementioned LMM, *subject* was used as a random effect. We hypothesized that the medium intensity stimulation paired with the high intensity cue (HM) would lead to a higher rating of

perceived stimulus intensity compared to the medium stimulus paired with the low intensity cue (LM).

2.7.2 Periodic response

To assess whether the amplitude at the FOI was significantly different from zero, a right tailed multi-sensor cluster-based permutation test using Wilcoxon signed-rank test as test statistic was used. To do this, for each condition, the corresponding data was merged into one file, containing all participants. The test compared each signal to 0, using a Bonferroni corrected alpha level of 0.0125 (the standard alpha level 0.05 divided by the number of conditions). The threshold for the cluster-based permutation was also set to 0.0125, and 2000 permutations were computed. The multi-sensor analysis was set to a threshold of 0.161, which sets the threshold for the sensor connection so each channel has 4 neighbors on average. This approach allowed to control for a non-normal distribution of the data, while taking potential type I error inflation due to multiple testing into account. The electrode with the highest test statistic was chosen for further analysis.

Based on previous results from this lab (Colon et al., 2017; Leu et al., 2023; Mulders et al., 2020) we expected a periodic response in the EEG signal elicited by the sustained periodic stimulation significantly larger than zero.

To investigate whether the high intensity cue paired with the medium intensity stimulation (HM) would lead to a higher amplitude at the FOI for the phase-locked EEG signal compared to the low intensity cue paired with the medium intensity stimulation (LM), we used a LMM with the following factors: stimulation *temperature* and *cue* as independent (fixed) variables (IV) with an interaction, while *subject* was a random factor. The *amplitude* at the FOI was used as dependent variable (DV).

2.7.3 Modulation of ongoing oscillations

As for the phase-locked signal, we examined whether the amplitude at the FOI was significantly larger than zero with a right tailed multi-sensor cluster-based permutation test using Wilcoxon signed-rank test as test statistic. The electrode with the highest test statistic was used for the continuation of the analysis.

We expected the amplitude at the FOI to be significantly larger than zero in all frequency bands (Colon et al., 2017; Leu et al., 2023; Liberati et al., 2019). To test our main hypotheses, we used a LMM with the same structure as described above. The IVs were *temperature* and *cue*, while *subject* was added as a random factor, accounting for the variation in the regression model between participants. Finally, *amplitude* was the DV in this model. A separate LMM was calculated for the amplitude at the FOI in each frequency band.

We hypothesized that the amplitude at the FOI would be larger if the medium intensity stimulation was preceded by a high intensity cue (HM) compared to a low intensity cue (LM). If this was the case and the cue-based expectation modulation would change intensity perception in the same direction, these results would suggest that the modulation of ongoing oscillation could be functionally related to pain perception.

2.7.4 Outliers

Any participant unable to complete data acquisition would have been excluded from the analysis. This was not the case in our data set. Further, any data points that violated the LMM assumptions after fitting the LMM were identified using a Shapiro-Wilk test to assess the normal distribution of the data as well as a Levene's test, testing the data set for homoscedasticity. In case the data did not conform to normality, a log-transform was applied, which conforms data to the assumption of

normality by correcting right-skewed data into a more normal form (Bland & Altman, 1996). Any data point that still violated any of the assumptions after the transformation or disproportionately affected the dataset after fitting the LMM was removed from the data set and was not replaced. To ensure that we will still reach the targeted sample size and statistical power, a slightly larger group of participants will be recruited than required by the sample size calculation. Additionally, data points that over-proportionally influence the data set were identified using Cook's Distance [D]. This method calculates how much the fitted values of a given data set change if just one data point is removed. The influence of a data point is expressed in the "distance" D; the larger it is, the more influential the data point (Cook, 1977). Therefore, any data point exceeding a D of 1 was removed from the data set. Cook's distance was calculated for each datapoint within a condition. Thus, for each condition and frequency band, a separate calculation was done. Overall, data points exceeding the threshold for Cook's distance were identified only in the phase-locked response. Results without removed outliers are reported in the Supplementary Materials.

3. Results

3.1 Behavioral results

The cue significantly influenced the expectation of the participants regarding the upcoming thermonociceptive stimulation ($F(1,1239)= 6108$, $p<0.001$, $\eta^2_p= 0.83$). The perception of the stimulation was also significantly modulated by both cue and stimulation temperature, as well as their interaction (Table 1, Figure 3). Post-hoc pairwise comparisons revealed that the medium intensity stimulation was perceived as significantly more

intense when preceded by a high intensity cue compared to a low intensity cue (t(1237)=25.950, p<0.001). Figure 4 illustrates the perception ratings for each participant in all conditions. Overall, stimuli were perceived as painful in condition HH (78.75% of trials), while this was rarely the case for condition LL (1.25% of trials). The medium intensity condition was perceived as mostly non-painful when preceded by a low intensity cue (LM, 9.7% rated as painful). Yet, the same stimulation preceded by a high intensity cue (HM) was rated as painful in more than twice as many trials (22.8% of trials).

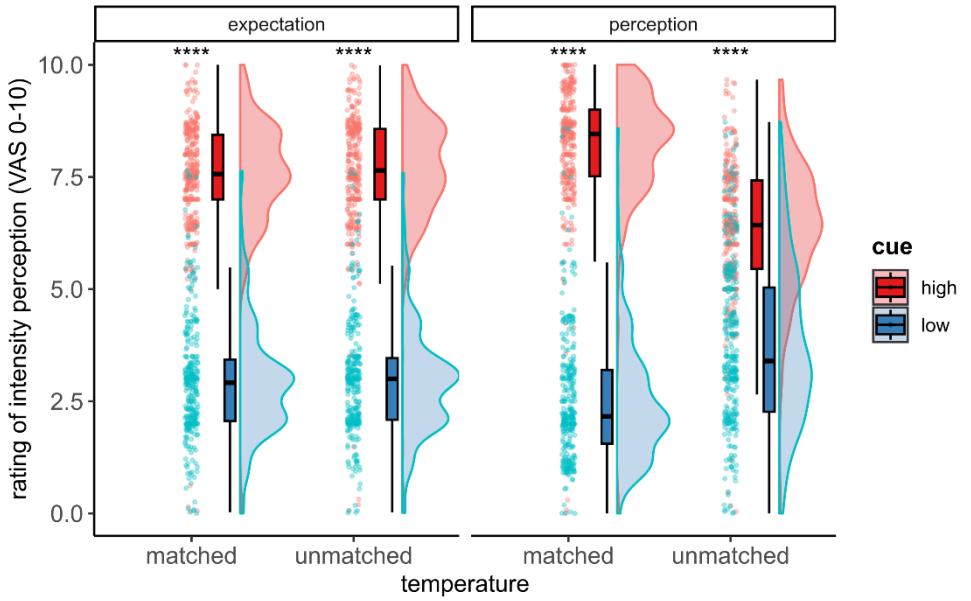

Figure 3: Ratings of expectation (left) and perception (right) collected on a Visual Analog Scale before and after each stimulation, illustrated in Raincloud plots (Allen et al., 2021). Dots indicate single subject ratings. Results of the post-hoc pairwise comparisons are indicated at the top; p<0.001=****. "Matched" refers to conditions HH and LL, while "unmatched" refers to conditions HM and LM (cue / temperature).

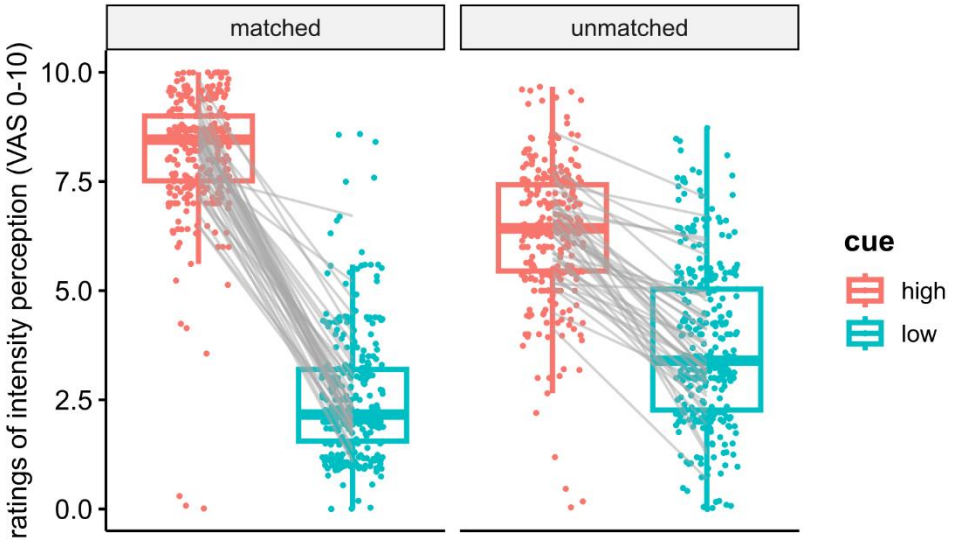

Figure 4: Ratings of intensity perception for each subject in each condition, given on a Visual Analog Scale (VAS). Grey lines connect the mean ratings of the same subject. Matched conditions equal the condition HH and LL, while unmatched conditions represent HM and LM (cue / temperature).

3.2 EEG

3.2.1 Phase-locked response

The Wilcoxon signed-rank test showed that a periodic modulation on the phase-locked response was only found in the HH condition. No significant periodic modulation was found in any of the other conditions. The electrode with the largest modulation was Fz, which was subsequently chosen as the electrode of interest for the remaining analysis of the phase-locked response. The data points of one subject were partially removed because they were identified as outliers, even after using a log-transform to increase the normality of the data distribution. Hence statistical analysis was done on the log-transformed data. The original amplitudes are shown in the figures to increase the intuitive understanding of the graphs. The LMM showed a significant effect of cue as well as of the temperature x cue interaction on the amplitude at the FOI (Table 1). Post-hoc pairwise

comparison revealed a significant difference between the matched conditions (HH vs LL, $p<0.001$), but no significant difference between the unmatched conditions (HM vs LM, $p=0.11$). Further analysis revealed a significant difference between conditions HH and HM ($p<0.0001$) but not between LM and LL ($p=0.073$).

3.2.2 Modulation of ongoing oscillations

Similar to the phase-locked response, only condition HH lead to a significant modulation at the FOI in the different frequency bands. The electrode with the largest modulation in the theta, alpha and beta frequency band were C2, PO3 and FCz. Scalp topographies illustrating the obtained Wilcoxon test-statistics can be found in Figure 5.

As for the phase-locked response, all data sets were log-transformed to conform to the assumption of normality. While the statistical analysis was done on the log-transformed data, we chose to show the original amplitudes in the plots for enhanced readability. The LMM's in the different frequency bands all yielded similar results (Table 1). While significant effects of cue, stimulus temperature and their interaction were observed in almost all frequency bands, all post-hoc pairwise comparisons revealed that the difference in amplitude at the FOI was not significant between conditions that were presented using the same stimulation temperature (HM and LM). Yet, in all comparisons, condition HH led to significantly larger amplitudes at the FOI than condition LL (illustrated in Figure 6). Additional pairwise comparisons revealed that in all frequency bands, condition HH elicited significantly larger amplitude at the FOI than condition HM ($p=0.011$, $p<0.001$, $p<0.001$, respectively, for theta, alpha and beta frequency band), while no significant differences were observed between conditions LM and LL. Illustrations of the spectra up to 1 Hz for each frequency band can be found in the Supplementary Materials.

Dependent variable	cue			condition			interaction		
	F-value	*p*	η^2_p *[95% CI]*	*F-value*	*p*	η^2_p *[95% CI]*	*F-value*	*p*	η^2_p *[95% CI]*
Perception ratings	(1,1237) 3357.926	**<0.001**	0.73 [0.71, 1]	20.634	**<0.001**	0.02 [0.01, 1]	451.532	**<0.001***	0.27 [0.23, 1]
Phase-locked response	(1,114.68) 7.912	**0.006**	0.06 [0.01, 1]	6.36	**0.013**	0.05 [0.01, 1]	26.026	**<0.001**	0.18 [0.09, 1]
Theta	(1,117) 4.992	**0.027**	0.04 [0.00, 1]	4.588	**0.034**	0.04 [0.00, 1]	2.248	0.147	0.02 [0.00, 1]
Alpha	(1,117) 10.761	**0.001**	0.08 [0.02, 1]	4.470	**0.037**	0.04 [0.00 ,1]	8.861	**0.004**	0.07 [0.01, 1]
Beta	(1,117) 10.374	**0.002**	0.08 [0.02, 1]	1.921	0.168	0.02 [0.00, 1]	13.784	**<0.001**	0.11 [0.03, 1]

Table 1: Results of the Linear Mixed model with the formula *dependent variable ~ cue + condition + cue : condition + (1|subject).* Significant p-values are highlighted in bold font. η^2_p was calculated as a measure of the partial effect size of each fixed effect, including its 95% confidence interval. Asterisks mark interactions that showed a significant difference in the post-hoc pairwise comparison between the conditions HM and LM (which used the same stimulus intensity, the only difference being the concomitantly presented cue). Electrodes of interest: Phase-locked: Fz, Theta: C2, Alpha: PO3, Beta: FCz.

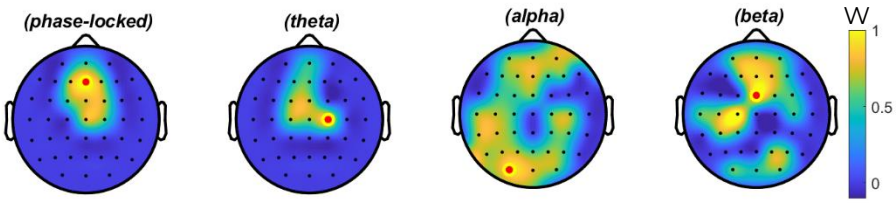

Figure 5: Topographies displaying the results of the multi-sensor cluster-based Wilcoxon signed-rank test (W) for the condition HH (cue for high intensity + high intensity stimulation). The electrode with the largest test statistic – which was used for the subsequent statistical analysis – is marked with a red dot.

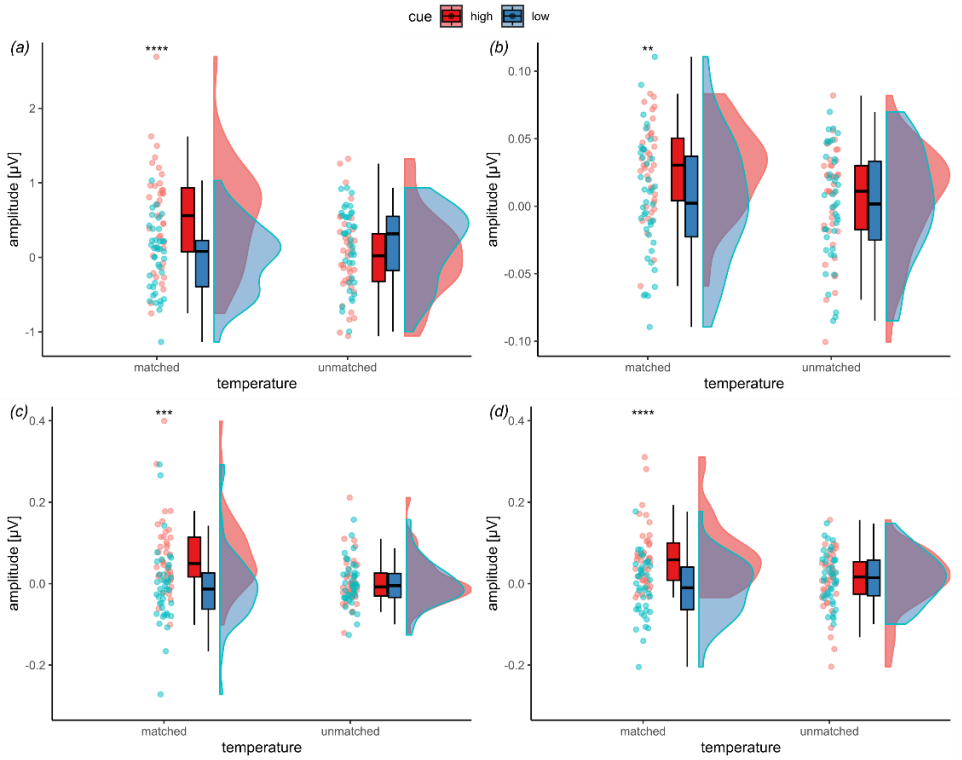

Figure 6: Raincloud plots (Allen et al., 2021) illustrating the amplitudes at the frequency of interest for ***(a)*** : phase-locked response, electrode Fz, ***(b)***: theta frequency band (4-8 Hz), electrode C2, ***(c)***: alpha frequency band (8-12 Hz), electrode PO3 and ***(d)***: beta frequency band (12-40 Hz), electrode FCz. "Matched" refers to conditions HH and LL, while "unmatched" refers to conditions HM and LM (cue / temperature). Significant differences in the post-hoc paired t-test are noted as follows: p<0.01= **, p<0.001=***, p<0.001=****.

4. Discussion

The cue-based expectation modulation paradigm, which was adapted from Atlas et al. (2010) and Keltner et al. (2006), influenced the participants' stimulus intensity expectation and perception as intended; both positive controls regarding the behavioral aspect of the experiment have been met. The visual cue changed the expectation of the participants towards the upcoming stimulus and participants anticipated the correct level of

stimulus intensity based on the cue they were given. Moreover, the cue also significantly changed the stimulus intensity perception of the participants in the medium intensity stimulation trials: participants experienced the stimulation as more painful and intense when shown a cue indicating a high stimulus intensity compared to being shown a cue for a low intensity stimulus. Consequently, given our hypothesis, we expected the modulation of ongoing oscillations to reflect these cue-based changes in stimulus perception during the stimuli delivered at a medium intensity (HM and LM).

A significant modulation of ongoing oscillations at the frequency of interest was only found in the high intensity stimulation condition. Additionally, while significant differences were found for the main effects and interactions between cue and stimulation temperature, post-hoc pairwise comparisons uncovered that these differences were mainly driven by the conditions HH and LL; the conditions of interest HM and LM did not differ significantly in their modulation at the frequency of interest for the specified electrodes in any of the analyzed frequency bands. Moreover, significant differences in amplitude found between HH and HM indicate the intensity at which the stimulus is delivered is mainly contributing to the amplitude observed at the frequency of interest, and not the expected level of stimulus intensity. This suggests a potential dissociation of stimulus intensity perception and the modulation of ongoing oscillations measured using scalp EEG.

While the frequency-tagging approach has been used numerous times in our labs, the present stimulation parameters diverged from previous experiments in their duration as well as in the stimulus temperatures. Notable, stimuli were shorter (10 instead of 15 cycles) and intensities lower (44°C and 47°C instead of only 50°C) compared to the previous publications using this technique (Colon et al., 2017; Leu et al., 2023;

Mulders et al., 2020). While the numbers of cycles were carefully chosen following the re-analysis of the data sets of these previous investigations, it was less clear how much the stimulation temperature would affect the modulation of ongoing oscillations. As shown by Colon et al. (2017), these slow sustained periodic stimuli recruit predominantly C-fibers, for which the activation threshold lies around 37°C to 49°C (Schmidt et al., 1997; Treede et al., 1990). Since we were not able to detect a significant modulation at the frequency of interest for the low and medium stimulation intensities, one possible explanation would be that the temperatures were too low to recruit enough afferent fibers to elicits a periodic activation of higher order neurons. Especially given the temperature of the low intensity stimulus, which was set just around the threshold for pain perception for most people, it seems reasonable that no large effects would be seen. Importantly, while we measured the neural responses to all 4 conditions, we were mainly interested in the responses to stimuli using the medium stimulation intensity (47°C). For conditions HM and LM it was indeed rather surprising to not find a periodic response at the frequency of interest. This might be a result of the lower stimulation temperature in combination with the very slow stimulation paradigm, as temporal summation (nociceptor discharge frequency > 0.5 Hz) is thought to be one of the means through which innocuous warm stimuli can activate nociceptive C-fibers (Tillman et al., 1995). While the low frequency of stimulation was chosen due to its superior signal-to-noise ratio (Colon et al., 2017), a higher temperature for the medium intensity trials might have led to a larger response at the frequency of interest. Yet, as we tried to create a paradigm that had 3 clearly discernable stimulation temperatures that were also tolerable for the high intensity stimulation, the range of temperatures to choose from for the paradigm was limited.

Nonetheless, while the response at the frequency of interest might have not been significant for certain conditions, we could theoretically still observe difference in the modulation of the ongoing oscillations at that frequency. Importantly, those differences will have to be interpreted with caution, as the observed responses were clearly rather small and not statistically different from zero. As expected, a significant difference between high and low intensity stimulation was found in all frequency bands, with the intensity of stimulation as the main differentiator. For both conditions, the expectations matched the applied stimulus. The comparison between the conditions preceded by the high expectation cue showed a similar pattern; the more intense stimulation led to a larger response at the frequency of stimulation in all frequency bands. Thus, neither the expectation of a high intensity stimulus nor the mismatch between expected and perceived stimulus intensity for condition HM seemed to have an influence on the recorded amplitude.

On the contrary, the medium intensity conditions (HM and LM) did not show any differences in their modulation, despite the strong effects the visual cues had on the intensity perception associated with the stimulation. While various investigations have found effects of pain stimulus expectation on EEG correlates (Hauck, Lorenz, Zimmermann, et al., 2007; Huneke et al., 2013; Strube et al., 2023; Thomaidou et al., 2021; Tiemann et al., 2015; Wager et al., 2006), other recent publications found a similar dissociation between stimulus perception and oscillatory activity. Albu and Meagher (2016) recorded an increase in oscillatory activity between 8 and 10 Hz related to thermonociceptive stimuli following a nocebo treatment. Yet, these changes were correlated to the catastrophizing of the individual and not the perceived pain intensity or unpleasantness. In a paradigm comparable to the one used in the present study, Nickel et al. (2022) found a similar modulation of thermonociceptive

stimulus perception based on visual cues, but failed to detect related changes in either event-related potentials (ERPs) or oscillatory activity in their time-frequency analysis.

With our frequency-tagging approach, we aimed to overcome some of the pitfalls of other - more standard - EEG analyses, such as the focus on phase-locked responses and brief stimuli. However, it appears that scalp EEG might not have the specificity or spatial resolution to relay the complex network of activity that shapes human pain perception when the activity of a specific electrode is considered. Nevertheless, this does not imply that EEG cannot be used to assess relevant information on how neural activity guides pain perception.

On one hand, expanding traditional scalp EEG assessments to connectivity analyses and source modeling has been shown to be a promising tool to further understand the complex processes that integrate sensory and contextual information. Bott et al. (2023) have provided interesting results using the same cue-based expectation paradigm as in Nickel et al. (2022), expanding the analysis from local oscillatory activity to interregional connectivity in a network of 6 pre-selected regions of interest associated with pain perception (such as contralateral primary somatosensory cortex, anterior cingulate and prefrontal cortices). While sensory information was mostly encoded in local activity, expectations were shaped exclusively by interregional connectivity, predominantly in the alpha frequency band from the prefrontal to the somatosensory cortex. These results highlight that the perception of pain, which depends on both sensory as well as contextual factors, can hardly be measured by a single electrode using scalp EEG. Thus, future EEG investigations should focus rather on the connectivity between different brain regions to further unravel how pain perception emerged from neural activity.

On the other hand, intracerebral EEG could overcome some limitations of scalp EEG. Previous investigations from our lab have shown that thermonociceptive stimuli (delivered in the same slow sustained periodic manner) are preferentially modulated in the human insula compared to non-nociceptive vibrotactile stimuli (Liberati et al., 2019). By using electrodes which are implanted in patients undergoing pre-surgical evaluation for focal refractory epilepsy, it is possible to assess the activity of brain regions which are difficult to assess using scalp EEG due to the depth of their locations with a very high spatial as well as temporal resolution (Bradley et al., 2017).

Finally, the statistical power given our sample size should be considered for the interpretation of our results. As outlined in our hypotheses table, while we had enough power (given the limitations of an alpha level of 0.02 and target power of 0.9) to find expected effect sizes based on previous investigations and our initial estimation, our sample size did not allow us to reach a statistical power that would allow us to find the "smallest possible effect that we would still be interested in" (Dienes, 2021). Frequently, the targeted effect size is the observed effect in previous literature; yet, this approach might lead to the lack of support for a hypotheses only because the effect might have been smaller than in previous investigations and not because there was truly no effect (Dienes, 2021). Additionally, since the amplitudes related to the medium intensity stimulation were smaller than expected, this could have led us to overestimate the initial effect size. The large range of the confidence intervals of the post-hoc estimated effect sizes suggest that our effect size is not very precise, and a different investigation might yield different results. Thus, even though we did not find any modulations in the ongoing oscillations related to the differences in pain perception induced by the cue-based expectation modulation, we cannot fully reject this hypothesis

based on our study alone and further investigations are needed to confirm our results.

5. Conclusion

Despite a strong effect of the visual cues on stimulus perception, no significant differences were observed in the modulation of ongoing oscillations at the frequency of interest between the conditions of interest (medium intensity stimulation preceded by either a cue for a high or a low stimulation intensity). These results could suggest a dissociation between stimulus perception and the modulation of ongoing oscillations measured using scalp EEG. While our results parallel other recent investigations using a cue-based expectation modulation, we cannot exclude that our sample size was not large enough to detect a potentially small effect and definitive conclusions should not be drawn.

It appears that more advanced analysis procedures (such as source localization and connectivity analysis) or more spatially precise recordings of neural activity (such as iEEG) could be more beneficial to understand how our perception of pain emerges from neural activity.

Question	Hypothesis	Sampling plan (power analysis)	Analysis Plan	Interpretation given different outcomes	Outcome
Behavioural response					
(1) Does the intensity cue influence the rating of expected pain?	A high pain cue will lead to a higher expected pain rating than a low pain cue.	See below. Expected detectable effect size is around η^2=0.058 (see Supplementary Materials for in-depth justifications).	rating_expected = cue + (1|subject) - DV: expected *intensity rating* - IV: *cue* - random coefficient: *subject*	*Positive control:* If the rating matches our expectations, we confirm that the cue is influencing pain expectations as intended. If not, the experiment cannot be used.	Hypothesis confirmed
(2) Do different cues differentially influence the perception of the same painful stimulus?	A medium pain trial paired with a high intensity cue will lead to a higher perceived intensity rating than a medium pain trial paired with a low intensity cue.	See below. Expected detectable effect size is around η^2=0.058 (see Supplementary Materials for in-depth justifications).	rating_perceived = temperature * cue + (1|subject) - DV: perceived *intensity rating* - IV: *temperature, cue* - random coefficient: *subject*	*Positive control:* A correct hypothesis would confirm that the expectation shapes the perception of the cue-associated stimuli. A dissociation of expectation and perception indicates that the cue-based paradigm was not successful at changing subjective intensity perception.	Hypothesis confirmed
Time locked, phase-locked response					
(3) Does the sustained periodic stimulation lead to a periodic EEG modulation at the frequency of interest?	The slow sustained periodic stimulation will elicit a periodic response at the frequency of interest.	See below. This sample size will allow us to detect an estimated effect size of around η^2=0.083 (see Suppl. Materials for in-depth justifications).	Multi-sensor cluster-based permutation Wilcoxon signed-rank test (Bonferroni corrected) of aggregated and averaged amplitudes at FOIs.	A periodic response shows that the stimulation paradigm induces the expected neural activity. ‡	Hypothesis confirmed only for condition HH; no definitive conclusion possible (see sample size limitation).

Time locked, phase locked response					
(4) Does a cue-based expectation task modulate the EEG signal at the FOI in the frequency domain?	The amplitude at the FOI induced by the medium intensity stimulation will exhibit a larger modulation following a cue indicating high intensity than a cue for low intensity.	To reach a statistical power of 0.9 with an alpha level of 0.02, 40 participants were enrolled. Calculations are based on power simulations using the simr package in R (Green et al., 2016). This sample size will allow us to detect an effect around η^2_p =0.09 (see Suppl. Materials for in-depth discussion).	amplitude_FOI = temperature * cue + (1|subject) - DV: *amplitude* at the FOI - IV: *temperature, cue* - random coefficient: *subject*	A change in modulation congruent to the change in intensity perception would reveal a possible connection between perceived pain and ongoing oscillations. ‡	Hypothesis disconfirmed; no definitive conclusion possible (see sample size limitation).
Time locked, non-phase locked response					
(3) Does a slow sustained periodic stimulation lead to a periodic neural response at the frequency of interest for the different frequency bands?	A periodic modulation will be elicited in all frequency bands.	See above. This sample size will allow us to detect an effect size of η^2=0.083 (see Supplementary Materials for in-depth justifications).	Multi-sensor cluster-based permutation and Wilcoxon signed-rank test of aggregated and averaged amplitudes at FOIs in the different frequency bands†.	A modulation at the frequency of stimulation indicates that sustained periodic stimulation leads to a periodic response also in the different frequency bands (Colon et al., 2017). ‡	Hypothesis confirmed only for condition HH; no definitive conclusion possible (see sample size limitation).
(4) Does a cue-based expectation task modulate the ongoing oscillations in the different frequency bands in the time-frequency domain?	The medium intensity stimulation will lead to a larger modulation of amplitude at the FOI following a high intensity cue compared to the same stimulation followed by a cue for low intensity.	See above. This sample size will allow us to detect an effect size around η^2_p=0.09 (see Supplementary Materials for in-depth justifications).	amplitude_FOI_OO† = temperature * cue + (1|subject) - DV: *amplitude* at the FOI for each frequency band - IV: *temperature, cue* - random coefficient: *subject*	A modulation of ongoing oscillations mirroring the level of intensity suggested by the cue would suggest that pain rating and ongoing oscillations might be functionally connected. ‡	Hypothesis disconfirmed; no definitive conclusion possible (see sample size limitation).

FOI: frequency of interest; DV: dependent variable; IV: independent variable; LMM: linear mixed model; amplitude_FOI: amplitude of phase-locked neural response; amplitude_FOI_OO: amplitude of non-phase locked neural response for each frequency band (theta, alpha, beta).

† One model for each frequency band (theta, alpha, beta).
‡Since the sample size is not sufficient to detect the smallest possible effect one would still be interested in (n=150) (Dienes, 2021), a non-significant result of this statistical test does not necessarily indicate that there is a definitive absence of an effect and no definitive conclusions will be drawn from a non-significant result

Table 2: Hypotheses table defined prior to data collection, detailing hypotheses, analysis plans and interpretations given different outcomes. Further information on the sampling plan can be found in section 2.2 and the Supplementary Materials.

Appendices

I. Effect and relevance of the detectable effect size

a) Linear mixed model - EEG

Estimating effect sizes for Linear Mixed Models (LMMs) is not a straightforward process, and there is still much debate about the ideal procedure. Since the power calculation is based on a simulated data set, our first approach was to repeat the simulation, but with 40 instead of the initial 12 participants of the original data set. The means and standard deviations stayed the same. Based on this simulation, a LMM was calculated, and the F-values transformed to partial η^2 values. This resulted in an estimated effect size of 0.09 for the interaction between cue and temperature for the phase-locked response in the EEG signal. We thus estimate to detect a slightly larger effect size than found in the study of Mulders et al. (2020) (η^2_p = 0.06 for the interaction in the phase-locked response). Therefore, we would theoretically still be interested in a smaller effect than found in the simulated model, which means that a non-significant result will not necessarily indicate that our hypotheses was wrong.

Additionally, the software "G*Power" (V. 3.1.9.7) (Faul et al., 2007) was used to calculate the required effect size to reach specified power (0.98), alpha error probability (0.02) and the sample size values (n=40). Unfortunately, the software does not offer this calculation for LMMs, and we were not able to find any adequate alternative. Instead, we approximated the model using the calculation for a repeated measures ANOVA, with within factors only. 1 group was compared along 4 measurements, with a correlation among repeated measures of 0.5 and a nonsphericity correction of 1. This resulted in a calculated required effect size f= 0.282, which equals an η^2_p of

0.074. This calculation shows that the targeted sample size should allow us to detect at least effect sizes similar to previous investigations. Since the ANOVA does not take the variance within subjects into account and is therefore less robust than an LMM, we can expect to be able to detect even smaller effect sizes with our model.

b) Linear Mixed Model - Ratings

Large effects for differences in perception of painful stimuli using expectation cues were found in previous investigations (effect sizes approximated from reported test- statistics) (Atlas et al., 2010; Hauck, Lorenz, Zimmermann, et al., 2007). This is supported by our pilot data, which showed very clear differences (similar percentage change between conditions as in Atlas et al. (2010)) between conditions HM and LM. We therefore expect to find at least an intermediate effect size in our data. Since structurally, the same LMM will be used for the estimation of the effect of cue and temperature on pain ratings as for the effect on the amplitude of the EEG signal, we can assume that our sample size will be sufficient to inform about effects of temperature and condition on pain ratings. Therefore, a smaller effect would not be interesting. G*Power was used to calculate the sensitivity (required effect size) for the power, alpha error and sample size associated with the LMMs of the ratings, using a repeated measures ANOVA, within factors, as conservative approximation for the LMM. The estimated effect size corresponds to η^2=0.058.

c) Wilcoxon signed-rank test

The software G*Power was used to calculate the effect size required for the Wilcoxon signed rank test, which will be used to identify amplitudes at the frequency of interest which are significantly larger than zero. Specifically, the sensitivity of a one-tailed one sample case Wilcoxon signed rank test with a normal distribution and an alpha error probability of 0.0125 (corrected for multiple testing), a power of 0.9 and a sample size of 40

participants was assessed. This calculation estimated an effect size of d=0.6 which equals an η^2_p of 0.083 (medium effect). Since the amplitudes of the modulation of ongoing oscillations tend to be rather small, especially for the theta frequency band, we will also be interested in effects that are smaller than η^2 =0.083.

II. Pilot Study

A behavioral pilot study was conducted to assess whether the changes in the stimulation paradigm compared to the original publication (Atlas et al., 2010) would still lead to the desired modulation of participants' pain perception. Specifically, we needed to ensure that the effect of the expectation modulation paradigm on the perceived intensity would last for the entire stimulation, which was extended from 10s in Atlas et al. to 50s in the present paradigm to accommodate for the frequency tagging approach. To achieve this, participants rated their perception of the thermonociceptive stimuli continuously *during* the application of the stimulus on the VAS, allowing to track the time course of their perception over the entire stimulation. 10 healthy participants (24.3 ± 2.9, 2 males) were recruited. The procedure of the pilot was identical to the experimental setup described previously, with the addition of the continuous rating.

The results of the continuous rating were analyzed qualitatively, while the rating of perceived stimulation intensity was assessed using the LMM proposed in the main experiment (rating ~ cue*temperature+(1|subject)). The independent variables had two levels (cue: low, high and temperature: matched, unmatched). A clear difference could be observed between all 4 conditions in the continuous ratings (Figure S1). Importantly, condition LM led to ratings that were noticeably lower compared to condition HM, despite the stimuli being delivered using the same temperature. This

difference seems to persist over the course of the trial, encouraging us that this paradigm is indeed effective for the slow sustained periodic stimulation paradigm we chose instead of a short tonic heat application.

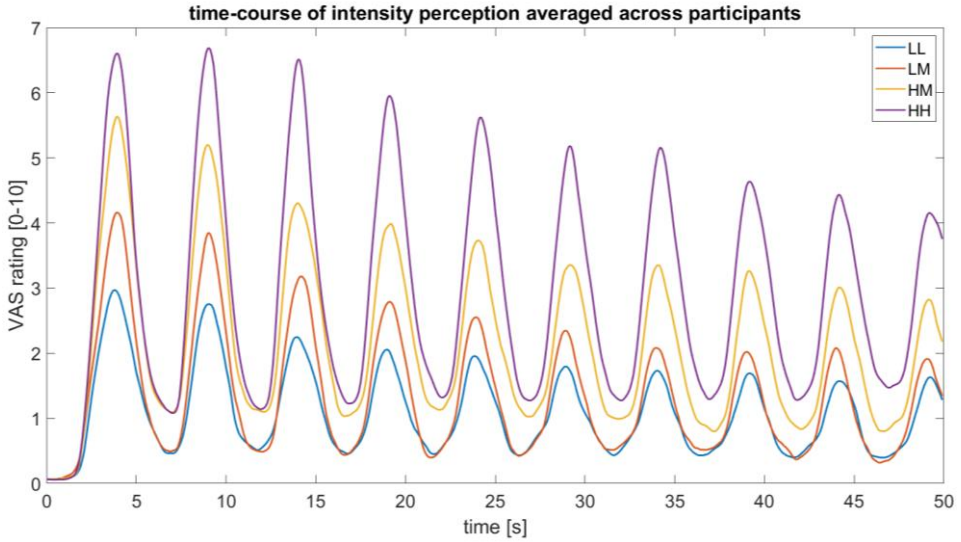

Figure S1. Average of the continuous rating across participants for each condition (LL: cue for low intensity stimulation + low stimulation temperature, LM: cue for low intensity stimulation + medium stimulation temperature, HM: cue for high intensity stimulation + medium intensity stimulation, HH: cue for high intensity stimulation + high intensity stimulation).

The ratings of expected and perceived intensity are shown in Figure S2. The cue appeared to be effective in influencing participants' expectation towards the following stimuli, as the cue for high intensity stimulation led to quite high expected levels of stimulus intensity, while the cue lor low intensity stimulation had the opposite effect. Additionally, the expected and perceived intensity levels are almost the same for the matched conditions (LL and HH). While the expectations did not change for the unmatched conditions (LM and HM), the perceived intensities graduated more towards the middle of the scale, reflecting that the stimulation temperature was at a medium intensity for both conditions. Yet, the most important contrast lies in the difference between the perceived

stimulation intensity for LM and HM. Although the temperature of stimulation was the same for the two conditions, perceptions of intensity varied significantly (main effect of interaction: $F(227,1)=73.561$, $p<0.0001$; *pairwise comparison*, unmatched temperature high cue vs low cue $p<0.0001$) between the conditions. This is consistent with the continuous ratings and indicates that even when asked to provide a single rating describing the overall perception of the stimulation, the effect of the cue-based expectation modulation paradigm persists. These results confirm the effectiveness of the chosen paradigm to change the subjective intensity perception of the applied stimuli towards the presented cue.

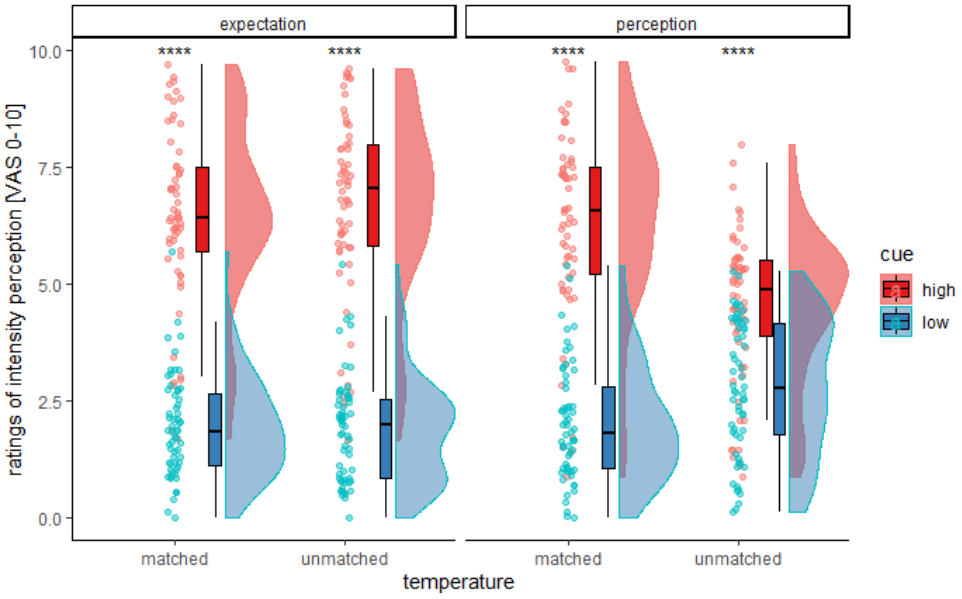

Figure S2. Averaged ratings of expected and perceived intensity of stimulation, given before and after each stimulus. The ratings were converted to a scale from 0-10 for readability. Matched conditions: low cue + low intensity stimulation, high cue + high intensity stimulation: unmatched conditions: low cue + medium intensity stimulation, high cue + medium intensity stimulation. Pairwise comparison; $p<0.0001$=****.

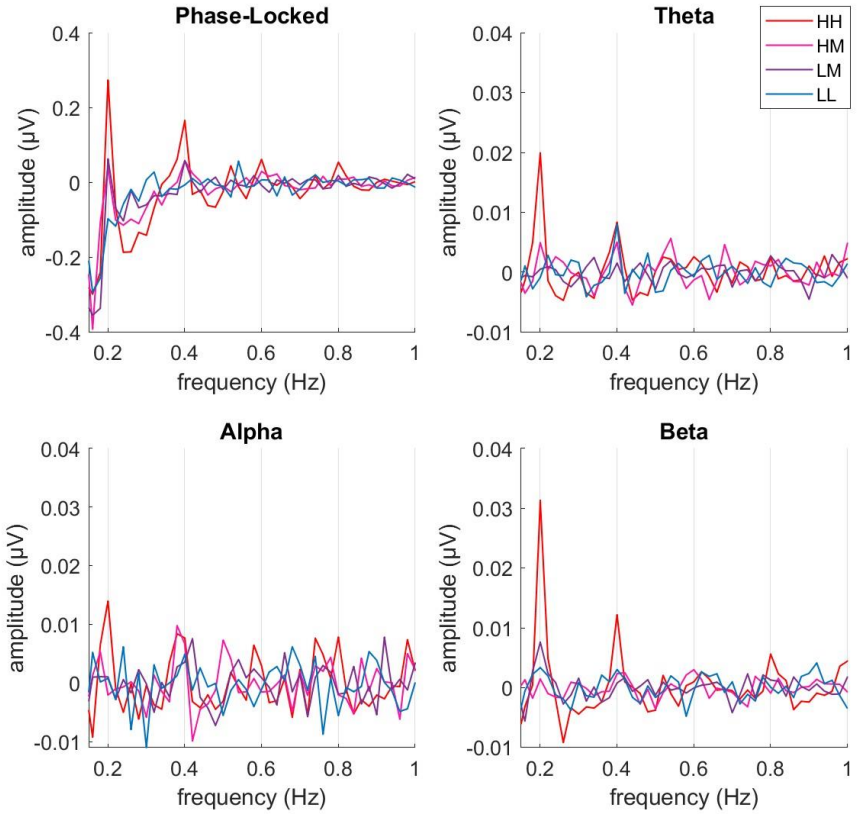

Figure S3: Illustration of the spectra up to 1 Hz for each analysis. The harmonics of the stimulation's frequency are indicated using vertical grey lines. Note that the results presented in the main publication reflect the aggregated harmonics of the stimulations frequency. HH: cue for high intensity + high intensity stimulation; HM: cue for high intensity + medium intensity stimulation; LM: cue for low intensity + medium intensity stimulation; LL: cue for low intensity + low intensity stimulation. Electrodes of interest: Phase-locked: Fz, Theta: C2, Alpha: PO3, Beta: FCz.

Addendum

I. Additional analysis of the aggregated harmonics

Following the unexpected lack of a significant periodic modulation in most conditions, we decided to carry out post-hoc exploratory analyses which were not pre-registered in the Registered Report after the manuscript had been accepted for publication. Specifically, the aggregation of the harmonics for the analysis of the amplitude at the frequency of interest and its potential to introduce noise in the aggregated amplitude introduced some doubts in the obtained results. An in-depths discussion of the significance of the harmonics in the frequency-tagging approach can be found in Chapter 1.

Initially, the opinion prevailed that the aggregation (=" summing up") of all of the harmonics in the spectrum would not be influenced by potential noise in later harmonics, as the sum of random noise should cancel out to zero in the aggregation. This was also the method that was used in the previous chapter, where harmonics were aggregated up to 40 Hz (Leu et al., 2023). Since we applied a Butterworth 4th order bandpass filter between 0.05 and 40 Hz in the first steps of the preprocessing in the present analysis (in contrast to a 0.05 – 100 Hz bandpass filter and 50 Hz multi-notch filter in the previous experiment), we were confident that we could aggregate the entire spectrum to achieve the same result.

Yet, considering that no periodic response was found in most of the conditions in this experiment, the question arose whether the aggregation method we used could not have had unexpected detrimental effects on the signal-to-noise ratio. To answer that question, three additional analyses were conducted: either to not aggregate the harmonics at all and only analyze the amplitude at the frequency of stimulation, as it has been done in the majority of publications from our lab using pain-related frequency

tagging (Colon et al., 2017; Liberati et al., 2019; Mulders et al., 2020). Nevertheless, a recent review on the summation of harmonics in frequency-tagging by Retter et al. (2021) came to the conclusion that disregarding the harmonics would also disregard an important aspect of the obtained neural response (see Chapter 1 for an in-depth discussion). Thus, two additional aggregation methods were added to the post-hoc analysis: to identify the harmonics that show a periodic response and only aggregate those (as it has been done in other frequency-tagging investigations (Retter & Rossion, 2016)) and to use the same aggregation method as in chapter 2, summing up the first 199 harmonics of the spectrum.

Thus, the amplitude at the frequency of stimulation (i.e. 0.2 Hz) was extracted, and the multi-sensor cluster-based Wilcoxon signed-rank test including Bonferroni correction was applied to test whether the amplitudes are significantly larger than zero. The analysis of the harmonics showed that overall, the first 4 harmonics were significantly larger than zero, i.e. displayed a periodic response at the frequency of interest. Therefore, the first 4 harmonics were aggregated for each frequency-band as well as the phase-locked response and the same Wilcoxon test was applied to test whether a significant periodic response was present. Finally, to match the exact aggregation method used in my previous experiment and to test whether our assumption would be correct, the first 199 harmonics were aggregated and analyzed as described above. The results can be found in table S5.

For the amplitude measured only at the frequency of stimulation, the phase-locked response did not show a significant periodic response anymore in any of the conditions. The results stayed comparatively the same for the activity in the theta, alpha and beta frequency band. Interestingly though, the topography of the neural activity changed, and

the distribution of the electrodes with the largest activity was more coherent with previous investigations from the lab. This might indicate that even though the results did not change for the different conditions, we might have aggregated some noise in our original analysis.

		No aggregation				**Aggregation of first 4 harmonics**			
		Phase-locked	Theta	Alpha	Beta	Phase-locked	Theta	Alpha	Beta
HH	*W*	-	4.940	4.389	5.289	3.246	4.805	4.415	5.289
	electrode	-	C2	C3	C3	Cz	C2	C3	C3
HM	*W*	-	-	-		-	-	3.434	-
	electrode	-	-	-		-	-	C3	-
LM	*W*	-	-	-	-	-	-	-	3.784
	electrode	-	-	-	-	-	-	-	C3
LL	*W*	-	-	-	-	-	-	-	-
	electrode	-	-	-	-	-	-	-	-

		Aggregation of first 199 harmonics			
		Phase-locked	Theta	Alpha	Beta
HH	*W*	3.891	3.945	4.281	4.671
	electrode	Fz	C2	PO3	FCz
HM	*W*	-	-	-	-
	electrode	-	-	-	-
LM	*W*	-	-	-	-
	electrode	-	-	-	-
LL	*W*	-	-	-	-
	electrode	-	-	-	-

Table S4: Results of post hoc exploratory analysis of the multi-sensor cluster-based Wilcoxon signed-rank test assessing whether a significant periodic response is present in the measured amplitude. The same procedure was carried out for either: only the peak at the frequency of stimulation (0.2 Hz, "no aggregation"), for the aggregated first 4 harmonics or for the aggregated first 199 harmonics.

A similar development was observed for the amplitudes in condition HH following the aggregation of the first 4 harmonics, with the addition of a significant periodic response for the phase-locked results. Additionally, condition HM in the alpha frequency band and condition LM in the beta

frequency band also displayed a significant periodic response at the aggregated amplitude.

Since different electrodes of interest were identified than in the original analysis, the LMM's were re-calculated for both additional analyses, using the either the amplitude at the frequency of stimulation or the aggregated amplitude of the first 4 harmonics. These LMM's showed that the two additional aggregation methods did not change the results that were previously obtained while aggregating the harmonics of the whole spectrum. Finally, we applied the multi-sensor cluster-based Wilcoxon signed-rank test to the aggregated amplitude consisting out of the first 199 harmonics. As expected, the results did not differ from our initial results while aggregating the whole spectrum.

II. Frequency spectra

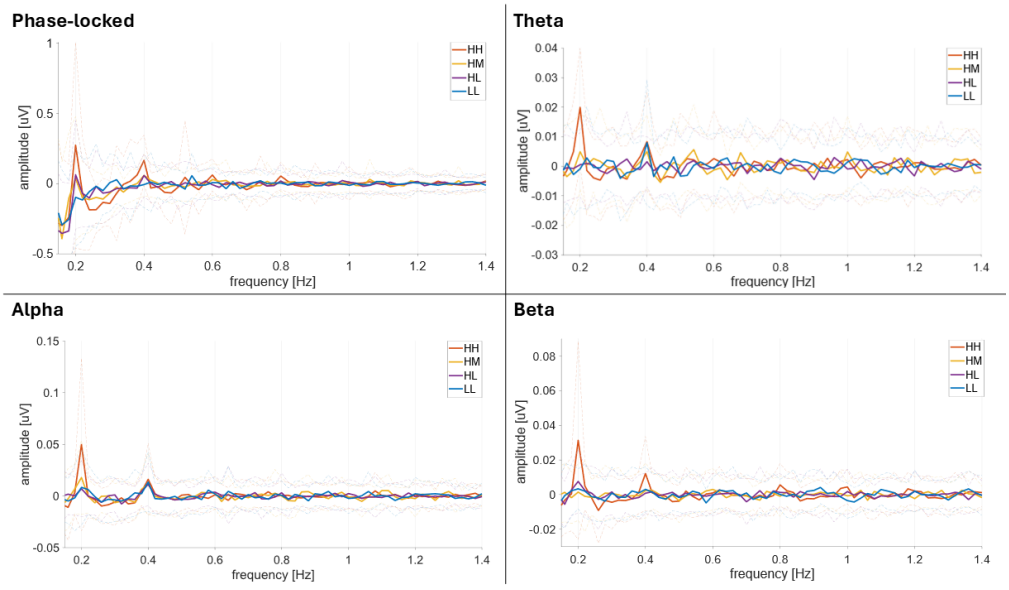

Figure S4: Frequency spectra illustrating the means ± standard deviations (dashed lines) of each condition for the phase-locked response, and the signal in the theta, alpha and beta frequency bands up to 3 Hz.

CHAPTER 4. The effect of stimulus saliency on the modulation of thermonociception-related ongoing neural oscillations

Abstract

Ongoing oscillations have been shown to be modulated in different frequency bands following phasic, tonic as well as periodic thermonociceptive stimulation. Yet, it remains unclear whether these modulations are related to pain perception, saliency (i.e., the ability of a stimulus to stand out from its environment) or solely the intensity of these stimuli. Thirty-five participants were recruited to investigate the relationship between pain perception and ongoing oscillations as well as the factors likely to modulate them, combining a sustained periodic thermonociceptive stimulation paradigm including periodic oddball events with a frequency-tagging analysis approach. Oddballs were delivered either at a higher or lower intensity ("high oddball" vs "low oddball" condition) than baseline stimuli. Continuous ratings of pain perception were collected during the stimulation to track participants' perception.

Overall, the stimuli were barely perceived as painful, which hinders conclusions about the relationship to pain perception. Only in the "high oddball" condition, the continuous ratings of perception clearly reflected the variations of stimulus intensity. Consistently, the oddball stimulus modulated ongoing oscillations in the "high oddball", but not in the "low oddball" condition. Because of the lack of differentiation between baseline and oddball cycles in the "low oddball" condition – both in perception and at the neural level – these findings do not allow disentangling the differential effects of stimulus intensity and saliency on the perception of thermonociceptive stimuli, or on the modulation of oscillatory activities related to thermonociception. However, they indicate the modulation of ongoing oscillations reflects subjects' perception of thermonociceptive stimuli that are both salient and intense.

1. Introduction

Saliency can be defined as the feature of a stimulus that makes it stand out from its environment (Egeth & Yantis, 1997). Painful stimuli emerge from the activity of the nociceptive system which is made to respond to high-intensity and potentially damaging somatosensory stimuli. These stimuli are therefore inherently salient and facilitate the involuntarily capture of attention (Eccleston & Crombez, 1999). The effects of saliency on event-related brain potentials (ERPs) evoked by nociceptive stimuli have been broadly studied (Iannetti et al., 2008; Legrain, Bruyer, et al., 2003; Valéry Legrain et al., 2009; Roa Romero et al., 2013) , and evidence emerged that, in the experimental procedures in which they are usually elicited, the modulation of the magnitude of those ERPs can be mostly driven by the saliency of the eliciting nociceptive stimulus rather than its intensity and its painfulness. This dissociation between the saliency of the nociceptive stimuli and their painfulness was demonstrated, among others, by studies showing that the relationship between pain and ERP magnitude can be disrupted when nociceptive stimuli are repeated: repeating the stimulation reduces ERP magnitude while pain perception remains constant (Iannetti et al., 2008). Moreover, novel nociceptive stimuli elicit ERPs of larger magnitude and distract more participants from their primary task than stimuli of the same intensity but presented more frequently (Legrain et al., 2009).

Lately, it has also been shown that painful stimuli not only elicit ERPs, but also modulate the synchrony of ongoing neural oscillations in different frequency bands (Gross et al., 2007; Mouraux et al., 2003; M. Ploner et al., 2006; Schulz et al., 2011). Yet, it remains unclear whether these pain-related modulations of neural oscillations reflect changes in pain perception, stimulus saliency or merely objective stimulus intensity. Recent investigations were able to show the effects of bottom-up modulation on

ongoing oscillatory activity by applying thermonociceptive stimuli of different intensities (Hauck et al., 2015; Tiemann et al., 2015; H. Wang et al., 2022; Zhang et al., 2012) or longer durations (Nickel et al., 2017; Schulz et al., 2015). While these studies provided evidence that the intensity of a stimulus modulates oscillations in the theta, alpha, beta and gamma frequency band, it remains ambiguous whether the observed effects are related to the saliency of the applied stimuli or solely their intensity.

Using a frequency-tagging approach (Regan, 1989), investigations from our lab demonstrated modulations of ongoing oscillations at the frequency of stimulation within different frequency bands following slow sustained periodic thermonociceptive stimulation in a range of investigations (Colon et al., 2017; Leu et al., 2023; Leu et al., 2024; Liberati et al., 2019; Mulders et al., 2020). While the manipulation of attention (Leu et al., 2023) and modulation of stimulus intensity expectation in (Leu et al., 2024) did not seem to have an effect on the modulation of ongoing oscillations, differences in oscillatory activity were found either between modalities (thermonociceptive vs vibrotactile stimulation) or between different stimulation intensities (i.e. temperature of stimulation). Yet, whether these differences in modulation are related to variations in the painfulness, intensity or purely the saliency of the applied stimuli remains unclear. Further clarifying this relationship would be an important step to deepen our understanding of the potential association between the modulation of ongoing oscillations and pain perception. More specifically, this could tell us whether the observed neural modulations could indeed be a sign of a preferential modulation of painful stimuli rather than a response related to contextual and unspecific features such as stimulus intensity and saliency. Thus, the clarification whether the modulation of ongoing oscillations is more closely related to stimulus saliency or intensity

would help to understand whether the modulation of ongoing oscillations could potentially be used as a physiological marker of pain in humans.

To shed light on the potential role of ongoing oscillations in the perception of salient stimuli, we adopted an oddball paradigm during periodic nociceptive stimulation. Continuously oscillating thermonociceptive stimuli were applied at the same location at a certain frequency, but every fourth stimulus was presented at a higher stimulus intensity (creating the oddball effect, since these stimuli "stood out" from the other stimuli). This effect allowed us to deliberately make some stimuli more salient than others and thus observe the corresponding brain responses, which we hypothesized are not merely related to changes in stimulus intensity. Previous studies using periodic visual stimuli have shown that oddball sensory events embedded in a regular series of stimuli (e.g., human faces among neutral objects, words among nonwords, etc.) elicited in the EEG spectrum, in addition to the baseline response, a response peak specifically at the frequency of occurrence of those oddball stimuli (e.g. (De Keyser et al., 2018; Lochy et al., 2016; Rossion et al., 2015), analyzed using a frequency-tagging approach. To this date, no study has extended this oddball approach to the perception of painful nociceptive stimuli.

The aim of this study was to investigate whether changes in stimulus saliency induced a corresponding modulation of ongoing oscillations, and whether these modulations relate more closely to the saliency or the intensity of the stimulus. As saliency and stimulus intensity are inherently tied to each other, this investigation did not aim to quantify the exact contribution of each factor. More so, the goal was to achieve a better understanding of how both these factors (and their interaction) can modulate ongoing oscillations. To this aim, intensity was varied using an oddball paradigm during which the stimulation intensity changes periodically between baseline and oddballs which were delivered at a

higher stimulation intensity (i.e., “high” oddball). Based on Rossion et al. (2015), we expected to be able to “tag” both the baseline and the oddball response at their respective frequency of stimulation. To disentangle the effect of saliency and intensity, we employed a control condition, during which the oddball was delivered at the same frequency as in the high oddball condition, but with a *lower* stimulation intensity (i.e., “low” oddball). Thus, the main characteristic of this oddball was its saliency, since its low intensity made it different (i.e. “standing out”) in comparison to the baseline stimuli. We hypothesized that the oddballs in both conditions would be perceived at a different intensity compared to the stimulation at baseline frequency. Further, we expected that the oddball would lead to a peak at its stimulation frequency for the high oddball condition. While we also expected a modulation for the low oddball if saliency affected the EEG response, no periodic modulation of this oddball would indicate a predominant role of intensity in the modulation of ongoing oscillations. If the amplitude of the neural response in the low oddball condition was similar to the amplitude at the oddball frequency in the high oddball condition, it would suggest that the modulation of ongoing oscillations is mostly affected by change detection rather than intensity. Conversely, if a periodic modulation was found in both conditions, but smaller for the low compared to the high oddball, the results would suggest that the modulation of ongoing oscillations was more closely related to the intensity of the stimulation, but still had an underlying contribution of the saliency of the stimuli.

2. Methods

The Stage 1 manuscript of this Registered Report (RR) has been formally registered on the Open Science Framework (OSF) by PCI RR after receiving in-principal-acceptance (https://osf.io/tn6z8/). The OSF project repository associated with this RR can be found under the following link: https://osf.io/s3879/ . All anonymized raw data sets and digital study materials are available in the public archive of Harvard Dataverse (https://doi.org/10.7910/DVN/542CLY).

2.1 Participants

We recruited 35 healthy adults (15 males, 25.4 ± 4.25 (mean ± std deviation)) who were between 18 and 35 years old (Creac'H et al., 2015). Due to non-compliance or artifacted signals, data of some participants were discarded from the analysis. Ultimately, the EEG data of 31 participants and behavioral data of 33 participants was used for the analysis. Participants were recruited via an established website and social media and were compensated with 25 € for the duration of the experiment (2 visits, lasting around 1.5h for the EEG assessment and 1h for the perception assessment). The number of participants was based on a power and effect size estimation using the software G*Power (Faul et al., 2007). A more detailed sample size rationale can be found in the Supplementary Materials. Previous EEG investigations of bottom-up modulations of ongoing oscillations have recruited between 7 (Zhang et al., 2012) and 20 participants (Hauck et al., 2015; Tiemann et al., 2015), while investigations using a visual oddball paradigm with a frequency-tagging approach recruited 12 participants (De Keyser et al., 2018; Rossion et al., 2015). Other pain-related frequency-tagging investigations recruited between 8 and 15 participants (Colon et al., 2017; Mulders et al., 2020). The experiment was split into two separate visits to the lab: one to record EEG data and one to

record continuous ratings during the same thermonociceptive stimulation paradigm. The order of the visits was counterbalanced across participants.

Exclusion criteria included regular use of psychotropic medication, intake of pain killers such as paracetamol and nonsteroidal anti-inflammatory drugs (NSAIDs) within 12h before the experiment, as well as any severe neurological diseases, psychiatric disorders, or recent upper limb trauma. The local Research Ethics Committee approved all experimental procedures (Commission d'Ethique hospitalo-facultaire, Saint-Luc Hospital & UCLouvain, B403201316436). Participants were informed about all procedures and signed an informed consent form prior to data acquisition. All procedures were carried out according to relevant guidelines and regulations.

2.2 Thermonociceptive stimulation

Thermonociceptive stimuli were applied using a contact heat thermode (TCS II, QST.Lab, Strasbourg, France) using a probe (°T03) applied on the dominant volar forearm of the participant (2 left-handed). The probe consisted of 15 micro-Peltier elements in groups of 3, resulting in a stimulation surface of 115,5 mm2. The maximal heating ramp of this thermode is 300°C/s. The stimuli were applied in a sustained periodic manner at a frequency of 0.5 Hz and oscillated between baseline temperature (35°C, approximately skin temperature) to a target temperature determined by the staircase procedure in the beginning of the visit (see section 2.3). The stimulation was delivered over a period of 80s and the full stimulation surface was used for each stimulation. The inter-stimulus-interval was self-paced by the experimenter (min. 10s) and the thermode was displaced after each trial to avoid habituation or sensitization.

2.2.1 *Oddball paradigm*

To introduce an oddball paradigm, every 4th stimulus (oddball frequency: 0.125 Hz) was delivered using a higher stimulus intensity (i.e., individual target temperature + 2°C) to make the oddball stimulus stand out from its environment. An illustration of the stimulation pattern can be found in Figure 1. A similar oddball paradigm using visual stimuli has been shown to elicit responses which can be easily identified using a frequency-tagging approach (Rossion et al., 2015). We also conducted a pilot study to ensure that the oddball would indeed be perceived as different from the baseline stimulation, and an additional pilot following changes post in-principal-acceptance (IPA) (see Supplementary Materials S.III).

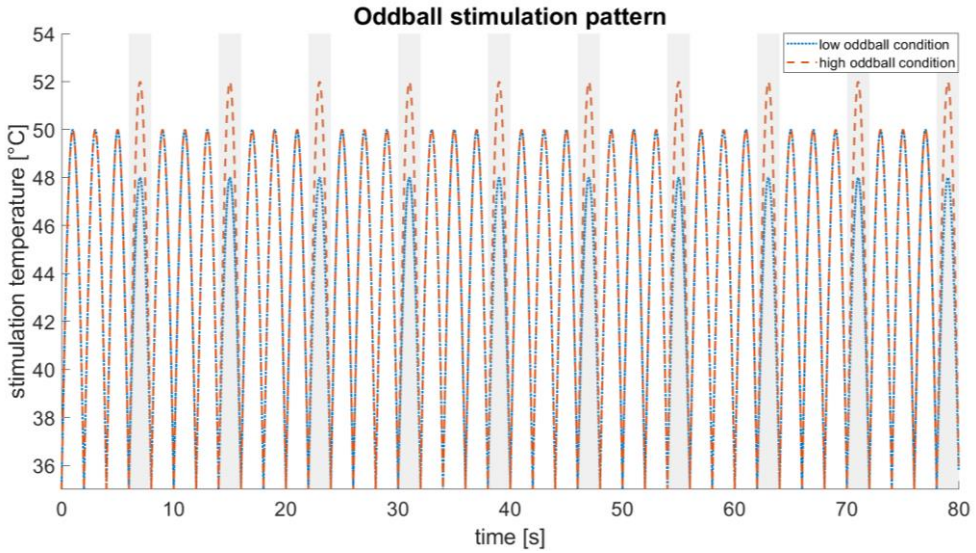

Figure 1: Illustration of the sustained periodic stimulation pattern during the "low oddball" (blue) and "high oddball" (red) condition with the example of 50°C as baseline target temperature. Every fourth stimulation (i.e., $F_{oddball}$=0.125Hz) will be delivered at 52°C, which is 2°C higher than the baseline stimulation or 48°C, respectively. One trial consists out of 80s of stimulation (i.e., 10 oddball cycles).

2.2.2 *Control condition*

To disentangle whether possible effects (behavioral and in the EEG) were at least partially related to the saliency of the stimulus or rather to the

change in stimulus intensity, a control condition (i.e., “low oddball”) was added to the experiment. To ensure that the oddball was still perceived as different but not more intense, the stimulation was delivered at the same frequency as previously described (0.125 Hz), but at a *lower* intensity (individual target temperature - 2°C) than the baseline stimulation (Figure 1). For some participants, the oddball elicited a qualitatively different perception (i.e. not painful) compared to the other stimuli. While this could be considered a confounding factor, it is this attribute which allowed the stimulus to be salient, i.e. stand out from its environment (the painful baseline stimuli). We then compared behavioral and neural responses between the oddballs (high oddball vs low oddball), which are both salient (i.e., a change from the previous stimuli) but different in their intensity.

2.3 Staircase procedure

A staircase procedure (Claus et al., 1990) was implemented to identify the individual pain threshold to which the stimulation temperature of the baseline temperature would be adapted to. The aim was to find a temperature which was tolerable for the full experiment (including high oddball trials), but still painful throughout the entirety of each trial (at the peaks of the stimulation). The stimuli applied in the staircase procedure were 40s long and were delivered in the same periodic sustained fashion as the stimuli in the rest of the experiment, but without the addition of an oddball stimulus. The first stimulus always reached a temperature of 49 °C at every peak. Participants were asked whether they perceived the stimulation as painful (at the peaks) throughout the 40s trial (if so, -0.5°C for the following stimulus), only painful in the first half of the trial (+0.5°C for the following stimulus) or as not painful (+1°C for the next stimulus). Participants were instructed that painfulness related to either a burning or pricking sensation (since we are predominantly stimulating C-fibers (Colon et al., 2017)). The threshold for sufficient painfulness of the

stimulation was identified when a single step in temperature led to a change in perception of the painfulness in two consecutive trials. For example, in the temperature was increased and the following trial was perceived as “generally painful”, the following trial would have a 0.5°C lower stimulation temperature. If this lower temperature trial was then perceived as “painful only in first half”, we selected the stimulation temperature of the preceding trial for the experiment. This temperature was then used as the “baseline peak temperature”, on which the stimulation temperatures for the high and low oddball depend on. The goal of this staircase was to reach a baseline stimulation temperature that was perceived as VAS 5 or higher at its peaks during the entire 80s of the stimulation. The maximal temperature that could be chosen for the baseline stimulation temperature was 51°C. On average, the selected baseline stimulation temperature was 50.197 ± 0.984 °C.

2.4 Behavioral measures

Ratings of perceived stimulus intensity were collected using a Visual Analog Scale (VAS) in the form of a slider implemented in a potentiometer. The continuous ratings were digitized at 100 Hz with an analog/digital converter (USB-6343, National Instruments, Texas). No ratings were collected during EEG data acquisition, as the arm movement would have likely artifacted the recordings. Thus, ratings were collected in a separate visit during which no EEG data was acquired. Before the start of the VAS part of the experiment, participants underwent a familiarization phase during which warm innocuous stimuli were delivered at the baseline stimulation frequency of 0.5 Hz onto the dominant volar forearm of the participant, while they had to rate their perception on the VAS scale. This phase was not considered for the analysis. The minimum of the VAS represented “no perception” and the maximum represented the “maximal pain imaginable”, while the middle of the scale (i.e. VAS 5) represented the

threshold to pain perception. Participants were asked to trace their perception using the VAS during each thermonociceptive stimulus following the familiarization phase. A pilot study examining whether participants would be able to trace the sustained periodic stimulation and detect the oddball stimuli in both conditions was conducted, a detailed description thereof can be found in the Supplementary Materials.

2.5 Experimental procedure

Participants were seated comfortably in a chair during the experiment, while their dominant arm was resting on the table with its volar surface upwards. They were instructed to move as little as possible and kept their gaze constant to avoid interference with the EEG signal acquisition during the thermonociceptive stimulation. They were not informed about the stimulation paradigm or any other details regarding the stimuli or the aim of the investigation. For each condition (i.e., high oddball / low oddball), 12 trials were delivered, distributed over 6 blocks of 4 thermonociceptive stimulation trials (Figure 4). The breaks between the stimulation blocks were self-paced, with a minimum of 2 minutes and a maximum of 5 minutes, while the breaks between trials were self-paced by the examinator (usually between 10s to 30s). The order of the conditions was randomized and counterbalanced across subjects, which was implemented to make the appearance and nature of the oddball less predictable. The same stimuli were delivered on both visits. At the beginning of the first visit, the staircase procedure was implemented to define the stimulation temperatures. The visit including the EEG assessment lasted around 1.5 hours in total, while the VAS assessment lasted around 1h per participant.

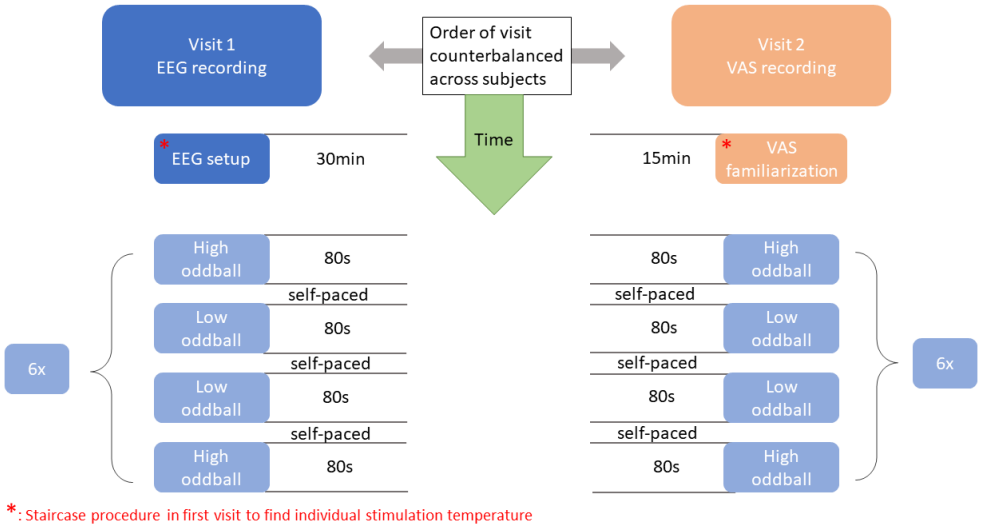

Figure 2: Illustration of the organization of the experiment. The visits were one week apart and conducted around the same time of day, and the same stimuli were delivered in both visits. A staircase procedure was implemented at the beginning of the first visit to find the ideal stimulation temperature for each participant, at which the experiment is tolerable but still painful throughout the entire stimulation.

2.6 EEG recordings

An elastic electrode-cap with 64 active, pre-amplified Ag-AgCl electrodes (BioSemi, Netherlands) arranged in accordance with the international 10-10 system was used to record EEG. To maintain a clear signal, the direct-current offset was limited to 30 mV. All electrodes were re-referenced offline to the average electrode activity and the sampling rate was set to 1024 Hz.. The BioSemi ActiView software stored the recorded signal for subsequent offline analyses.

2.7 EEG analysis

The EEG recordings were analyzed using the Letswave7 (www.letswave.org) toolbox in MATLAB (2022a The MathWorks).

2.7.1 Analysis of the phase-locked response

We employed a frequency-tagging analysis approach (Regan, 1989) to analyze the periodic response induced by the slow sustained periodic stimuli, which allowed us to differentiate between oscillatory activity related to our stimuli and other unrelated ongoing activity (Colon, Nozaradan, et al., 2012). The frequency-tagging method is based on the notion that a periodic stimulus elicits a periodic activity which can be identified as periodic responses at the frequency of stimulation in the recorded EEG signals (Colon, Legrain, et al., 2012; Mouraux, Diukova, et al., 2011) (illustrated in Figure 3). This approach has been frequently used in our lab, leading to a standardized analysis approach (Colon et al., 2017; Leu et al., 2023; Leu et al., 2024; Mulders et al., 2020). The obtained EEG signal was first filtered using a Butterworth band-pass filter between 0.05 and 30 Hz. Then, the signal was segmented into epochs of the length of stimulation (80s), relative to the onset of the stimuli. To remove potential muscular artifacts (i.e., from eye movements), an Independent Component Analysis (Fast ICA algorithm) (Hyvarinen & Oja, 2000) was applied, and any trial containing amplitudes larger than ± 500 µV was removed. On average, 4.5 ± 2.1 independent components supposed to reflect noise signals were removed per participant. 1.3% of trials was removed due to large artifacts (> 500 µV) that could not be removed using the ICA. In 3 participants noisy channels were interpolated using its 3 neighboring electrodes. The electrode locations were flipped for the 2 left-handed participants. The remaining signal was re-referenced to the average of the electrode set, and the waveforms were then averaged across participants. To analyze the signal in the frequency domain, a discrete Fourier transform (FFT) (Frigo & Johnson, 1998) was used. Finally, we subtracted at each electrode and at each frequency bin the average amplitude of the signal measured at the maximum amount of neighboring frequencies (depending on the location of the electrode, this number varies from 2-5) to remove residual

noise (Mouraux, Iannetti, et al., 2011). The peak at the frequency of the oddball stimulation (FoS) in each condition was selected for the continuation of the analysis (FoS_{base}= 0.5 Hz). In a similar (visual) oddball paradigm, it has been shown that responses related to the periodic oddball are the strongest at the first 3 harmonics (i.e., $FoS_{oddball}$= 0.125 Hz, FoS_{H2}= 0.25 Hz and FoS_{H3}= 0.375 Hz) (Rossion et al., 2015). The signal with the largest response within the first three harmonics was selected and used in the continuation of the analysis.

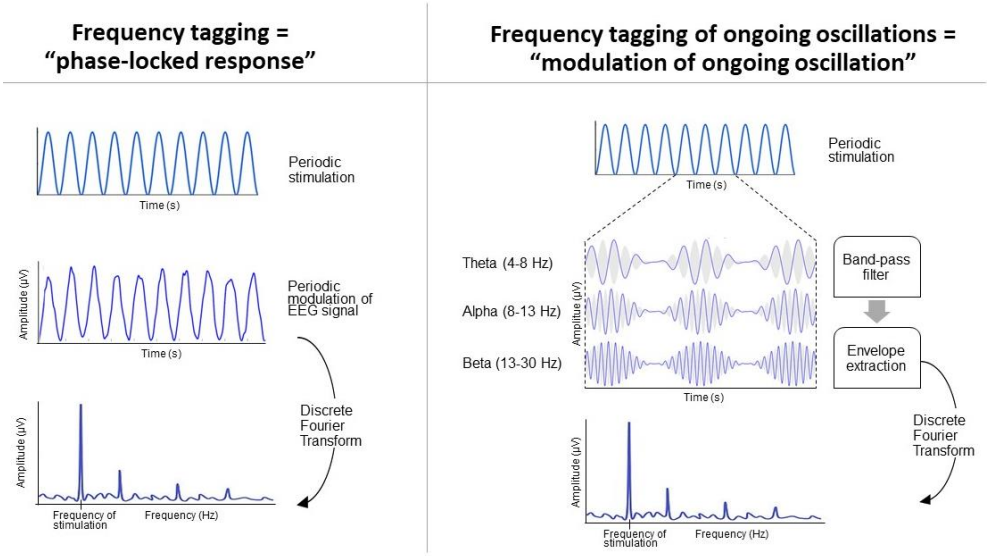

Figure 3: Illustration of the frequency-tagging method as well as its extension for the frequency-tagging of ongoing oscillations.

2.7.2 Analysis of the modulation of ongoing oscillations

The analysis of the modulation of ongoing oscillations only differed from the previously described steps in two points. To isolate the activity related to specific frequency bands (theta: 4-8 Hz, alpha: 8-13 Hz, beta: 13-30 Hz, in accordance with the COBIDAS recommendations (Pernet et al., 2020)), a 4th order Butterworth bandpass filter was used to filter the EEG signal after the re-referencing step. Additionally, a Hilbert transform was applied to

estimate the envelope of the signal. The remaining steps were the same as described in the analysis of the phase-locked response (averaging, FFT, removal of residual noise). The resulting amplitude at the $FoS_{oddball}$ and FoS_{base} in each frequency band, condition, and for all electrodes was considered for the statistical analysis. As for the phase-locked response, the first 3 harmonics of the oddball stimulus were considered in each condition, and the harmonic with the largest modulation was selected.

2.8 Statistical Analysis

Statistical analyses were done using R Statistical Software (Version 4.3.1, R Core Team 2023) and MATLAB (2020b The MathWorks). The significance level was set at $p<0.05$. A Kenward-Roger approximation generating appropriate type 1 error rates for smaller sample sizes was used to test the significance of the results.

2.8.1 Behavioral data

To analyze the continuous ratings and find peaks related to the oddball in both conditions, each condition was averaged for each participant. A time-window of 1-2.6s seconds after each oddball stimulus (i.e. peak of the stimulation) was assessed and the highest rating within this window was selected. The length of this time-window was based on Mulders et al. (2020), who reported that peaks in continuous rating followed on average between 1.35 and 2 seconds after the peak of the stimulus delivered at a frequency of 0.2 Hz. Similar results were found in our own pilot data (see Supplementary Materials S.II). The same procedure was carried out to identify peaks associated with the baseline stimulation. The detected peaks were averaged (summed up and divided by the number of peaks) for each stimulus and condition. To assess whether the ratings related to the oddball differed from the rating of the baseline stimuli, two linear mixed models were used, assessing the effect of the factor *stimulus*

(baseline/oddball) on the ratings of perception given during either the high oddball (model 1) or during the low oddball (model 2) condition. *Subject* was added as a random effect to adjust the intercept of the regression model for each participant. Based on the assumption that the high oddball was more salient than the baseline stimuli, we expected that it would be perceived as more painful than the baseline stimuli. In the low oddball condition, we expected the oddball to be perceived as less painful than baseline stimuli, since the oddball was delivered using a lower stimulus intensity. If we failed to get evidence for a difference between baseline and oddball ratings in one of the conditions, we would not expect to find a modulation of ongoing oscillations at the frequency of stimulation of the corresponding oddball ($FoS_{oddball}$).

To be able to compare the ratings related to the oddball in the two conditions relative to the baseline peaks (which are not necessarily of the same amplitude in the two oddball conditions), the difference between baseline and oddball was calculated for each condition (=Δhigh and Δlow). A paired t-test was applied to compare the difference between oddballs across the conditions. We expected that the high oddball would be rated as more painful than the low oddball stimuli.

2.8.2 Phase-locked response

To control for a non-normal distribution of the data set and to account for potential type I error inflations due to multiple testing, a right-tailed multi-sensor cluster-based permutation test using a one-sample Wilcoxon signed-rank test as test statistic was used to identify amplitudes at the FoS which were significantly different from zero. A Bonferroni corrected alpha level of 0.0125 (the standard alpha level 0.05 divided by the number of conditions) was used to account for multiple testing (the median being compared to 0 at each of the 64 channels). The threshold for the cluster-based permutation was also set to 0.0125, and 2000 permutations were

computed. The sensor connection threshold for the multi-sensor analysis was set to 0.161, thus each channel had 4 neighbors on average. A periodic response was considered when the Wilcoxon signed-rank test (with the conditions specified above) identified an amplitude as significantly different from zero. Electrodes showing a periodic response that are neighboring each other were pooled and analyzed as a cluster (Hauck et al., 2015; Tiemann et al., 2015). Since most of the responses at $FOS_{oddball}$ proved to be not significantly different from zero or not clustered, we created the electrode clusters of interest based solely on the test statistic for FOS_{base} (Figure 7).

Based on the frequency-tagging premise, we expected to find a periodic response at both FoS_{base}, in both conditions. Previous investigations in our lab using a stimulation frequency of 0.2 Hz showed that this elicits a very consistent response (Colon et al., 2017; Leu et al., 2023; Mulders et al., 2020). If none of the electrodes showed a significant increase in periodic response at the FoS_{base}, we would have to assume that we failed to induce a periodic modulation of the EEG signal, rendering the data unusable as the fundamental objective of the investigation was not achieved (positive control).

We further expected to find a periodic response at the $FoS_{oddball}$, in both conditions. A peak at the $FoS_{oddball}$ would show that the periodic oddball paradigm adapted from a visual stimulation paradigm also works as intended using much slower, painful stimuli. If a periodic response was found in the high oddball condition but not in the low oddball condition, we could assume that the intensity of the stimulus contributed more to the periodic response than saliency (since both stimuli should be salient, but only one of them is delivered at a high stimulation intensity). A response larger than zero at the $FoS_{oddball}$ in the low oddball condition

would show that a stimulus with a lower intensity than baseline could also elicit an oddball response, potentially due to the saliency of the stimulus.

If the oddball response in both conditions was larger than zero, the relative amplitude of the oddball responses was calculated for each condition (=Δhigh and Δlow) and compared using a paired t-test. The relative amplitude had been chosen to mitigate potential differences between the responses at the FOS'_{base}. Given the difference in oddball stimulation intensity, the baseline stimuli could also be perceived differently in the different conditions, potentially leading to non-identical responses between the conditions. If the periodic response was driven mainly by the intensity of the stimulus, we expected the amplitude of the high oddball to be larger than the low oddball. If saliency had an additional contribution to the periodic response, the oddballs would show a similar amplitude.

2.8.3 Modulation of ongoing oscillations

The analysis of the modulation of ongoing oscillations was identical to the analysis of the phase-locked response but was done separately for each frequency band. Therefore, a right-tailed multi-sensor cluster-based permutation test using a Wilcoxon signed-rank test as test statistic was be used to identify the electrodes with an amplitude significantly larger than zero at both FoS' and in each condition. Corresponding to the analysis of the phase-locked response, for each frequency band, neighboring electrodes exhibiting a large modulation at the frequency of stimulation (i.e., a high test-statistic) were pooled into clusters. We expected to find clusters over contralateral central-parietal areas for the alpha and beta frequency band (Colon et al., 2017; Leu et al., 2023; Mulders et al., 2020) and more fronto-central for the theta frequency band (Colon et al., 2017; Leu et al., 2024; Mulders et al., 2020; Tiemann et al., 2015). As for the phase-locked response, clusters were based on the modulation of ongoing oscillations found at FOS_{base}. As for the phase-locked response, we expected a periodic

response at both FoS'_{base} and $FoS'_{oddball}$ in the different frequency bands and conditions. No response at the $FoS_{oddball}$ in the low oddball condition would show that the saliency of the stimulus does not contribute significantly to the modulation of ongoing oscillations and that stimulus intensity was the main contributing factor.

As for the phase-locked response, the difference between baseline and oddball was calculated for each condition and frequency band (if both show a modulation at their FoS). Then, for each frequency band, a paired t-test was employed to compare the peaks related to Δhigh and Δlow. If the intensity of the stimulus was the main factor in the modulation of ongoing oscillations, the amplitude for Δhigh would be larger than the amplitude for Δlow (not excluding that saliency might also influence this modulation). If saliency was more relevant than stimulus intensity, the amplitudes of the oddball in the normal and the control condition would be similar to each other.

2.8.4 Outliers

Only participants that completed both experimental sessions fully were considered for the analysis. Further, we removed outliers (identified using Cook's distance (Cook, 1977)) as well as data points that violate LMM assumptions of linearity and normality.

Violations of LMM assumptions were identified using a Shapiro-Wilk test to assess the normal distribution of the data. To test the data set for homoscedasticity, Levene's test was used. In case the data did not conform to normality, a log-transform was applied, which conformed data to the assumption of normality by correcting right-skewed data into a more normal form (Bland & Altman, 1996). Any data point that still violated any of the assumptions after the transformation or disproportionately affected

the dataset after fitting the LMM was removed from the data set without being replaced.

Cook's Distance [D] was used to identify data points that over-proportionally influenced the data set. This method calculated how much the fitted values of a given data set change if just one data point was removed. The influence of a data point was expressed in the "distance" D; the larger it was, the more influential the data point (Cook, 1977). Therefore, any data point exceeding a D of 1 was removed from the data set. Cook's distance was calculated for each datapoint within a condition, using a separate calculation for each condition and frequency band.

Removing outliers can be tricky and offers a certain analytical flexibility which should be mitigated as much as possible in a Registered Report (Leys et al., 2019). In case outliers were removed from the data set, we added the complete analysis with the full data set (no outliers removed) in the Supplementary Materials for comparison purposes. No outliers were removed from the dataset apart from the participants which were rejected pre-statistical analysis.

2.9 Exploratory analyses

2.9.1 Behavioral response

Given the periodicity of the VAS ratings, an exploratory visual analysis was conducted as a direct comparison to the analysis of the neural responses by transforming the perception ratings into the frequency domain. Mirroring the preprocessing steps of the EEG data, we calculated the group average for each condition, then applied the FFT and corrected the baseline by removing 2-5 neighboring frequency bins from the signal.

2.9.2 Neural response

In the primary registered analysis, the amplitude at the frequency of the oddball (or one of the first 2 harmonics) was considered by itself. Yet, in a compelling review by (Retter et al., 2021), it is demonstrated that harmonics are indeed an important part of the neural response in the frequency domain. This theoretical framework was supported by the EEG spectra found in this investigation in e.g. the alpha frequency band, which showed visually identifiable peaks at the 1st and 2nd harmonic of the oddball of about the same magnitude as the main response at $FOS_{oddball}$ (see Figure 9). Therefore, to avoid the pitfall of disregarding the harmonics completely and potentially lose information, we added an exploratory analysis to this RR, in which the amplitude at the oddball frequency is aggregated (i.e. summed up) with the amplitudes at the first 2 harmonics. This new amplitude (FOS_{agg}), comprising the amplitudes at 0.125 Hz, 0.25 Hz and 0.375 Hz, and therefore more adequately representing the complete neural response to the oddball stimulation, will then be treated as the $FOS_{oddball}$ for the consecutive analysis (i.e. multi-sensor cluster-based Wilcoxon signed rank test to identify amplitudes significantly larger than 0, and the comparison of the relative amplitudes if both conditions show a modulation of ongoing oscillations at the FOS_{agg}).

3. Results

Data from 1 participant were entirely excluded from the dataset due to non-compliance with the instructions of the experimenter in both sessions and 1 participant did not complete the 2nd testing session. Data from 2 additional participants had to be excluded from the EEG dataset, because the data was too contaminated by artifacts (i.e. amplitudes over 500 µV after ICA).

3.1 Stimulus perception

While many participants were able to track the periodic stimulation using the VAS, the baseline stimulation cycles were often not clearly perceived, rendering the identification of the rating peaks on a single subject level rather difficult (see Supplementary Material S.IV for single subject average examples). Yet, on a group level, rating peaks relating to both oddball and baseline stimulation were clearly identifiable in both conditions (Figure 4).

The high oddball stimulation was overall perceived as more intense than the low oddball stimulation. Interestingly, only for the high oddball condition, the subjects perceived on average that the oddball cycles were painful (Figure 4), even though we had aimed to elicit the sensation of pain in both conditions. The oddballs in the high oddball condition were visually clearly distinguishable from baseline stimulation cycles, which was not the case in the low oddball condition (relating to hypothesis 1). Nevertheless, the rating peaks related to either oddball were observed with almost the same time delay after the peak of the stimulation (see vertical lines in Figure 4, avg. delay high oddball: (mean ± std. dev.) 1.834s ± 0.164s, delay low oddball: 1.717s ± 0.215s). The ratings peaks relating to the oddball stimulation cycles were rated at group average at a VAS of 5.1 ± 0.2 following high oddball and VAS 4.3 ± 0.4 for low oddball stimulation (Figure 4). On group average, participants rated the baseline stimulation cycles at VAS 4.6 ± 0.3 in the high oddball trials, and at VAS 4.3 ± 0.4 in the low oddball trials. While these values were based on the group average, for the LMM individual ratings relating to baseline and oddball peaks were extracted based on the maximal rating within a time-window of 1-2.6 sec after the stimulation peak for each trial and participant. This is a rather wide span for such a window and given the high heterogeneity in ratings (see Supplementary Materials S.4 for single subject average examples) it is not surprising that the peaks that were identified with this method deviate

slightly in their average from the data reported above. The oddball cycles in the high oddball condition were identified to be rated at VAS 5.5 ± 2.4, while the oddball cycles in the low oddball condition were identified at VAS 4.7 ± 2.3.

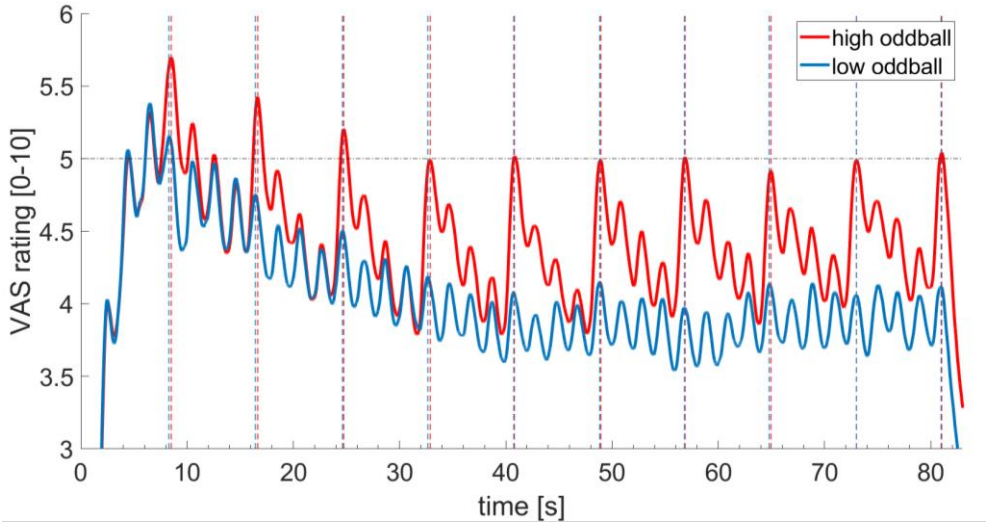

Figure 4: Group averages of the continuous ratings of perceived stimulus intensity [0-5] and painfulness [5-10] given on a visual analog scale (VAS) during each stimulus. The high oddball stimulation is colored in red, the low oddball stimulation is colored in blue. Vertical lines indicate the detected peak of the ratings for each condition. The horizontal line indicates the threshold from intensity to painfulness on the VAS.

Rating peaks related to the baseline stimulation cycles were identified at VAS 5.0 ± 2.1 for the high oddball condition and VAS 4.7 ± 2.0 for the low oddball condition. The LMM for each condition showed that oddballs were perceived as more intense than baseline in the high oddball condition ($F(750)=30.066$, $p<0.001$), while no significant difference was found between oddball and baseline stimulation in the low oddball condition ($F(750)= 0.0404$, $p=0.841$)(Figure 5). This confirmed hypothesis 1 for the high oddball, but not the low oddball condition. The relative difference between the VAS ratings relating to the oddball and baseline ratings peaks was calculated for each condition (hypothesis 2). This showed that the relative oddball ratings were significantly different from each other

(t(391)=7.437, p<0.001), high oddball peaks were perceived as more intense/painful than low oddball peaks (Figure 8).

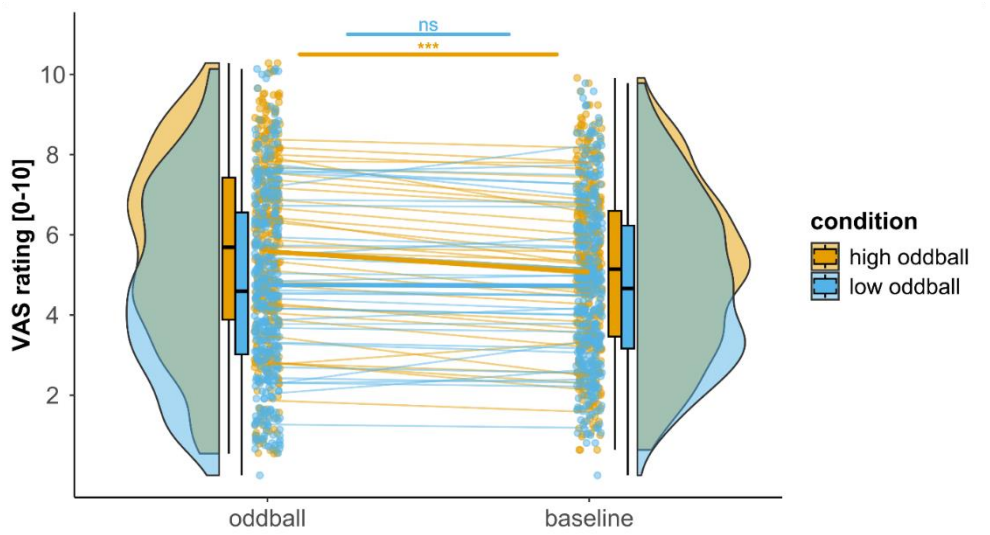

Figure 5: Continuous VAS ratings extracted at the maximal rating 1-2.6 sec after the stimulation peaks of both oddball and baseline stimulation. A separate model was run for each condition. The results of both LMM's are indicated using asterisks: ***p<0.001, ^{ns}p<0.05.

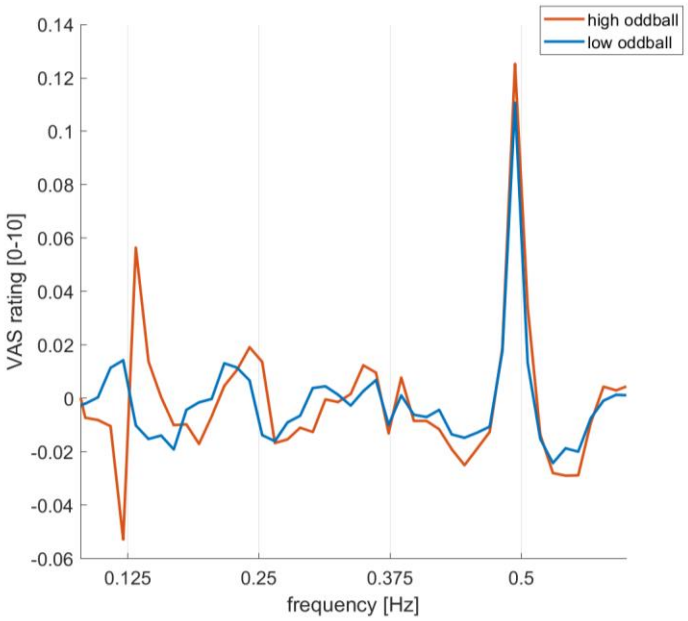

Figure 6: Exploratory behavioral analysis. Frequency-tagged continuous VAS ratings. Vertical lines indicate the FOS-oddball and its harmonics (i.e. 0.125 Hz, 0.25 Hz) as well as FOSbase (i.e. 0.5 Hz).

3.2 EEG recordings

3.2.1 Phase-locked response

In the phase-locked response, amplitudes significantly larger than zero (i.e. significant periodic response) were found at the FOS_{base} in both the high and low oddball condition (hypothesis 3a, positive control). Similarly, the right-tailed multi-sensor cluster-based permutation Wilcoxon signed-rank test identified a significant peak at the $FOS_{oddball}$ in both conditions (hypotheses 4a and 4b). A full table with the test-statistics can be found in the Supplementary Materials. Based on the electrodes with the largest test statistics at the FOS_{base} that were adjacent to each other, clusters of interest were built. Given the different topographies, these clusters vary between the conditions: for the high oddball condition, a fronto-central cluster was identified (CPz, Cz, C2, FC2, FCz). In the low oddball condition, the cluster was shifted towards contralateral parietal regions (C3, C5, CP5). A secondary cluster was identified which resembled more the cluster in the high oddball condition (CPz, Cz, C2, FCz, FC2, Fz).

The relative change in amplitude between oddball and baseline response was calculated for each condition and the relative change was compared between the conditions. While the peak related to the oddball stimulus was clearly distinguishable in the high oddball condition ($W(31)=414$, $p<0.001$), this was not the case in the clusters in the low oddball condition ($W(31)=299$, $p=0.327$; $W(31)=219$, $p=0.581$) (Figure 7). The comparison of the relative change between the conditions using a non-parametric paired t-test (hypothesis 5) revealed that the relative peak at the FOSoddball in the high oddball condition was significantly larger than the peaks at $FOS_{oddball}$ of the central ($W(31)=430$, $p<0.001$) and parietal cluster ($W(31)=365$, $p=0.021$) in the low oddball condition (Figure 8).

3.2.2 *Modulation of ongoing oscillations*

In the theta frequency band, the right-tailed multi-sensor cluster-based permutation Wilcoxon signed-rank test identified amplitudes significantly different from zero only at the FOS_{base} (hypothesis 3b) in the high oddball condition, but not at either of the $FOS_{oddball}$ (hypotheses 6a and 6b) (Figure 7). Two clusters were identified, a centro-parietal one contralateral (CP1, CP3, CP5, P5) as well as a smaller cluster ipsilateral to the stimulation side (CP4, C4, C2).

In the alpha frequency band, the responses at the FOS_{base} were significantly different from zero (i.e. showing a modulation of ongoing oscillations) in both conditions (hypothesis 3b). In the high oddball condition, a cluster at central electrodes contralateral to the stimulation side was identified (C1, C3, CP3, FC3). A very similar cluster was detected in the low oddball condition, shifted slightly to more parietal regions (C3, C5, CP3, CP5). Figure 9 illustrates the alpha band responses in those clusters in the frequency spectrum. No significant periodic response was detected at either $FOS_{oddball}$ (hypotheses 6a and 6b).

Only in the beta frequency band, a modulation of ongoing oscillations was found at both the FOS_{base} (hypothesis 3b) as well as the $FOS_{oddball}$ in the high oddball condition (hypothesis 6a). The response at FOS_{base} was relatively widespread in both conditions, leading to the identification of the same large cluster including central electrodes and electrodes contralateral to the stimulation side (Fz, F1, FCz, FC1, FC3, Cz, C1, C3). While no significant modulation was found at the $FOS_{oddball}$ in the low oddball condition (hypothesis 6b), some electrodes in the baseline cluster were also modulated in the response at $FOS_{oddball}$. Thus, 2 clusters of activity were identified at the $FOS_{oddball}$. One cluster composed of central electrodes (FCz, FC1, FC3, Cz, C1,C3) and one cluster of parietal electrodes (C5, CP3, CP5, P5).

As no modulation of ongoing oscillations was found at the frequency of the oddball in the low oddball condition in any of the frequency bands, no comparison of the relative oddball amplitudes between high and low oddball condition were carried out (as pre-registered, hypothesis 7).

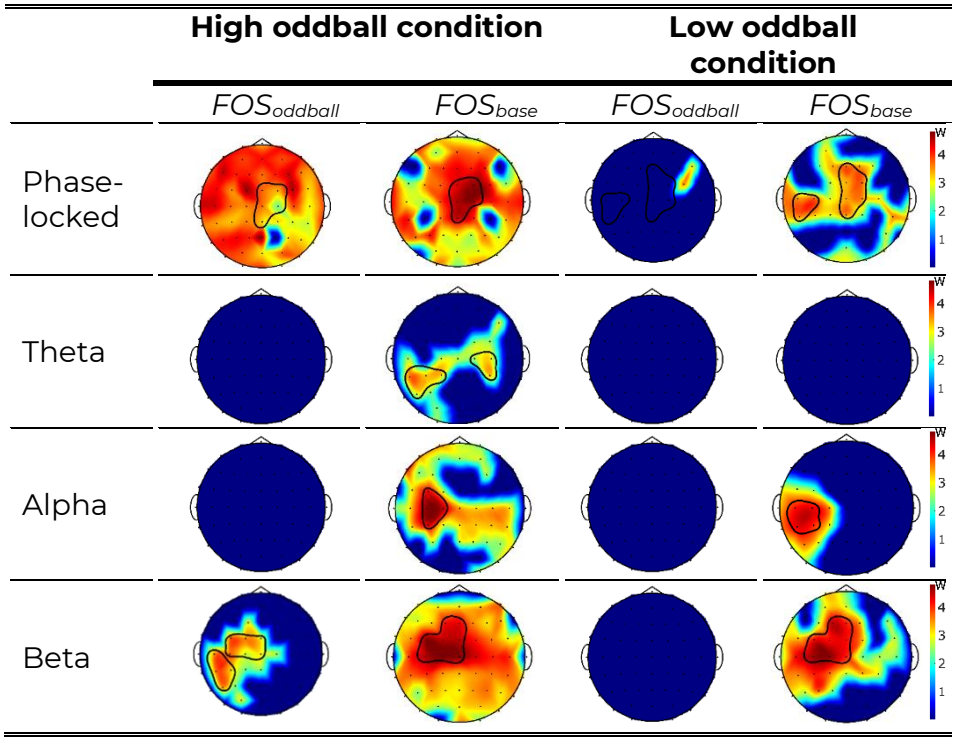

Figure 7: Topographies illustrating the magnitude of the right-tailed multi-sensor cluster-based permutation Wilcoxon signed-rank test statistic (W) for each condition and stimulation type. No significant modulation of ongoing oscillations was found at the FOSoddball in the low oddball condition. All topographies were plotted using the same scale.

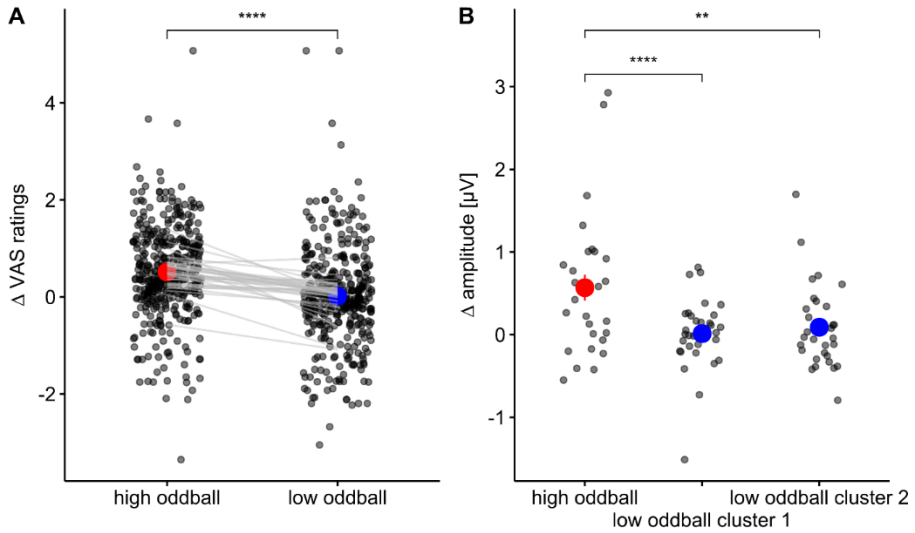

Figure 8: Oddball ratings (A) and phase-locked amplitudes (B) relative to each condition's baseline. Grey horizontal lines indicate the mean for each subject, colored dots indicate the mean for each condition. The following electrode clusters were formed: high oddball condition CPz, Cz, C2, FC2, FCz, low oddball condition cluster 1: CPz, Cz, C2, FCz, FC2, Fz and cluster 2: C3, C5, CP5 for the phase-locked response. Wilcoxon paired t-test: **p<0.01, ****p<0.0001.

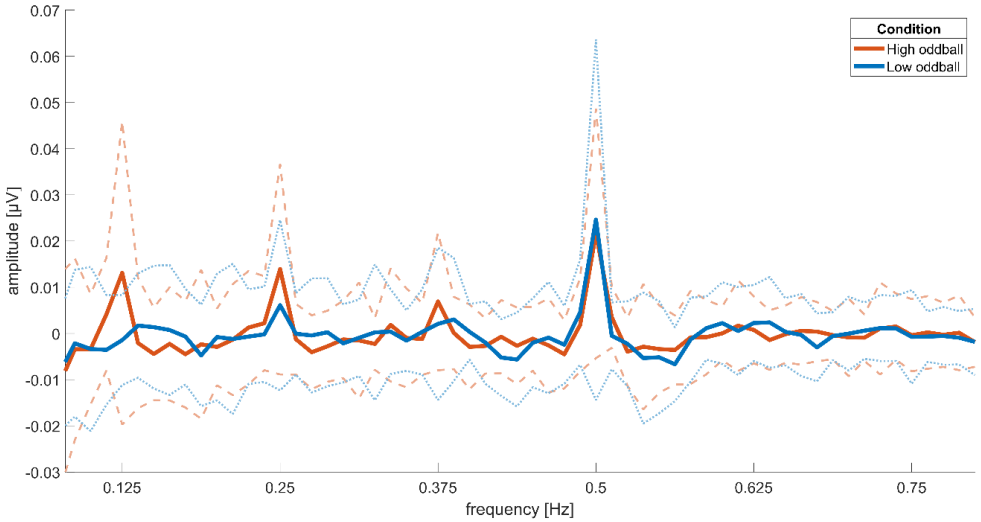

Figure 9: Spectrum of the estimated envelope of the EEG response in the alpha frequency band, illustrating the modulation of ongoing oscillations at the first few harmonics. X-axis indicators match the frequency of the oddball stimulation ($FOS_{oddball}$=0.125 Hz). The group mean for each condition is indicated in bold, dashed lines indicate the standard deviation from the mean. The electrode cluster in the high oddball condition comprises electrodes C1, C3, CP3, FC3; the low oddball cluster is made of electrodes C3, C5, CP3, CP5.

3.3 Exploratory analyses

3.3.1 Ratings

In addition to the registered analysis, we also employed the frequency-tagging analysis method to the continuous VAS rating. Given its high periodicity at the group-level, this exploratory analysis seemed to be an informative addition to the study as it allows a direct comparison with the obtained EEG responses. The continuous ratings in the frequency domain are illustrated in Figure 6. The visualization of the frequency spectrum of the continuous ratings highlights the tendency which has already been visible in the time domain: while a (visually) clear response was found at the $FOS_{oddball}$ in the high oddball condition, this was not the case for the low oddball condition. At the FOS_{base}, the magnitude of the responses seems to be similar. Generally, the rating peaks that relate to the FOS's are very close to the actual stimulation frequencies, showing that overall, the participants were quite accurate at following the periodicity of the stimulation with only small, but consistent delays.

3.3.2 EEG

Based on the clear peaks that could be visually identified in the spectra of the neural response in the frequency bands (see Figure 9 for an example), an exploratory analysis was added which took all harmonics up to the FOS_{base} into account for the analysis of the oddball response. Interestingly, the aggregation of the $FOS_{oddball}$ and its first two harmonics up to FOS_{base} (i.e. FOS_{agg}) did not change any results for the low oddball condition; as for the main analysis, no modulation of ongoing oscillations was found at the FOS_{agg}. Contrarily, including the first two harmonics in the high oddball condition (additional to the frequency of stimulation) showed that the oddball stimulation did lead to a significant modulation of ongoing oscillations at the aggregated amplitude in all three frequency bands

(Figure 10). To be consistent with the previous analysis, no new electrode clusters of interests were formed, but rather the clusters identified by the Wilcoxon signed-rank test at FOS_{base} were fitted onto the topographies of the FOS_{agg} test statistic. For the alpha and beta frequency bands, this approach led to a rather good match of electrodes with a high Wilcoxon test statistic between FOS_{base} and FOS_{agg}. Since none of the frequency bands showed a response at FOS_{agg} in the low oddball condition that was significantly different from zero, the relative oddball amplitudes were not compared (as pre-registered).

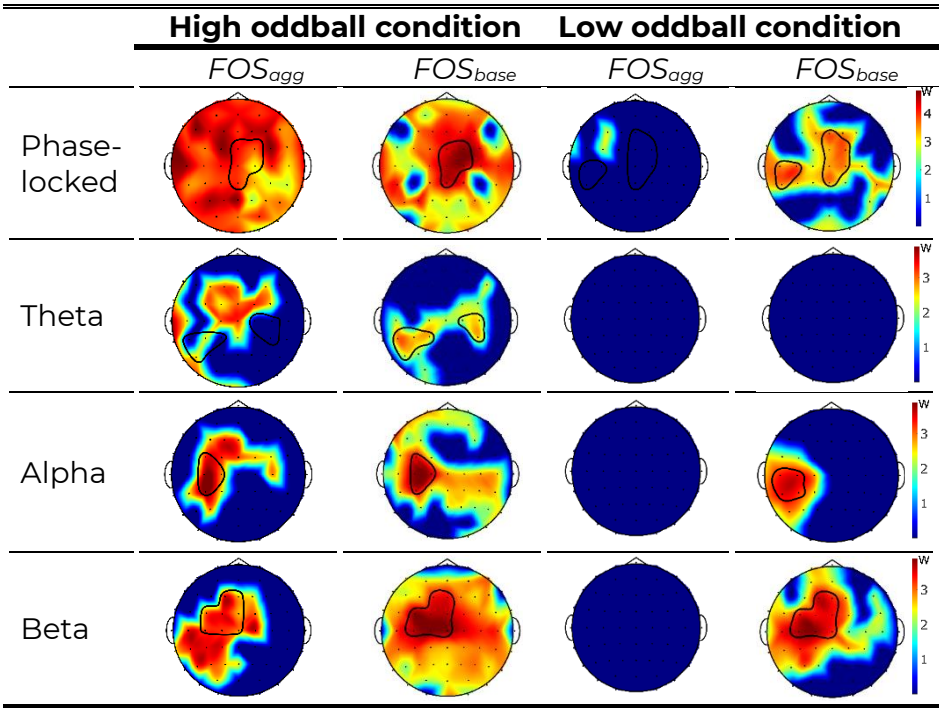

Figure 10: Exploratory analysis. The EEG signal at $FOS_{oddball}$ and its first 2 harmonics (i.e. 0.125 Hz, 0.25 Hz, 0.375 Hz) were aggregated into the FOS_{agg}, Topographies illustrate the magnitude of the right-tailed multi-sensor cluster-based permutation Wilcoxon signed-rank test statistic (W) for each condition and extracted amplitudes. No significant modulation of ongoing oscillations was found at the $FOS_{oddball}$ in the low oddball condition.

4. Discussion

In this investigation, we aimed to disentangle the relationship between the stimulus intensity, saliency and the thereby elicited modulation of ongoing oscillations. To achieve this, a sustained periodic oddball paradigm was designed, eliciting two main responses in the frequency domain at the $FOS_{oddball}$ (i.e. 0.125 Hz) and FOS_{base} (i.e. 0.5 Hz), which were measured both using scalp EEG as well as continuous ratings on a VAS scale. To differentiate between effects of intensity and saliency which are inherently tied to each other in a high intensity stimulation, a lower intensity control oddball stimulation was added.

At the group level, participants were able to trace the cycles of the sustained periodic stimulation throughout the entire trial in both conditions. The ratings associated to the oddball cycles in the high oddball condition were clearly distinguishable from the ratings relating to the baseline stimulation cycles, which was not the case for the low oddball condition. Further, the ratings of the high and low oddball cycles relative to their baseline differed significantly from each other. Taken together, these results suggest that – in this experimental design and in absence of a valid control condition - it was mainly the intensity of the stimulation that drove the ratings of perception.

A significant modulation of ongoing oscillations was found at the FOS_{base} in the theta, alpha and beta frequency bands in electrode clusters mostly contralateral to the stimulation side at frontal, central and parietal electrodes. Only in the beta frequency band during the high oddball condition, a modulation of ongoing oscillations was evidenced at $FOS_{oddball}$. Exploratory analyses demonstrated the importance of taking the harmonics of the $FOS_{oddball}$ into account and revealed that a modulation of

ongoing oscillations could be found at the $FOS_{oddball}$ in all frequency bands, but only in the high oddball condition.

These results could indicate that both stimulus perception as well as the modulation of ongoing oscillations are mainly influenced by stimulus intensity. Yet, the fact that the oddball was not perceived as significantly different from the baseline stimulation in the low oddball condition indicates that the chosen parameters might have not been sufficient to create an oddball that is salient (or intense) enough to elicit a clear response and is therefore not a valid control condition for our hypotheses. These results can therefore not disentangle the involvement of stimulus saliency or intensity in stimulus perception or modulation of ongoing oscillations.

4.1 Behavioral response

Extracting ratings for oddball and baseline stimulation cycles using the pre-registered method proved difficult at the single-subject level. Particularly in the low oddball condition, many participants struggled to perceive the individual stimulation cycles. Given these ambiguous ratings, the wide 1-2.6 second time window after the peak of each stimulus cycle resulted in potentially arbitrary data points, as it was unclear whether they truly corresponded to the perception at the peak of the stimulus cycle. Comparing single-subject data (Figure 5) to group averages (Figure 4) revealed a consistent shift of VAS 0.3., and given the consistency of this difference, the data points extracted on single subject level seemed appropriate for further analysis.

The LMM's confirmed that the oddball cycles led to significantly higher ratings of perception compared to baseline cycles of the stimulation in the high oddball condition. Additionally, this was the only stimulation that was on average perceived as painful (i.e. VAS rating ≥5). On the contrary, in the

low oddball condition, the oddball cycles were not perceived significantly different from baseline cycles of the stimulation. Thus, hypothesis 1 could only be confirmed for the high oddball condition. A similar difference between a high and low intensity (unattended) deviants has been observed in an ERP studies using auditory stimuli (Rinne et al., 2006) and brief laser stimuli (Legrain, Guérit, et al., 2003), in which only the strong intensity deviants led to the emergence of the P3a - an ERP component linked to novelty detection / involuntary orienting of attention - suggesting that the stimulus was not salient enough to capture involuntary attention. The underlying neuronal mechanism might be “transient detection”, a mechanism through which brief changes in the environment reset the neuronal adaptation to a stimulus, contributing to its saliency (Escera et al., 2000). This mechanism is highly relevant, especially in the context of painful stimuli, as they imply potential physical harm and an early detection of such an event is thus an innate protection mechanism.

There are other probable reasons as to why the low oddball cycles were not perceived as salient, such as the speed of the stimulation; it might be that the dip in intensity of the oddball stimulation cycle was too fast to be differentiated from the quickly following baseline stimulation cycle, creating a more diffuse sensation rather than a clearly perceivable negative peak. This is supported by the fact that for many participants, it was not possible to trace the stimulation cycle by cycle even for the baseline stimulation, making it even more difficult to perceive a brief change in the stimulation pattern at a lower intensity. Additionally, the temperature of the low oddball stimulation cycles in combination with the relatively low temporal precision of the underlying nociceptors should be considered. On one hand, C-fiber nociceptors (which are known to be primarily in this slow sustained periodic paradigm (Colon et al., 2017)) have rather low firing rate of around 15-20 Hz and it has been demonstrated that

this firing rate correlates / rises with the steepness of the heating ramp of the applied thermonociceptive stimulation (Yarnitsky et al., 1992). On the other hand, the temperature and heating profile with which the stimulation is applied at the skin surface does not necessarily correspond to the properties reaching the nociceptors (Magerl & Treede, 1996). This so called “heat sink-effect” from skin surface to the nociceptor level gets progressively larger, the faster the heating rate of the applied thermonociceptive stimulation (Tillman et al., 1995). Additionally, pain perception related to C-fiber nociceptor activation has been shown to be strongly influenced by spatial and temporal summations (Treede et al., 1990). Using stimuli of different durations (0.5s, 1s, 2s), a recent investigation demonstrated that only the longest stimulus duration led to pain ratings which could be differentiated (H. Wang et al., 2022).While direct comparison with their study is not possible due to individualized target temperatures ,this investigation highlights that - especially considering lower stimulation temperatures – temporal precision of perception limited. This effect is potentially amplified in the present experiment, as only a fraction of the 2s cycle was spent at the target temperature. Conversely, slower periodic stimulation paradigms have been shown to be easily trackable using continuous ratings, despite relatively small differences in stimulation intensity (Guo et al., 2020; Mulders et al., 2020), supporting the notion that temporal summation is an important aspect in the pain response to C-fiber activation using heat stimulation.

Furthermore, the offset analgesia phenomenon – characterizing a disproportionally large reduction in pain perception to a relatively small decrease in applied temperature of stimulation (Grill & Coghill, 2002)) - should be considered as a contributing factor for the relatively low ratings of stimulus perception. Even though the underlying mechanisms are not yet fully elucidated and are likely a combination of peripheral and central

mechanisms, the effect seems to be generally driven by a temporal filtering of the sensory experience (Mørch et al., 2015). Thus, an offset analgesic-like effect in the downward slope of the thermonociceptive stimulation could have overall attenuated the pain perception of the participants, despite the stimulation temperature being over generally accepted C-fiber related pain threshold (Treede et al., 1990).

Unsurprisingly given the above-mentioned results, the relative oddball ratings in the high oddball condition were significantly larger than in the low oddball condition (confirming hypothesis 2). While this could be interpreted as stimulation intensity being the main driving factor behind the perception of sustained periodic thermonociceptive stimulation, it should not be disregarded that the oddball in the low oddball condition failed to be perceived as significantly different from the baseline stimulation in the first place and is therefore not a valid control condition. Hence, no direct conclusions can be made regarding the involvement of saliency in the perception of these stimulations.

4.2 Neural response

The stimulation led to a significant periodic response at FOS_{base}, thus confirming the predefined positive control for the EEG response to the sustained periodic thermonociceptive stimulation (hypothesis 3a). In the phase-locked response, a widespread periodic response was found at the $FOS_{oddball}$ in the high oddball condition (confirming hypothesis 4a). In contrast, while a periodic modulation was found in very few electrodes also at $FOS_{oddball}$ in the low oddball condition (hypothesis 4b), the localization of those electrodes suggests that the recorded activity might be related to muscular artifacts. Additionally, many electrodes showed a periodic response between 0.1 Hz and 0.125 Hz, further supporting the notion that the low oddball stimulation was potentially “washed out” among the other

ongoing activities. The comparison of the amplitude relative to baseline at the $FOS_{oddball}$' showed a significantly larger periodic response in the high oddball condition (hypothesis 5). Yet, before these results are interpreted as evidence that intensity is the main contributing factor for the periodic response, it should be considered that the clusters of activity did not match between responses to oddball and baseline stimulation, making it difficult to build meaningful comparisons. Furthermore, given the minimal and diffuse effect the oddball had in the low oddball condition, this comparison should be interpreted cautiously.

A modulation of ongoing oscillations was found at the FOS_{base} of each frequency band in both conditions (hypothesis 3), except for the low oddball condition in the theta frequency band. This illustrates that generally, the sustained periodic stimulation pattern was successful, even though slightly adapted parameters were used compared to previous experiments using this approach (Colon et al., 2017; Leu et al., 2023; Leu et al., 2024; Mulders et al., 2020). The electrode clusters found in the alpha frequency band that showed a modulation of ongoing oscillation were located over the contralateral central-parietal (/sensorimotor) areas, matching previous results using sustained periodic sinusoidal stimulations (Colon et al., 2017; Leu et al., 2023; Leu et al., 2024; Mulders et al., 2020). The electrodes exhibiting a modulation of ongoing oscillations in the beta band were more widespread to frontal electrodes than expected; the previously mentioned investigations found activity within this frequency band to be primarily located at the same central-parietal electrodes as in the alpha band. Nevertheless, the clusters in both frequency bands were fairly consistent in the high and low oddball condition. This was not the case for the theta frequency band; instead of exhibiting a modulation in fronto-central electrodes as expected, activity was observed in an ipsilateral and contralateral parietal cluster (similar to

Colon et al. (2017)). Electrodes showing a modulation of ongoing oscillations have been inconsistent in previous experiments using similar stimulation parameters (Colon et al., 2017; Leu et al., 2023; Leu et al., 2024); some did not even find a significant modulation at all (Mulders et al., 2020).

Given the behavioral result, we did not expect to see a significant neural response at the $FOS_{oddball}$ (i.e. 0.125 Hz) in the low oddball condition. At the $FOS_{oddball}$ (i.e. 0.125 Hz), the main analysis revealed a significant modulation only in the beta frequency band at central and parietal electrodes at the $FOS_{oddball}$ in the high oddball condition (hypothesis 6a). This could indicate that the oddball stimulation cycles were not able to elicit a consistent modulation of ongoing oscillations (disconfirming hypothesis 6b), regardless of the stimulation intensity and thus that ratings and neural response were dissociated from each other. Yet, at the time of writing the Stage 1 of this RR, the author team had underestimated the relevance of the harmonics that are inherently present in the frequency representation of a signal. Retter et al. (2021) published a compelling discussion of the importance of these harmonics and provided evidence that, if harmonics are neglected in the analysis, a relevant portion of the neural response is lost. Additionally, they demonstrated that both low stimulation frequencies and non-sinusoidal stimulation patterns led to a larger number of relevant harmonics (Retter et al., 2021). Given our experimental setup, it was thus worth examining the obtained frequency spectra (see Figure 9) and relevant activity was found at least at the first 2 harmonics of the $FOS_{oddball}$ before the frequency relating to the baseline stimulation (FOS_{base}). We therefore added an exploratory analysis to this RR, which included these two harmonics for the assessment of the response at the $FOS_{oddball}$ (Heinrich et al., 2009; Milton et al., 2020). The results of this exploratory analysis showed a significant modulation of ongoing oscillations at the aggregated oddball frequency (FOS_{ass}) in the high

oddball condition for all frequency bands (confirming hypothesis 6a). The lack of such a modulation in the low oddball condition (disconfirming hypothesis 6b) might indicate that (at least given the present experimental setup) stimulus intensity could be the main driving factor behind the magnitude of synchronized neural activity leading to a measurable modulation of ongoing oscillations.

4.3 Relationship between neural and behavioral responses

While not a primary outcome of this Registered Report, the obtained results invite for a comparison between the obtained neural and behavioral responses. Specifically, this potential relationship is illustrated in the comparison of modulation of ongoing oscillations and variations in the perception of the stimulation in the frequency domain. Both spectra show significant peaks at the $FOS_{oddball}$ in the high oddball condition only, suggesting that perception and modulation of ongoing oscillations are to some extent related to each other. This falls in line with other investigations that found that ongoing oscillations are modulated relative to the (perceived) intensity of the applied stimulation (Hauck et al., 2015; Huishi Zhang et al., 2016; Nickel et al., 2017; Schulz et al., 2015; Tiemann et al., 2015; H. Wang et al., 2022; Zhang et al., 2012). Yet, just as these other investigations, we were not able to determine to which extent the observed relationship is based on the (perceived) stimulus intensity or saliency.

In closing, we would like to highlight the difficulty of designing an experimental paradigm that is able to differentiate between stimulus intensity and saliency, two factors that are inherently tied to each other. The “triplet ERP paradigm” is a very elegant solution to this problem, applying triplets (i.e. three consecutive stimuli applied with a fixed 1s

interstimulus interval within the consecutive stimuli) of brief laser stimulations delivered at the same intensity, thereby reducing the saliency of the stimulation with each repetition while keeping the objective intensity constant (Iannetti et al., 2008). Adapting this approach to fit the necessary periodic stimulation parameters to be able to frequency-tag the modulation of ongoing oscillations proved to be a challenge. While in the final paradigm, a rather simple variation of intensity was used to elicit the oddball sensation, we piloted a multitude of alternatives involving changing stimulation surfaces, temperatures and frequencies of stimulation, of which all had serious caveats for the interpretation of the results. Thus, it seems that frequency-tagging is perhaps not the ideal technique to disentangle effects of saliency and intensity in behavioral and neural responses elicited by thermonociceptive stimulation.

5. Conclusion

In conclusion, our results suggest that stimulus intensity has a potentially large effect on both the modulation of ongoing oscillations and the stimulus perception elicited by sustained periodic thermonociceptive stimulation. Yet, given the fact that our control condition did not have the desired effects on the behavioral and neural level, we are not able to disentangle to which extent stimulation saliency affected the observed responses. These findings highlight the challenges of unraveling the contributions of saliency and intensity to the modulation of ongoing oscillations by integrating an oddball paradigm into the frequency-tagging approach.

Acknowledgements

This study was supported by the FRIA doctoral grant of CL by the Belgian Fund for Scientific Research (F.R.S.–FNRS, grant number: 5118622) and by a prize from the Fondation Medicale Reine Elisabeth (F.M.R.E) awarded to GL. GL is funded by F.R.S.-FNRS. We would like to thank Wumeng Wang for his help with data acquisition and subject recruitment, the NOCIONS lab for insightful discussions and the CATL team of our department for technical assistance.

The authors declare no conflict of interest.

Author contributions

Conceptualization: CL, GL; Methodology: CL, SF, GL; Software: CL, SF; Investigation: CL, SF; Formal analysis: CL; Funding Acquisition: CL, GL; Writing – original draft: CL; Writing – review & editing: CL, SF, VL, GL

Appendices

I. Hypotheses table and sampling plan

Question	Hypothesis	Analysis Plan	Interpretation given different outcomes
1) Is the oddball perceived as different than the baseline stimulation in both conditions (i.e., high and low oddball)?	The intensity rating of the oddball stimulation will be different than the rating for the baseline stimulation in both conditions.	LMMs: $Rating_{high}$ ~ stimulus+(1|subject) $Rating_{low}$ ~ stimulus + (1|subject) $Rating_{high}$= high oddball $Rating_{low}$= low oddball	A significant simple effect of "stimulus" would indicate that the oddball paradigm is working as intended and elicited a change in perception in this condition. If no difference is perceived in one specific condition, the oddball might not have been salient enough to change perception. In those cases, based on our main hypothesis, we would not expect to find a modulation of ongoing oscillations at the frequency of stimulation of the corresponding oddball ($FoS_{oddball}$). ‡
2) Does the relative peak of the rating related to the high oddball differ from the rating of the low oddball?	If the oddball perception is driven by the intensity of the stimulus, the high oddball will be perceived as more intense than the low oddball.	Paired t-test of the Δ (baseline-oddball) between high and low condition.	A difference between the ratings would show that the objective intensity of the oddball is driving the subjective perception. If the oddballs had similar peaks, it could indicate that the perception is rather based on the saliency of the stimulus. ‡
Time-locked, phase-locked response			
3a) Does the sustained periodic stimulation lead to a periodic EEG modulation at FoS_{base} in both conditions?	The slow sustained periodic stimulation paradigm will lead to a periodic modulation of the EEG signal at the FoS_{base}.	Multi-sensor cluster-based permutation Wilcoxon signed-rank test of amplitudes at the FoS_{base}.	Positive control: If the expected neural activity is not induced by the baseline stimulation in the stimulation paradigm (results of the one-sided Wilcoxon signed-rank test show that the amplitude at FoS_{base} is not significantly different from zero), the fundamental assumption for using the frequency-tagging approach in this study would not be met.
4a) Does the oddball stimulation lead to a periodic modulation of the EEG signal at the $FoS_{oddball}$ in the high oddball condition?	The oddball paradigm will lead to a periodic modulation of the EEG signal at the frequency at which the oddball was presented in the high oddball condition.	Multi-sensor cluster-based permutation Wilcoxon signed-rank test of amplitudes at the $FoS_{oddball}$ in the high oddball condition.	A modulation (amplitude significantly larger than zero in Wilcoxon signed-rank test) at the frequency of the high oddball would indicate that the paradigm was successful in eliciting a periodic response related to the oddball. If no peak can be detected, the paradigm did not work as intended for the phase-locked response. ‡
4b) Does the oddball stimulation lead to a periodic modulation of the EEG signal at the $FoS_{oddball}$ in the low oddball condition?	The oddball paradigm will lead to a periodic modulation of the EEG signal at the frequency at which the oddball was presented in the low oddball condition.	Multi-sensor cluster-based permutation Wilcoxon signed-rank test of amplitudes at the $FoS_{oddball}$ in the low oddball condition.	Control condition: A modulation (amplitude significantly larger than zero in Wilcoxon signed-rank test) at the frequency of the low oddball would indicate that an oddball with a lower stimulation intensity than the baseline stimulation is able to elicit a neural response. No peak might indicate that the oddball delivered at a low stimulation intensity was not intense or salient enough to induce a periodic response. ‡
5) Does the high oddball lead to a larger relative response in the EEG signal at the $FoS_{oddball}$ than the low oddball in the frequency-domain?	The amplitude at the $FoS_{oddball}$ in the high oddball condition will be similar to the amplitude at the $FoS_{oddball}$ in the low oddball condition.	Paired t-test of the difference (Δbaseline-oddball) between high and low oddball condition.	A similar amplitude of the oddball in the high and low oddball condition would support the notion that the oddball response is mainly driven by the saliency of the stimulus. If the oddball in the low oddball condition leads to a smaller response compared to the oddball in the high oddball condition, it could suggest that the intensity of the stimulus is more prominently reflected in the periodic response related to the oddball than saliency. ‡

Time-locked, non-phase-locked response			
3b) Does the sustained periodic stimulation lead to a periodic EEG modulation at FoS_{base} in both conditions?	A periodic modulation of the EEG signal will be elicited in all frequency bands for the FoS_{base} in both conditions.	Multi-sensor cluster-based permutation Wilcoxon signed-rank test of amplitudes at the FoS_{base} †.	A modulation (amplitude significantly larger than zero in Wilcoxon signed-rank test) at the frequency at FoS_{base} indicates that sustained periodic stimulation leads to a periodic response in the different frequency bands (Colon et al., 2017) in both conditions. No periodic response would indicate that the sustained periodic stimulation paradigm was not successful in inducing a periodic modulation.
6a) Does the oddball stimulation lead to a modulation of ongoing oscillations at the $FoS_{oddball}$ in the high oddball condition?	The oddball paradigm will lead to a modulation of ongoing oscillations at $FoS_{oddball}$ in the high oddball condition.	Multi-sensor cluster-based permutation Wilcoxon signed-rank test of amplitudes at the $FoS_{oddball}$ in the high oddball condition.	A modulation (amplitude significantly larger than zero in Wilcoxon signed-rank test) at the frequency of the oddball would indicate that the paradigm was successful in eliciting a neural response related to the oddball. No peak at $FoS_{oddball}$ would indicate that the chosen oddball parameters were not intense or salient enough to elicit a modulation of ongoing oscillations. ‡
6b) Does the oddball stimulation lead to a periodic modulation of the EEG signal at the $FoS_{oddball}$ in the low oddball condition?	The oddball paradigm will lead to a modulation of ongoing oscillations at $FoS_{oddball}$ in the low oddball condition.	Multi-sensor cluster-based permutation Wilcoxon signed-rank test of amplitudes at the $FoS_{oddball}$ in the low oddball condition.	Control condition: A modulation (amplitude significantly larger than zero in Wilcoxon signed-rank test) at the frequency of the oddball would indicate that an oddball with a lower stimulation intensity than the baseline stimulation is able to elicit a neural response. No peak at $FoS_{oddball}$ might indicate that the oddball in the low oddball condition was not intense or salient enough to lead to the expected response. ‡
7) Does the high oddball lead to a larger relative response in the EEG signal at the $FoS_{oddball}$ than the low oddball in the different frequency bands?	The amplitude at the $FoS_{oddball}$ in the high oddball condition will be similar to the amplitude at the $FoS_{oddball}$ in the low oddball condition.	Paired t-test of the Δ (baseline-oddball) between high and low oddball condition. †	A similar amplitude of the oddball in the high and low oddball condition would suggest that the oddball response is mainly driven by the saliency of the stimulus. If the oddball in the low oddball condition would lead to a smaller response compared to the oddball in the high oddball condition it would suggest that the intensity of the oddball stimulus is reflected more prominently in the corresponding modulation of ongoing oscillations than saliency.

Abbreviations. LMM: Linear mixed model; $amplitude_{FoS}$: amplitude at the frequency of stimulation FoS_{base}: amplitude at frequency of baseline stimulation; $FoS_{oddball}$: amplitude at frequency of oddball stimulation. † One test for each frequency band (theta, alpha, beta)

‡ As the sample size is not sufficient to detect the smallest possible effect one would still be interested in (see explanation below), a non-significant result does not necessarily indicate that there is a definitive absence of an effect and no definitive conclusions can be drawn from a non-significant result (Dienes, 2021).

Sampling plan:

To reach an overall statistical power of 0.9 with an alpha level of 0.02, 30 participants would suffice according to our data stimulation (using estimated effects based on previous investigations). To account for potential dropouts (e.g., statistical outliers, incomplete data sets) and to ensure that we will still reach out targeted power, 35 participants will be enrolled. Calculations were carried out in the software G*Power (V. 3.1.9.7.) (Faul et al., 2007) (see below). This sampling size also surpasses previous investigations investigating bottom-up modulations of ongoing oscillations (n= 21, 20) (Hauck et al., 2015; Tiemann et al., 2015), using a frequency-tagging approach (n=8, 15) (Colon et al., 2017; Mulders et al., 2020) or using periodic oddball paradigms (n = 10 to 12) (De Keyser et al., 2018; Lochy et al., 2015; Rossion et al., 2015).

Rationale for deciding the sensitivity of the test for confirming or disconfirming the hypothesis:

For each statistical test, the effect size was estimated and the sample size necessary to reach the desired statistical power was calculated separately. For the EEG analysis, G*Power was used to calculate the required sample sizes for the Wilcoxon signed-rank test as well as for the paired t-test. In summary, adopting observed effect sizes from previous investigations using similar paradigms, the proposed statistical tests require 10, 30, 16 and 22 participants respectively to reach a power of 0.9 with an alpha level of 0.02. Therefore, to satisfy the minimum requirements for each test, we will aim for a minimum sample size of 30 participants and enroll 35 participants in the experiment.

To control for type II error rates beyond the effects found in previous studies, the “smallest effect ones does not want to miss out on” was calculated and used as the targeted effect size for each statistical test (Dienes, 2021). To find these effect sizes, the 80% confidence interval of the

expected effect was calculated and the lower bound chosen for the final expected power calculation (Perugini et al., 2014). Unfortunately, our lab does not have the resources to recruit such large sample sizes (see detailed description below). This means that for the statistical tests where the sample size is not sufficient to detect the smallest effect that we would still be interested in, no final conclusions will be made on the definitive absence of an effect in case of non-significant results.

Based on previous results from our lab (Leu et al., 2023) and results from oddball investigation in the visual field (Rossion, 2014; Rossion et al., 2015), we expect a large effect in our sample for the detection of a peak at the frequency of the baseline stimulation. Given a normally distributed sample, an alpha level of 0.0125 (corrected for multiple comparisons) and a one-sided Wilcoxon signed-rank test against a constant and an effect size of Cohen's d=1.4, we would need to recruit 10 participants to reach the targeted statistical power. To control for the smallest possible effect we would still be interested in, the data of ~30 participants would suffice. The effect size associated with this sample size would be d=0.69 for this statistical test.

Based on other oddball paradigm investigations (Rossion et al., 2015), we expect a medium-to-large effect size for the detection of peaks related to the oddball stimuli in the two conditions (amplitudes about half the size of the baseline responses). Given a normally distributed sample, a one-sided Wilcoxon signed-rank test against a constant, an alpha level of 0.0125, power of 0.9 and an effect size of d=0.7, we would need to recruit 30 participants to reach our target. To test for the smallest effect we would still be interested in, the recruitment of 160 participants would be necessary.

Since the comparison between the EEG amplitudes related to the painful periodic oddballs in the two conditions using a paired t-test is rather

experimental, we could unfortunately not find any data from which we could approximate an effect size. Additionally, the t-test will only be carried out in case of significant result in all Wilcoxon one-sample t-tests. This also means that the eventual results of this test will have to be interpreted with caution, and eventual negative (i.e., non-significant) results do not necessarily mean that there is no effect present, since we are not sure whether we missed small effects that we would theoretically still be interested in (Dienes, 2021).

Data on the perceived level of stimulus intensity following sustained periodic heat stimuli is scarce. As an approximation, we used the effect size of the ANOVA main effect of *temperature* reported in Mulders et al. (2020), since a similar sustained periodic stimulation paradigm was used in that investigation with varying surface temperatures (warm, cold). The main effect of *temperature* had an effect size n_2^p=0.658. As we do not use cold stimuli in a separate trial, but heat stimuli of different intensities, we expect that the effect size in our sample will be smaller. Nevertheless, as the effect found in Mulders et al. (2020) was very large, we can still assume to find effects that are on the larger side. Specifically, for the high oddball condition, we expect a slightly larger effect than for the low oddball condition, based on the observations in our pilot experiment. We estimated an effect size of n_2^p=0.2 for the high oddball condition and an effect size of n_2^p=0.15 for the low oddball condition. As sample size calculations for LMMs are not feasible in G*Power, we approximated the model using the calculation for a repeated measures ANOVA, with within factors only. 1 group was compared along 2 measurements, with a correlation among repeated measures of 0.5 and a non-sphericity correction of 1. A separate calculation was done for each oddball condition. Given the effect size we estimated, a target power of 0.09 with an alpha level of 0.02, we should test 16 participants for the high oddball condition

and 22 participants for the low oddball condition. After transforming the n_2 into an effect size expressed in Cohen's d, the conversion table proposed in Perugini et al. (2014) was used to find the sample size needed to test for the smallest effect size that would still be interesting. This led to a recommendation of between 74 (high oddball) and 160 (low oddball) participants for this experiment.

II. Pilot study

To make sure that participants will be able to trace their perception of the sustained periodic stimulation paradigm on the VAS slider (min: no perception, middle: starting to be painful, max: maximal painfulness imaginable) and perceive differences between baseline and oddball stimuli, we conducted a behavioral pilot study (10 healthy participants, 5 female, age: 24.4 ± 2.4 years old, 5 left handed) using the same parameters as described in the main manuscript. One participant had to be removed from the pilot data set due to corrupted data.

After a brief familiarization using 2 trials of warm periodic stimuli at the frequency of stimulation of the main experiment (i.e., 0.5 Hz) during which participants learned how to use the VAS slider was implemented, the staircase procedure defined the individual pain threshold was carried out.

In the main pilot experiment, 8 trials were administered in 2 blocks of 4 stimuli, counterbalanced between high and low oddball condition. The participants were asked to trace their perception of the stimulation as well as they could on the VAS. Additionally, they had to provide a verbal description of their perception of the stimuli. This was done to assess whether they would be able to perceive any sort of periodicity or oddball within each of the conditions. Across all subjects, the pain threshold was identified at 50.1°C (range: 51°C to 48.5°C). All participants were able to follow the periodic stimulation pattern with the VAS but were not able to

consciously detect a pattern in the stimulation. The group average of the VAS responses following stimulation using the high oddball condition is illustrated in Figure S.1. On average, the peak of the ratings followed 1.28 ± 0.17 seconds after the peak of the oddball stimulation. Generally, the peaks were rated somewhat faster at the beginning of the stimulation and slowed down towards the end of the stimulation (1st peak rating: 0.92s after stimulation peak, 9th peak rating 1.39s after the peak of the stimulation). Participants clearly perceived the high oddball as more painful than baseline stimulation. As temperatures were adapted to the individual, only one person had to stop a trial due to discomfort.

Trials delivered using a low intensity oddball were overall perceived as less painful (Figure S.2). Still, the oddball can be clearly differentiated from the baseline stimulation. The peak of the oddball ratings followed on average 2.33 ± 0.19 seconds after the peak of the oddball stimulus and didn't vary much across the duration of the stimulation. The peaks of the baseline stimulation were always perceived as painful, whereas the peaks associated with the low oddball were merely perceived as very intense (rating below 5 on the VAS).

Overall, the pilot study confirmed that both the high and low oddball stimuli can be differentiated from the baseline stimuli and lead to a periodic response in the VAS ratings. Additionally, we were able to show that even though ratings vary based on the applied stimuli, participants were not able to detect a pattern within the trials, minimizing effects of e.g., expectation. Thus, this pilot study supports that – using the proposed experimental setup –, we will be able to modulate pain perception as planned.

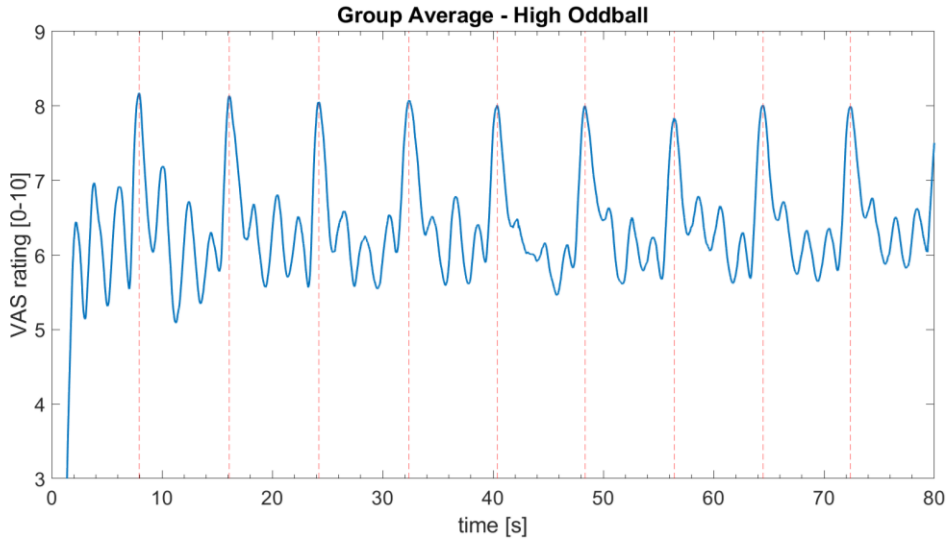

Figure S.1: Group and trial averages of the continuous rating provided by the participants during the stimulation on a Visual Analog Scale (VAS) during stimulation trials using a high intensity oddball stimulation. Vertical red lines represent the peak of the rating related to the oddball stimulation. The VAS scale ranged from 0 (start of perception) over 5 (start of painfulness) to 10 (maximum painfulness imaginable).

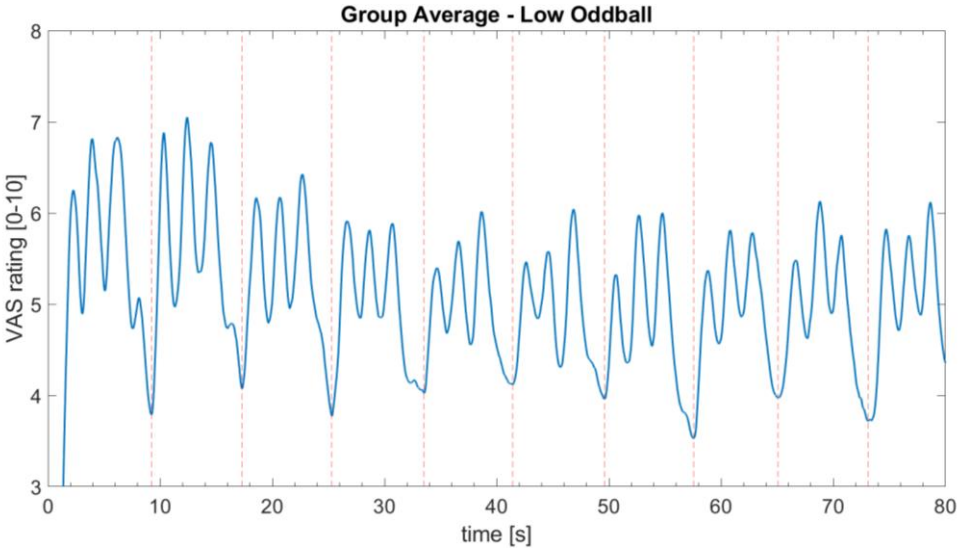

Figure S.2*:* Group and trial averages of the continuous rating provided by the participants during the stimulation on a Visual Analog Scale (VAS) during stimulation trials using a low intensity oddball stimulation. Vertical red lines represent the peak of the rating related to the oddball stimulation. The VAS scale ranged from 0 (start of perception) over 5 (start of painfulness) to 10 (maximum painfulness imaginable).

III. Amendment of methods: Pilot study with adapted parameters for RR Stage I

Despite our previous pilots, it appeared that the final experiment was not as well tolerated as we expected. We therefore decided to adapt the parameters of the stimulation to make the experiment overall less painful, while keeping the same paradigm and hypotheses. To show that these adaptations do not lead to a deviation from the registered hypotheses, a pilot experiment was conducted on 7 healthy participants (age: 25.9 ± 3.3 years old, 2 males). The pilot subjects had to trace their perception of the stimuli using a Visual Analog Scale (VAS) with the same scale as for the registered experiment, following the same staircase procedure as previously described. The general parameters of the registered experiment were used except for:

We adapted the range of the oddball. Instead of adding/subtracting 3°C to the baseline for the high/ low oddball condition, we used a 2°C difference. Additionally, the staircase procedure to identify the pain threshold started at 49°C instead of 50°C, hoping to set a lower “anchor” for the perception of the participants. A further change was that the participants could only chose a baseline stimulus up to 51°C instead of 53°C, to avoid any potential skin damage due to the long-lasting nature of our stimuli. Finally, we also changed the probe that was used to deliver the thermonociceptive stimuli. We chose the “standard” T03 probe (also provided by QST.labs), which has been previously used in our lab for similar experiments (Leu et al., 2023; Mulders et al., 2020). The probe has a maximal heating rate of 300°C/s and is set with 15 micro-Peltier elements, resulting in a stimulation surface of 115,5 mm^2. This last adaptation was chosen to avoid excessive sensitization of the skin, as we noticed that the much larger probe, we used previously did not allow us to change the position of the probe sufficiently without touching previously stimulated skin areas.

None of the participants were able to find a stimulation pattern in either of the oddball conditions. As illustrated in Figure S.3, the high intensity oddballs still led to a clear difference in perception. Overall, the perception of the stimulus is lower than in the previously registered pilot, but we believe that this is a necessary adjustment to ensure that the experiment is tolerable for the participants in its full length. On average, the peak of the ratings followed 1.84 ± 0.23 seconds after the peak of the high oddball stimulation. Figure S.4 illustrates the results following stimuli in the low oddball condition. It seems that the changed parameters lead to a less clearly perceivable decrease in stimulation intensity. Yet, the changes observed in this pilot could indeed be related to the saliency of the lower oddball (as described in the first hypotheses). Low intensity oddballs were perceived at a similar delay as for the high intensity (1.67 ± 0.15 seconds after the peak).

We would therefore argue that the adapted parameters are a necessary modification of the registered experiment, which does not dramatically change the perception of the stimuli and seems to make the experiment more tolerable for the participants.

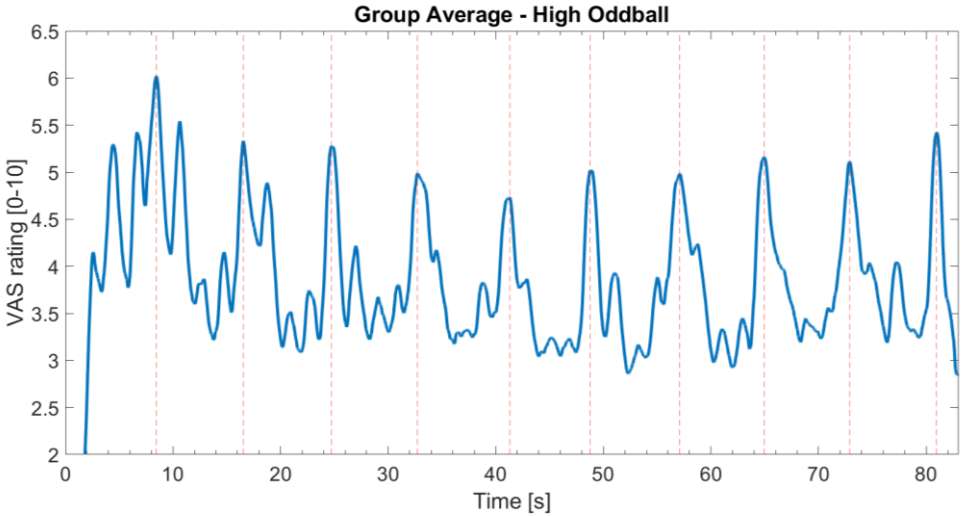

Figure S.3: Group and trial averages of the continuous rating provided by the participants during the stimulation on a Visual Analog Scale (VAS) during stimulation trials using a high intensity oddball stimulation. Vertical red lines represent the peak of the rating related to the oddball stimulation. The VAS scale ranged from 0 (start of perception) over 5 (start of painfulness) to 10 (maximum painfulness imaginable).

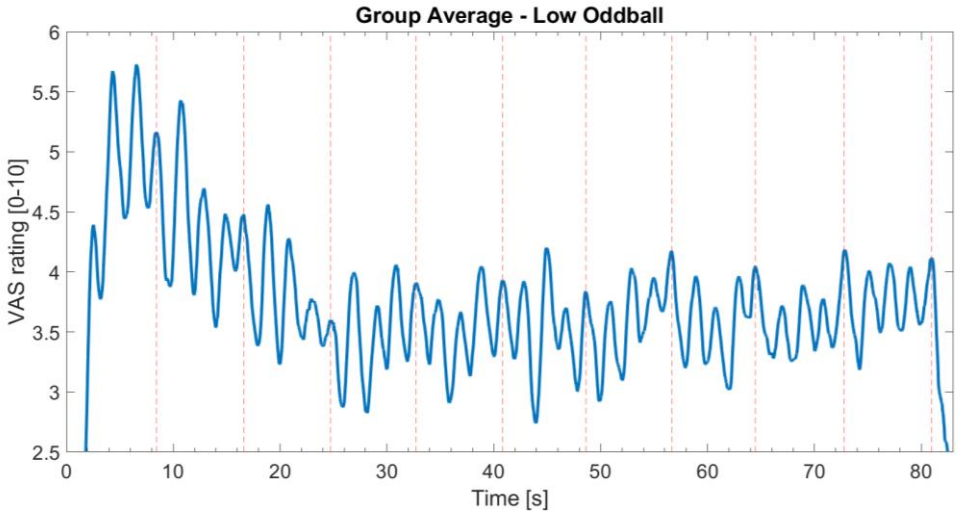

Figure S.4: Group and trial averages of the continuous rating provided by the participants during the stimulation on a Visual Analog Scale (VAS) during stimulation trials using a low intensity oddball stimulation. Vertical red lines represent the peak of the rating related to the oddball stimulation. The VAS scale ranged from 0 (start of perception) over 5 (start of painfulness) to 10 (maximum painfulness imaginable).

VI. Single subject average examples of stimulus perception ratings

High intensity oddball condition

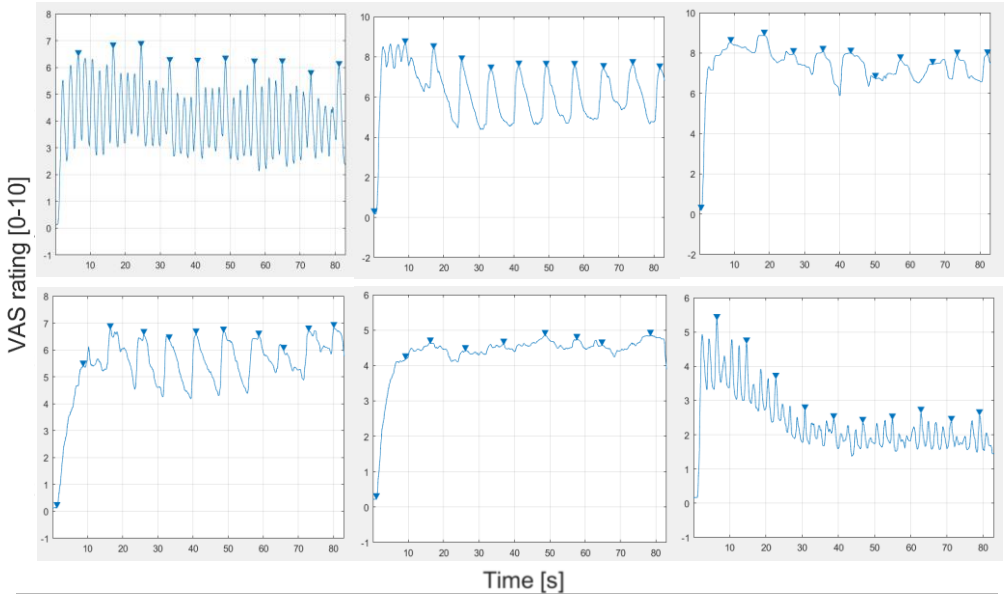

Low intensity oddball condition

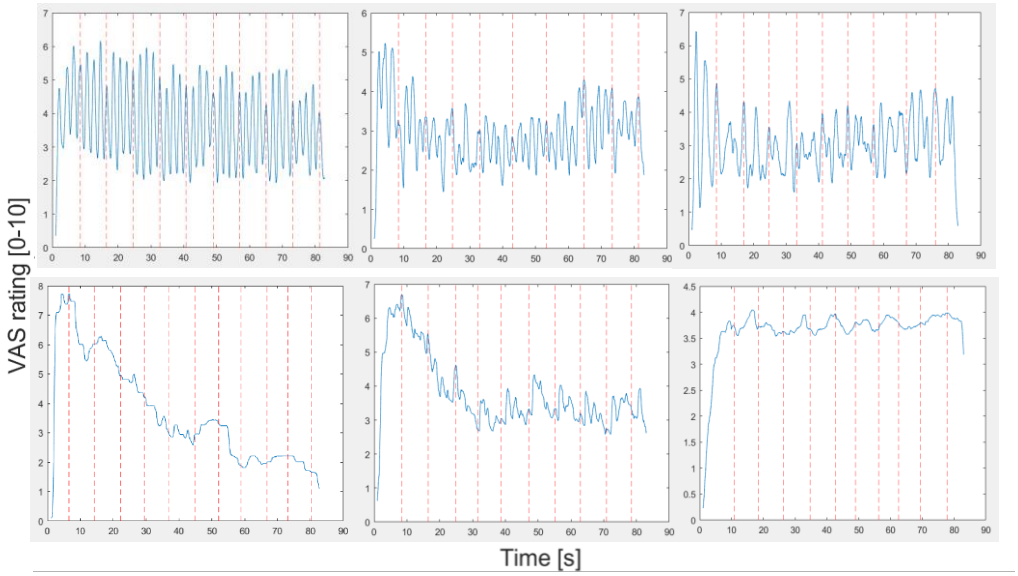

VII. Frequency spectra

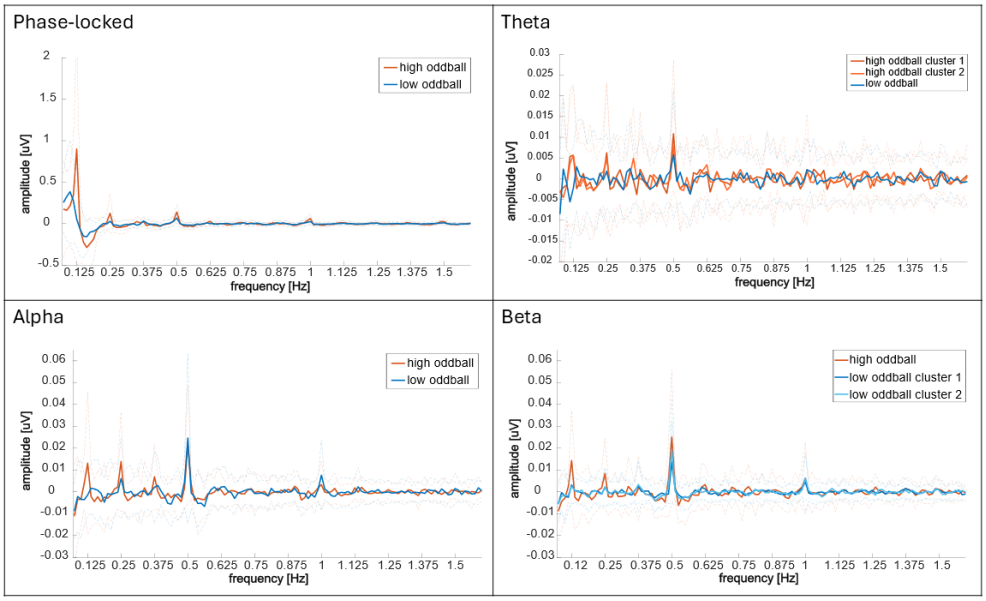

Figure S.5: Frequency spectra illustrating the means ± standard deviation of each condition and cluster for the phase-locked response, and the signal in the theta, alpha and beta frequency bands.

CHAPTER 5. Linking the modulation of ongoing neural oscillations to thermonociception using intracerebral EEG: insights from the posterior insula

Abstract

The human insular cortex is involved in a multitude of processes essential for survival, but its precise role in pain perception remains debated. While it has been shown that ongoing oscillatory activity in the posterior insula is preferentially modulated by thermonociceptive input, it is unclear whether these modulations are functionally related to changes in pain perception. To assess this link, neural responses to sustained periodic thermonociceptive and non-nociceptive vibrotactile stimulation delivered at a frequency of 0.2 Hz were measured using intracerebral electrode contacts located in the anterior (n= 48) and posterior (n= 19) insular cortices of 8 patients undergoing presurgical evaluation for focal epilepsy. An arithmetic task was employed concomitant to the stimulation, aiming to shift the participants' attentional focus away from the stimulation. A frequency-tagging analysis approach was used to assess the modulation of the ongoing neural oscillations. As expected, the perception of the stimulation was significantly reduced during the arithmetic task in both modalities, with a stronger decrease during vibrotactile stimulation. Moreover, in the posterior insula, the arithmetic task led to a significant reduction of the modulation of ongoing alpha oscillations induced by thermonociceptive stimulation, whereas the modulation of these oscillations did not differ between conditions for the vibrotactile stimulation. The concomitant decrease in the perception of the thermonociceptive stimulation and in the modulation of ongoing oscillations in the posterior insula during the distraction task suggests that this region could be functionally related to the perception of thermonociceptive stimulation. Additionally, the absence of such a relationship following vibrotactile stimulation suggests that this relationship could be preferential for thermonociceptive stimulation.

1. Introduction

Pain perception is associated to the interaction of multiple brain regions such as the anterior cingulate cortex (ACC), primary and secondary somatosensory cortices (S1, S2), thalamus, prefrontal cortex (PFC) and the insular cortex (Apkarian et al., 2005; Treede et al., 1999). Yet, the underlying mechanisms leading to the experience of pain caused by a nociceptive stimulus remain elusive (Mouraux & Iannetti, 2018). The human insular cortex is a promising target to deepen the understanding of these mechanisms, as it has been shown to be consistently activated by nociceptive stimuli perceived as painful (Apkarian et al., 2005; Becerra et al., 1999; Freund et al., 2009), serves as a relay and integration "hub" for sensory information, and plays an important role in interoception and emotional regulation (Gogolla, 2017; Kurth et al., 2010; Shura et al., 2014; Zhang et al., 2024). Crucially, while the anterior portion of the insular cortex is mainly involved in the cognitive and emotional processing of a painful stimulus (Geuter et al., 2017; Hein & Singer, 2008; Kong et al., 2006; Singer et al., 2004; Stancak & Fallon, 2013), some investigations argue that its activation reflects the perceived level of intensity of a nociceptive stimulus (Craig et al., 2000; Davis et al., 1998). Conversely, activation in the posterior insula has been claimed to be predominantly related to the actual intensity of such a stimulus (Frot et al., 2006; Geuter et al., 2017; Andrew R. Segerdahl et al., 2015). Thus, the distinct role of the insular cortex in the perception of pain is still disputed (Davis et al., 2015; A. R. Segerdahl et al., 2015).

To further investigate the involvement of the insular cortex in pain perception, intracerebral electroencephalography (iEEG) is a useful tool to study the temporal aspects of pain processing with a high spatial resolution within different regions of the insula. In recent years, the use of slow and continuously fluctuating stimulation has been proposed as a

paradigm to more closely approximate processes involved in sustained pain, activating predominantly slow unmyelinated C-fibers (Colon et al., 2017). This technique is called “frequency-tagging” (Regan, 1989), and underlies the rationale that a periodic stimulation elicits periodic activity within higher order neurons which in turn generates a response at the frequency of stimulation and its harmonics in the EEG signal in the frequency spectrum. Importantly, this approach yields a very high signal-to-noise ratio and enables the differentiation between ongoing neural activity related to the stimulus and unrelated activity (Colon, Nozaradan, et al., 2012; Mouraux, Iannetti, et al., 2011). Using this type of stimulation, iEEG recordings from the dorsal posterior insula have shown that ongoing neural oscillations are preferentially modulated by sustained periodic thermonociceptive stimuli in the theta and alpha frequency bands at the frequency of stimulation (Liberati et al., 2019). These findings suggest a relationship between nociception and ongoing oscillations, but it remains unclear whether these modulations play a significant role in the perception of pain. If this is the case, cognitive processes known to affect pain perception should also affect these ongoing oscillations. Thus, changes in the attentional state of the subject should be reflected in changes in pain perception (Valéry Legrain et al., 2009), and consequently also in the modulation of ongoing oscillations in the posterior insula measured using iEEG. Importantly, such an attention modulation paradigm using an arithmetic distraction task has already been used in a scalp EEG investigation following the same rationale (Leu et al., 2023). The results of this investigation were not conclusive, possibly due to the analysis of a singular electrode of interest and the low spatial resolution of scalp EEG. It is plausible that any activity from cortical areas that are located deep in the brain would be drowned out by noise in the scalp EEG measurement (Ramantani et al., 2016). Given the potential involvement of the insula in the processing of nociceptive stimuli, we expect to obtain a

better understanding of the underlying mechanisms using iEEG with electrode contacts located in the anterior and posterior insula. Thus, the same ultra-slow sustained periodic stimulation paradigm at a frequency of 0.2 Hz was applied, using both thermonociceptive and non-nociceptive vibrotactile stimulation (Leu et al., 2023).

We hypothesized that a distraction task would lead to a decrease in the perceived intensity in both modalities. A concomitant decrease in amplitude of the modulation of ongoing oscillations exerted by the stimulation would indicate a link to intensity perception. If the modulation is preferential for pain perception, the neural response following non-painful sustained periodic vibrotactile stimuli will be different compared to the thermonociceptive stimuli.

2. Methods

2.1. Participants

8 patients (age: 30.25 ± 8.21 years (mean ± standard deviation), 2 female) undergoing pre-surgical evaluation for refractory focal epilepsy were recruited at the Department of Neurology at the Saint-Luc University Hospital (Brussels, Belgium). Recruitment, electrode implantation and iEEG recordings were performed as described in our previous collaborations with the Refractory Epilepsy Centre, and our sample size matches these previous investigations (Liberati et al., 2019; Liberati et al., 2017; Liberati et al., 2016; Liberati et al., 2020). As part of their evaluation, all patients had depth electrodes implanted in different regions of the brain that were suspected to be the origin of their seizures. We focused only on electrodes implanted in the anterior (n=48) and posterior (n=19) insula. These regions were identified as either the region surrounding the short

insular gyri, the pole of the insula and the transverse insular gyrus for the anterior insula or the regions encompassing the anterior and posterior long insular gyri for the posterior insula (Naidich et al., 2004). 6 Participants had depth electrodes implanted in the anterior and posterior insula, 1 patient only in the anterior and 1 patient only in the posterior insula. MNI coordinates for all electrode contacts can be found in Table 1. This data will be publicly available by the time of publication, containing anonymized DICOM images of each patient. For each image, it will be ensured that no facial features that could lead to the identification of the patient are recognizable.

None of the participants had a medical history (psychiatric diseases, sensory abnormalities, or cognitive deficits) that would hinder their participation in the experiment. Additionally, no ictal discharges were detected during the experiment in any of the participants. Prior to signing an informed consent form, all participants were informed by the responsible neurologist that this experiment would not influence their treatment and that they were free to choose whether they wanted to participate. The experiment was conducted in agreement with the Declaration of Helsinki, and the local research ethics committee approved the investigation (Commission d'Ethique Hospitalo-Facultaire Saint-Luc UCLouvain, B403201316436).

2.2. Experimental setup

The same protocol described in Leu et al. (2023) was used for the experimental setup, carried out at the patient's bedside. Very slow periodic sustained thermonociceptive and vibrotactile stimuli were used in separate blocks, at a frequency of 0.2 Hz over a duration of 75 s per trial, during which participants either were not requested to do anything in

particular (i.e. baseline condition) or had to solve an arithmetic task (i.e. distraction task).

The temperature of the thermonociceptive stimuli varied between baseline temperature (35°C) and 50°C in a sinusoidal manner over a duration of 5 s per cycle. Stimuli were delivered using a thermal cutaneous stimulator (TCS II, QST.Lab, Strasbourg, France). The probe (model T03, set with 15 micro-Peltier elements over a 30mm diameter surface) was placed on the volar forearm of the participant, contralateral to where the highest number of insular contacts were located. The non-nociceptive vibrotactile stimuli were delivered using a 251 Hz sine wave whose amplitude was periodically modulated at a frequency of 0.2 Hz (Figure 1), using a recoil-type vibrotactile transducer (Haptuator, Tactile Labs Inc., Canada) positioned between the thumb and the index of the arm contralateral to where the highest number of insular contacts were located. This non-nociceptive stimulation, generally perceived as non-painful but intense (Liberati et al., 2019), was chosen to assess the selectivity of the observed brain responses for nociceptive stimulation and/or pain perception.

The distraction task consisted of continuously subtracting 7 from a 3-digit starting number throughout the stimulation (Dowman et al., 2008) and to report the final number after the end of the trial. Since our main aim was to keep the patients engaged and motivated for the task, they had the possibility to subtract 3 instead of 7 if they felt like the task was too demanding. This was the case for 2 patients. After each stimulus, the patients provided a rating of the intensity of the stimulus on a numerical ratings scale from 0 to 10 (0: no perception, 10: most intense perception imaginable) and classified the stimulation as painful or not (yes/no).

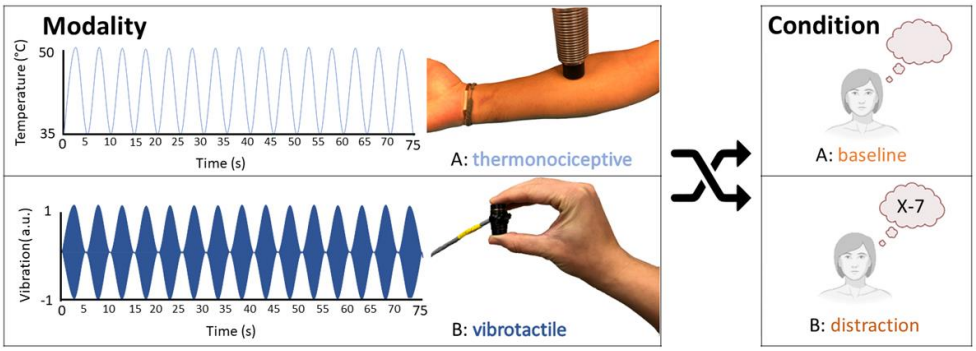

Figure 1. Experimental setup, adapted from Leu et al. (2023). Each modality was paired with each condition for a block of 10 trials.

2.3. Electrode implantation

For each patient, the most probable sites of the epileptogenic focus were determined by a multidisciplinary team. Commercially available depth electrodes for stereo electroencephalography (SEEG) (Dixi Medical, Besancon, France) were implanted vertically at those sites through burr holes using a frameless neuronavigational approach, as described in Budke et al. (2018); Joris et al. (2023). Post-implantation 3D-1T MRI scans confirmed the accurate placement of each electrode on the day of or the day after the operation.

2.4. Electrode contact localization

The exact anatomical location of the implanted electrode rods was determined using BrainVoyager (Brain Innovation, Maastricht, The Netherlands), by normalizing the acquired MRI scans to a standard T1 template in MNI space and manually identifying the MNI coordinates of the insular electrode contacts. The exact location of the coordinates was then assessed using the Automated Anatomical labelling Atlas 3 (Rolls et al., 2020) and if there were doubts, the probabilistic Harvard-Oxford cortical structural atlas (25% probability), both running in the open-source toolbox

Statistical Parametric Mapping (SPM12) in MATLAB. Due to discrepancies between the localization identified using the atlases and the suggested location of the electrode contacts by the neurologists, all electrode contacts which were identified as being in the insula by the neurologist team at St-Luc university hospital were used for the analysis presented in this chapter. All electrode contacts are reported in Table 1.

2.5. Intracerebral recordings

In 2 patients, the signal from the implanted electrodes was acquired using a DeltaMed system (Natus Europe, Paris, France). Electromyographic (EMG) and electrocardiographic activity was recorded from the patient's nondominant arm at the triceps and biceps and from two electrodes respectively located on the right and left side of the sternum, one electrode located centrally under the sternum, and one electrode on the right lateral side, respectively. The reference electrodes were located between Cz and Pz. For all other participants, the signal from the implanted electrodes was acquired using a "BRAIN QUICK ®" acquisition system by MicroMed (Natus Europe, Paris, France). The reference electrode was placed 2 cm behind the usual Fz location in the 10-20 International System. Additionally, electromyographic (EMG) and electrocorticographic activity (ECG) were recorded to account for artifacts related to movement and heart rate. These bipolar electrodes were placed on each upper limb on the deltoid muscle, as well as in the center of the chest and on the right upper part of the abdomen. For both systems, the sampling rate was 512 Hz. The EEG recordings were analyzed offline using the Letswave7 (www.letswave.org) toolbox in MATLAB (2022a The MathWorks).

patient	electrode	hemi-sphere	contact	description	MNI coordinates
P1	1	left	1	Anterior insula	[33.00, 21.11, -11.33]
			2	Anterior insula	[36.54, 20.08, -11.08]
			3	Anterior insula	[40.00, 20.11, -11.33]
	2		1	Posterior insula	[51.00, -6.89, -15.33]
			2	Posterior insula	[54.00, -7.89, -15.33]
			3	Posterior insula	[56.00, -10.20, -14.80]
P2	1	right	1	Anterior insula	[49.71, 15.29, -4.50]
			2	Anterior insula	[56.20, 15.67, -4.53]
			3	Anterior insula	[61.17, 16.08, -4.42]
	2		1	Posterior insula	[52.90, -8.90, -6.40]
			2	Posterior insula	[55.58, -7.84, -6.32]
P3	1	right	1	Anterior insula	[-38.29, -2.00, -16.00]
			2	Anterior insula	[-38.00, -1.00, -14.00]
			3	Anterior insula	[-38.00, 2.00, -11.00]
			4	Anterior insula	[-35.00, 5.00, -9.00]
			5	Anterior insula	[-34.00, 7.11, -7.33]
			6	Anterior insula	[-34.00, 9.11, -4.33]
			7	Anterior insula	[-32.00, 12.88, -1.88]
			8	Anterior insula	[-31.50, 15.00, 0.00]
	2		1	Anterior insula	[33.00, -1.00, 7.00]
			2	Anterior insula	[-36.00, -1.13, 7.13]
			3	Anterior insula	[-39.00, -1.00, 7.14]
	3		1	Posterior insula	[-39.00, -2,00, 2.00]
			2	Posterior insula	[-43.00, -2.00, 4.00]
			3	Posterior insula	[-46.00, -2.00, 5.00]
	4		1	Anterior insula	[-42.00, -3.13, -3.88]
			2	Anterior insula	[-45.00, -2.67, -3.89]
			3	Anterior insula	[-48.00, -2.13, -3.88]
P4	1	right	1	Posterior insula	[-37.00, -32.00, 2.00]
			2	Posterior insula	[-40.33, -30.75, 1.67]
P5	1	right	1	Anterior insula	[-39.00, -15.00, -7.00]
	2		1	Posterior insula	[-33.00, -25.88, 0.88]
			2	Posterior insula	[-35.90, -24.80, 0.40]
			3	Posterior insula	[-39.00, -24.75, 0.13]
			4	Posterior insula	[-42.00, -24.80, 0.20]
	3		1	Posterior insula	[-45.00, -23.36, -0.09]

			2	Posterior insula	[-35.90, -28.40, 7.00]
	4		1	Anterior insula	[-30.00, -6.00, 5.00]
			2	Anterior insula	[-33.00, -6.00, 6.00]
			3	Anterior insula	[-36.00, -5.88, 7.13]
			4	Anterior insula	[-39.18, -5.45, 7.91]
P6	1	left	1	Anterior insula	[43.00, 9.00, -15.00]
			2	Anterior insula	[45.00, 9.00, -12.86]
			3	Anterior insula	[48.00, 9.00, -10.67]
	2		1	Posterior insula	[45.75, 1.00, 9.00]
			2	Posterior insula	[49.00, 1.00, 11.00]
			3	Posterior insula	[54.46, 1.54, 13.00]
P7	1	right	1	Anterior insula	[-37.00, 10.14, -4.00]
			2	Anterior insula	[-40.00, 12.00, -1.00]
P8	1	left	1	Anterior insula	[-34.00, 29.13, -3.13]
			2	Anterior insula	[-36.27, 30.00, -3.36]
			3	Anterior insula	[-38.88, 30.25, -4.00]
	2		1	Anterior insula	[-34.00, 25.00, 10.00]
			2	Anterior insula	[-36.86, 26.00, 9.43]
			3	Anterior insula	[-40.25, 26.13, 9.00]
			4	Anterior insula	[-45.00, 27.00, 9.00]
	3		1	Anterior insula	[-35.00, 9.00, 4.00]
			2	Anterior insula	[-38.75, 9.00, 4.88]
			3	Anterior insula	[-41.00, 9.00, 5.86]
			4	Anterior insula	[-43.00, 9.00, 7.86]
	4		1	Posterior insula	[-31.00, -19.00, 9.00]
			2	Posterior insula	[-34.00, -19.00, 0.00]
			3	Posterior insula	[-37.45, -19.00, 0.09]
			4	Posterior insula	[-41.00, -19.00, 1.00]
	5		1	Anterior insula	[-33.00, 18.00, -7.00]
			2	Anterior insula	[-32.00, 18.50, -4.00]
			3	Anterior insula	[-31.00, 19.00, -1.00]
			4	Anterior insula	[-29.89, 19.00, 2.44]
			5	Anterior insula	[-30.00, 17.00, 5.00]
			6	Anterior insula	[-29.00, 18.00, 8.00]
			7	Anterior insula	[-28.00, 18.00, 12.00]
			8	Anterior insula	[-26.00, 18.00, 16.00]

Table 1. Description and MNI-coordinates of the electrode contacts used in this investigation, implanted in either the anterior or posterior insula.

A 4th order Butterworth filter over the range of 0.05 to 100 Hz was applied and 75 s epochs were segmented based on the onset of the stimulation. Artifacts related to heartbeat and movements were removed using an Independent Component Analysis (Fast ICA algorithm (Hyvarinen & Oja, 2000)) and the signal re-referenced to the average of the electrode contacts for each participant separately. The remaining signal was then averaged per participant, condition and modality. To assess the periodic response at the frequency of the stimulation (i.e. “frequency tagging”, (Regan, 1989), the signal was transformed into the frequency domain using a Fast Fourier Transform (FFT) (Frigo & Johnson, 1998), resulting in a frequency resolution of 0.013 Hz. The signal was then baseline corrected by subtracting the average amplitude measured at the 2-5 surrounding bins, at each electrode and frequency bin and thus largely removing residual noise (Mouraux, Iannetti, et al., 2011), which is inherently present particularly in lower frequencies. The baseline correction is based on the notion that without the periodic response, the signal at the frequency (bin) of interest should not differ from the average of the surrounding frequency bins.

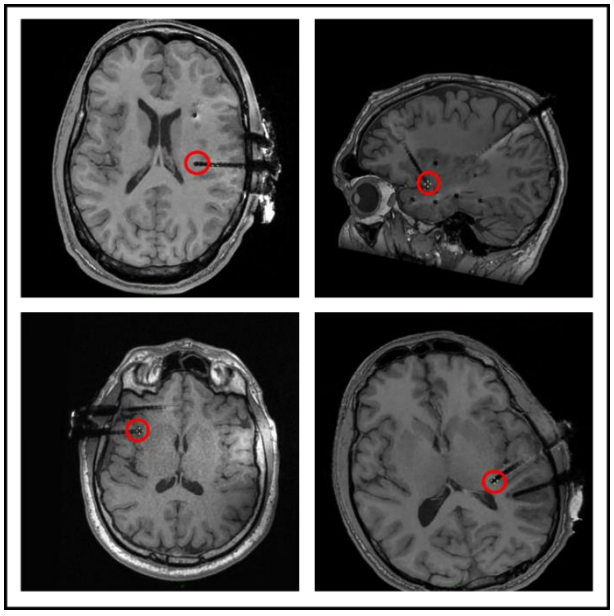

Figure 2. Examples of intracerebral electrode contacts implanted in the anterior or posterior insula.

The modulation of ongoing neural oscillations was assessed in the theta (4-8 Hz), alpha (8-12 Hz),beta (12-40 Hz) and gamma (40-100 Hz) frequency bands using a “frequency-tagging of ongoing oscillations” approach (Colon et al., 2017; Leu et al., 2023; Leu et al., 2024; Liberati et al., 2019; Mulders et al., 2020). This approach is an extension of the commonly used frequency-tagging (Regan, 1989), applied to ongoing oscillations by filtering the data for the respective frequency band and estimating the signal envelope using a Hilbert transform before converting the signal into the frequency domain using a FFT. The iEEG data was averaged across subjects and conditions and finally, the signal was baseline corrected as described above.

2.6. Statistical analysis

R Statistical Software (V. 4.3.1,(R Core Team, 2023)) was used for the statistical analysis of the data. All harmonics in the frequency spectrum were summed up to form the amplitude at the “frequency of interest” (FOI). This procedure is based on the rationale that not taking into account the harmonics elicited by a periodic stimulation would disregard an important portion of the evoked response (Retter et al., 2021). Because the neural response to a periodic stimulus is not perfectly sinusoidal, the elicited activity is distributed over multiple harmonics rather than being centered only at the frequency of stimulation. To this end, the harmonics have to be taken into account to accurately reconstruct the time-domain signal. We therefore summed up all harmonics for each condition and modality, for the phase-locked response as well as for the frequency bands (Courtin & Mouraux, 2024 Preprint; Leu et al., 2023; Leu et al., 2024; Rossion et al., 2020). The amplitudes at these FOIs were consequently used in the statistical analysis. A Bonferroni-corrected non-parametrical right-tailed Wilcoxon signed-rank test was performed at the FOI for the phase-locked response as well as the modulation of ongoing oscillations in the

frequency bands, to assess whether a statistically significant response (i.e. amplitude larger than zero) was present.

A linear mixed model (LMM) was used to assess 1) the effect of condition and modality on perceived intensity of the stimulation. Additional LMMs were used to estimate the effect of condition, modality, and location of the electrodes (anterior/ posterior) on 2) periodic response of the EEG signal and 3) the modulation of ongoing modulations in the different frequency bands at the frequency of interest. A REML approximation was used to fit the LMMs. Significant results ($p<0.05$) were further assessed using post-hoc pairwise comparisons. All amplitudes were log-transformed to conform them to the assumptions underlying the LMM. In the gamma frequency band, one participant had to be removed almost entirely from the data set, as the amplitudes violated assumptions even after log-transformation (outliers identified using Cook's distance [D] (Cook, 1977)). In the theta band, this was the case for 3 data points.

Additionally, to assess whether potential effects of the distraction task on the modulation of ongoing oscillations were due to differences in baseline amplitudes between the modalities, the relative change in log amplitude (to match the LMM's) was calculated for each modality and compared to each other using a paired t-test.

3. Results

3.1. Perception

During the distraction task, perceived stimulation intensity was significantly decreased during the thermonociceptive ($p=0.0129$) as well as vibrotactile stimuli ($p=0.0002$) (Figure 2). The thermonociceptive stimuli were perceived as painful during less than half of the baseline condition

(40%), and to an even lesser extent during distraction (28.75%). Vibrotactile stimuli were never perceived as painful in both conditions (0%).

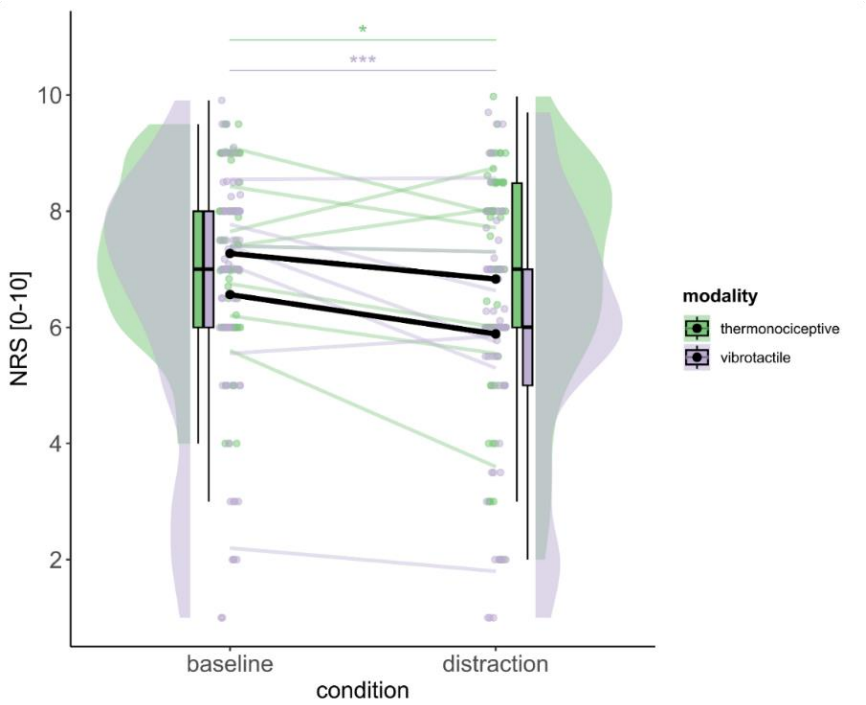

Figure 2. Ratings of perceived stimulus intensity using a Numerical Rating Scale [NRS] between 0 (no perception) and 10 (most intense perception imaginable) following thermonociceptive and vibrotactile stimulation. Horizontal lines mark the individual average (colored) as well as the group averages (black) for each modality. P-values indicate the results of the post-hoc pairwise comparison (*p<0.05, ***p<0.001).

3.2. Neural response to the sustained periodic thermonociceptive and vibrotactile stimuli

3.2.1. Periodic response and modulation of ongoing oscillations induced by the frequency-tagging paradigm

A significant periodic phase-locked response was found at the FOI for both modalities and insular regions (Table 2). Similarly, the modulation of ongoing oscillations at the FOI was significantly different from zero in the

theta and alpha frequency bands for all tested factors apart from the amplitude at the FOI exerted by thermonociceptive stimulation in the anterior insula. Conversely, in the beta frequency band, only the modulation elicited by vibrotactile stimulation did not lead to a response significantly different from zero. Finally, in the gamma frequency band, all orientations and modalities showed a significant modulation of ongoing oscillations apart from the thermonociceptive response in the posterior insula. Figures 4.1 and 4.2 illustrate the neural responses for each modality and condition across the frequency spectrum.

3.2.2. Comparison of conditions and modalities

The results of the LMM are summarized in Table 3 and 4 and differences between baseline and distraction conditions are illustrated in Figure 3 for all frequency bands. In the phase-locked response, a significant effect of modality, electrode contact location, and their interaction was found in the LMM (Table 3). The theta and alpha frequency bands displayed significant effects of location, the interaction between location, condition and modality, as well as an interaction between condition and modality. In the beta frequency band, significant effects of condition, location and an interaction between condition and modality were found and finally in the gamma frequency band, only an interaction between condition and modality was found (Table 4). In the following section, pairwise comparisons showing significant differences are reported. The complete tables of these comparisons can be found in the Supplementary Materials (S.Table 1).

The phase-locked amplitude at the FOI elicited by thermonociceptive stimulation was significantly larger than the FOI elicited by vibrotactile stimulation in the posterior insula during baseline condition ($t(190)=2.170$, $p=0.0312$). Further post-hoc comparison of the phase-locked response showed that showed that the baseline thermonociceptive stimuli led to a

significantly larger periodic response in the posterior compared to the anterior insula (t(205)=-4.942, p<0.001), as did vibrotactile stimuli (t(217)=-2.704, p=0.007). Differences between baseline and distraction task were only found for thermonociceptive stimulation in the anterior insula (t(183)=2.053, p=0.042).

	modality	location	n	W	p.adj
phase-locked	thermonociceptive	anterior	96	3469	**<0.001**
	vibrotactile	anterior	90	3448	**<0.001**
	thermonociceptive	posterior	38	735	**<0.001**
	vibrotactile	posterior	32	515	**<0.001**
theta	thermonociceptive	anterior	96	2284	1.000
	vibrotactile	anterior	90	3309	**<0.001**
	thermonociceptive	posterior	36	610	**<0.001**
	vibrotactile	posterior	31	456	**<0.001**
alpha	thermonociceptive	anterior	96	2694	0.363
	vibrotactile	anterior	90	3162	**<0.001**
	thermonociceptive	posterior	38	710	**<0.001**
	vibrotactile	posterior	32	491	**<0.001**
beta	thermonociceptive	anterior	96	3010	**0.026**
	vibrotactile	anterior	90	2519	0.116
	thermonociceptive	posterior	38	593	**0.002**
	vibrotactile	posterior	32	450	**0.001**
gamma	thermonociceptive	anterior	96	3009	**0.026**
	vibrotactile	anterior	90	2876	**0.002**
	thermonociceptive	posterior	36	424	0.314
	vibrotactile	posterior	28	351	**0.001**

Table 2. Results of the right-tailed Wilcoxon signed-rank test to assess whether the amplitude at the FOI was significantly different from zero (baseline condition). Bonferroni correction was applied to correct for multiple comparisons.

In the theta frequency band, amplitudes were significantly larger in the posterior compared to the anterior insula following thermonociceptive (t(203)=-5.583 , p<0.001), as well as vibrotactile stimuli (t(212)=-2.827, p=0.005). The modulation of ongoing oscillations elicited by

thermonociceptive stimuli was significantly larger during baseline than during distraction in the posterior insula (t(181)=2.044, p=0.042). Vibrotactile stimuli elicited the opposite response in the anterior insula (t(181)=-3.708, p<0.001). Moreover, thermonociceptive stimulation elicited significantly smaller responses than vibrotactile stimulation in the anterior insula during baseline condition (t(183)=-2.561, p=0.011).

Post-hoc pairwise comparisons of the amplitudes at the FOI in the alpha frequency band showed that in the posterior insula, thermonociceptive stimulation elicited significantly larger responses than vibrotactile stimulation in the baseline condition (t(188)=2.739, p=0.007). Further, the modulation of ongoing oscillations exerted by thermonociceptive (t(160)=-6.735, p<0.001) as well as vibrotactile stimuli (t(177)=-3.523, p=0.001) was significantly larger in the posterior than in the anterior insula. Finally, in the posterior insula, the arithmetic task led to a significant reduction in the modulation exerted by thermonociceptive stimuli at the FOI (t(183)=2.205, p=0.029) while vibrotactile stimuli led to a larger response during the arithmetic task in the anterior insula (t(183)=-3.400, p=0.001).

	phase-locked response		
	F-value	p	η^2_p
condition	0.259	0.611	0.001
modality	4.581	**0.034**	0.024
orientation	42.846	**< 0.001**	0.415
condition:modality	0.627	0.429	0.004
condition:orientation	1.755	0.187	0.010
modality:orientation	6.959	**0.009**	0.036
condition:modality:orientation	0.126	0.723	0.001

Table 3. Results of the Linear Mixed Model (amplitude ~ modality * condition * orientation + (1| electrode contact:patient) and estimated partial effect sizes and their confidence intervals. Significant results are indicated in bold font.

As for the other frequency bands, the modulation of ongoing oscillations was significantly larger in the posterior than in the anterior insula in the beta frequency band (*thermonociceptive*: t(223)= -2.184, p=0.030; *vibrotactile*: t(231)= -2.398, p=0.017). Moreover, the vibrotactile stimuli led to significantly larger modulation of ongoing oscillations during the distraction condition compared to baseline in the anterior (t(184)=-2.483, p=0.014) as well as posterior insula (t(184)=-2.216, p=0.028).

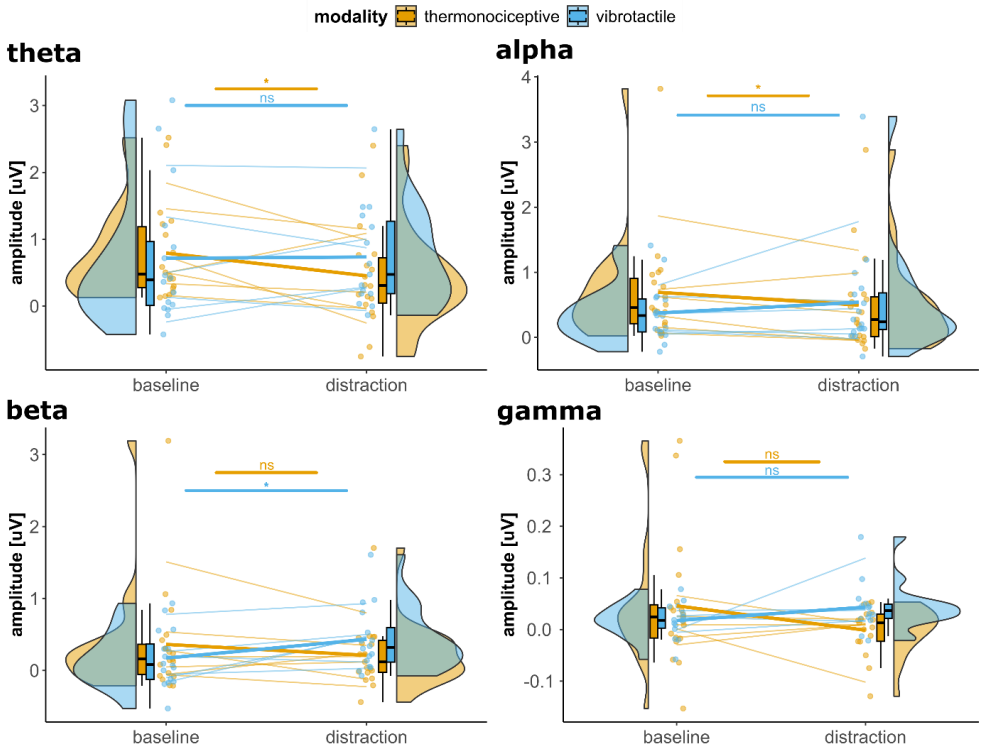

Figure 3. Modulation of ongoing oscillations in the theta, alpha, beta and gamma frequency bands at electrode contacts in the posterior insula. Background horizontal lines represent patient means, while the bold line illustrates the group mean. Results of post-hoc pairwise comparisons are displayed using the original amplitudes: * p<0.05, ns p>0.05.

Finally, modulations in the gamma frequency band were assessed. Overall, relatively small amplitudes were measured (see Figure 3), and no difference between amplitudes in the anterior and posterior insula were found. Only following vibrotactile stimulation in the anterior insula, the modulation of ongoing oscillations was significantly larger during the arithmetic task compared to the baseline condition (t(178.093)=-3.049, p=0.003)

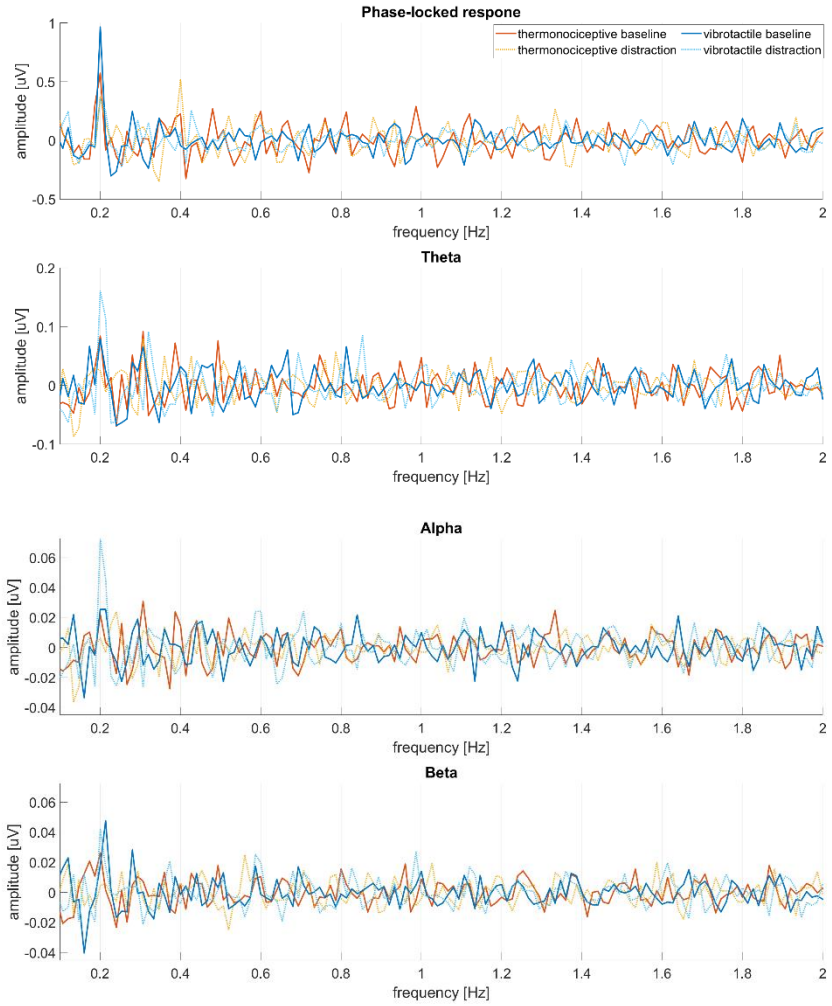

Figure 4.1. Frequency spectra representing the group and electrode contact averages for the different modalities and conditions in the *anterior* insula.

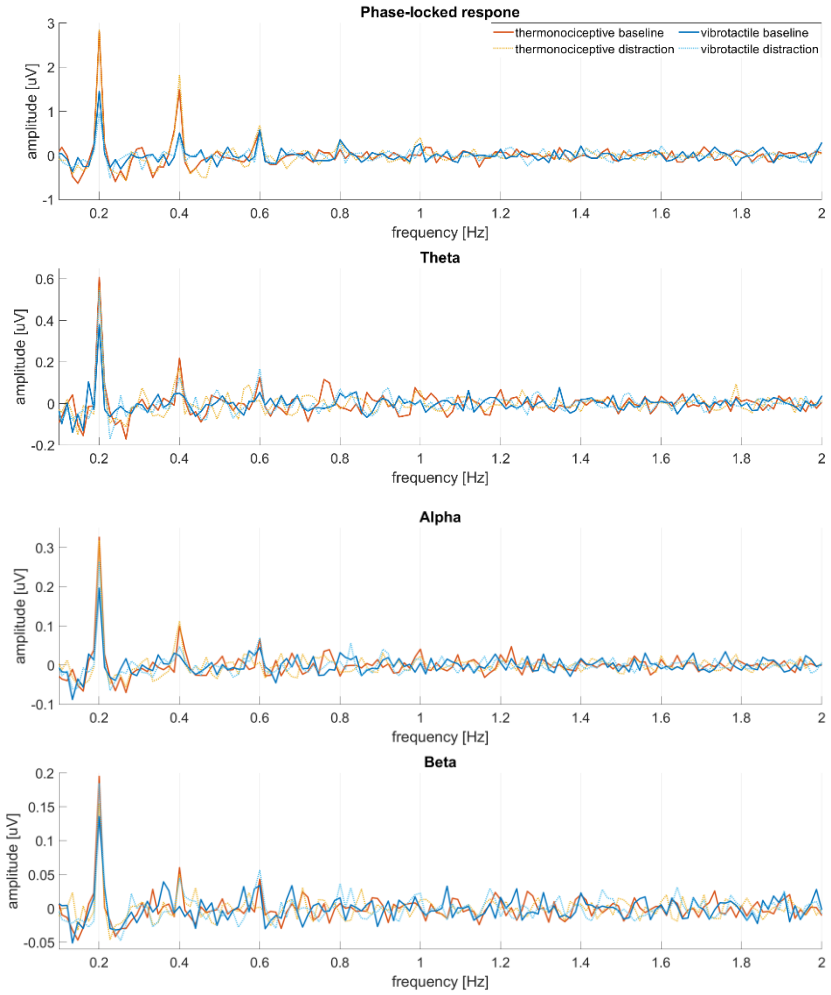

Figure 4.2. Frequency spectra representing the group and electrode contact averages for the different modalities and conditions, measured in the posterior insula.

	theta			***alpha***		
	F-value	p	η^2_p	F-value	p	η^2_p
condition	0.975	0.325	0.006	0.602	0.439	0.003
modality	9.773	0.002	0.049	0.012	0.913	0.000
orientation	20.360	< 0.001	0.250	32.349	< 0.001	0.325
condition: modality	5.990	0.0154	0.033	8.616	0.004	0.045
condition:orientation	7.119	0.008	0.039	4.655	0.032	0.025
modality:orientation	5.284	0.023	0.027	9.223	0.003	0.046
condition:modality: orientation	0.405	0.525	0.002	0.595	0.441	0.003

	beta			***gamma***		
	F-value	p	η^2_p	F-value	p	η^2_p
condition	4.334	**0.039**	0.024	0.297	0.586	0.002
modality	0.294	0.588	0.002	1.988	0.160	0.011
orientation	12.337	**< 0.001**	0.168	0.355	0.556	0.007
condition:modality	7.294	**0.008**	0.039	9.551	**0.002**	0.055
condition:orientation	0.007	0.932	0.000	1.044	0.308	0.006
modality:orientation	0.454	0.501	0.002	0.057	0.812	0
condition:modality: orientation	2.833	0.094	0.016	0.068	0.794	0

Table 4. Results of the Linear Mixed Model (amplitude ~ modality * condition * orientation + (1| electrode_contact:patient) and estimated partial effect sizes, for each frequency band. Significant results are indicated in bold font.

3.3. Relative change in modulation of ongoing oscillations

Finally, the comparison of the relative change (amplitude baseline – amplitude distraction) between the conditions showed that only in the posterior insula and following thermonociceptive stimulation, the distraction task led to a reduction of amplitudes compared to baseline (Figure 5). However, this relative amplitude was only significantly different from zero in the alpha frequency band ($t(15)=2.452$, $p=0.027$). Interestingly, the opposite effect was found in the beta frequency band in the posterior

insula, where vibrotactile stimulation led to significantly increased responses relative to baseline (t(15)=-2.431, p=0.028). In the anterior insula, the same relative change in amplitude was observed for vibrotactile stimulation (*theta*: t(44)=-3.509, p=0.001; *alpha*: t(44)=-6.670, p=0.001, *beta*: t(44)=-2.189, p=0.034, *gamma*: t(44)=-3.408, p=0.001).

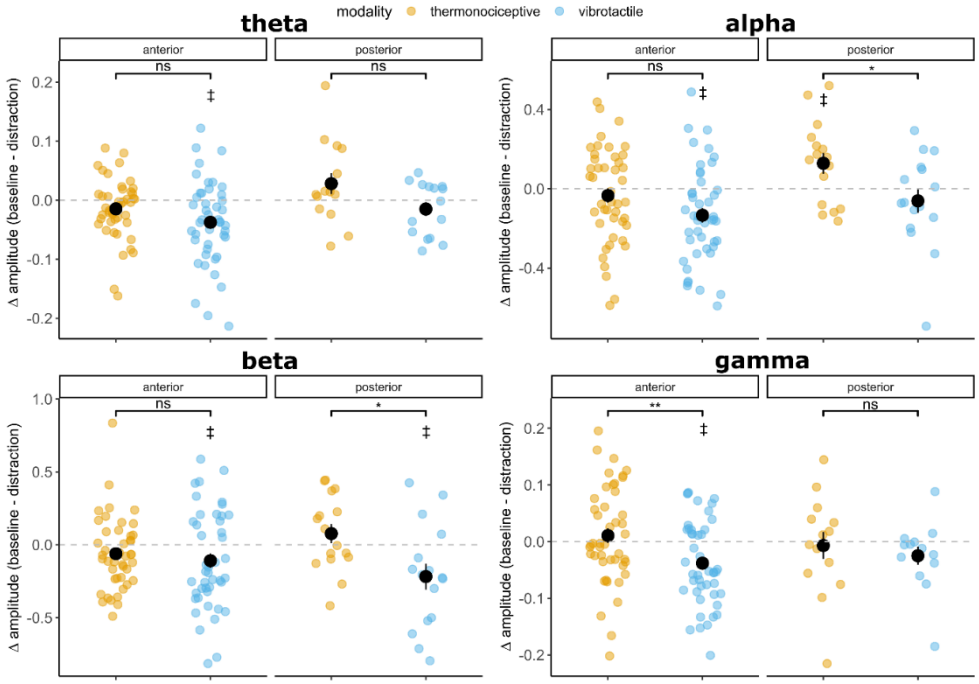

Figure 5: Relative (Δ) amplitudes (log amplitude baseline condition – log amplitude distraction condition) were calculated to assess potential baseline effects of condition on effects found in the LMM. The mean and the confidence interval are indicated in black for each group. *p<0.05, ^{ns}p>0.05. A one sample t-test (two-sided) was used to determine whether the obtained relative amplitudes were significantly different from zero (indicated with ‡, p<0.05). Pairwise t-tests were used to compare the relative amplitudes between conditions (*p<0.05, ^{ns}p>0.05).

The modalities did not differ significantly from each other neither in the anterior nor the posterior insula in the theta frequency band (t(44)=1.565, p=0.125; t(14)=1.964, p=0.070). In the alpha frequency band, the relative amplitude at the FOI was significantly larger for thermonociceptive than vibrotactile stimulation (t(15)=2.746, p=0.015). No such difference was found

in the anterior insula ($t(44)=1.797$, $p=0.079$). While similar relationships were found in the beta ($t(44)=0.769$, $p=0.446$; $t(15)=2.652$, $p=0.018$) and gamma frequency band ($t(44)=3.268$, $p=0.002$; $t(13)=0.561$, $p=0.585$), the difference between the modalities in the posterior insula seemed to be mediated by the increase in amplitude elicited by the vibrotactile stimulation during the distraction task, as the relative change for the amplitudes elicited by thermonociceptive stimulation was not significantly different from zero.

4. Discussion

To further understand the involvement of the insula in pain perception, sustained periodic thermonociceptive and vibrotactile stimuli were delivered at a frequency of 0.2 Hz to refractory epilepsy patients who had intracerebral electrodes temporarily implanted in the anterior and posterior insula. Using a frequency-tagging approach, we aimed to assess whether ongoing oscillatory activity in the insula is functionally related to pain perception by distracting patients from the stimuli using an arithmetic task during half of the trials.

Intensity perception was modulated by the arithmetic distraction task as expected, leading to a significant decrease in the perceived stimulus intensity in both modalities. Concomitantly, the modulation of ongoing oscillations elicited by thermonociceptive stimulation was decreased in the alpha and theta frequency bands in the posterior insula. Even though the arithmetic task led to a reduction in intensity ratings during vibrotactile stimuli in our experiment, an increase in modulation of ongoing oscillations was observed during the arithmetic task in all frequency bands in the anterior insula as well as in the beta frequency band in the posterior insula.

A significant periodic response and modulation of ongoing oscillations was found across both modalities in the anterior and posterior insula. The comparison of the amplitudes at the FOI demonstrated a consistently larger modulation of ongoing oscillations in the posterior insula for both modalities. Thermonociceptive and vibrotactile stimulation did not differ much in the modulation of ongoing oscillations that they induced during baseline condition; solely in the posterior insula in the alpha frequency band, thermonociceptive stimulation led to larger amplitudes, while the opposite was the case in the anterior insula in the theta frequency band. Our evidence largely falls in line with the results of Liberati et al. (2019), who found a larger modulation of ongoing oscillations exerted by thermonociceptive stimulation in the posterior compared to the anterior insula. Moreover, a preferential modulation of ongoing oscillations following thermonociceptive stimulation in the dorsal-posterior insula in the alpha and theta frequency band was observed in their study. Our results support these findings in the alpha, but not in the theta frequency band. The consistent difference in the modulation of ongoing oscillations between the modalities in the alpha frequency band could reflect the preferential modulation of thermonociceptive stimuli over non-nociceptive vibrotactile stimuli within the posterior insula and illustrates its potential involvement in the processing of thermonociceptive stimuli.

The modulation of ongoing oscillations was significantly reduced during the arithmetic task in both the theta and alpha frequency band in the posterior insula. However, differences in the magnitude of the modulation of ongoing oscillations in the baseline condition could potentially mediate the observed effects, i.e. a baseline modulation of larger magnitude has more capacity for a decrease than an already small modulation. To control for this, the relative difference between baseline and distraction condition was compared for each modality and frequency band. While differences

between the modalities were found in the alpha, beta and gamma frequency band, it seems for the latter two, the observed differences could be mediated by the significant decrease of the relative amplitude for vibrotactile stimulation which was found in the anterior insula in all frequency bands. This indicates that, for vibrotactile stimulation, the modulation of ongoing oscillations actually increased during the arithmetic task in this modality even when taking the baseline into account, confirming the effect observed in the LMM. Interestingly, even though post-hoc comparisons revealed a significant decrease of the modulations of ongoing oscillations induced by thermonociceptive stimulation during the arithmetic task in the theta frequency band, no difference was found between the modalities in the comparison of the modulations relative to their baseline. This indicates that, despite the relationship between the relative modulations going in the same direction, the decrease in modulation during the arithmetic task should be interpreted cautiously for the theta frequency band. Additionally, Liberati et al. (2019) found a significant difference between the modalities in the theta frequency band, which we were not able to replicate in our baseline condition. A potential explanation for this discrepancy could be the perception of the stimulation; the laser stimulation used in Liberati et al. (2019) was generally perceived as painful, whereas this was not the case in the present experiment. This might suggest that activity in the theta frequency band is indeed preferential for pain, but not thermonociception. Collectively, it seems that the modulations of ongoing oscillations induced by experimentally induced pain / thermonociception in the theta frequency band remains somewhat inconclusive, as contradicting results have also been found in a range of scalp EEG investigations (Kim & Davis, 2021). Finally, in the alpha frequency band, the comparison of the induced amplitudes at the FOI relative to baseline confirmed the prior result of the LMM that the arithmetic task led to a significant reduction in the

modulation of ongoing oscillations following thermonociceptive stimulation. We can therefore be certain in the evidence that modulations in activity in the alpha frequency band could be substantially involved in the shift in stimulus perception evoked by the arithmetic task concomitant to the thermonociceptive stimulation.

This evidence aligns with previous research, suggesting a predominantly posterior involvement of the insula in the processing of nociceptive stimulation (Labrakakis, 2023), demonstrating that magnitude of stimulus perception relates to activity in the posterior insula (Baliki et al., 2009; Andrew R. Segerdahl et al., 2015; Wiech et al., 2005). A number of investigations studied the effect of distraction (through e.g. mental arithmetic tasks or the Stroop working memory task) on pain perception in relation to insular activity, and generally found a decrease during distraction from nociceptive stimulation concomitant to a decrease in pain perception (Bantick et al., 2002; Petrovic et al., 2000; Seminowicz & Davis, 2006; Valet et al., 2004). An investigation of the ultra-late responses to brief thermonociceptive laser stimuli (which likely reflect C-fiber activity) also found a decrease in insular activity during a mental calculation task (Qiu et al., 2004). The reduction in neural response magnitude in the posterior insula solely in the alpha frequency band might be related to active inhibition, as the thermonociceptive stimulation was not relevant for the completion of the arithmetic distraction task. Similar results have been found in a spatial attention task employing vibrotactile stimulation, where during the task, responses in the posterior insula were attenuated (Goltz et al., 2013).

It should be considered that the alpha frequency band is arguably the most prominent band in the modulation of attentional processes (Palva & Palva, 2007). Thus, activity in this frequency band is likely pain-unspecific, and the decrease in modulation of ongoing oscillations in the alpha

frequency band during distraction might reflect the inhibition in insular activity which has been observed in many functional imaging studies alongside reductions in the ACC, S1/S2 and thalamic activity (Bantick et al., 2002; Longe et al., 2001; Schlereth et al., 2003; Valet et al., 2004). However, the fact that no decrease in modulation during the arithmetic task was found in response to vibrotactile stimulation even though it elicited a strong effect on perception suggests that the observed effect is not purely attentional but related to the thermonociceptive properties of the stimulus.

In scalp EEG studies, the alpha frequency band power has been shown to relate to intensity perception (Nickel et al., 2022) as well as being reduced during a distraction task (Peng et al., 2014). Yet, other investigations were not able to find this link (Leu et al., 2023; Schulz et al., 2015). Comparing the present results to Leu et al. (2023), the perception of the stimulation has generally been more intense in the patients, while the change in the ratings of perceived stimulation intensity across conditions were similar in patients and healthy volunteers. Yet, although the same method of summation of the harmonics was used, no difference could be found at the electrode with the largest modulation in the scalp EEG study for either of the modalities. The signal recorded at these scalp electrodes likely recorded activity mainly originating in the somatosensory cortices (Apkarian et al., 2005; Dowman et al., 2008), not able to pick up activity of deep-brain structures such as the insula. This difference underlines the importance of the posterior insula in the processing of somatosensory input and further highlights the need for research that goes beyond the scalp surface to disentangle how the brain shapes pain perception.

The anterior and posterior insula differ in both structural and resting state connectivity with other brain regions involved in pain perception, with pain awareness being related mostly to the anterior insula (Wiech et al.,

2014). Similarly, cognitive factors influencing pain perception (i.e. top-down pain modulators) such as attention and expectation have been shown to be integrated with the objective properties (i.e. bottom-up modulation) of the nociceptive stimulation in the anterior insula (Atlas et al., 2010). Other investigations showed that while nociceptive stimulation elicited activity in the posterior part of the insula, distraction mostly attenuated activity in the anterior insula (Brooks et al., 2002; Silvestrini & Corradi-Dell'Acqua, 2023). Similarly, effects of expectation (i.e. prediction error) were found in the anterior insula, while the stimulus intensity was encoded in the posterior insula (Geuter et al., 2017). It is therefore unexpected that the effects of the distraction task for thermonociceptive stimulation seem to be mainly located in the posterior insula, and differences in the anterior insula were only found following vibrotactile stimulation.

Indeed, an increase in modulations at the FOI induced by vibrotactile stimulation was found in the anterior insula during the arithmetic task in all frequency bands. Without any task, vibrotactile stimulation seems to primarily activate the primary and secondary somatosensory cortices, as well as the posterior insula (Albanese et al., 2009; Francis et al., 2000; Nelson et al., 2004). Yet, if a working memory task such as a frequency discrimination task is being performed, fMRI investigations have demonstrated that activity shifts to the anterior insula (Albanese et al., 2009; Li Hegner et al., 2007; Sörös et al., 2007). Considering that the insula receives input from somatosensory cortices (Augustine, 1996), which are then relayed along the posterior-anterior axis of the insula to higher-order cortical structures such as the prefrontal region (Cloutman et al., 2012; Uddin et al., 2014), the observed effects are likely related to cognitive task monitoring and short-term memory retention of the perceived tactile stimulation which are integrated in the anterior insula (Cieslik et al., 2015). Additionally, studies examining the circuits involved in emotional

regulation found the anterior insula to be active during distraction tasks, e.g. mental arithmetic tasks (Dörfel et al., 2014; Morawetz et al., 2017). We can only speculate as to why this effect was not observed in the thermonociceptive modality. One potential explanations is that the modalities were not adequately matched in terms of saliency (i.e. the ability of a stimulus to stand out from its environment (Egeth & Yantis, 1997)). Painful stimuli are inherently salient, as they pose a potential physical threat to the body. And while the perceived intensity of the stimulations did not differ between the modalities at baseline, at least some of the thermonociceptive stimulations were perceived as painful, which makes them by definition more salient. One could speculate that the saliency of the thermonociceptive stimuli interfered with the arithmetic task and potentially disrupted the task execution. This is supported by the reports of some patients who mentioned being distracted by the task, leading to a reduced perception of intensity, but at times also very aware of the painful stimulation. In contrast, they were less aware of the vibrotactile stimulation during the task. These statements are validated by the recorded difference in intensity perception between the modalities during the arithmetic task.

The valuable data obtained from intracerebral recordings introduce some limitations to this investigation that are challenging to overcome. First, we were not able to balance the location of the implanted electrodes between the anterior and posterior insula, resulting in a dataset containing more than twice as many data points in the anterior insula. Any conclusions drawn regarding activity in the posterior insula and their relationship to the perception of thermonociceptive stimulation thus need to be interpreted with caution and future investigations must confirm our findings. Secondly, while the stimulation in both modalities was perceived as more intense by patients than by healthy participants, this increase in

intensity did not lead to an increase in the number of stimulations which were perceived as “painful”. One possible explanation for this discrepancy is the setting of the experiment; at the patient’s bedside, few days after a highly invasive brain surgery is a stark contrast to the laboratory setting in which the scalp EEG experiment took place. It is plausible that this environmental factor, interacting with potential painful side-effects of the electrode implantation, led patients to (consciously or not) adapt their evaluation of what constitutes a painful stimulation in this situation (McGrath, 1994). Nevertheless, the fact that most stimulations were not perceived as painful prevents us from drawing conclusions regarding the relationship between the modulation of ongoing oscillations and pain perception *per se*, as we can only assume a link between changes in intensity perception and pain. Thus, our conclusions are limited to the relationship between the modulation of ongoing oscillations and thermonociception.

5. Conclusion

The arithmetic distraction task led to a decrease in perceived stimulation intensity following both thermonociceptive and vibrotactile stimulation. Yet, only for thermonociceptive stimulation, a concomitant decrease in modulation of ongoing oscillations was observed in the alpha frequency band in the posterior insula. This data supports the notion that these stimulations are preferentially modulated in the alpha frequency band and suggests the involvement of the posterior insula in thermonociception. As most of the thermonociceptive stimulations were not perceived as intense, but not painful, further investigations should clarify whether this relationship extends to pain perception. Nonetheless, future investigations could focus on using non-invasive brain stimulation to target the posterior insula for the development of novel therapeutic approaches for the treatment of chronic pain.

Acknowledgements

We wish to thank Julien Lambert of the CATL team of the Université catholique de Louvain for technical assistance. We would further like to thank all the master's students that were interns of the lab between 2022-2024 and helped with data acquisition.

Author contributions

Conceptualization: CL, GL; Methodology (experiment): CL, GL; Methodology (surgical implantation of intracerebral electrodes): VJ, PF; Investigation: CL; Formal analysis: CL; Funding acquisition: CL, GL; Resources (patients): SFS, AF; Supervision: GL; Writing – original draft: CL; Writing – review and editing: CL, SFS, AF, VJ, PF, GL

Funding sources

This study was supported by the FRIA doctoral grant of Chiara Leu by the Belgian Fund for Scientific Research (F.R.S.–FNRS). Giulia Liberati is supported by the Fonds de la Recherche Scientifique (F.S.R.–FNRS) and by the Fondation Médicale Reine Elisabeth (F.M.R.E).

CHAPTER 6: Harmonic aggregation and their signal-to-noise ratio in the frequency spectrum

On the relevance of harmonic aggregation and signal-to-noise estimations in the frequency spectrum following sustained periodic stimulation

Exploratory analyses of the data collected in the intracerebral EEG investigation presented in chapter 5

1. Significance of harmonic aggregation

As mentioned in the explanation of the rationale for the aggregation of all harmonics in the frequency spectrum in the introduction of this thesis (see chapter 1, “Harmonics” and corresponding Figure 6 for illustration), it remains debated which number of harmonics should be aggregated to obtain an adequate measurement of the neural response to sustained periodic stimulation (Retter et al., 2021). While our decision to aggregate over the entire spectrum in the studies presented in this thesis has a sound rationale, following frequent discussions in the lab, we wanted to ensure that we did not incorporate too much noise with the aggregation of late harmonics (which are less likely to carry responses to the periodic stimulation). Therefore, we introduce a secondary analysis of the iEEG data presented in chapter 5, aggregating only the first few harmonics which are consecutively different from zero (Retter & Rossion, 2016). This approach was chosen due to the stark contrast to the primary analysis, as only few harmonics will be selected, and very little noise should be present in those signals.

1.1. Rationale and methods for alternative aggregation of harmonics

A non-parametrical right-tailed Wilcoxon signed-rank test was performed at each harmonic up to 1 Hz for the phase-locked response as well as the modulation of ongoing oscillations in the frequency bands, to assess whether a statistically significant periodic response (i.e. peak larger than zero) was present (Figure 1). The harmonics that showed a significant periodic response were then summed up to form the peak at the “frequency of interest” (FOI). This procedure is based on the rationale that not taking into account any of the harmonics elicited by a periodic stimulation would disregard an important portion of the evoked response

(Retter et al., 2021). The neural response to a periodic stimulus is not perfectly sinusoidal, resulting in activity distributed across multiple harmonics rather than being centered only at the frequency of stimulation. Thus, these harmonics must be considered to accurately reconstruct the time-domain signal.

While the exact number of harmonics that should be summed up is still debated and the sum of all harmonics potentially incorporates unnecessary noise into the signal at the FOI, we aimed to find the ones that are meaningful to the periodic response, i.e. showing an amplitude which is significantly different from zero. In previous iEEG studies using a frequency-tagging approach, the first 3 harmonics were identified to be modulated (0.2 Hz, 0.4 Hz, 0.6 Hz) (Liberati et al., 2019). We therefore expected to sum up a similar number of harmonics for each signal. Yet, the Wilcoxon signed-rank test revealed that the number of harmonics that showed a significant modulation of ongoing oscillations was not constant across the different frequency bands (Figure 1), and we therefore summed up a different number of harmonics for the phase-locked response and for each frequency band. The amplitudes at these FOIs were consequently used in the statistical analysis. We did not differentiate between conditions for this step.

1.2. Wilcoxon signed-rank test

A significant periodic EEG response was found consistently only for some of the first harmonics (Figure 1). Following these results, concurrent significant modulations of ongoing oscillations elicited by thermonociceptive stimulation were chosen as the “modality of interest”, hence the first 2 harmonics and the peak at the frequency of stimulation were summed up for the phase-locked response. No summation was carried out in the theta and gamma frequency bands, as only the

amplitude at the frequency of stimulation was shown to be significantly different from zero. Finally, for the alpha and beta frequency bands, the amplitudes at 0.2 Hz as well as the first harmonic in the frequency spectrum (0.4 Hz) were summed up. These amplitudes built of the sum of the harmonics were used for the statistical analysis.

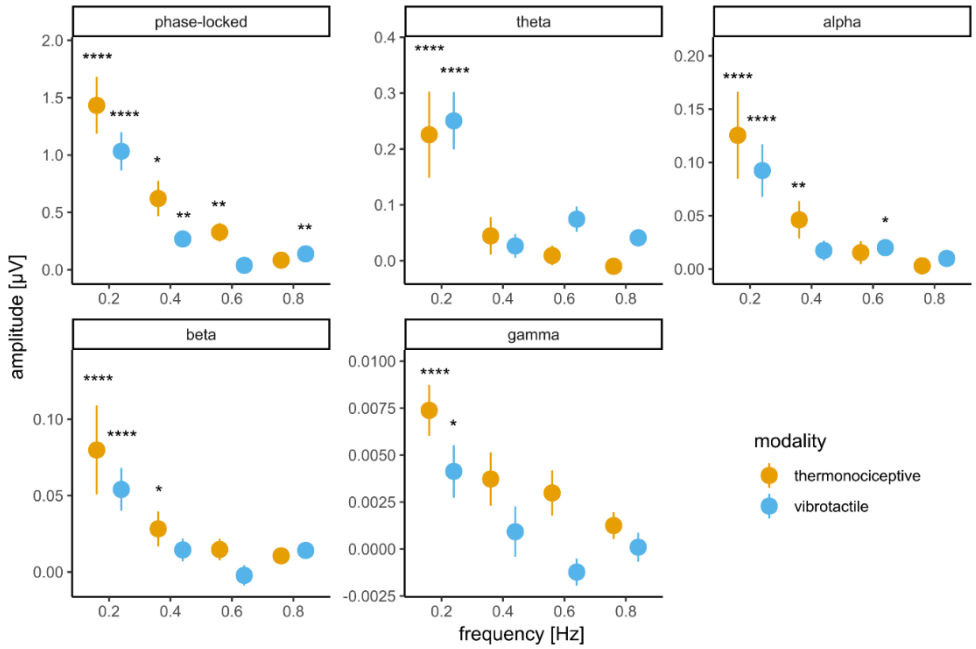

Figure 1. Mean and confidence intervals of the amplitude recorded at the frequency of stimulation (0.2 Hz) and the first 3 harmonics (0.4 Hz, 0.6 Hz, 0.8 Hz) for the phase-locked response as well as all frequency bands during the baseline condition. Results of the right-tailed Wilcoxon signed-rank test against zero (Bonferroni corrected) are displayed as follows: *p<0.05, **p<0.01, ****p<0.0001.

1.3. Linear mixed models

The results of the LMM are summarized in Table 1 and 2 and illustrated in Figure 2, and the same model was used as in the previous chapter (amplitudeFOI ~ condition * modality * localization + (1| subject:electrode).

Significant effects of modality, location and their interaction were found in the LMM of the phase-locked response. Post-hoc comparison showed that

the baseline thermonociceptive stimuli led to a significantly larger periodic response in the posterior compared to the anterior portion of the insula (t=-3.611(211), p<0.001), as did vibrotactile stimuli (t(191)=-3.023, p=0.003). No differences were found in the responses recorded from either the anterior or posterior insula comparing activity elicited during the arithmetic task and baseline condition.

In the theta frequency band, amplitudes were significantly larger in the posterior compared to the anterior insula (t(163)=-4.254, p<0.001) following thermonociceptive, as well as vibrotactile stimuli (t(175)=-2.117, p=0.036). The modulation of ongoing oscillations elicited by thermonociceptive stimuli was significantly larger during baseline than during distraction in the anterior insula (t(182)=1.822, p=0.070). Vibrotactile stimuli elicited the opposite response in the same region (t(182)= 3.570, p=0.001). No differences between the conditions were observed in the posterior insula.

Significant differences between the location of the electrode contacts and their interaction with condition and modality were found in the alpha frequency band. Post-hoc pairwise comparisons illustrated that the modulation of ongoing oscillations was significantly larger in the posterior than in the anterior insula elicited by thermonociceptive (t(137)=-4.177, p=0.0001) as well as vibrotactile stimuli (t(148)=-3.091, p=0.002). Additionally, only in the anterior insula, the arithmetic task led to a significant reduction in the modulation elicited by thermonociceptive stimuli at the frequency of interest (t(182)= 2.078, p=0.039) while vibrotactile stimuli led to a larger response during the arithmetic task (t(182)=-3.570, p=0.001).

	phase-locked response		
	F-value	p	η^2_p
condition	1.940	0.165	0.011
modality	15.775	**< 0.001**	0.078
orientation	33.410	**< 0.001**	0.345
condition:modality	0.397	0.530	0.002
condition:orientation	0.067	0.795	0.000
modality:orientation	10.208	**0.002**	0.052
condition:modality:orientation	0.748	0.388	0.004

Table 1. Results of the Linear Mixed Model (amplitude ~ modality * condition * orientation + (1| electrode contact:patient) and estimated partial effect sizes and their confidence intervals. Significant results are indicated in bold font.

As for the other frequency bands, the modulation of ongoing oscillations in the beta frequency band was significantly larger in the posterior than in the anterior insula (*thermonociceptive*: t(208)= -2.581, p=0.011; *vibrotactile*; t(216)= -2.885, p=0.004). Moreover, the vibrotactile stimuli led to significantly larger modulation of ongoing oscillations during the distraction condition compared to baseline in the anterior (t(182)=-2.214, p=0.028) as well as posterior insula (t(182)=-2.053, p=0.042).

The modulation of ongoing oscillations in the gamma frequency band was significantly larger in the posterior insula (*thermonociceptive*: t(223.308)= -2.774, p=0.006). In the baseline condition, amplitudes did not differ between the modalities. Finally, post-hoc pairwise comparisons showed that during distraction, amplitudes at the frequency of interest (i.e. 0.2 Hz) were significantly larger than in the baseline condition following vibrotactile stimulation, both in the anterior (t(183.650)=-2.124, p=0.035) and posterior insula (t(183.650)=-2.538, p=0.012).

	theta			***alpha***			***beta***		
	F-value	p	η^2_p	F-value	p	η^2_p	F-value	p	η^2_p
condition	4.683	0.032	0.025	4.695	0.032	0.025	4.480	0.036	0.025
modality	7.364	0.007	0.037	0.036	0.849	0.000	2.382	0.124	0.012
orientation	21.108	< 0.001	0.243	24.517	<0.001	0.272	27.686	<0.001	0.312
condition: modality	6.513	0.012	0.035	3.421	0.066	0.018	4.415	0.037	0.024
Condition :location	0.543	0.462	0.003	1.011	0.316	0.006	3.047	0.083	0.017
modality: location	16.646	< 0.001	0.080	13.198	<0.001	0.065	0.101	0.751	0.001
condition: modality: location	2.265	0.134	0.012	5.338	0.022	0.028	0.688	0.408	0.004

	gamma		
	F-value	p	η^2_p
condition	0.259	0.61	0
modality	4.581	**0.034**	0.003
orientation	42.846	**< 0.001**	0.006
condition: modality	0.627	0.430	0.067
condition:location	1.755	0.187	0.016
modality:location	6.959	**0.009**	0.044
condition: modality: location	0.126	0.723	0.015

Table 2. Results of the Linear Mixed Model (amplitude ~ modality * condition * orientation + (1| electrode contact:patient) and estimated partial effect sizes and their confidence intervals, for each frequency band. Significant results are indicated in bold font

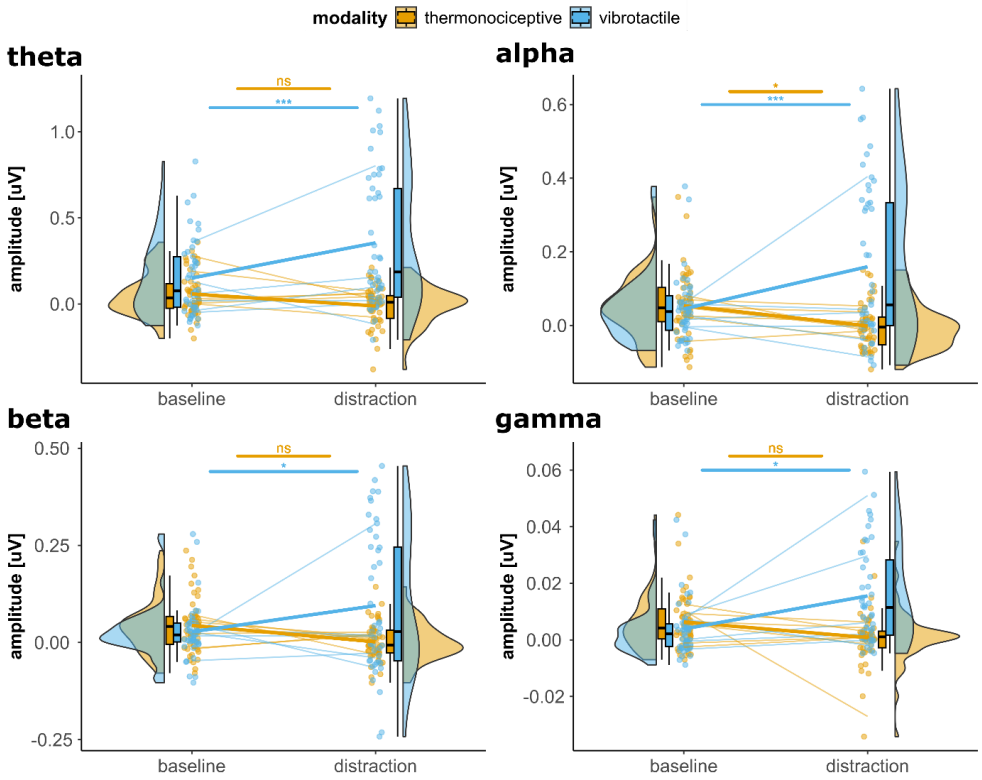

Figure 2. Modulation of ongoing oscillations in the theta, alpha, beta and gamma frequency bands at electrode contacts in the **anterior insula**. For each frequency band, the first few harmonics with amplitudes that were significantly different from zero were summed up into the FOI (theta: 0.2 Hz, alpha: 0.2 Hz + 0.4 Hz, beta: 0.2 Hz + 0.4 Hz, gamma: 0.2 Hz). Background horizontal lines represent patient means, while the bold line illustrates the group mean. Results of post-hoc pairwise comparisons are displayed: *p<0.5, ***p<0.001.

1.4. Assessment of signal to noise ratio across the frequency spectrum

The differences between the results in our primary analysis in chapter 5 and exploratory analysis here were larger than expected, demonstrating the importance of a careful selection of the number of harmonics which should be aggregated for the FOI. While there is not a clear right or wrong in the harmonic aggregation by assessing the LMMs, we would like to

examine a potential method to objectively identify the “ideal” sum of harmonics, i.e. the sum that carries the largest signal-to-noise ratio (SNR) in the spectrum. To do so, for each condition, modality and frequency band, the amplitudes at each harmonic were consecutively summed up, with the calculation of the SNR after each addition to the FOI. Noise was defined using the mean of the ± 10 frequency bins surrounding the harmonic frequency (i.e. ± 0.13 Hz), a frequently used range for noise subtraction in frequency-tagging paradigms using fast periodic visual stimuli (Meigen & Bach, 1999; Retter & Rossion, 2016; Rossion et al., 2012; Rossion et al., 2015; Srinivasan et al., 1999). The following formula was used:

$$SNR\ [dB] = 20 * log_{10}\left(\frac{\sqrt{s_1^2+s_2^2+\cdots+s_n^2}}{\sqrt{n_1^2+n_2^2+\cdots+n_n^2}}\right)$$

in which *s* = baseline corrected signal at harmonic frequency and *n* = mean baseline corrected signal of the frequency bins surrounding the harmonic frequency which were defined as noise (i.e. ± 10 bins).

Figure 3 illustrates the obtained SNRs of the consecutively accumulated amplitudes at the harmonics of the frequency of stimulation. However, the initial SNR values are relatively low compared to its maximum in all frequency bands, which is unexpected, considering that we found few harmonics significantly different from zero above 1 Hz in the analysis of the response in the frequency spectrum (without any summation at the harmonics, see Figure 1). In fact, the SNR for the thermonociceptive modality was negative at the frequency of stimulation in all frequency bands, contradicting the signal at 0.2 Hz in the frequency spectrum which usually shows the largest modulation at this frequency.

Thus, to further understand the difference in results obtained by either summing up all harmonics in the frequency spectrum or just the first few, the same SNR analysis was conducted, but with a much narrower window

for the definition of the noise surrounding the amplitude at the harmonic frequency (± 3 frequency bins, i.e. ± 0.039 Hz) (Figure 4). An illustration of the potential impact of the number of frequency bins used for noise estimation can be found in Figure 5, with examples for the phase-locked response and the beta frequency band.

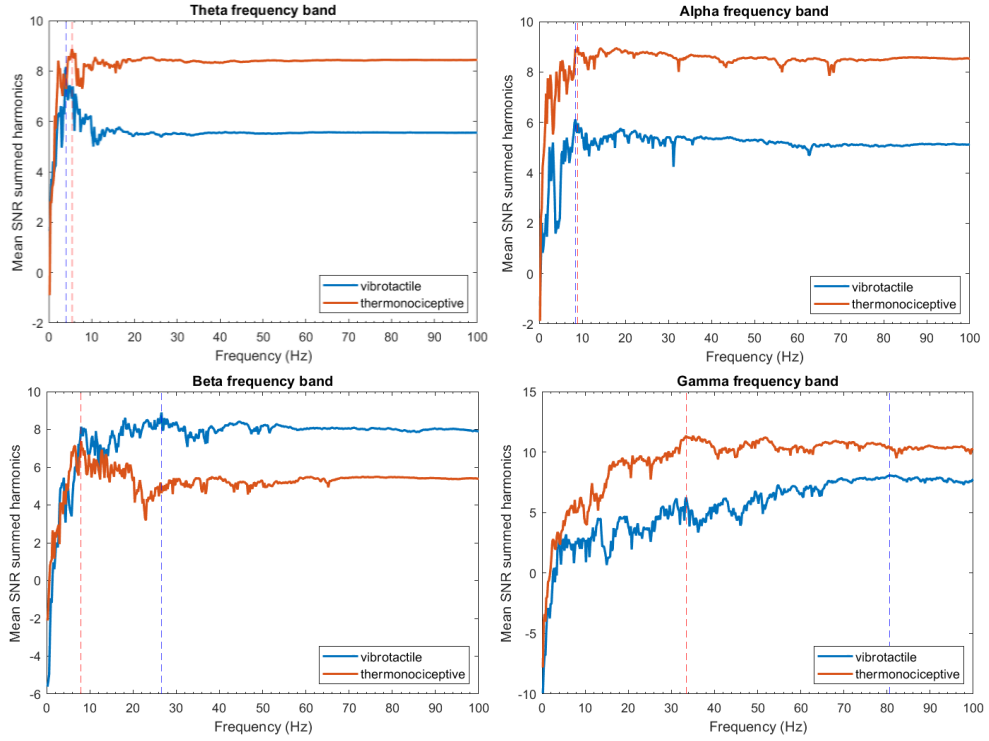

Figure 3. Mean signal-to-noise ratio (SNR) of the consecutively summed up harmonics in the frequency spectrum of each frequency band. Noise was defined as the mean signal at the ± 10 frequency bins surrounding the harmonic of interest (± 0.13 Hz). Vertical lines represent the maximal SNR measured in the spectrum for the respective modality and frequency band.

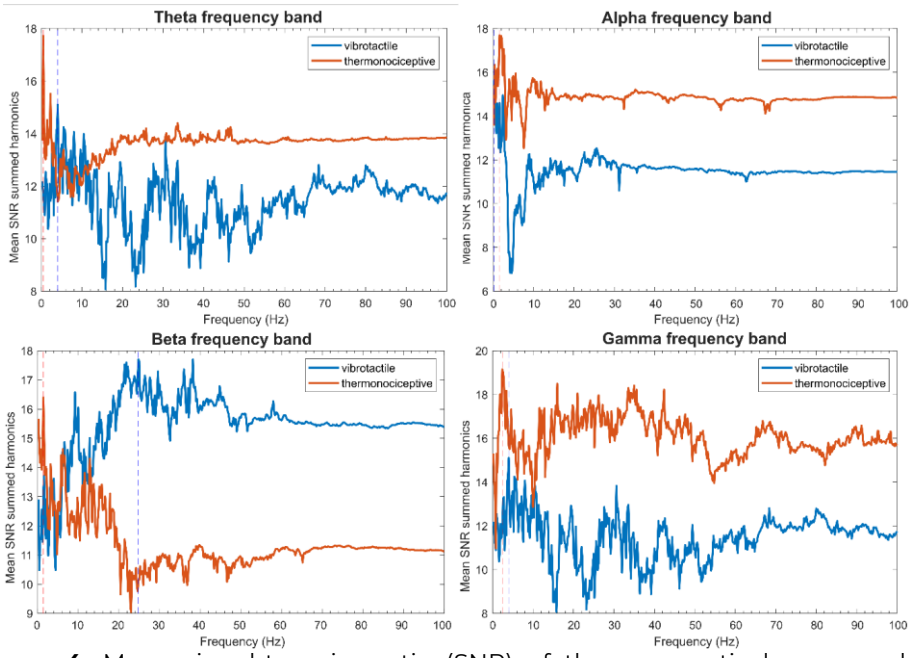

Figure 4. Mean signal-to-noise ratio (SNR) of the consecutively summed up harmonics in the frequency spectrum of each frequency band. Noise was defined as the mean signal at the ± 3 frequency bins surrounding the harmonic of interest (± 0.039 Hz). Vertical lines represent the maximal SNR measured in the spectrum for the respective modality and frequency band.

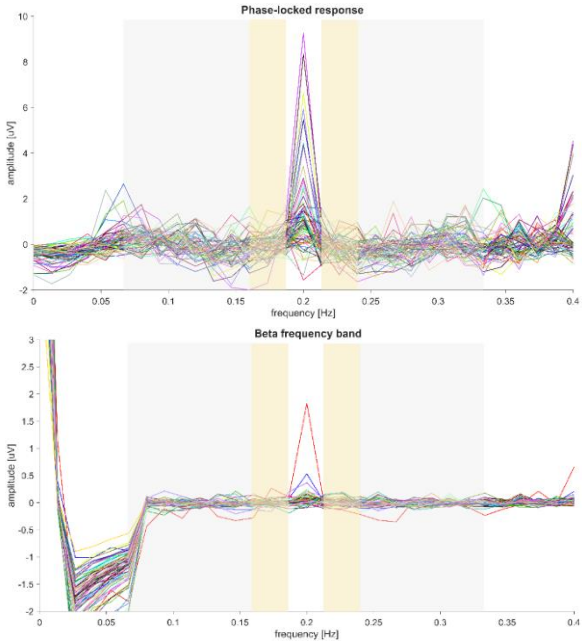

Figure 5. Illustration of the bin-width defined for the estimation of the noise surrounding the harmonic of interest. Group averages with pooled electrode contacts of the phase-locked and estimated beta frequency band response following thermonociceptive stimulation in the baseline condition. Note how for beta (like all other frequency bands), the applied baseline correction leads to a distortion of the signal between 0 and 0.08 Hz. Yellow column = ± 3 frequency bins, i.e. ± 0.039 Hz, grey column = ± 10 frequency bins, i.e. ± 0.13 Hz.

2. Discussion

Due to the ongoing discussions about the ideal number of harmonics that should be aggregated to adequately reflect the neural response to a (periodic) stimulation in the frequency domain both in the literature (Retter et al., 2021) and in our lab, the comparison of the results by aggregation of a different number of harmonics seemed to be a good opportunity to explore this debate and potentially find a solution that is suitable for the slow sustained periodic sinusoidal stimulation that is often used in our lab. Since the results of the main investigation (i.e. potential relationship between the modulation of ongoing oscillations and pain perception in the posterior insula) are discussed in chapter 5, the present discussion will focus solely on the differences and similarities in the results obtained by the two methods of harmonic aggregation and potential future directions using an SNR assessment as basis for the decision on how many harmonics should be aggregated.

The obtained number of harmonics with an amplitude significantly different from zero seemed relatively low across all tested frequency spectra, but are in fact comparable to the results of an investigation using the same stimulation modalities (albeit laser stimulations instead of thermal cutaneous stimulations) and parameters (Liberati et al., 2019). The most notable difference is that our predecessor found almost no significant modulation of ongoing oscillations following vibrotactile stimulation. In the present experiment however, we found that the modulation of ongoing oscillations induced by vibrotactile stimulation was generally lower compared to thermonociceptive stimulation, but still significantly different from zero for most of the tested harmonics (< 1 Hz). Since a similar number of patients / electrode contacts in the insula were part of the experiment and the same stimulation parameters were used, it is not entirely clear as to how this difference originated. One explanation

could be that the distribution of anterior / posterior electrode contacts is not the same in the two investigations and were also not accounted for in the assessment of the amplitudes at each harmonic. Given the potentially differential involvement of the anterior and posterior insula in the perception of somatosensory stimuli, this is likely to have an impact.

Generally, it seems that the amplitude of the harmonics in the thermonociceptive modality decreases linearly, while this is not the case in the vibrotactile modality. In fact, in most frequency bands, the 2nd or 3rd harmonic was larger than the previous one. This disparity between the modalities could be due to the stimulation itself; while for thermonociceptive stimulation, an almost perfectly sinusoidal shape of the stimulation was applied (with the possibility to have a feedback of the applied temperature profile), the vibrotactile stimulation profile was potentially not as precise since the device that was used was not primarily designed for sustained periodic vibrotactile stimulation, had no feedback of the stimulation and there was a certain degree of variability in how participants held the device (e.g. the amount of pressure applied). Hence, the stimulation was potentially less sinusoidal, leading to a less sinusoidal neural response which translates into the formation of more harmonics (see Retter et al. (2021) for a visual illustration of this effect). Moreover, peripheral mechanoreceptors activated by the vibrotactile stimulation relay their activity through large, myelinated fibers which are relatively slow, possibly distorting the sinusoidal shape of the stimulus. And finally, since the haptuator that was used to deliver the stimulation was held by the patient between thumb and index, the applied pressure could potentially also lead to differences in the stimulation (i.e. level of mechanoreceptor activation) which makes the average of the trials more variable and potentially less sinusoidal. Nevertheless, as we did observe a consistent periodic modulation at the frequency of the stimulation, the

above-mentioned considerations do not imply that the vibrotactile stimulation used was not a valid control condition.

The LMM comparing effects of the few aggregated harmonics on electrode contact localization, modality and condition did not differ from the previous results in the main analysis (chapter 5) in terms of amplitude magnitudes in the anterior and posterior insula. It appears that the larger amplitudes found in the posterior insula are a fairly consistent feature of the modulation of ongoing oscillations induced by thermonociceptive and vibrotactile stimulation, as the same relationship was found in Liberati et al. (2019) and the primary analysis of this dataset that aggregated all the harmonics. Additionally, while a consistent increase in the modulation of ongoing oscillations in the anterior insula was found during the arithmetic task compared to baseline following vibrotactile stimulation, similar results were obtained using the "aggregation of all harmonics" method in chapter 5. The first notable difference between the aggregation methods is that, when aggregating only few harmonics, statistical differences in modulation between the modalities during baseline condition (which were present in the theta and alpha frequency band in the primary analysis) disappear. Finally, the arguably largest discrepancy is the almost complete abolishment of the effects that were found in the posterior insula in the primary analysis. Interestingly though, it seems that there is at least a partial shift to the anterior insula, as the effect of the distraction task on the modulation of ongoing oscillations induced by thermonociceptive stimulation is present solely in the alpha frequency band in the anterior insula when aggregating only few harmonics.

As discussed in chapter 5, top-down modulation of pain perception through distraction has been shown to affect the anterior insula by decreasing the neural activity (Atlas et al., 2010; Brooks et al., 2002; Silvestrini & Corradi-Dell'Acqua, 2023). Yet, in this chapter, the focus is not

on the neural underpinnings of the observed activity, but rather on the methodological differences leading to these diverging results in the two different ways of summing up the harmonics in the frequency spectrum.

The first consideration is that, by only aggregating the first few harmonics, a relevant portion of the response to the periodic stimulation at higher harmonics was ignored, leading to the differences in the obtained results. This is in some ways the opposite criticism that was received for the aggregation of all harmonics, in which the summation of noise was a potential issue. Thus, to gain a better understanding of the distribution of the neural response at different harmonics in the frequency spectrum, the mean SNR was calculated for each harmonic sum consecutively (i.e. SNR of the sum of the current harmonic plus the previous harmonics) up to 100 Hz. First, the noise surrounding the harmonic was approximated by the averaging 10 frequency bins to the left and right of the harmonic frequency bin, a method which has often been used in frequency-tagging investigations in the visual domain (Retter & Rossion, 2016; Rossion et al., 2012; Rossion et al., 2015; Srinivasan et al., 1999). The SNRs in all frequency bands showed a similar plateau towards higher frequencies, illustrating that (as assumed in the primary methods in chapter 5) random noise at those higher harmonics cancelled each other out and does not affect the signal to noise ratio any longer. For both the theta and alpha frequency band, the highest SNR can be found at ~3 Hz and ~8 Hz respectively, which seems reasonable given the lower bound of the applied bandpass filter for the respective frequency band. In the beta and gamma frequency bands, the modalities showed larger differences between the maximal SNR and the signal plateaus at higher frequencies. In the thermonociceptive modality, the highest SNR could still be found close to the lower bound of the applied bandpass filter (even lower in the beta frequency band). The vibrotactile stimulation however led to SNR maxima that are past the

middle of the filtered bandwidth. Notably, only in the beta band, the SNR was overall larger for vibrotactile than for thermonociceptive stimulation.

As mentioned previously, to understand the observed negative SNRs at the first harmonics (which are normally seen as the ones carrying the highest signal to noise ratio), the same SNR calculation was applied using a much narrower bandwidth for the estimation of the noise surrounding the signal at the harmonics. This additional analysis highlights how seemingly small details can have a considerable impact on this type of analysis. While the SNRs were generally larger and the difference between modalities remained comparable to the wider noise range, the largest SNRs could now be found almost exclusively at the first few harmonics. Especially for thermonociceptive stimulation, the largest SNR was located within the first 5 harmonics (<1 Hz), reflecting the results of the Wilcoxon signed rank-test on the single harmonic analysis more closely. The visualization of the number of frequency bins used for the estimation of the noise surrounding the amplitude at the harmonic revealed how these relatively larger differences in SNR emerge, particularly at early harmonics. As illustrated in Figure 5, using 10 frequency bins to on each side of the harmonic frequency leads to overlap between the noise considered for each harmonic. As previous investigations using this bin width for SNR estimation used much higher frequencies of stimulation with a similar frequency resolution as us, this problem might have not emerged in those SNR calculations. More importantly, the baseline correction which was applied to the signal after the frequency transform (FFT) leads to a characteristic distortion of the signal between 0 and 0.8 Hz. This has been observed in other investigations using this pipeline (Leu et al., 2023; Leu et al., 2024; Liberati et al., 2019). If 10 frequency bins are considered for the noise estimation, this distorted signal is part of the estimate, despite not truly reflecting baseline neural noise (i.e. random ongoing neural activity).

Since the aggregation method sums up subsequent harmonics and noise bins, this leads to the negative SNR values that were observed in the first SNR calculation. Using only 3 frequency bins for the noise estimation eradicates this problem, as the baseline correction artifact is not taken into account for the noise estimation / SNR calculation. Yet, it could be argued that only 3 frequency bins do not provide an accurate reflection of the noise (i.e. randomly oscillating neural activity unrelated to the stimulus) surrounding the amplitude at the harmonic of interest. Thus, future investigation using a similar sustained periodic stimulation paradigm at low frequencies should consider using a width of 5-7 bins for the estimation of the average noise surrounding the harmonics of interest and the consider summing the amplitudes at all harmonics up to the one with the highest SNR.

While these considerations on an appropriate SNR estimation are relevant, the larger question here was whether the aggregation of the amplitudes at all harmonics in the frequency spectrum (i.e. to the upper end of the bandpass filter, max. 100 Hz) would lead to the aggregation of a lot of noise that would subsequently diminish or "overshadow" the signal that is actually related to our stimulation. While the presented data may not allow for a definitive conclusion on this subject, it seems that the notion that random noise (both positive and negative) at higher harmonics will cancel out if consecutively aggregated - resulting in no net increase in noise – is plausible. This suggests that this approach is valid for frequency tagging analyses.

CHAPTER 7: General Discussion

In this dissertation, we set out to understand the potential functional relationship between the perception of painful stimuli and the modulation of ongoing oscillations using a frequency-tagging analysis approach. Four complementary experiments were conducted: three scalp EEG investigations probing the effects of bottom-up and top-down modulation of pain perception and its effects on the modulation of ongoing oscillations, as well as an additional investigation with the same aim but using depth electrodes implanted in the insular cortex in a cohort of patients undergoing presurgical evaluation for the treatment of refractory epilepsy.

The underlying hypothesis behind all investigations was the same: if a functional relationship between pain perception and the modulation of ongoing oscillations exists, then changes in the perception of the painful stimulation should consequently lead to changes in the modulation of ongoing oscillations. To be able to primarily study the relationship between perception and ongoing oscillatory activity, we chose well-known paradigms that are able to modulate pain perception, either “bottom-up” via variations in the stimulation itself, or “top-down” through cognitive activity. It is important to underline that we were not interested in how the paradigms modulated pain perception *per se*, but rather how these changes would influence the modulation of ongoing oscillations. To evoke the perception of pain, slow sustained periodic thermonociceptive stimulations were used in all experiments, with small variations in stimulation frequency, temperature and duration. This specific stimulation pattern allowed us to “tag” the neural response at the frequency of stimulation in the frequency spectrum (Regan, 1989), efficiently differentiating between activity related to the applied stimulation and other unrelated ongoing neural activity (Colon, Nozaradan, et al., 2012; Mouraux, Iannetti, et al., 2011).

1. Main findings

In **study 1** (Leu et al., 2023), we aimed to affect stimulus perception by distracting 25 healthy participants from the slow sustained periodic thermonociceptive stimulation using an unrelated arithmetic task. Vibrotactile stimulation was used as a control modality for the specificity to nociception of potentially observed effects. The task was successful in diverting participant's attention away from the stimulation and lowered the perceived intensity in both stimulation modalities, yet no such difference was observed in the modulation of ongoing oscillations. While these results might suggest a dissociation between pain perception and modulation of ongoing oscillations, we also found that the task was far less effective than expected. Therefore, it cannot be excluded that a different task with a larger effect would lead to a change in the modulation of ongoing oscillations. The main difference in modulation of ongoing oscillations was found between the modalities, where thermonociceptive stimulation led to consistently larger modulations than vibrotactile stimulation. Potentially, these differences emerge from the inherent difference in saliency between the nociceptive and non-nociceptive stimulation, or the difference in perceived level of intensity between the modalities.

The second attempt to use a top-down modulation of pain perception to investigate the link between perception and the modulation of ongoing oscillations was described in **study 2** (Leu et al., 2024). The expectation of 40 healthy participants concerning the upcoming stimulation was influenced using visual cues, suggesting that either a high intensity or low intensity stimulation would follow. Unknown to the participants, a medium intensity stimulation was intermittently applied, preceded by a misleading cue. Large differences in intensity perception of this medium intensity stimulation were found, depending on which stimulation

intensity participants expected. Thus, it seemed that this time, the chosen cognitive manipulation was more successful than in study 1. Yet again, no difference in the modulation of ongoing oscillations was found between stimulations of the same intensity that were perceived differently due to the preceding cue (i.e. medium intensity stimulation + high intensity cue / low intensity cue). A preliminary interpretation of these results could be to dismiss the link between pain perception and modulation of ongoing oscillations. Taking a closer look though revealed that only in the high intensity stimulation, the modulation of ongoing oscillations was significantly larger than zero. This suggests that in both the medium and low intensity stimulation, the periodic stimulation paradigm did not succeed in eliciting a significant periodic modulation, potentially due to the relatively low peak temperature of the applied stimulation. The EEG results should therefore be interpreted cautiously in this investigation. Thus, even though we did not find a link between changes in perception and the modulation of ongoing oscillations, we cannot exclude that we would obtain different results using a higher stimulation temperature for the medium intensity condition. Similar to study 1, we found a consistent difference in modulation of oscillations between the high and low intensity condition, suggesting that the intensity of the applied stimulation plays a substantial role in shaping the magnitude of the oscillatory activity.

The final scalp EEG experiment of this dissertation aimed to uncover how “bottom-up” modulations in perception influence the modulation of ongoing oscillations in 35 healthy participants (**study 3**). By using a periodic oddball paradigm embedded in the sustained periodic stimulation, we aimed to disentangle effects of stimulus saliency and intensity on both stimulus perception as well as the elicited modulation of ongoing oscillations. The conceptualization of this experiment was challenging, since saliency and intensity are inherently tied to each other

and notoriously hard to differentiate, especially when constricted to the use of a slow sustained periodic stimulation. After many pilot experiments, we settled on a relatively straightforward design, with a high intensity / high saliency oddball in one condition, and a low intensity / high saliency oddball in the control condition. While this design worked well in terms of behavioral and neural response in the “high intensity oddball” condition, it was much more difficult to differentiate the “low intensity oddball” from the main stimulation (i.e. “baseline” stimulation). Given the lack of effect on the perceptual level, we also did not expect to find differences in the oscillatory activity at the oddball frequency. Hence, we were not able to disentangle effects of saliency and intensity neither on perception nor on the modulation of ongoing oscillations. Given the periodicity which is necessary for the frequency-tagging analysis, it might not be the ideal approach to study the effects of saliency on oscillatory activity. Nevertheless, our results were consistent with our previous findings, demonstrating that an intense and salient stimulation leads to modulations in perception and of ongoing oscillatory activity that reflect these properties.

Finally, we had to acknowledge that scalp EEG recordings might not be able to give us the insight we were looking for. Even though we used a 64-channel setup in the scalp EEG investigations, electrical activity recorded at the surface hardly reflects the activity of deep-brain structures such as the insula. Moreover, the initial results which pointed towards a relationship between pain perception and the modulation of ongoing oscillations were found in intracerebral recordings of the insula (Liberati et al., 2019). Thus, the main goal of the final **study 4** using iEEG was to assess whether changes in pain perception induced by an arithmetic task (the same distraction task that was used in study 1) would lead to a congruent modulation of ongoing oscillations. Using the same experimental protocol

would also allow us to directly compare scalp EEG and iEEG results. Secondarily, we aimed to replicate the findings of Liberati et al. (2019) in our non-task condition (i.e. baseline condition), using a thermal cutaneous stimulator instead of a CO_2-laser. The first patient for this experiment was tested shortly after the data collection for study 1 began, while the last patient was added to the data set less than 6 months before this dissertation was submitted. In this period, 8 patients undergoing pre-surgical evaluation for the treatment of refractory epilepsy were tested at their bedside in the St-Luc university hospital in Brussels. While we set out with the idea to use exactly the same experimental paradigm as in study 1 in the patients, we soon had to realize that 30 minutes of arithmetic calculation task in a 1.5h experiment are not an easy feat just days after a highly invasive brain surgery. Thus, for most participants, the data acquisition was spread over multiple days to avoid mental fatigue and make the study feasible in the hospital setting. On a behavioral level, the results were relatively similar to study 1: a decrease in intensity perception was present in both modalities during the arithmetic task, with a stronger effect on the perception of the vibrotactile stimulation. A key difference was the perception of pain. While most healthy participants had perceived the stimulation as painful, this was the case for less than half of the thermonociceptive stimulations in the iEEG sessions. This was further surprising since the same sustained periodic thermonociceptive stimulation (applied with a CO_2-laser) elicited a largely painful sensation in Liberati et al. (2019). Perhaps for this reason we were also not able to replicate the preferential modulation of thermonociceptive stimulation in the theta frequency band which Liberati et al. (2019) had found in the theta and alpha frequency band in the posterior insula. Indeed, we found a significant periodic modulation at the frequency of stimulation in both modalities that was only larger for thermonociceptive stimulation in the alpha frequency band in the posterior insula. This was also the frequency

band and location at which a significant decrease in modulation of ongoing oscillations concomitant to the decrease in intensity perception was observed, supporting our initial hypothesis of a functional relationship between perception and ongoing oscillations. However, since only about half of the thermonociceptive stimulation were perceived as painful, we cannot claim any immediate link to pain perception *per se*, but rather to thermonociception.

2. Interpretation

While frequency-tagging is frequently used in many different sensory domains (such as vision (Rossion et al., 2020), rythm (Nozaradan, 2014) and tactile perception (Moungou et al., 2016)), it is still relatively novel to the assessment of neural responses to nociceptive stimulation. At first, relatively fast (> 3 Hz) electrical (Colon, Nozaradan, et al., 2012) and CO_2-laser (Colon et al., 2014; Mouraux, Iannetti, et al., 2011) stimulations were used to elicit steady-state evoked potentials (SS-EP, equivalent to the "phase-locked response"), predominantly related to Aδ-fiber activity with maximal responses over fronto-central regions. Comparing these responses to concurrently applied tactile and visual stimulation showed that each modality elicited activity in a distinct subgroup of neuronal populations (Colon, Legrain, et al., 2012), but that selectively attending either of the modalities did not alter the magnitude of the SS-EP responses (Colon et al., 2014). However, only at slower stimulation frequencies (i.e. 0.2 Hz), SS-EPs relating to the activation of slowly-adapting C-fibers were found (Colon et al., 2017). Being related to the "secondary", burning and lasting sensation of pain as well as being implicated in e.g. tissue inflammation (Campbell & Meyer, 1983), these SS-EPs could potentially aid in the understanding of the role of C-fibers in pain perception.

Using the same slow sustained periodic sinusoidal stimulation paradigm (0.2 Hz, 75s / trial), but a slightly lower stimulation peak temperature (48°C) and a thermal cutaneous stimulator, Mulders et al. (2020) obtained similar results in terms of topography and magnitude compared to the previously used CO_2-laser for the SS-EP (i.e. phase-locked response) as well as the modulation of ongoing oscillations, which were first characterized by Colon et al. (2017). Moreover, they found that the perception of the stimulation and the recorded EEG responses in the time domain shared many similarities (e.g. larger responses for warm than for cold stimulation, stronger habituation with fixed than with variable surface), suggesting a potential correlation. Following these developments, Liberati et al. (2019) employed the frequency tagging approach in an investigation using intracerebral EEG with electrode contacts implanted in the insula. Interestingly, they found a preferential modulation of thermonociceptive stimulation over vibrotactile stimulation in the dorsal-posterior insula in the alpha and theta frequency bands, suggesting a potential link to pain perception.

Thus, this thesis sets out to define this potential relationship between pain perception and the modulation of ongoing oscillations assessed using frequency-tagging. Yet, the results presented in chapters 2, 3 and 4 do not allow us to make any final conclusion regarding this relationship using scalp EEG. Nevertheless, they have deepened our understanding of the possibilities and limitations of the frequency-tagging approach in the assessment of neural oscillatory activity elicited by thermonociceptive stimulation. The one consistent link we found in all scalp EEG experiments was between the applied stimulation intensity and the magnitude of the modulation of ongoing oscillations. This relationship has already been evidenced in other investigations assessing the effect of (tonic) heat pain on oscillatory activity, showing that the higher the stimulation intensity,

the larger the observed effect (e.g. stronger ERD / power decrease in the alpha frequency band) (Hauck et al., 2015; Huishi Zhang et al., 2016; Nickel et al., 2017; Tiemann et al., 2015; H. Wang et al., 2022). Nickel et al. (2017) investigated the translation from stimulus intensity to pain perception closer using 10 minutes of sustained thermonociceptive stimulation and revealed that stimulus intensity is likely encoded by the oscillatory activity in the alpha and beta frequency band over sensorimotor areas contralateral to the stimulated limb. These results fall in line with functional imaging studies demonstrating that S1 activation relates to spatial and temporal summation at peripheral nociceptors (Peyron et al., 2000) and support the notion that the decrease in oscillatory activity in sensorimotor areas relates to the alerting function of pain (Markus Ploner et al., 2006; M. Ploner et al., 2006), which is more imminent if the stimulus intensity is stronger.

Furthermore, we extended the previously used stimulation parameters (peaks at 48°C/50°C, stimulation frequency of 0.2 Hz, 15 cycles of the sinusoidal period per stimulation trial) and analysis in many ways. In chapter 3, we showed the selection of the peak temperature is highly important to achieve a significant modulation at the frequency of the stimulation and cannot be inferred solely from the C-fiber activation threshold, as we did not observe the expected response using 47°C. Moreover, we demonstrated that – given a sufficiently high peak stimulation temperature – 8 cycles in one stimulation trial and are enough to elicit a periodic response and modulation of ongoing oscillations, effectively shortening the trial duration to 50s. Ee also showed that using 8 trials per condition is enough to obtain a good signal-to-noise ratio in the averaged signal. To account for potentially artifact trials and inter-individual differences, we would recommend using 10 cycles / trial and 10 trials / condition in a setup with a stimulation frequency of 0.2 Hz. These

adaptations increase the feasibility of this type of experiment especially if multiple conditions with the thermonociceptive stimulation are applied, since it decreases the overall duration of the experiment considerably. In chapter 4, we demonstrated that it is possible to integrate a periodic oddball into the slow sustained periodic thermonociceptive stimulation, without participants being aware of the periodicity in the oddball even when they are asked to track their perception of the stimulation. Moreover, given sufficiently high intensity of stimulation (or potentially slower stimulations), the neural response to this oddball can be differentiated from the main stimulation in the frequency domain.

We have also deepened our understanding of how these slow sustained periodic stimulations and their variations are being perceived by healthy participants. The perception of the same stimulation varies considerably between participants, which can be easily shown across the 100 healthy participants that took part in the experiments for this thesis. While reasons for this are manyfold (McGrath, 1994; Quiton & Greenspan, 2008), and would probably fill an entire thesis for themselves, we would like to focus on how to best respond to this variability when conducting experiment using thermonociceptive stimulation and frequency tagging. Given the slow fluctuations of the stimulation temperature, it was also not easy for many participants to define whether the stimulation was “painful”, especially since we only assessed this in a binary fashion at the end of the stimulation in chapter 2, 3 and 5. Additionally, very little time of the stimulation is actually spent at the peak temperature, making each cycle in itself not very painful. It is likely the summation of cycles applied at the same site which make the stimulation painful. We improved the assessment of “pain” in study 4, in which we used a continuous VAS with a clear threshold for “starting to be painful” in the middle of the scale. This allowed for a much more nuanced evaluation of the (pain) perception, and

further enables the tracking of the evolution of the perception cycle by cycle. The results of this experiment impressively demonstrated the differences in the ability to track sustained periodic stimulations as well as how much the perception differed in terms of intensity and painfulness. However, the complication with this scale is that the movement of the arm, which is as periodic as the stimulation, would interfere with the EEG recordings. Thus, while it can offer a lot of information about the perception of the stimulation, it effectively doubles the time of the experiments, as any EEG data will have to be recorded separately. Of note, if the perception of "pain" is crucial for the experiment or its interpretation, stimulation temperatures should be adapted to the individual, using either thresholding or staircase procedures (Doll et al., 2014; Yarnitsky et al., 1995). This will of course lead to the confound of using different stimulation intensities, which as we have already seen in the preceding chapters, heavily influences the modulation of ongoing oscillations. Thus, each investigation needs to carefully consider whether the perception of pain (as opposed to the mere activation of the (thermo-) nociceptive system) is crucial to answer their hypothesis.

In terms of analysis, we moved from assessing mostly the amplitude at the frequency of the stimulation (as done in previous studies from our lab) to taking the response at each harmonic in the frequency spectrum into account. The rationale for this summation of harmonics has been extensively discussed in chapter 1 and 6, and while there is still no clear consensus on what is the "perfect" amount of harmonics to sum (Retter et al., 2021; Zhou et al., 2016) (if this could even be generalized across different investigations / modalities), we are confident that by taking harmonics into account, we are closer to assessing the full neural response induced by the stimulation.

Finally, we should consider the results of the iEEG experiment in chapter 5. This was the only experiment in which we found a relationship between changes in intensity perception and the modulation of ongoing oscillations, despite using exactly the same paradigm and analysis in a scalp EEG experiment in healthy volunteers. This disparity highlights the fundamental differences between intracerebral and scalp EEG. The main difference is the activity that is being recorded; while iEEG records electrical potentials generated by the transmembrane current flow between relatively small, localized groups of neurons (Eccles, 1951), scalp EEG samples activity predominantly related to postsynaptic potentials of relatively large groups of pyramidal neurons close to the scalp (Luck, 2014), whose electrical potentials are distorted by cerebral fluid, bone and skin before it reaches the recording electrode. Thus, while iEEG can inform us about neuronal activity even in deep brain structures (depending on the placement of the recording electrode), the same deep brain activity would not generate a signal that could be picked up and differentiated from other sources at the scalp level. Much more likely, scalp EEG recordings reflect mostly activity of "superficially" located regions such as S1, explaining the difference in the results we obtained in the two experiments employing the same distraction task. The insula has been implicated in pain processing in many investigations, but the specific involvement of its subregions remains less clear (Labrakakis, 2023). Our results suggest a relationship between thermonociception and modulation of oscillations in the alpha frequency band in the posterior insula, which is one of the bands in which Liberati et al. (2019) found a preferential modulation of (painful) thermonociceptive stimuli. However, while the theta frequency band has exhibited the same preferential modulation in their study, we could not find such a relationship, perhaps because most of our stimuli did not elicit a painful percept. Hence, the precise role of the posterior insula in pain perception remains ambiguous.

Future research could focus on disentangling these relationships using neuromodulation, as these interventions can provide us a more causal effect of the relationship between stimulation and perception.

In a more general context, we should consider the differences and similarities between assessing ongoing oscillatory brain activity and the "standard" ERP approach, which has characterized the understanding of the temporal aspects of neural responses to somatosensory (and nociceptive) stimuli for much of the last decades. ERPs are usually recorded in response to brief stimuli, eliciting a neural response time-locked to the onset of the stimulus, and are composed of a series of positive and negative deflections in the EEG recording (e.g. N1, N2-P2 complex, P3), each attributed to a sequential stage of stimulus processing (Luck, 2014). As such, they reflect e.g. stimulus detection, saliency attribution, and cognitive stimulus evaluation over a timeframe of a few hundred milliseconds, therefore providing detailed temporal information about somatosensory processing (Sokhadze et al., 2017). In contrast, ongoing oscillations are not time-locked to a stimulus, but ever-present fluctuations of brain activity, which are involved in the integration of information across different brain regions and build the foundation for the "state" of the brain at any given moment. Thus, they represent a broader state of cortical excitability and connectivity, which can be perturbed by a somatosensory stimulus or sustained cognitive processes. Prominent examples of such processes are attention or expectation, which have been shown to modulate both ERPs as well as ongoing oscillations. Distraction (e.g. attention away from a stimulus) has been demonstrated to decrease the amplitude of the N2 and P2 component (Garcia-Larrea et al., 1997; Yamasaki et al., 1999) while attention towards the stimuli can lead to an increase in the same component (Legrain et al., 2002), potentially deriving from the allocation of attentional resources towards the detection of the

sensory input (Legrain et al., 2012). Arguably, all components of the ERP seem to be to some extent influenced by attentional modulation (Ohara et al., 2004). Stimulus expectation has also been shown to influence components of the ERPs (Miyazaki et al., 1994). Thus, ERPs reflect a transient response to a specific event and potentially highlight the role of specific cortical regions such as SII and the ACC (Treede, 2003). Ongoing oscillations on the other hand reflect the changes in the current "state", which can stretch beyond the timeframe of the applied stimulus. As already discussed in this dissertation, attention leads to a decrease in alpha band power (i.e. ERD), likely linked to cortical inhibition / gaiting of information (Pfurtscheller, 2003), whereas gamma band power increases, potentially strengthening local and inter-regional connectivity (Clayton et al., 2015). Similarly, effects of expectation on ongoing oscillations are marked by a change in activity in the alpha and beta frequency band, associated with a pre-stimulus "preparation" towards the expected stimulus as well as a "predictive coding" feedback, which reacts depending on whether the stimulus matches the expectations (Bauer et al., 2014). Thus, while ERPs inform us about the immediate processing of a stimulus and its temporal dynamics, ongoing oscillations provide context about the cortical states and network dynamics surrounding the same event. They are closely linked to each other, as it has been found that the P3 (or P300) magnitude of the ERP modulates alpha ERD (Yordanova et al., 2001) and early evoked gamma oscillations match the P3 response in discrimination tasks (Herrmann & Mecklinger, 2001).

In a similar vein, there has been a longstanding debate around what exactly these frequency-tagged neural responses represent (Capilla et al., 2011; Doelling et al., 2019; Haegens & Zion Golumbic, 2018; Heinrich, 2010; Henin et al., 2023; Herrmann, 2001; Norcia et al., 2015; Zhou et al., 2016; Zoefel et al., 2018). Are they merely superimposed evoked potentials, or do they

reflect neural entrainment induced by the stimulation? While answering this question was by no means a goal of this thesis, it is an important discussion to contextualize the obtained results and how they can inform us about the neural processes underlying pain perception. Here, we should differentiate between the "phase-locked" response (i.e. steady-state response), and the "non-phase-locked" response (i.e. modulation of ongoing oscillations). There is accumulating evidence that the "phase-locked" response indeed corresponds to the linear superposition of transient ERPs in the frequency domain (Capilla et al., 2011; Ding & Simon, 2013; Zhou et al., 2016). This is supported by the notion that any frequency domain signal (if summed at its harmonics) is simply the reconstruction of the original time domain signal (Retter et al., 2021). Thus, as ERPs and their relationship to pain perception are already well characterized (Iannetti et al., 2008; Legrain, Iannetti, et al., 2011; Mouraux & Iannetti, 2009), the phase-locked response has not been of primary interest in the different experiments that were conducted for this dissertation. The modulation of ongoing oscillations however is considered to reflect the "non-phase-locked" oscillatory response to the applied stimulation, due to the estimation of the signal envelope through the Hilbert transform. This linear operation creates a 90° phase shift in the signal, allowing us to not only assess the Fourier-transformed magnitude of the response but also take its phase angle into account. As phase resetting (i.e. a shift in the phase of the oscillation, often to synchronize with other activity) has been proposed as one of the underlying mechanisms of intrinsic oscillatory synchronization (Doelling et al., 2019; Schroeder & Lakatos, 2009), modulations thereof by the applied stimulation might be uncovered by this approach and contribute to the understanding of the neural dynamics of pain perception. And indeed, Guo et al. (2020) demonstrated that following sustained periodic thermonociceptive stimulation at 0.1 Hz over 30s, the modulation of oscillatory activity outlasted the stimulation,

suggesting an entrainment of the oscillatory activity. Interestingly, the authors chose to remove any part of the signal that was potentially generated by a transient evoked response to the stimulation through a series of elaborate filters. Perhaps due to this stringent filtering, they found that pain sensitivity was related to the strength of the neural entrainment on a group level, indicated by participants having higher pain sensitivity showing that the phase of the entrainment was closer to the actual stimulation as well as a larger increase in power. Thus, modulating intrinsic oscillatory activity by sustained periodic thermonociceptive stimulation could reveal the neuronal synchronization involved in the formation of pain perception at least to some extent, and therefore open the door for potential treatment interventions using non-invasive brain stimulation that could alter the (potentially maladapted) synchronization of these neuronal populations in chronic pain conditions.

3. Limitations

While the frequency-tagging approach allows us to efficiently differentiate ongoing neural activity related to our stimulation from unrelated activity, this methodology also has its limitations. To obtain a good signal-to-noise ratio, rather low frequencies of stimulation have to be used (Colon et al., 2017), and between 8-10 cycles of the periodic stimulation should be present within each trial. This makes the stimulation quite long and tedious for the participants. While any cognitive task gets exhausting over this period of time, a “no-task” condition also gets very boring, making it difficult for the subject to focus on the stimulation. Additionally, the required duration of the stimulation and the repetition of the cycles on the same patch of skin surface also make it difficult to deliver thermonociceptive stimulations that are perceived as painful but are also

bearable and do not harm the participants. Finding a compromise between these factors led to many of our stimulations to be perceived as non-painful, effectively preventing us from drawing any conclusions regarding the involvement of “pain” in the observed neural responses.

In hindsight, there are a few points that could be improved in the different studies of this thesis, that could possibly lead to clearer findings. While the arithmetic task in **study 1** managed to distract participants to a certain degree, we would have hoped for a stronger effect. Interestingly, in our pilot study in 20 healthy participants in which we tested the effect of the arithmetic task on the perception of the thermonociceptive stimulation, the task was highly successful. Thus, the addition of the vibrotactile stimulation as a control modality, which effectively doubled the duration of the experiment, might have led to participants getting tired and hence focus less on the calculations. A shorter experiment (in terms of trial duration or trial repetitions) might have been more suitable to optimize task performance. Another confound for the analysis was that we did not really have a readout of how engaged the participants were in the task. While they had to report the final number that they calculated, we were not able to say whether they just calculated very slowly, only did the task in the last 10 seconds, made few or many mistakes etc. Given a more comprehensive understanding of the participant’s involvement in the task, we could have potentially stratified the sample into a “distracted” and “not distracted” group and examined whether this affects our results. Individualizing task difficulty could have likely also improved task performance. Considering these limitations it also should be noted that it was rather difficult to find a distraction task that is in no way periodic (to not interfere with the periodic vibrotactile and thermonociceptive stimulation) and does not require any non-cognitive neural action (i.e.

reading something, listening, clicking buttons) since this would have also interfered with our EEG recordings.

In **study 2**, we had not anticipated how well the task manipulated participant's perception of the thermonociceptive stimulation for the entire 50s of the stimulation. Of course, this task had previously been used successfully (Atlas et al., 2010), but over shorter stimulus durations. This being said, while the task was highly effective, the chosen stimulation temperatures were not ideal. The aim was to choose 3 different stimulation peak temperatures that could be easily differentiated into a "low intensity" and a "high intensity" stimulation, with the medium intensity stimulation sitting somewhere in between, ideally with the same temperature difference to the high and low intensity stimulation. While we were not necessarily interested in the neural response to the low intensity stimulation, it was a prerequisite to be able to compare responses in the medium intensity condition following different visual cues. Prior investigations using ultra-slow sustained periodic sinusoidal stimulations used peak temperatures between 48 and 50°C (Colon et al., 2017; Guo et al., 2020; Mulders et al., 2020). Yet, given that this type of stimulation primarily activates C-fibers (Colon et al., 2017), which have an activation threshold of around 40°C, we assumed that we could safely lower the stimulation temperature without losing the periodic response. As previous investigations using this cue-based expectation modulation did not use long sustained periodic thermonociceptive stimulation, we could not base our temperature range solely on that, and we chose the temperatures 44°C, 47°C and 50°C, thinking that, at least, this paradigm will be bearable for all subjects across the 36 applied trials. In hindsight maybe naively, while we piloted the expectation paradigm behaviorally, we did not pilot the EEG response to the different stimulation temperatures prior to starting the experiment and given the requirements for a level 1

Registered Report, we also did not analyze the data until the end of data acquisition, to avoid creating any potential bias during the experiment. Then, unfortunately, we had to acknowledge during the analysis of the data that the medium intensity stimulation peaking at 47°C each cycle was probably too low to elicit a periodic neural response or modulation of ongoing oscillations, as we could only observe these in the high intensity condition (50°C). In retrospect, to be sure to elicit a periodic modulation and a modulation of ongoing oscillations, we should have used a medium intensity stimulation at 48°C or higher (based on Mulders et al. (2020)). Consequently, the low and medium intensity stimulation would also have to be adjusted. To stay within a bearable limit for the participants, the high intensity stimulation could be between 50 and 51°C, while the low intensity stimulation would then be between 46 and 47°C. However, whether the difference between high and low is enough to be clearly differentiated and whether the overall increase of stimulation temperature would make the experiment less bearable would have to be part of new pilot experiments.

The last scalp EEG experiment (**study 3**) was arguably the most challenging to conceptualize. While the goal of having a sustained periodic oddball stimulation embedded within a "baseline" sustained periodic stimulation that would elicit a change in the saliency of the stimulation was clear, it was much less clear how this could be achieved without also varying the intensity of the stimulation, which would be a confound for the interpretation of the saliency effect. Many pilot experiments were conducted in a bid to find a study design that would be able to differentiate between effects of saliency and intensity. We tried probes of different shapes and sizes and to cycle across the zones independently in different sequences (e.g. activating each zone alone, then all together for the oddball, activating only one zone consistently and all zones for the oddball, activating zones clockwise and then anticlockwise

for the oddball). The main aim of those attempts was to not change the applied stimulation intensity itself (i.e. the temperature of the probe). Yet clearly, if one zone is activated more frequently than other zones it creates a confound, as there could be sensitization or habituation at peripheral receptors. Moreover, each zone of the TCS is relatively small, and we had to accept that our participants were not able to differentiate between the activity of them if they were activated in a cyclic manner. For these reasons, we circled back to our initial plan, which is to vary the intensity of the oddball stimulation cycles compared to the baseline stimulation cycles and implement a control condition to differentiate between effects of intensity and saliency. As evidenced by chapter 4, this approach was not very successful. However, given our extensive piloting, we don't see that many options to improve the experimental paradigm if it has to be organized around a sustained periodic stimulation suitable for frequency tagging. Because even if the stimulation frequencies would be lowered to enable participants to track the stimulation more clearly, and thus hopefully make the control condition more effective, the stimulation would turn out to be extremely long, as 8-10 cycles of the oddball are needed for a good signal-to-noise ratio. Indeed, it might be that frequency tagging is not the most ideal approach to disentangle effects of saliency and intensity on oscillatory activity.

Finally, we should also consider limitations in the iEEG experiment (**study 4**). Many of them have already been discussed in chapter 5 and are inherently tied to this type of experiment (i.e. hospital setting, tiredness of participants, no control over implanted electrode locations). Yet, the design of the experiment could be improved to be more suitable for this environment. Naturally, as the same paradigm was used as in study 1, many of the discussed limitations of the arithmetic task also apply to the iEEG to this experiment. Moreover, since the patients had just recently

undergone a highly invasive brain surgery, the entire experiment should not take more than 1h to not fatigue them more than necessary. This could be achieved by shortening the trial duration to 50-60s and apply 1-2 trials less per block. Given the high signal-to-noise ratio of intracerebral recordings, a lower number of trials should suffice to achieve a clean signal compared to scalp EEG investigations.

4. Perspective

4.1. Functional connectivity

A possible limitation in study 1 and study 2 is the selection of only one electrode of interest out of a 64-channel setup for the analysis. We chose to investigate the modulation of ongoing oscillations based on their dynamic and flexible nature, and their role in neural communication. Consequently, it is unlikely that the electrical potentials measured at a singular electrode can adequately reflect the underlying neural activity and the potential changes induced by our interventions / tasks. Thus, a more holistic approach that takes clusters of electrodes into account might be more reasonable, as it has been done in few other investigations assessing how ongoing oscillatory activity is affected by painful stimuli (Bott et al., 2023; Nickel et al., 2022; Tiemann et al., 2015). A further step to view the brain as a network of activity that shapes the perception of pain through its interactions would be to incorporate source connectivity analyses (Schoffelen & Gross, 2009). While there are many different ways to assess the temporal and spatial correlations between nodes of EEG activity (recently reviewed by Chiarion et al. (2023)), all with pros and cons relative to the experimental paradigm and research question, an in-depth review discussion would be beyond the scope of this chapter. Of note, EEG-based

source localization should be interpreted cautiously and as a complementary approach to “traditional” EEG readouts, as the signal at different electrodes correlated thus many different combinations of sources can explain the same topography of activity. Nevertheless, there is a growing body of research focusing on the functional connectivity of small and large scale neural networks and their relationship with pain (Bott et al., 2023; Modares-Haghighi et al., 2021; Nickel et al., 2017; Nickel et al., 2020; Schulz et al., 2015).

4.2. Brain-state dependent non-invasive neuromodulation:

Using the techniques presented in this thesis, any changes elicited in the modulation of ongoing oscillations related to pain perception are merely correlational evidence. To fully understand the functional relationship between ongoing oscillations and pain perception, it is imperative to investigate a causal link between these phenomena.

Non-invasive neuromodulation techniques such as transcranial magnetic stimulation (TMS) allow the direct and focal stimulation of the brain through the creation of a magnetic pulse, inducing an electrical field which can activate neural networks in the cortex by depolarizing superficial axons (Zewdie & Kirton, 2016). Traditionally, these magnetic pulses are delivered in a single-pulse manner over the sensorimotor cortex 1 (M1), eliciting a motor-evoked potential (MEP) at peripheral muscles, which is widely accepted as a correlate for cortical excitability (Ilmoniemi et al., 1997). In more recent years, repetitive TMS (rTMS) paradigms emerged which added a large sequence of TMS pulses in a series, leading to changes in cortical excitability which can outlive the duration of the TMS intervention (Desideri et al., 2018; Zrenner et al., 2018). This technique has since been successfully used in the treatment of e.g. clinically depressed adults (Nahas et al., 2001).

Not unlike TMS, pain has been shown to alter corticomotor excitability, as illustrated by a reduction in MEPs following experimental pain interventions (Bank et al., 2013; Burns et al., 2016; Rohel et al., 2021). Thus, the stimulation of the motor cortex could potentially interact with/modulate cortical excitability and consequently alter pain perception. As rTMS has been shown to induce long-lasting effects of neuronal circuitry, it seems like an ideal technique to use for the treatment of chronic pain conditions. Indeed, rTMS has since been used in different groups of neuropathic pain patients with promising results, as reviewed by Attia et al. (2021). Yet, the underlying mechanisms are still poorly understood. A comprehensive review on the analgesic effects of rTMS has been conducted by Moisset et al. (2016), documenting the successful use of TMS not only over M1 but also over the dorsolateral prefrontal cortex (DLPFC). While possible pathways of action are discussed, there is no complete grasp on how rTMS leads to its analgesic effect. Yet, recently published comprehensive reviews comparing the effectiveness of TMS over M1 or DLPFC using a large body of evidence came to the conclusion that M1 is the superior target to produce analgesic effects (Garcia-Larrea, 2023; Garcia-Larrea & Quesada, 2022). Nevertheless, while rTMS effects are often reliable on a group-level, the cause for the observed large intra- and inter-individual differences in response to the stimulation remain unclear (Horvath et al., 2015; Wiethoff et al., 2014). A more individualized approach might be the solution to develop effective treatment solutions. To achieve this, a better understanding of the cortical activity during and following rTMS is imperative. Amongst other factors, the brain-state of the individual at the time of stimulation might be a contributing factor to the observed variability in TMS outcomes (Li et al., 2015; Ridding & Ziemann, 2010).

While MEPs have been frequently used to assess the corticomotor excitability, they can only provide limited insights into the underlying

mechanisms since they merely reflect the “sum” of activities from cortical and peripheral levels. The recent developments in electroencephalography (EEG) devices which are more robust towards TMS-evoked artifacts have enabled researchers to gather information measured directly from the cortex in the form of TMS-evoked potentials (Farzan et al., 2016; Ilmoniemi & Kičić, 2010). The henceforth emerging research branch of TMS-EEG (combining these two techniques) enabled the assessment of cortical properties such as excitability, inhibition, plasticity, and connectivity (Ilmoniemi et al., 1997; Miniussi & Thut, 2010). Additionally, it facilitates the online measurement of the ongoing brain state of the individual before, during, and after TMS. Current state-of-the-art methodology has been discussed in the recently published review by an expert panel in the field (Hernandez-Pavon et al., 2023). The research group of Prof. Paolo Belardinelli has hence specialized in the brain-state dependent use of TMS, working towards a closed-loop application of non-invasive neurostimulation (Zrenner et al., 2016).

In this line of research, specific brain-states (measured by EEG) are identified which can potentiate the cortical excitability induced by TMS if triggered at the appropriate state. To this end, either the positive or negative peak (i.e. trough) are identified online by a real-time system based on the EEG traces of a specific electrode of interest, creating a forward prediction and estimating the phase of the ongoing activity in a specified range at a specific time point. The stimulation is consequently triggered when a specific phase condition is met (Figure 1). The different phases are related to the presence of different neurotransmitters; the positive peak is associated with the release of GABA in the postsynaptic cleft, leading to an inhibition. Conversely, signal troughs are linked to the release of Glutamate, a facilitatory neurotransmitter (Sears & Hewett, 2021). Zrenner et al. (2018) showed that a high frequency μ-rhythm phase-

dependent rTMS intervention (200 stimulation triplets at 100Hz at 80% of the resting motor threshold (RMT)) led to increased corticospinal excitability as measured by MEP amplitude, with a long-term potentiation like increased excitability up to 30 min after the intervention. Triggering the stimulation at the negative peak led to significantly increased corticospinal excitability compared to random phase stimulation. Conversely, TMS pulses triggered at the positive peak led to a reduction in MEP amplitude, illustrating a decrease in corticospinal excitability. Thus, phase-dependent high-frequency rTMS interventions allow us to selectively modulate the corticospinal excitability.

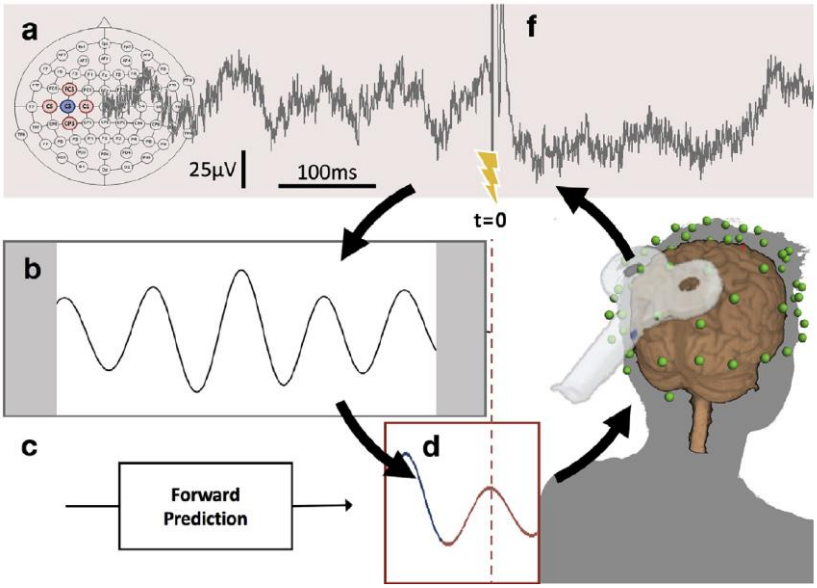

Figure 1: illustration of the phase-dependent TMS loop. The ongoing µ-rhythm is measured, and when a desired state (i.e., peak or through) is predicted, the TMS pulse is triggered. (Zrenner et al., 2018)

In an extension of this investigation, Desideri et al. (2018) examined the resting-state EEG correlates of cortical excitability following µ-rhythm phase-dependent burst rTMS. Additionally, MEPs and single-pulse TMS evoked and induced EEG responses were compared before and after the burst rTMS intervention. While the previously observed effect on MEPs was

reproduced no significant differences were found in any of the EEG measures. Yet, other investigations did find increased phase-locked EEG responses and a higher synchronization with interconnected contralateral homologous regions following single-pulse TMS over M1 targeting the trough of the μ frequency band. These results show that phase-dependent stimulation over M1 does not only create local effects, but can also influence the magnitude and reliability of within-network synchronization (Momi et al., 2022).

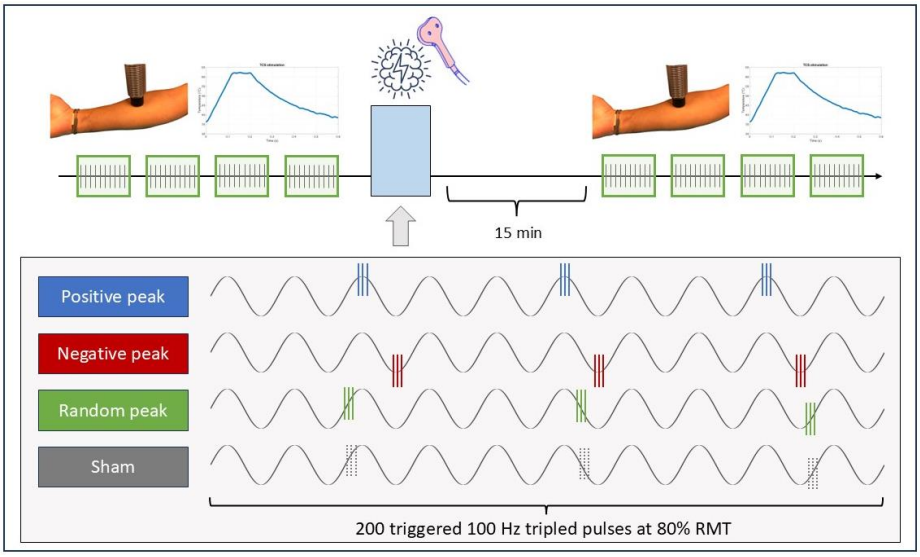

Figure 2: Illustration of the proposed experimental paradigm to assess whether changes in cortical excitability have an effect on pain perception and / or processing. Brief painful stimuli will be used to assess this relationship before and after the phase-dependent rTMS intervention.

These advances will allow us to directly probe the relationship between the modulation of ongoing oscillations and pain perception by modulating corticospinal excitability using non-invasive neuromodulation. Thus, I will use the opportunity of having a few months left before my PhD fellowship expires to embark on a collaboration with the lab of Prof. Belardinelli at CIMeC / University of Trento. Our collaboration will employ a high-frequency phase-dependent rTMS intervention as described above to

selectively increase or decrease corticospinal excitability. Using a pre-/post-intervention paradigm (Figure 2) will allow us to assess changes in the response to thermonociceptive stimuli in cortical activity measured by EEG as well as in the subjective perception of the individual.

Following a high-frequency rTMS intervention targeting the trough of the μ frequency band, we expect to induce a state of higher cortical excitability. We hypothesize that this will cause an increase in the modulation of ongoing oscillations as well as in the pain perception. On the other hand, the rTMS intervention targeting the peak of the μ frequency band will lead to a decrease in modulation of ongoing oscillations and pain perception. As a control condition, a high-frequency rTMS intervention stimulating at random point of the μ frequency band will be used. In this condition, we do not expect major changes in the EEG responses or the pain perception. A successful implementation of this phase-dependent rTMS intervention could potentially lead to novel therapeutical intervention for chronic pain patients.

5. Conclusion

This dissertation highlighted many of the advantages and limitations of employing a frequency-tagging approach to study the neural processing of thermonociceptive stimulation. Using scalp EEG, we were not able to fully characterize the functional relationship between pain perception and the modulation of ongoing oscillations. Indeed, given the underlying complexities of the dynamic system of ongoing oscillatory activity, the adopted scalp EEG measures might not have been sufficient to elucidate this question. Nevertheless, the obtained intracerebral recordings from the posterior insula provided evidence that thermonociception could indeed be related to the modulation of alpha band oscillations. Moreover, in synergy with the findings of Liberati et al. (2019), they suggested that theta band oscillations could be linked to pain perception, paving the way for future investigations assessing this relationship causally using neuromodulation.

(BONUS) CHAPTER 8: Registered Reports

While not directly a part of the research conducted in this thesis, I would like to spend some time on the concept of "**Registered Reports**", a publication method that I used for all scalp EEG experiments presented here (chapter 2,3, and 4).

It has long been known that academic publishing favors positive findings, leading to the development of publication bias (Fanelli, 2010; Jennions & MØLler, 2002) and selective reporting (John et al., 2012; Simmons et al., 2011). These practices further disincentives direct replications, as they are not considered "novel" and can often end in negative results (Collaboration, 2015). Yet, replications are necessary to solidify novel findings. Furthermore, the way the sample size has been derived is often unclear, leading to underpowered studies and overestimation of effects (Button et al., 2013). Taken together, the reproducibility and transparency of the academic publishing system was highly questionable. But in a career in which one "publishes or perishes", it is not surprising that many scientists see themselves forced to find novel and exciting findings in all their experiments, if the alternative is to lose out on grants and career opportunities because they cannot get their work published (Nosek et al., 2012).

In an attempt to combat these developments, Chambers (2013) started the Registered Report initiative at the journal *Cortex* and further developed the idea by creating an independent non-profit peer-review platform: the "Peer-Community in Registered Reports" (PCI RR) (https://rr.peercommunityin.org). The aim was to make publications accessible, transparent and the scientific methods rigorous and the main criteria for publication. This is achieved by a peer-review process *prior* to data acquisition (see Figure 1). In this "Stage 1", authors submit a manuscript containing a detailed description of the methods (including extensive sample size justifications, analysis plan and preliminary

interpretations of main outcomes) as well as a brief introduction. This manuscript is then peer-reviewed by experts in the field, based on pre-defined criteria (can be found here: https://rr.peercommunityin.org/help/guide_for_reviewers). Importantly, these criteria are focused on scientific soundness of the chosen methods, making sure that each step is described and adequately justified.

Once the peer-review process is complete, the manuscript receives "in-principal-acceptance" (IPA). This means that the investigation will be published regardless of the outcome, as long as the authors adhere 100% to the registered methods. After Stage 1 acceptance, the manuscript cannot be changed anymore and any deviation need to be communicated as soon as possible, potentially leading to a review of the IPA. Additionally, the manuscript has to be stored in a publicly available repository, such as the Open Science Framework (OSF).

Once the data is acquired, analyzed and discussed, the "Stage 2" manuscript is sent for peer-review. Ideally, the same reviewers as for Stage 1 also review Stage 2, as the goal here is to not critique the already approved methods, but only review the results and discussion of the experiment. While exploratory analyses can be conducted and added to the manuscript, they cannot constitute the main findings of the investigation. All acquired data and digital study materials have to be made publicly available for Stage 2 to be completed. Finally, after this peer-review stage is passed, the manuscript is ready for publication in one of the growing number of journals that accept Registered Report.

Previously, RRs were registered directly with the respective journal that would publish it. Recently, the peer-community in Registered Reports (PCI RR, https://rr.peercommunityin.org/) has been established and newer RRs are being reviewed through this community-based non-profit platform. PCI RR does not publish the RRs themselves but collaborates with journals

that offer RR publications. Therefore, the authors only have to decide at the end of the manuscript process in which journal (that accepts RRs from PCI RR) they would like to publish their results. It is also a part of the PCI RR process to upload all manuscript versions (including all stages of the review process), as well as raw data and analysis scripts on a publicly available server such as OSF.

In a recent review by Chambers and Tzavella (2022), the last 10 years of development of Registered Reports, its current state and future trajectory are discussed. Yet, as noted by the authors, the initiative is successful in improving reproducibility and transparency in academic publishing, and One major drawback of the Registered Report process is the time it takes to actually start an experiment. Since IPA has to be attained *before* data acquisition can start, the timeline is highly dependent on the speed of the Stage 1 review process. Especially for early career researchers with short-term contracts this might pose a problem and could potentially discourage them from pursuing a Registered Report.

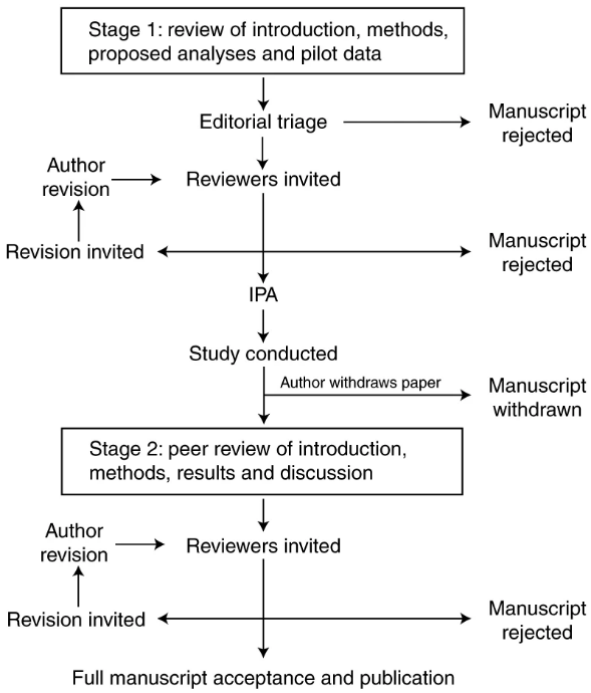

Figure 1. Workflow scheme for Registered Reports. Adapted from Chambers and Tzavella (2022)).

Past, ongoing and future projects related to this dissertation

Leu, C., Courtin, A., Cussac, C., & Liberati, G. (2023). *The role of ongoing oscillation in pain perception: Absence of modulation by a concomitant arithmetic task.* Cortex, 168, 114-129. https://doi.org/https://doi.org/10.1016/j.cortex.2023.08.005

Leu, C., Glineur, E., & Liberati, G. (2024). *Cue-based modulation of pain stimulus expectation: do ongoing oscillations reflect changes in pain perception? A registered report.* Royal Society Open Science, 11(6), 240626. https://doi.org/doi:10.1098/rsos.240626

Leu, C., Forest, S., Legrain, V. & Liberati, G. (under review). *The effect of stimulus saliency on the modulation of ongoing neural oscillations related to thermonociception: a Registered Report.*

Leu, C., Boutachkourt, A., Ferrao Santos, S., Fierain, A. Finet, P., Joris, V. & Liberati, G. (in preparation[3]). *Linking the modulation of ongoing neural oscillation to thermonociception using intracerebral EEG: insights from the posterior insula.*

*Castellano, P., ****Leu, C.,** Mazzetti, M., & Liberati, G. (in preparation[3]) *Fast Periodic Visual Stimulation to study the processing of health-related images in the human brain.*

* These authors contributed equally to this work

[3] Data collection and analysis completed

Zolezzi, M.D., **Leu, C.,** Graven-Nielsen, T., & Liberati, G. (in preparation[3]). *The effect of HFS on C-fiber responses elicited by sustained periodic thermonociceptive stimulation.* Preregistration: https://osf.io/up96w

Leu C., Herbillon G., Liberati, G., Legrain V. (in preparation[4]). *Bilateral frequency-tagging using slow sustained periodic sinusoidal thermonociceptive stimulation.*

Leu, C., Null, M., Mouraux, A., Liberati, G., & Belardinelli, P. *Unraveling the relationship between ongoing oscillations and pain perception using high-frequency rTMS: a brain-state dependent TMS-EEG investigation*. Exchange research project, supported by the SofinaBoël Fellowship 2024 and carried out at the University of Trento (Italy) in spring 2025.

[4] Data collection ongoing

Acknowledgements

While the journey towards this dissertation has taught me a lot about science and about myself, I also got to meet a whole bunch of wonderful people along the way, both in and out of the university. I want to thank every single of you, who was in some way involved in helping me through these 3.5 years, be it with feedback on my research, supporting me in moments of doubt or simply sharing a laugh.

First, I want to acknowledge the over 100 volunteers who participated (more or less happily) in my scalp EEG experiments and endured hours of pain for me to be able to complete this dissertation. I am also extremely grateful to the 10 patients of the Reference Center for Refractory Epilepsy of the Saint-Luc university hospital for participating in my experiment, as well as to the entire unit for helping me acquire the intracerebral data.

Further, I would like to extend my gratitude to the external members of the PhD jury, Prof. Markus Ploner and Prof. Paolo Belardinelli, for taking the time out of their busy schedules to read and evaluate this dissertation. I would also like to thank the members of my steering committee, Prof. Sylvie Nozaradan, Prof. Valérie Goffaux, Prof. André Mouraux and Prof. Valéry Legrain for taking the time to review my work every year, give me critical feedback and ensuring that I stay on the right path. While these meetings were sometimes daunting, I will never forget the 2nd year "confirmation meeting", after which I felt for the first time like I might actually not be an imposter anymore.

But most importantly, I need to thank my supervisor, Prof. Giulia Liberati, who - I am still convinced - hired my initially because I was born on the same day as her son. Giulia, while it took a while for you to accept that I am not Italian despite my name, you put your trust in me immediately and gave me the freedom to do things my own way, for which I am very

grateful. Being a “single child” for the first 2 years of my PhD and building the Liberati Lab by your side was truly a special experience. Thank you for always having an open door for me and whatever I felt the need to tell you (even if they were the most random things), being always available for last-minute revisions, and for passing on every opportunity that crossed your desk. Now I am spoiled, and my future supervisors will have to deal with the high expectations you set in terms of reliability, support and kindness.

Speaking of the Liberati Lab, having “siblings” turned out to be not all that bad. Aïcha, I already miss having you sit about an elbow-length away from me, being open to discuss and think through each and every idea and question that crosses my mind, be it scientific or not. You have often made me feel heard and understood when I thought no one else shared my views. Thank you for your honesty, your encouragements in times of doubt, your feedback, your ability to read my mind and say the exact same words I just wanted to say and the many many laughing fits we had late in the afternoon in our office.

There are plenty more people in NOCIONS who helped me along the way, shared a laugh with me when I was most frustrated, volunteered to have lunch at a Swiss lunch time or supported me in my attempts to impose some sort of order in the TCS storage room or start the lab meeting on time. Every single one of you made my time at UCLouvain unique, and I am grateful to all of you. Avu (& Hary), Delia, Giulia E., Julien, Lieve, Manu, Alessandra and Paola (as honorary NOCIONS members), and all the others, thank you for the many times you listened to me yap about frequency-tagging in our lab meetings, the good times at Ad Hoc, and all the small moments in between.

Maddie and Monika, my cheerleaders during the first two years of this journey, your support and friendship means the world to me. Thank you for sharing your academia wisdom, for listening to me whenever I was

discouraged, answering even the most random questions about “how to do science”, for holding my hand while submitting my first paper review and for teaching me that it is ok to celebrate the big (and small) wins along the way. Having you in my corner (or in the same office) during this time has made all the difference. I can almost forgive you for both leaving Brussels in the same week to live in the UK while I was only half-way done with my PhD.

While my family was often far away, the weeks spent together in the mountains always compensated for the constant drizzle in Brussels. Maybe this thesis can finally convince you that during this PhD, I did more than just cycle around Belgium, trying to find a hill to climb. Thank you for teaching me that hard work pays off and that you first have to believe in yourself before others can do the same.

I also want to thank my “home away from home”, the DeHavens. You welcomed me with open arms, from the first moment I stepped into your house. Being able to get out of the city on the weekends and be part of your family has allowed me to escape from this sometimes-all-consuming journey I was on, for which I’ll be forever grateful.

And finally, Robbert, I’ll never be able to thank you enough for your support and understanding during these 3.5 years. From being a pilot subject for every single one of my experiments, over being my taxi driver while my foot was in a cast but I still wanted to go to the lab, to brainstorming ideas and concepts of my studies with me. This dissertation has taken center-stage during much of the last years, and you were in it for the good and the bad, listening patiently to every single one of my problems and keeping me grounded when I got too excited. We both know how much I pride myself in being “independent” and doing things on my own; but this one would have not been possible without you.

Bibliography

Adrian, E. D., & Matthews, B. H. (1934). The interpretation of potential waves in the cortex. *J Physiol*, *81*(4), 440-471. https://doi.org/10.1113/jphysiol.1934.sp003147

Akam, T., & Kullmann, D. M. (2014). Oscillatory multiplexing of population codes for selective communication in the mammalian brain. *Nature Reviews Neuroscience*, *15*(2), 111-122. https://doi.org/10.1038/nrn3668

Albanese, M.-C., Duerden, E. G., Bohotin, V., Rainville, P., & Duncan, G. H. (2009). Differential Effects of Cognitive Demand on Human Cortical Activation Associated With Vibrotactile Stimulation. *Journal of Neurophysiology*, *102*(3), 1623-1631. https://doi.org/10.1152/jn.91295.2008

Albu, S., & Meagher, M. W. (2016). Expectation of nocebo hyperalgesia affects EEG alpha-activity. *International Journal of Psychophysiology*, *109*, 147-152. https://doi.org/https://doi.org/10.1016/j.ijpsycho.2016.08.009

Alhajri, N., Boudreau, S. A., & Graven-Nielsen, T. (2023). Decreased Default Mode Network Connectivity Following 24 Hours of Capsaicin-induced Pain Persists During Immediate Pain Relief and Facilitation. *The Journal of Pain*, *24*(5), 796-811. https://doi.org/https://doi.org/10.1016/j.jpain.2022.12.004

Allen, M., Poggiali, D., Whitaker, K., Marshall, T., van Langen, J., & Kievit, R. (2021). Raincloud plots: a multi-platform tool for robust data visualization [version 2; peer review: 2 approved]. *Wellcome Open Research*, *4*(63). https://doi.org/10.12688/wellcomeopenres.15191.2

Almashaikhi, T., Rheims, S., Jung, J., Ostrowsky-Coste, K., Montavont, A., De Bellescize, J., Arzimanoglou, A., Keo Kosal, P., Guénot, M., Bertrand, O., & Ryvlin, P. (2014). Functional connectivity of insular efferences. *Human Brain Mapping*, *35*(10), 5279-5294. https://doi.org/https://doi.org/10.1002/hbm.22549

Apkarian, A. V., Bushnell, M. C., Treede, R.-D., & Zubieta, J.-K. (2005). Human brain mechanisms of pain perception and regulation in health and disease. *European Journal of Pain*, *9*(4), 463-484. https://doi.org/https://doi.org/10.1016/j.ejpain.2004.11.001

Appelbaum, L. G., Wade, A. R., Vildavski, V. Y., Pettet, M. W., & Norcia, A. M. (2006). Cue-Invariant Networks for Figure and Background Processing in Human Visual Cortex. *The Journal of Neuroscience*, *26*(45), 11695-11708. https://doi.org/10.1523/jneurosci.2741-06.2006

Atlas, L. Y., Bolger, N., Lindquist, M. A., & Wager, T. D. (2010). Brain Mediators of Predictive Cue Effects on Perceived Pain. *The Journal of Neuroscience*, *30*(39), 12964-12977. https://doi.org/10.1523/jneurosci.0057-10.2010

Atlas, L. Y., & Wager, T. D. (2012). How expectations shape pain. *Neuroscience Letters*, *520*(2), 140-148. https://doi.org/https://doi.org/10.1016/j.neulet.2012.03.039

Attia, M., McCarthy, D., & Abdelghani, M. (2021). Repetitive Transcranial Magnetic Stimulation for Treating Chronic Neuropathic Pain: a Systematic Review. *Current Pain and Headache Reports*, *25*(7), 48. https://doi.org/10.1007/s11916-021-00960-5

Augustine, J. R. (1996). Circuitry and functional aspects of the insular lobe in primates including humans. *Brain Research Reviews*, *22*(3), 229-244. https://doi.org/https://doi.org/10.1016/S0165-0173(96)00011-2

Babiloni, C., Brancucci, A., Percio, C. D., Capotosto, P., Arendt-Nielsen, L., Chen, A. C. N., & Rossini, P. M. (2006). Anticipatory Electroencephalography Alpha Rhythm Predicts Subjective Perception of Pain Intensity. *The Journal of Pain*, *7*(10), 709-717. https://doi.org/https://doi.org/10.1016/j.jpain.2006.03.005

Babiloni, F., Cincotti, F., Babiloni, C., Carducci, F., Mattia, D., Astolfi, L., Basilisco, A., Rossini, P. M., Ding, L., Ni, Y., Cheng, J., Christine, K., Sweeney, J., & He, B. (2005). Estimation of the cortical functional connectivity with the multimodal integration of high-resolution EEG and fMRI data by directed transfer function. *NeuroImage*, *24*(1), 118-131. https://doi.org/https://doi.org/10.1016/j.neuroimage.2004.09.036

Baier, B., zu Eulenburg, P., Geber, C., Rohde, F., Rolke, R., Maihöfner, C., Birklein, F., & Dieterich, M. (2014). Insula and sensory insular cortex and somatosensory control in patients with insular stroke. *European Journal of Pain*, *18*(10), 1385-1393. https://doi.org/https://doi.org/10.1002/j.1532-2149.2014.501.x

Baliki, M. N., Geha, P. Y., & Apkarian, A. V. (2009). Parsing pain perception between nociceptive representation and magnitude estimation. *Journal of Neurophysiology*, *101*(2), 875-887. https://doi.org/10.1152/jn.91100.2008

Bank, P. J. M., Peper, C. E., Marinus, J., Beek, P. J., & van Hilten, J. J. (2013). Motor consequences of experimentally induced limb pain: A systematic review. *European Journal of Pain*, *17*(2), 145-157. https://doi.org/https://doi.org/10.1002/j.1532-2149.2012.00186.x

Bantick, S. J., Wise, R. G., Ploghaus, A., Clare, S., Smith, S. M., & Tracey, I. (2002). Imaging how attention modulates pain in humans using functional MRI. *Brain*, *125*(2), 310-319. https://doi.org/10.1093/brain/awf022

Barlow, J. S. (1983). Electroencephalography: Basic Principles, Clinical Applications and Related Fields. *JAMA*, *250*(22), 3108-3108. https://doi.org/10.1001/jama.1983.03340220076048

Bates, D., Mächler, M., Bolker, B., & Walker, S. (2015). Fitting Linear Mixed-Effects Models using lme4. *Journal of Statistical Software*, *67*(1), 1-48. https://doi.org/10.18637/jss.v067.i01

Bauer, M., Stenner, M.-P., Friston, K. J., & Dolan, R. J. (2014). Attentional Modulation of Alpha/Beta and Gamma Oscillations Reflect Functionally Distinct Processes. *The Journal of Neuroscience*, *34*(48), 16117-16125. https://doi.org/10.1523/jneurosci.3474-13.2014

Baumgärtner, U., Iannetti, G. D., Zambreanu, L., Stoeter, P., Treede, R.-D., & Tracey, I. (2010). Multiple Somatotopic Representations of Heat and Mechanical Pain in the Operculo-Insular Cortex: A High-Resolution fMRI Study. *Journal of Neurophysiology*, *104*(5), 2863-2872. https://doi.org/10.1152/jn.00253.2010

Becerra, L. R., Breiter, H. C., Stojanovic, M., Fishman, S., Edwards, A., Comite, A. R., Gonzalez, R. G., & Borsook, D. (1999). Human brain activation under controlled thermal stimulation and habituation to noxious heat: An fMRI study. *Magnetic Resonance in Medicine*, *41*(5), 1044-1057. https://doi.org/https://doi.org/10.1002/(SICI)1522-2594(199905)41:5<1044::AID-MRM25>3.0.CO;2-M

Beecher, H. K. (1956). RELATIONSHIP OF SIGNIFICANCE OF WOUND TO PAIN EXPERIENCED. *Journal of the American Medical Association*, *161*(17), 1609-1613. https://doi.org/10.1001/jama.1956.02970170005002

Bell, A. J., & Sejnowski, T. J. (1995). An information-maximization approach to blind separation and blind deconvolution. *Neural Comput*, *7*(6), 1129-1159. https://doi.org/10.1162/neco.1995.7.6.1129

Benedetti, F., Amanzio, M., Rosato, R., & Blanchard, C. (2011). Nonopioid placebo analgesia is mediated by CB1 cannabinoid receptors. *Nature Medicine*, *17*(10), 1228-1230. https://doi.org/10.1038/nm.2435

Berger, H. (1929). Über das Elektroenkephalogramm des Menschen. *Archiv für psychiatrie und nervenkrankheiten*, *87*(1), 527-570.

Beydoun, A., Morrow, T. J., Shen, J. F., & Casey, K. L. (1993). Variability of laser-evoked potentials: attention, arousal and lateralized differences. *Electroencephalography and Clinical Neurophysiology/Evoked Potentials Section*, *88*(3), 173-181. https://doi.org/https://doi.org/10.1016/0168-5597(93)90002-7

Bingel, U., & Tracey, I. (2008). Imaging CNS Modulation of Pain in Humans. *Physiology*, *23*(6), 371-380. https://doi.org/10.1152/physiol.00024.2008

Bland, J. M., & Altman, D. G. (1996). Statistics Notes: Transforming data. *BMJ*, *312*(7033), 770. https://doi.org/10.1136/bmj.312.7033.770

Bott, F. S., Nickel, M. M., Hohn, V. D., May, E. S., Gil Ávila, C., Tiemann, L., Gross, J., & Ploner, M. (2023). Local brain oscillations and interregional connectivity differentially serve sensory and expectation effects on pain. *Science Advances*, *9*(16), eadd7572. https://doi.org/doi:10.1126/sciadv.add7572

Bouchatta, O., Aby, F., Sifeddine, W., Bouali-Benazzouz, R., Brochoire, L., Manouze, H., Fossat, P., Ba M'Hamed, S., Bennis, M., & Landry, M. (2022). Pain hypersensitivity in a pharmacological mouse model of attention-deficit/hyperactivity disorder. *Proceedings of the National Academy of Sciences*, *119*(30), e2114094119. https://doi.org/doi:10.1073/pnas.2114094119
Boyle, Y., El-Deredy, W., Martínez Montes, E., Bentley, D. E., & Jones, A. K. P. (2008). Selective modulation of nociceptive processing due to noise distraction. *Pain*, *138*(3), 630-640. https://doi.org/https://doi.org/10.1016/j.pain.2008.02.020
Bradley, C., Bastuji, H., & Garcia-Larrea, L. (2017). Evidence-based source modeling of nociceptive cortical responses: A direct comparison of scalp and intracranial activity in humans. *Human Brain Mapping*, *38*(12), 6083-6095. https://doi.org/https://doi.org/10.1002/hbm.23812
Brodin, E., Ernberg, M., & Olgart, L. (2016). Neurobiology: General considerations–from acute to chronic pain. *Nor. Tannlegeforen. Tid*, *126*, 28-33.
Brodski, A., Paasch, G.-F., Helbling, S., & Wibral, M. (2015). The Faces of Predictive Coding. *The Journal of Neuroscience*, *35*(24), 8997-9006. https://doi.org/10.1523/jneurosci.1529-14.2015
Brooks, J. C. W., Nurmikko, T. J., Bimson, W. E., Singh, K. D., & Roberts, N. (2002). fMRI of Thermal Pain: Effects of Stimulus Laterality and Attention. *NeuroImage*, *15*(2), 293-301. https://doi.org/https://doi.org/10.1006/nimg.2001.0974
Brooks, J. C. W., & Tracey, I. (2007). The insula: A multidimensional integration site for pain. *Pain*, *128*(1), 1-2. https://doi.org/10.1016/j.pain.2006.12.025
Budke, M., Avecillas-Chasin, J. M., & Villarejo, F. (2018). Implantation of Depth Electrodes in Children Using VarioGuide® Frameless Navigation System: Technical Note. *Operative Neurosurgery*, *15*(3), 302-309. https://doi.org/10.1093/ons/opx192
Buhle, J. T., Stevens, B. L., Friedman, J. J., & Wager, T. D. (2012). Distraction and Placebo:Two Separate Routes to Pain Control. *Psychological Science*, *23*(3), 246-253. https://doi.org/10.1177/0956797611427919
Burns, E., Chipchase, L. S., & Schabrun, S. M. (2016). Primary sensory and motor cortex function in response to acute muscle pain: A systematic review and meta-analysis. *European Journal of Pain*, *20*(8), 1203-1213. https://doi.org/https://doi.org/10.1002/ejp.859
Button, K. S., Ioannidis, J. P. A., Mokrysz, C., Nosek, B. A., Flint, J., Robinson, E. S. J., & Munafò, M. R. (2013). Power failure: why small sample size undermines the reliability of neuroscience. *Nature Reviews Neuroscience*, *14*(5), 365-376. https://doi.org/10.1038/nrn3475
Buzsáki, G., Anastassiou, C. A., & Koch, C. (2012). The origin of extracellular fields and currents — EEG, ECoG, LFP and spikes. *Nature Reviews Neuroscience*, *13*(6), 407-420. https://doi.org/10.1038/nrn3241
Buzsáki, G., & Chrobak, J. J. (1995). Temporal structure in spatially organized neuronal ensembles: a role for interneuronal networks. *Current Opinion in Neurobiology*, *5*(4), 504-510. https://doi.org/https://doi.org/10.1016/0959-4388(95)80012-3
Buzsáki, G., & Draguhn, A. (2004). Neuronal Oscillations in Cortical Networks. *Science*, *304*(5679), 1926-1929. https://doi.org/10.1126/science.1099745
Caldichoury, A., Garcia-Larrea, L., & Frot, M. (2024). Focal changes in alpha oscillations during short-term memorization of pain: a high-density electroencephalogram study with source localization. *European Journal of Neuroscience*, *59*(10), 2778-2791. https://doi.org/https://doi.org/10.1111/ejn.16317
Campbell, J. N., & Meyer, R. A. (1983). Sensitization of unmyelinated nociceptive afferents in monkey varies with skin type. *Journal of Neurophysiology*, *49*(1), 98-110. https://doi.org/10.1152/jn.1983.49.1.98
Capilla, A., Pazo-Alvarez, P., Darriba, A., Campo, P., & Gross, J. (2011). Steady-State Visual Evoked Potentials Can Be Explained by Temporal Superposition of Transient Event-Related Responses. *PLOS ONE*, *6*(1), e14543. https://doi.org/10.1371/journal.pone.0014543

Cauda, F., Torta, D. M. E., Sacco, K., D'Agata, F., Geda, E., Duca, S., Geminiani, G., & Vercelli, A. (2013). Functional anatomy of cortical areas characterized by Von Economo neurons. *Brain Structure and Function*, *218*(1), 1-20. https://doi.org/10.1007/s00429-012-0382-9
Cerliani, L., Thomas, R. M., Jbabdi, S., Siero, J. C. W., Nanetti, L., Crippa, A., Gazzola, V., D'Arceuil, H., & Keysers, C. (2012). Probabilistic tractography recovers a rostrocaudal trajectory of connectivity variability in the human insular cortex. *Human Brain Mapping*, *33*(9), 2005-2034. https://doi.org/https://doi.org/10.1002/hbm.21338
Cervero, F. (2012). *Understanding pain: exploring the perception of pain*. Mit Press.
Chambers, C. D. (2013). Registered Reports: A new publishing initiative at Cortex. *Cortex*, *49*(3), 609-610. https://doi.org/https://doi.org/10.1016/j.cortex.2012.12.016
Chambers, C. D., & Tzavella, L. (2022). The past, present and future of Registered Reports. *Nature Human Behaviour*, *6*(1), 29-42. https://doi.org/10.1038/s41562-021-01193-7
Chang, P.-F., Arendt-Nielsen, L., Graven-Nielsen, T., Svensson, P., & Chen, A. C. N. (2001). Topographic effects of tonic cutaneous nociceptive stimulation on human electroencephalograph. *Neuroscience Letters*, *305*(1), 49-52. https://doi.org/https://doi.org/10.1016/S0304-3940(01)01802-X
Chang, P. F., Arendt-Nielsen, L., & Chen, A. C. N. (2002). Dynamic changes and spatial correlation of EEG activities during cold pressor test in man. *Brain Research Bulletin*, *57*(5), 667-675. https://doi.org/https://doi.org/10.1016/S0361-9230(01)00763-8
Chen, A. C., & Rappelsberger, P. (1994). Brain and human pain: topographic EEG amplitude and coherence mapping. *Brain Topogr*, *7*(2), 129-140. https://doi.org/10.1007/bf01186771
Chen, A. C. N., Rappelsberger, P., & Filz, O. (1998). Topology of EEG Coherence Changes May Reflect Differential Neural Network Activation in Cold and Pain Perception. *Brain Topography*, *11*(2), 125-132. https://doi.org/10.1023/A:1022254505510
Chiarion, G., Sparacino, L., Antonacci, Y., Faes, L., & Mesin, L. (2023). Connectivity Analysis in EEG Data: A Tutorial Review of the State of the Art and Emerging Trends. *Bioengineering*, *10*(3), 372. https://www.mdpi.com/2306-5354/10/3/372
Chowdhury, N. S., Chiang, A. K., Millard, S. K., Skippen, P., Chang, W.-J., Seminowicz, D. A., & Schabrun, S. M. (2023). Alterations in cortical excitability during pain: A combined TMS-EEG Study. *bioRxiv*, 2023.2004.2020.537735. https://doi.org/10.1101/2023.04.20.537735
Chowdhury, N. S., Skippen, P., Si, E., Chiang, A. K. I., Millard, S. K., Furman, A. J., Chen, S., Schabrun, S. M., & Seminowicz, D. A. (2023). The reliability of two prospective cortical biomarkers for pain: EEG peak alpha frequency and TMS corticomotor excitability. *Journal of Neuroscience Methods*, *385*, 109766. https://doi.org/https://doi.org/10.1016/j.jneumeth.2022.109766
Churyukanov, M., Plaghki, L., Legrain, V., & Mouraux, A. (2012). Thermal detection thresholds of A δ - and C-fibre afferents activated by brief CO2 laser pulses applied onto the human hairy skin. *PLOS ONE*, *7*(4), e35817. https://doi.org/10.1371/journal.pone.0035817
Cieslik, E. C., Mueller, V. I., Eickhoff, C. R., Langner, R., & Eickhoff, S. B. (2015). Three key regions for supervisory attentional control: Evidence from neuroimaging meta-analyses. *Neuroscience & Biobehavioral Reviews*, *48*, 22-34. https://doi.org/https://doi.org/10.1016/j.neubiorev.2014.11.003
Claus, D., Hilz, M. J., & Neundörfer, B. (1990). Thermal discrimination thresholds: a comparison of different methods. *Acta Neurologica Scandinavica*, *81*(6), 533-540. https://doi.org/https://doi.org/10.1111/j.1600-0404.1990.tb01015.x
Clayton, M. S., Yeung, N., & Cohen Kadosh, R. (2015). The roles of cortical oscillations in sustained attention. *Trends in Cognitive Sciences*, *19*(4), 188-195. https://doi.org/https://doi.org/10.1016/j.tics.2015.02.004
Cloutman, L. L., Binney, R. J., Drakesmith, M., Parker, G. J. M., & Lambon Ralph, M. A. (2012). The variation of function across the human insula mirrors its patterns of structural connectivity: Evidence from in vivo probabilistic tractography. *NeuroImage*, *59*(4), 3514-3521. https://doi.org/https://doi.org/10.1016/j.neuroimage.2011.11.016

Cobos, I., & Seeley, W. W. (2013). Human von Economo Neurons Express Transcription Factors Associated with Layer V Subcerebral Projection Neurons. *Cerebral Cortex*, *25*(1), 213-220. https://doi.org/10.1093/cercor/bht219
Collaboration, O. S. (2015). Estimating the reproducibility of psychological science. *Science*, *349*(6251), aac4716. https://doi.org/doi:10.1126/science.aac4716
Colon, E., Legrain, V., & Mouraux, A. (2012). Steady-state evoked potentials to study the processing of tactile and nociceptive somatosensory input in the human brain. *Neurophysiologie Clinique/Clinical Neurophysiology*, *42*(5), 315-323. https://doi.org/https://doi.org/10.1016/j.neucli.2012.05.005
Colon, E., Legrain, V., & Mouraux, A. (2014). EEG Frequency Tagging to Dissociate the Cortical Responses to Nociceptive and Nonnociceptive Stimuli. *Journal of Cognitive Neuroscience*, *26*(10), 2262-2274. https://doi.org/10.1162/jocn_a_00648
Colon, E., Liberati, G., & Mouraux, A. (2017). EEG frequency tagging using ultra-slow periodic heat stimulation of the skin reveals cortical activity specifically related to C fiber thermonociceptors. *NeuroImage*, *146*, 266-274. https://doi.org/https://doi.org/10.1016/j.neuroimage.2016.11.045
Colon, E., Nozaradan, S., Legrain, V., & Mouraux, A. (2012). Steady-state evoked potentials to tag specific components of nociceptive cortical processing. *NeuroImage*, *60*(1), 571-581. https://doi.org/https://doi.org/10.1016/j.neuroimage.2011.12.015
Cook, R. D. (1977). Detection of Influential Observation in Linear Regression. *Technometrics*, *19*(1), 15-18. https://doi.org/10.1080/00401706.1977.10489493
Courtin, A. S., & Mouraux, A. (2024 Preprint). *Exploration of the EEG response to periodic thermal and vibrotactile stimuli*. https://www.biorxiv.org/content/biorxiv/early/2024/01/16/2024.01.15.575576.full.pdf
Craig, A. D. (2002). How do you feel? Interoception: the sense of the physiological condition of the body. *Nature Reviews Neuroscience*, *3*(8), 655-666. https://doi.org/10.1038/nrn894
Craig, A. D. (2009). How do you feel — now? The anterior insula and human awareness. *Nature Reviews Neuroscience*, *10*(1), 59-70. https://doi.org/10.1038/nrn2555
Craig, A. D., Chen, K., Bandy, D., & Reiman, E. M. (2000). Thermosensory activation of insular cortex. *Nature Neuroscience*, *3*(2), 184-190. https://doi.org/10.1038/72131
Creac'H, C., Bertholon, A., Convers, P., Garcia-Larrea, L., & Peyron, R. (2015). Effects of aging on laser evoked potentials. *Muscle & Nerve*, *51*(5), 736-742. https://doi.org/https://doi.org/10.1002/mus.24458
Davis, K. D., Bushnell, M. C., Iannetti, G. D., St Lawrence, K., & Coghill, R. (2015). Evidence against pain specificity in the dorsal posterior insula. *F1000Res*, *4*, 362. https://doi.org/10.12688/f1000research.6833.1
Davis, K. D., Kwan, C. L., Crawley, A. P., & Mikulis, D. J. (1998). Functional MRI Study of Thalamic and Cortical Activations Evoked by Cutaneous Heat, Cold, and Tactile Stimuli. *Journal of Neurophysiology*, *80*(3), 1533-1546. https://doi.org/10.1152/jn.1998.80.3.1533
De Keyser, R., Mouraux, A., Quek, G. L., Torta, D. M., & Legrain, V. (2018). Fast periodic visual stimulation to study tool-selective processing in the human brain. *Experimental Brain Research*, *236*(10), 2751-2763. https://doi.org/10.1007/s00221-018-5331-2
De Martino, E., Casali, A., Casarotto, S., Hassan, G., Couto, B. A., Rosanova, M., Graven-Nielsen, T., & de Andrade, D. C. (2024). Evoked oscillatory cortical activity during acute pain: Probing brain in pain by transcranial magnetic stimulation combined with electroencephalogram. *Human Brain Mapping*, *45*(6), e26679. https://doi.org/https://doi.org/10.1002/hbm.26679
De Martino, E., Gregoret, L., Zandalasini, M., & Graven-Nielsen, T. (2021). Slowing in Peak-Alpha Frequency Recorded After Experimentally-Induced Muscle Pain is not Significantly Different Between High and Low Pain-Sensitive Subjects. *The Journal of Pain*, *22*(12), 1722-1732. https://doi.org/https://doi.org/10.1016/j.jpain.2021.06.004
Demarest, P., Rustamov, N., Swift, J., Xie, T., Adamek, M., Cho, H., Wilson, E., Han, Z., Belsten, A., Luczak, N., Brunner, P., Haroutounian, S., & Leuthardt, E. C. (2024). A novel theta-

controlled vibrotactile brain–computer interface to treat chronic pain: a pilot study. *Scientific Reports*, *14*(1), 3433. https://doi.org/10.1038/s41598-024-53261-3
Desideri, D., Zrenner, C., Gordon, P. C., Ziemann, U., & Belardinelli, P. (2018). Nil effects of μ-rhythm phase-dependent burst-rTMS on cortical excitability in humans: A resting-state EEG and TMS-EEG study. *PLOS ONE*, *13*(12), e0208747. https://doi.org/10.1371/journal.pone.0208747
Devue, C., Collette, F., Balteau, E., Degueldre, C., Luxen, A., Maquet, P., & Brédart, S. (2007). Here I am: The cortical correlates of visual self-recognition. *Brain Research*, *1143*, 169-182. https://doi.org/https://doi.org/10.1016/j.brainres.2007.01.055
Dienes, Z. (2021). Obtaining Evidence for No Effect. *Collabra: Psychology*, *7*(1). https://doi.org/10.1525/collabra.28202
Diers, M., de Vos, C. C., Gandhi, W., Hoeppli, M. E., Becker, S., Bock, E., Baillet, S., & Schweinhardt, P. (2020). Induced oscillatory signaling in the beta frequency of top-down pain modulation. *Pain reports*, *5*(1), e806. https://doi.org/10.1097/pr9.0000000000000806
Ding, N., & Simon, J. Z. (2013). Power and phase properties of oscillatory neural responses in the presence of background activity. *Journal of Computational Neuroscience*, *34*(2), 337-343. https://doi.org/10.1007/s10827-012-0424-6
Doelling, K. B., Assaneo, M. F., Bevilacqua, D., Pesaran, B., & Poeppel, D. (2019). An oscillator model better predicts cortical entrainment to music. *Proceedings of the National Academy of Sciences*, *116*(20), 10113-10121. https://doi.org/doi:10.1073/pnas.1816414116
Doll, R. J., Buitenweg, J. R., Meijer, H. G. E., & Veltink, P. H. (2014). Tracking of nociceptive thresholds using adaptive psychophysical methods. *Behavior Research Methods*, *46*(1), 55-66. https://doi.org/10.3758/s13428-013-0368-4
Dörfel, D., Lamke, J.-P., Hummel, F., Wagner, U., Erk, S., & Walter, H. (2014). Common and differential neural networks of emotion regulation by Detachment, Reinterpretation, Distraction, and Expressive Suppression: A comparative fMRI investigation. *NeuroImage*, *101*, 298-309. https://doi.org/https://doi.org/10.1016/j.neuroimage.2014.06.051
Dostrovsky, J. O., & Craig, A. (2006). Ascending projection systems. *Wall and Melzack's textbook of pain*, 187-203.
Dowman, R., Rissacher, D., & Schuckers, S. (2008). EEG indices of tonic pain-related activity in the somatosensory cortices. *Clinical Neurophysiology*, *119*(5), 1201-1212. https://doi.org/10.1016/j.clinph.2008.01.019
Downar, J., Crawley, A. P., Mikulis, D. J., & Davis, K. D. (2000). A multimodal cortical network for the detection of changes in the sensory environment. *Nature Neuroscience*, *3*(3), 277-283. https://doi.org/10.1038/72991
Downar, J., Mikulis, D. J., & Davis, K. D. (2003). Neural correlates of the prolonged salience of painful stimulation. *NeuroImage*, *20*(3), 1540-1551. https://doi.org/https://doi.org/10.1016/S1053-8119(03)00407-5
Drewes, A. M., Krarup, A. L., Detlefsen, S., Malmstrøm, M.-L., Dimcevski, G., & Funch-Jensen, P. (2008). Pain in chronic pancreatitis: the role of neuropathic pain mechanisms. *Gut*, *57*(11), 1616-1627. https://doi.org/10.1136/gut.2007.146621
Eccles, J. C. (1951). Interpretation of action potentials evoked in the cerebral cortex. *Electroencephalography and clinical neurophysiology*, *3*(4), 449-464. https://doi.org/https://doi.org/10.1016/0013-4694(51)90033-8
Eccleston, C. (1995). Chronic pain and distraction: An experimental investigation into the role of sustained and shifting attention in the processing of chronic persistent pain. *Behaviour Research and Therapy*, *33*(4), 391-405. https://doi.org/https://doi.org/10.1016/0005-7967(94)00057-Q
Eccleston, C., & Crombez, G. (1999). Pain demands attention: A cognitive–affective model of the interruptive function of pain. *Psychological Bulletin*, *125*(3), 356-366. https://doi.org/10.1037/0033-2909.125.3.356
Egeth, H. E., & Yantis, S. (1997). VISUAL ATTENTION: Control, Representation, and Time Course. *Annual Review of Psychology*, *48*(1), 269-297. https://doi.org/10.1146/annurev.psych.48.1.269

Egsgaard, L. L., Wang, L., & Arendt-Nielsen, L. (2009). Volunteers with high versus low alpha EEG have different pain–EEG relationship: a human experimental study. *Experimental Brain Research*, *193*(3), 361-369. https://doi.org/10.1007/s00221-008-1632-1

Elul, R. (1972). The Genesis of the Eeg. In C. C. Pfeiffer & J. R. Smythies (Eds.), *International Review of Neurobiology* (Vol. 15, pp. 227-272). Academic Press. https://doi.org/https://doi.org/10.1016/S0074-7742(08)60333-5

Engel, A. K., & Fries, P. (2010). Beta-band oscillations—signalling the status quo? *Current Opinion in Neurobiology*, *20*(2), 156-165. https://doi.org/https://doi.org/10.1016/j.conb.2010.02.015

Escera, C., Alho, K., Schröger, E., & Winkler, I. W. (2000). Involuntary Attention and Distractibility as Evaluated with Event-Related Brain Potentials. *Audiology and Neurotology*, *5*(3-4), 151-166. https://doi.org/10.1159/000013877

Fanelli, D. (2010). "Positive" Results Increase Down the Hierarchy of the Sciences. *PLOS ONE*, *5*(4), e10068. https://doi.org/10.1371/journal.pone.0010068

Farzan, F., Vernet, M., Shafi, M. M. D., Rotenberg, A., Daskalakis, Z. J., & Pascual-Leone, A. (2016). Characterizing and Modulating Brain Circuitry through Transcranial Magnetic Stimulation Combined with Electroencephalography [Review]. *Frontiers in Neural Circuits*, *10*. https://doi.org/10.3389/fncir.2016.00073

Faul, F., Erdfelder, E., Lang, A.-G., & Buchner, A. (2007). G*Power 3: A flexible statistical power analysis program for the social, behavioral, and biomedical sciences. *Behavior Research Methods*, *39*(2), 175-191. https://doi.org/10.3758/BF03193146

Ferracuti, S., Seri, S., Mattia, D., & Cruccu, G. (1994). Quantitative EEG modifications during the cold water pressor test: hemispheric and hand differences. *International Journal of Psychophysiology*, *17*(3), 261-268. https://doi.org/https://doi.org/10.1016/0167-8760(94)90068-X

Franciotti, R., Ciancetta, L., Della Penna, S., Belardinelli, P., Pizzella, V., & Romani, G. L. (2009). Modulation of alpha oscillations in insular cortex reflects the threat of painful stimuli. *NeuroImage*, *46*(4), 1082-1090. https://doi.org/https://doi.org/10.1016/j.neuroimage.2009.03.034

Francis, S. T., Kelly, E. F., Bowtell, R., Dunseath, W. J. R., Folger, S. E., & McGlone, F. (2000). fMRI of the Responses to Vibratory Stimulation of Digit Tips. *NeuroImage*, *11*(3), 188-202. https://doi.org/https://doi.org/10.1006/nimg.2000.0541

Freund, W., Klug, R., Weber, F., Stuber, G., Schmitz, B., & Wunderlich, A. P. (2009). Perception and suppression of thermally induced pain: A fMRI study. *Somatosensory & Motor Research*, *26*(1), 1-10. https://doi.org/10.1080/08990220902738243

Fries, P. (2005). A mechanism for cognitive dynamics: neuronal communication through neuronal coherence. *Trends in Cognitive Sciences*, *9*(10), 474-480. https://doi.org/10.1016/j.tics.2005.08.011

Fries, P. (2009). Neuronal Gamma-Band Synchronization as a Fundamental Process in Cortical Computation. *Annual Review of Neuroscience*, *32*(1), 209-224. https://doi.org/10.1146/annurev.neuro.051508.135603

Fries, P. (2015). Rhythms for Cognition: Communication through Coherence. *Neuron*, *88*(1), 220-235. https://doi.org/https://doi.org/10.1016/j.neuron.2015.09.034

Fries, P., Scheeringa, R., & Oostenveld, R. (2008). Finding Gamma. *Neuron*, *58*(3), 303-305. https://doi.org/10.1016/j.neuron.2008.04.020

Fries, P., Schröder, J.-H., Roelfsema, P. R., Singer, W., & Engel, A. K. (2002). Oscillatory Neuronal Synchronization in Primary Visual Cortex as a Correlate of Stimulus Selection. *The Journal of Neuroscience*, *22*(9), 3739-3754. https://doi.org/10.1523/jneurosci.22-09-03739.2002

Frigo, M., & Johnson, S. G. (1998, 15-15 May 1998). FFTW: an adaptive software architecture for the FFT. Proceedings of the 1998 IEEE International Conference on Acoustics, Speech and Signal Processing, ICASSP '98 (Cat. No.98CH36181),

Frot, M., Faillenot, I., & Mauguière, F. (2014). Processing of nociceptive input from posterior to anterior insula in humans. *Human Brain Mapping*, *35*(11), 5486-5499. https://doi.org/https://doi.org/10.1002/hbm.22565

Frot, M., Magnin, M., Mauguière, F., & Garcia-Larrea, L. (2006). Human SII and Posterior Insula Differently Encode Thermal Laser Stimuli. *Cerebral Cortex*, *17*(3), 610-620. https://doi.org/10.1093/cercor/bhk007
Furman, A. J., Meeker, T. J., Rietschel, J. C., Yoo, S., Muthulingam, J., Prokhorenko, M., Keaser, M. L., Goodman, R. N., Mazaheri, A., & Seminowicz, D. A. (2018). Cerebral peak alpha frequency predicts individual differences in pain sensitivity. *NeuroImage*, *167*, 203-210. https://doi.org/https://doi.org/10.1016/j.neuroimage.2017.11.042
Furman, A. J., Thapa, T., Summers, S. J., Cavaleri, R., Fogarty, J. S., Steiner, G. Z., Schabrun, S. M., & Seminowicz, D. A. (2019). Cerebral peak alpha frequency reflects average pain severity in a human model of sustained, musculoskeletal pain. *Journal of Neurophysiology*, *122*(4), 1784-1793. https://doi.org/10.1152/jn.00279.2019
Garcia-Larrea, L. (2023). Non-invasive cortical stimulation for drug-resistant pain. *Current Opinion in Supportive and Palliative Care*, *17*(3), 142-149. https://doi.org/10.1097/spc.0000000000000654
Garcia-Larrea, L., Peyron, R., Laurent, B., & Mauguière, F. (1997). Association and dissociation between laser-evoked potentials and pain perception. *NeuroReport*, *8*(17), 3785-3789. https://journals.lww.com/neuroreport/Fulltext/1997/12010/Association_and_dissociation_between_laser_evoked.26.aspx
Garcia-Larrea, L., & Quesada, C. (2022). Cortical stimulation for chronic pain: from anecdote to evidence. *European Journal of Physical and Rehabilitation Medicine*, *58*(2), 290-305. https://doi.org/10.23736/s1973-9087.22.07411-1
Gauriau, C., & Bernard, J.-F. (2004). Posterior Triangular Thalamic Neurons Convey Nociceptive Messages to the Secondary Somatosensory and Insular Cortices in the Rat. *The Journal of Neuroscience*, *24*(3), 752-761. https://doi.org/10.1523/jneurosci.3272-03.2004
Gehrlach, D. A., Weiand, C., Gaitanos, T. N., Cho, E., Klein, A. S., Hennrich, A. A., Conzelmann, K.-K., & Gogolla, N. (2020). A whole-brain connectivity map of mouse insular cortex. *eLife*, *9*, e55585. https://doi.org/10.7554/eLife.55585
Geisler, C. D. (1960). Average responses to clicks in man recorded by scalp electrodes.
Geuter, S., Boll, S., Eippert, F., & Büchel, C. (2017). Functional dissociation of stimulus intensity encoding and predictive coding of pain in the insula. *eLife*, *6*, e24770. https://doi.org/10.7554/eLife.24770
Giehl, J., Meyer-Brandis, G., Kunz, M., & Lautenbacher, S. (2014). Responses to tonic heat pain in the ongoing EEG under conditions of controlled attention. *Somatosensory & Motor Research*, *31*(1), 40-48. https://doi.org/10.3109/08990220.2013.837045
Gogolla, N. (2017). The insular cortex. *Current Biology*, *27*(12), R580-R586. https://doi.org/10.1016/j.cub.2017.05.010
Goldman, R. I., Stern, J. M., Engel, J., Jr., & Cohen, M. S. (2002). Simultaneous EEG and fMRI of the alpha rhythm. *NeuroReport*, *13*(18), 2487-2492. https://doi.org/10.1097/01.wnr.0000047685.08940.d0
Goltz, D., Pleger, B., Thiel, S., Villringer, A., & Müller, M. M. (2013). Sustained Spatial Attention to Vibrotactile Stimulation in the Flutter Range: Relevant Brain Regions and Their Interaction. *PLOS ONE*, *8*(12), e84196. https://doi.org/10.1371/journal.pone.0084196
Gray, C. M., Engel, A. K., König, P., & Singer, W. (1992). Synchronization of oscillatory neuronal responses in cat striate cortex: Temporal properties. *Visual Neuroscience*, *8*(4), 337-347. https://doi.org/10.1017/S0952523800005071
Green, P., & MacLeod, C. J. (2016). SIMR: an R package for power analysis of generalized linear mixed models by simulation. *Methods in Ecology and Evolution*, *7*(4), 493-498. https://doi.org/https://doi.org/10.1111/2041-210X.12504
Grill, J. D., & Coghill, R. C. (2002). Transient Analgesia Evoked by Noxious Stimulus Offset. *Journal of Neurophysiology*, *87*(4), 2205-2208. https://doi.org/10.1152/jn.00730.2001
Gross, J., Schnitzler, A., Timmermann, L., & Ploner, M. (2007). Gamma Oscillations in Human Primary Somatosensory Cortex Reflect Pain Perception. *PLoS biology*, *5*(5), e133. https://doi.org/10.1371/journal.pbio.0050133

Guldin, W. O., & Markowitsch, H. J. (1983). Cortical and thalamic afferent connections of the insular and adjacent cortex of the rat. *Journal of Comparative Neurology*, *215*(2), 135-153. https://doi.org/https://doi.org/10.1002/cne.902150203
Guo, Y., Bufacchi, R. J., Novembre, G., Kilintari, M., Moayedi, M., Hu, L., & Iannetti, G. D. (2020). Ultralow-frequency neural entrainment to pain. *PLoS biology*, *18*(4), e3000491. https://doi.org/10.1371/journal.pbio.3000491
Haegens, S., & Zion Golumbic, E. (2018). Rhythmic facilitation of sensory processing: A critical review. *Neuroscience & Biobehavioral Reviews*, *86*, 150-165. https://doi.org/https://doi.org/10.1016/j.neubiorev.2017.12.002
Hashmi, J. A., Baliki, M. N., Huang, L., Baria, A. T., Torbey, S., Hermann, K. M., Schnitzer, T. J., & Apkarian, A. V. (2013). Shape shifting pain: chronification of back pain shifts brain representation from nociceptive to emotional circuits. *Brain*, *136*(9), 2751-2768. https://doi.org/10.1093/brain/awt211
Hauck, M., Lorenz, J., Domnick, C., Gerloff, C., & Engel, A. (2015). Top-Down and Bottom-Up Modulation of Pain-Induced Oscillations [Original Research]. *Frontiers in human neuroscience*, *9*. https://doi.org/10.3389/fnhum.2015.00375
Hauck, M., Lorenz, J., & Engel, A. K. (2007). Attention to Painful Stimulation Enhances γ-Band Activity and Synchronization in Human Sensorimotor Cortex. *The Journal of Neuroscience*, *27*(35), 9270-9277. https://doi.org/10.1523/jneurosci.2283-07.2007
Hauck, M., Lorenz, J., Zimmermann, R., Debener, S., Scharein, E., & Engel, A. K. (2007). Duration of the cue-to-pain delay increases pain intensity: a combined EEG and MEG study. *Experimental Brain Research*, *180*(2), 205-215. https://doi.org/10.1007/s00221-007-0863-x
Healy, M. J. (1993). Data transformations. *Arch Dis Child*, *69*(2), 260-264. https://doi.org/10.1136/adc.69.2.260
Heid, C., Mouraux, A., Treede, R.-D., Schuh-Hofer, S., Rupp, A., & Baumgärtner, U. (2020). Early gamma-oscillations as correlate of localized nociceptive processing in primary sensorimotor cortex. *Journal of Neurophysiology*, *123*(5), 1711-1726. https://doi.org/10.1152/jn.00444.2019
Hein, G., & Singer, T. (2008). I feel how you feel but not always: the empathic brain and its modulation. *Current Opinion in Neurobiology*, *18*(2), 153-158. https://doi.org/https://doi.org/10.1016/j.conb.2008.07.012
Heinrich, S. P. (2010). Some thoughts on the interpretation of steady-state evoked potentials. *Documenta Ophthalmologica*, *120*(3), 205-214. https://doi.org/10.1007/s10633-010-9212-7
Heinrich, S. P., Mell, D., & Bach, M. (2009). Frequency-domain analysis of fast oddball responses to visual stimuli: A feasibility study. *International Journal of Psychophysiology*, *73*(3), 287-293. https://doi.org/https://doi.org/10.1016/j.ijpsycho.2009.04.011
Henin, S., Schwiedrzik, C. M., Ding, N., & Melloni, L. (2023). How Can I Investigate Perceptual and Cognitive Function Using Neural Frequency Tagging? In N. Axmacher (Ed.), *Intracranial EEG: A Guide for Cognitive Neuroscientists* (pp. 507-519). Springer International Publishing. https://doi.org/10.1007/978-3-031-20910-9_31
Hernandez-Pavon, J. C., Veniero, D., Bergmann, T. O., Belardinelli, P., Bortoletto, M., Casarotto, S., Casula, E. P., Farzan, F., Fecchio, M., Julkunen, P., Kallioniemi, E., Lioumis, P., Metsomaa, J., Miniussi, C., Mutanen, T. P., Rocchi, L., Rogasch, N. C., Shafi, M. M., Siebner, H. R., . . . Ilmoniemi, R. J. (2023). TMS combined with EEG: Recommendations and open issues for data collection and analysis. *Brain Stimulation*, *16*(2), 567-593. https://doi.org/https://doi.org/10.1016/j.brs.2023.02.009
Herrmann, C. S. (2001). Human EEG responses to 1–100 Hz flicker: resonance phenomena in visual cortex and their potential correlation to cognitive phenomena. *Experimental Brain Research*, *137*(3), 346-353. https://doi.org/10.1007/s002210100682
Herrmann, C. S., & Mecklinger, A. (2001). Gamma activity in human EEG is related to highspeed memory comparisons during object selective attention. *Visual Cognition*, *8*(3-5), 593-608. https://doi.org/10.1080/13506280143000142

Horvath, J. C., Forte, J. D., & Carter, O. (2015). Evidence that transcranial direct current stimulation (tDCS) generates little-to-no reliable neurophysiologic effect beyond MEP amplitude modulation in healthy human subjects: A systematic review. *Neuropsychologia*, *66*, 213-236. https://doi.org/https://doi.org/10.1016/j.neuropsychologia.2014.11.021

Hu, L., & Iannetti, G. D. (2019). Neural indicators of perceptual variability of pain across species. *Proceedings of the National Academy of Sciences*, *116*(5), 1782-1791. https://doi.org/doi:10.1073/pnas.1812499116

Hu, L., Peng, W., Valentini, E., Zhang, Z., & Hu, Y. (2013). Functional Features of Nociceptive-Induced Suppression of Alpha Band Electroencephalographic Oscillations. *The Journal of Pain*, *14*(1), 89-99. https://doi.org/https://doi.org/10.1016/j.jpain.2012.10.008

Hua, L. H., Strigo, I. A., Baxter, L. C., Johnson, S. C., & Craig, A. D. (2005). Anteroposterior somatotopy of innocuous cooling activation focus in human dorsal posterior insular cortex. *American Journal of Physiology-Regulatory, Integrative and Comparative Physiology*, *289*(2), R319-R325. https://doi.org/10.1152/ajpregu.00123.2005

Huber, M. T., Bartling, J., Pachur, D., Woikowsky-Biedau, S. v., & Lautenbacher, S. (2006). EEG responses to tonic heat pain. *Experimental Brain Research*, *173*(1), 14-24. https://doi.org/10.1007/s00221-006-0366-1

Huishi Zhang, C., Sohrabpour, A., Lu, Y., & He, B. (2016). Spectral and spatial changes of brain rhythmic activity in response to the sustained thermal pain stimulation. *Human Brain Mapping*, *37*(8), 2976-2991. https://doi.org/https://doi.org/10.1002/hbm.23220

Huneke, N. T. M., Brown, C. A., Burford, E., Watson, A., Trujillo-Barreto, N. J., El-Deredy, W., & Jones, A. K. P. (2013). Experimental Placebo Analgesia Changes Resting-State Alpha Oscillations. *PLOS ONE*, *8*(10), e78278. https://doi.org/10.1371/journal.pone.0078278

Hyvarinen, A., & Oja, E. (2000). Independent component analysis: algorithms and applications. *Neural Netw*, *13*(4-5), 411-430. https://doi.org/10.1016/s0893-6080(00)00026-5

Iannetti, G. D., Hughes, N. P., Lee, M. C., & Mouraux, A. (2008). Determinants of laser-evoked EEG responses: pain perception or stimulus saliency? *J Neurophysiol*, *100*(2), 815-828. https://doi.org/10.1152/jn.00097.2008

Ibañez, A., Gleichgerrcht, E., & Manes, F. (2010). Clinical effects of insular damage in humans. *Brain Structure and Function*, *214*(5), 397-410. https://doi.org/10.1007/s00429-010-0256-y

Ilmoniemi, R. J., & Kičić, D. (2010). Methodology for Combined TMS and EEG. *Brain Topography*, *22*(4), 233-248. https://doi.org/10.1007/s10548-009-0123-4

Ilmoniemi, R. J., Virtanen, J., Ruohonen, J., Karhu, J., Aronen, H. J., Näätänen, R., & Katila, T. (1997). Neuronal responses to magnetic stimulation reveal cortical reactivity and connectivity. *NeuroReport*, *8*(16), 3537-3540. https://journals.lww.com/neuroreport/fulltext/1997/11100/neuronal_responses_to_magnetic_stimulation_reveal.24.aspx

Innocenti, G. M., Lehmann, P., & Houzel, J.-C. (1994). Computational Structure of Visual Callosal Axons. *European Journal of Neuroscience*, *6*(6), 918-935. https://doi.org/https://doi.org/10.1111/j.1460-9568.1994.tb00586.x

Isnard, J., Magnin, M., Jung, J., Mauguière, F., & Garcia-Larrea, L. (2011). Does the insula tell our brain that we are in pain? *Pain*, *152*(4), 946-951. https://doi.org/10.1016/j.pain.2010.12.025

Jasmin, L., Granato, A., & Ohara, P. T. (2004). Rostral agranular insular cortex and pain areas of the central nervous system: A tract-tracing study in the rat. *Journal of Comparative Neurology*, *468*(3), 425-440. https://doi.org/https://doi.org/10.1002/cne.10978

Jennions, M. D., & MØLler, A. P. (2002). Publication bias in ecology and evolution: an empirical assessment using the 'trim and fill' method. *Biological Reviews*, *77*(2), 211-222. https://doi.org/10.1017/S1464793101005875

Jensen, O., Bonnefond, M., & VanRullen, R. (2012). An oscillatory mechanism for prioritizing salient unattended stimuli. *Trends in Cognitive Sciences*, *16*(4), 200-206. https://doi.org/https://doi.org/10.1016/j.tics.2012.03.002

Jensen, O., & Mazaheri, A. (2010). Shaping Functional Architecture by Oscillatory Alpha Activity: Gating by Inhibition [Hypothesis and Theory]. *Frontiers in human neuroscience*, *4*. https://doi.org/10.3389/fnhum.2010.00186
Jensen, O., & Tesche, C. D. (2002). Frontal theta activity in humans increases with memory load in a working memory task. *European Journal of Neuroscience*, *15*(8), 1395-1399. https://doi.org/https://doi.org/10.1046/j.1460-9568.2002.01975.x
Jensen, T. S., & Finnerup, N. B. (2014). Allodynia and hyperalgesia in neuropathic pain: clinical manifestations and mechanisms. *The Lancet Neurology*, *13*(9), 924-935. https://doi.org/10.1016/S1474-4422(14)70102-4
Jepma, M., Koban, L., van Doorn, J., Jones, M., & Wager, T. D. (2018). Behavioural and neural evidence for self-reinforcing expectancy effects on pain. *Nature Human Behaviour*, *2*(11), 838-855. https://doi.org/10.1038/s41562-018-0455-8
John, L. K., Loewenstein, G., & Prelec, D. (2012). Measuring the Prevalence of Questionable Research Practices With Incentives for Truth Telling. *Psychological Science*, *23*(5), 524-532. https://doi.org/10.1177/0956797611430953
Jones, S. R., Pritchett, D. L., Sikora, M. A., Stufflebeam, S. M., Hämäläinen, M., & Moore, C. I. (2009). Quantitative Analysis and Biophysically Realistic Neural Modeling of the MEG Mu Rhythm: Rhythmogenesis and Modulation of Sensory-Evoked Responses. *Journal of Neurophysiology*, *102*(6), 3554-3572. https://doi.org/10.1152/jn.00535.2009
Joris, V., Ribeiro-Vaz, J. G., Finet, P., El Tahry, R., Elkaim, L. M., Raftopoulos, C., & Ferrao-Santos, S. (2023). Stereoelectroencephalography Implantation Using Frameless Neuronavigation and Varioguide: Prospective Analysis of Accuracy and Safety in a Case Series of 11 Patients. *World Neurosurgery*, *174*, e62-e71. https://doi.org/https://doi.org/10.1016/j.wneu.2023.02.116
Kahneman, D. (1973). *Attention and effort* (Vol. 1063). Citeseer.
Kaiser, J., & Lutzenberger, W. (2003). Induced gamma-band activity and human brain function. *Neuroscientist*, *9*(6), 475-484. https://doi.org/10.1177/1073858403259137
Katz, J., & Melzack, R. (1999). MEASUREMENT OF PAIN. *Surgical Clinics of North America*, *79*(2), 231-252. https://doi.org/https://doi.org/10.1016/S0039-6109(05)70381-9
Keltner, J. R., Furst, A., Fan, C., Redfern, R., Inglis, B., & Fields, H. L. (2006). Isolating the Modulatory Effect of Expectation on Pain Transmission: A Functional Magnetic Resonance Imaging Study. *The Journal of Neuroscience*, *26*(16), 4437-4443. https://doi.org/10.1523/jneurosci.4463-05.2006
Kim, J. A., & Davis, K. D. (2021). Neural Oscillations: Understanding a Neural Code of Pain. *The Neuroscientist*, *27*(5), 544-570. https://doi.org/10.1177/1073858420958629
Klein, A. S., Dolensek, N., Weiand, C., & Gogolla, N. (2021). Fear balance is maintained by bodily feedback to the insular cortex in mice. *Science*, *374*(6570), 1010-1015. https://doi.org/doi:10.1126/science.abj8817
Klimesch, W. (1997). EEG-alpha rhythms and memory processes. *International Journal of Psychophysiology*, *26*(1), 319-340. https://doi.org/https://doi.org/10.1016/S0167-8760(97)00773-3
Klimesch, W. (2012). Alpha-band oscillations, attention, and controlled access to stored information. *Trends in Cognitive Sciences*, *16*(12), 606-617. https://doi.org/10.1016/j.tics.2012.10.007
Klimesch, W., Freunberger, R., Sauseng, P., & Gruber, W. (2008). A short review of slow phase synchronization and memory: Evidence for control processes in different memory systems? *Brain Research*, *1235*, 31-44. https://doi.org/https://doi.org/10.1016/j.brainres.2008.06.049
Knyazev, G. G. (2007). Motivation, emotion, and their inhibitory control mirrored in brain oscillations. *Neuroscience & Biobehavioral Reviews*, *31*(3), 377-395. https://doi.org/https://doi.org/10.1016/j.neubiorev.2006.10.004
Kong, J., White, N. S., Kwong, K. K., Vangel, M. G., Rosman, I. S., Gracely, R. H., & Gollub, R. L. (2006). Using fMRI to dissociate sensory encoding from cognitive evaluation of heat pain intensity. *Human Brain Mapping*, *27*(9), 715-721. https://doi.org/https://doi.org/10.1002/hbm.20213

Kowalczyk, T., Bocian, R., & Konopacki, J. (2013). The generation of theta rhythm in hippocampal formation maintained in vitro. *European Journal of Neuroscience*, *37*(5), 679-699. https://doi.org/https://doi.org/10.1111/ejn.12091
Koyama, T., McHaffie, J. G., Laurienti, P. J., & Coghill, R. C. (2005). The subjective experience of pain: Where expectations become reality. *Proceedings of the National Academy of Sciences of the United States of America*, *102*(36), 12950-12955. https://doi.org/10.1073/pnas.0408576102
Kucyi, A., & Davis, K. D. (2015). The dynamic pain connectome. *Trends in Neurosciences*, *38*(2), 86-95. https://doi.org/https://doi.org/10.1016/j.tins.2014.11.006
Kupers, R., & Kehlet, H. (2006). Brain imaging of clinical pain states: a critical review and strategies for future studies. *The Lancet Neurology*, *5*(12), 1033-1044. https://doi.org/10.1016/S1474-4422(06)70624-X
Kurth, F., Zilles, K., Fox, P. T., Laird, A. R., & Eickhoff, S. B. (2010). A link between the systems: functional differentiation and integration within the human insula revealed by meta-analysis. *Brain Structure and Function*, *214*(5), 519-534. https://doi.org/10.1007/s00429-010-0255-z
Labrakakis, C. (2023). The Role of the Insular Cortex in Pain. *International Journal of Molecular Sciences*, *24*(6), 5736. https://www.mdpi.com/1422-0067/24/6/5736
Le Pera, D., Svensson, P., Valeriani, M., Watanabe, I., Arendt-Nielsen, L., & Chen, A. C. N. (2000). Long-lasting effect evoked by tonic muscle pain on parietal EEG activity in humans. *Clinical Neurophysiology*, *111*(12), 2130-2137. https://doi.org/https://doi.org/10.1016/S1388-2457(00)00474-0
Legrain, V., Bruyer, R., Guérit, J.-M., & Plaghki, L. (2003). Nociceptive processing in the human brain of infrequent task-relevant and task-irrelevant noxious stimuli. A study with event-related potentials evoked by CO2 laser radiant heat stimuli. *Pain*, *103*(3), 237-248. https://doi.org/https://doi.org/10.1016/S0304-3959(02)00451-7
Legrain, V., Crombez, G., & Mouraux, A. (2011). Controlling Attention to Nociceptive Stimuli with Working Memory. *PLOS ONE*, *6*(6), e20926. https://doi.org/10.1371/journal.pone.0020926
Legrain, V., Damme, S. V., Eccleston, C., Davis, K. D., Seminowicz, D. A., & Crombez, G. (2009). A neurocognitive model of attention to pain: Behavioral and neuroimaging evidence. *Pain*, *144*(3), 230-232. https://doi.org/10.1016/j.pain.2009.03.020
Legrain, V., Guérit, J.-M., Bruyer, R., & Plaghki, L. (2002). Attentional modulation of the nociceptive processing into the human brain: selective spatial attention, probability of stimulus occurrence, and target detection effects on laser evoked potentials. *Pain*, *99*(1), 21-39. https://doi.org/10.1016/s0304-3959(02)00051-9
Legrain, V., Guérit, J.-M., Bruyer, R., & Plaghki, L. (2003). Electrophysiological correlates of attentional orientation in humans to strong intensity deviant nociceptive stimuli, inside and outside the focus of spatial attention. *Neuroscience Letters*, *339*(2), 107-110. https://doi.org/https://doi.org/10.1016/S0304-3940(02)01485-4
Legrain, V., Iannetti, G. D., Plaghki, L., & Mouraux, A. (2011). The pain matrix reloaded: A salience detection system for the body. *Progress in Neurobiology*, *93*(1), 111-124. https://doi.org/https://doi.org/10.1016/j.pneurobio.2010.10.005
Legrain, V., Mancini, F., Sambo, C. F., Torta, D. M., Ronga, I., & Valentini, E. (2012). Cognitive aspects of nociception and pain. Bridging neurophysiology with cognitive psychology. *Neurophysiologie Clinique/Clinical Neurophysiology*, *42*(5), 325-336. https://doi.org/https://doi.org/10.1016/j.neucli.2012.06.003
Legrain, V., Perchet, C., & García-Larrea, L. (2009). Involuntary Orienting of Attention to Nociceptive Events: Neural and Behavioral Signatures. *Journal of Neurophysiology*, *102*(4), 2423-2434. https://doi.org/10.1152/jn.00372.2009
Leu, C., Courtin, A., Cussac, C., & Liberati, G. (2023). The role of ongoing oscillation in pain perception: Absence of modulation by a concomitant arithmetic task. *Cortex*, *168*, 114-129. https://doi.org/https://doi.org/10.1016/j.cortex.2023.08.005
Leu, C., Glineur, E., & Liberati, G. (2024). Cue-based modulation of pain stimulus expectation: do ongoing oscillations reflect changes in pain perception? A registered report. *Royal Society Open Science*, *11*(6), 240626. https://doi.org/doi:10.1098/rsos.240626

Leys, C., Delacre, M., Mora, Y. L., Lakens, D., & Ley, C. (2019). How to classify, detect, and manage univariate and multivariate outliers, with emphasis on pre-registration. *International Review of Social Psychology*, *32*(1). https://doi.org/10.5334/irsp.289
Li Hegner, Y., Saur, R., Veit, R., Butts, R., Leiberg, S., Grodd, W., & Braun, C. (2007). BOLD Adaptation in Vibrotactile Stimulation: Neuronal Networks Involved in Frequency Discrimination. *Journal of Neurophysiology*, *97*(1), 264-271. https://doi.org/10.1152/jn.00617.2006
Li, L., Liu, X., Cai, C., Yang, Y., Li, D., Xiao, L., Xiong, D., Hu, L., & Qiu, Y. (2016). Changes of gamma-band oscillatory activity to tonic muscle pain. *Neuroscience Letters*, *627*, 126-131. https://doi.org/https://doi.org/10.1016/j.neulet.2016.05.067
Li, L. M., Uehara, K., & Hanakawa, T. (2015). The contribution of interindividual factors to variability of response in transcranial direct current stimulation studies [Review]. *Frontiers in Cellular Neuroscience*, *9*. https://doi.org/10.3389/fncel.2015.00181
Li, Z., Zhang, L., Zeng, Y., Zhao, Q., & Hu, L. (2023). Gamma-band oscillations of pain and nociception: A systematic review and meta-analysis of human and rodent studies. *Neuroscience & Biobehavioral Reviews*, *146*, 105062. https://doi.org/https://doi.org/10.1016/j.neubiorev.2023.105062
Liang, Z., Li, F., Hu, W., Huang, G., Oba, S., Zhang, Z., & Ishii, S. (2020). A Generalized Encoding System for Alpha Oscillations Through Visual Saliency Analysis. *IEEE Transactions on Neural Systems and Rehabilitation Engineering*, *28*(12), 2731-2743. https://doi.org/10.1109/TNSRE.2020.3038789
Liberati, G., Algoet, M., Klöcker, A., Ferrao Santos, S., Ribeiro-Vaz, J. G., Raftopoulos, C., & Mouraux, A. (2018). Habituation of phase-locked local field potentials and gamma-band oscillations recorded from the human insula. *Scientific Reports*, *8*(1), 8265. https://doi.org/10.1038/s41598-018-26604-0
Liberati, G., Algoet, M., Santos, S. F., Ribeiro-Vaz, J. G., Raftopoulos, C., & Mouraux, A. (2019). Tonic thermonociceptive stimulation selectively modulates ongoing neural oscillations in the human posterior insula: Evidence from intracerebral EEG. *NeuroImage*, *188*, 70-83. https://doi.org/https://doi.org/10.1016/j.neuroimage.2018.11.059
Liberati, G., Klöcker, A., Algoet, M., Mulders, D., Maia Safronova, M., Ferrao Santos, S., Ribeiro Vaz, J.-G., Raftopoulos, C., & Mouraux, A. (2017). Gamma-Band Oscillations Preferential for Nociception can be Recorded in the Human Insula. *Cerebral Cortex*, *28*(10), 3650-3664. https://doi.org/10.1093/cercor/bhx237
Liberati, G., Klöcker, A., Safronova, M. M., Ferrao Santos, S., Ribeiro Vaz, J.-G., Raftopoulos, C., & Mouraux, A. (2016). Nociceptive local field potentials recorded from the human insula are not specific for nociception. *PLoS biology*, *14*(1), e1002345.
Liberati, G., Mulders, D., Algoet, M., van den Broeke, E. N., Santos, S. F., Ribeiro Vaz, J. G., Raftopoulos, C., & Mouraux, A. (2020). Insular responses to transient painful and non-painful thermal and mechanical spinothalamic stimuli recorded using intracerebral EEG. *Scientific Reports*, *10*(1), 22319. https://doi.org/10.1038/s41598-020-79371-2
Linde, L. D., Ortiz, O., Choles, C. M., & Kramer, J. L. K. (2023). Pain-related gamma band activity is dependent on the features of nociceptive stimuli: a comparison of laser and contact heat. *Journal of Neurophysiology*, *129*(1), 262-270. https://doi.org/10.1152/jn.00357.2022
Liu, C. C., Moosa, S., Quigg, M., & Elias, W. J. (2021). Anterior insula stimulation increases pain threshold in humans: a pilot study. *J Neurosurg*, *135*(5), 1487-1492. https://doi.org/10.3171/2020.10.Jns203323
Lobanov, O. V., Zeidan, F., McHaffie, J. G., Kraft, R. A., & Coghill, R. C. (2014). From cue to meaning: Brain mechanisms supporting the construction of expectations of pain. *PAIN®*, *155*(1), 129-136. https://doi.org/https://doi.org/10.1016/j.pain.2013.09.014
Lochy, A., Van Belle, G., & Rossion, B. (2015). A robust index of lexical representation in the left occipito-temporal cortex as evidenced by EEG responses to fast periodic visual stimulation. *Neuropsychologia*, *66*, 18-31. https://doi.org/https://doi.org/10.1016/j.neuropsychologia.2014.11.007

Lochy, A., Van Reybroeck, M., & Rossion, B. (2016). Left cortical specialization for visual letter strings predicts rudimentary knowledge of letter-sound association in preschoolers. *Proceedings of the National Academy of Sciences*, *113*(30), 8544-8549. https://doi.org/doi:10.1073/pnas.1520366113
Longe, S. E., Wise, R., Bantick, S., Lloyd, D., Johansen-Berg, H., McGlone, F., & Tracey, I. (2001). Counter-stimulatory effects on pain perception and processing are significantly altered by attention: an fMRI study. *NeuroReport*, *12*(9), 2021-2025. https://doi.org/10.1097/00001756-200107030-00047
Lorenz, J., Hauck, M., Paur, R. C., Nakamura, Y., Zimmermann, R., Bromm, B., & Engel, A. K. (2005). Cortical correlates of false expectations during pain intensity judgments—a possible manifestation of placebo/nocebo cognitions. *Brain, Behavior, and Immunity*, *19*(4), 283-295. https://doi.org/https://doi.org/10.1016/j.bbi.2005.03.010
Lőrincz, M. L., Kékesi, K. A., Juhász, G., Crunelli, V., & Hughes, S. W. (2009). Temporal Framing of Thalamic Relay-Mode Firing by Phasic Inhibition during the Alpha Rhythm. *Neuron*, *63*(5), 683-696. https://doi.org/https://doi.org/10.1016/j.neuron.2009.08.012
Lu, L., Wang, Q., Sheng, J., Liu, Z., Qin, L., Li, L., & Gao, J.-H. (2019). Neural tracking of speech mental imagery during rhythmic inner counting. *eLife*, *8*, e48971. https://doi.org/10.7554/eLife.48971
Luck, S. J. (2014). *An introduction to the event-related potential technique*. MIT press.
Luke, S. G. (2017). Evaluating significance in linear mixed-effects models in R. *Behavior Research Methods*, *49*(4), 1494-1502. https://doi.org/10.3758/s13428-016-0809-y
Maddison, R., Nazar, H., Obara, I., & Vuong, Q. C. (2023). The efficacy of sensory neural entrainment on acute and chronic pain: A systematic review and meta-analysis. *British Journal of Pain*, *17*(2), 126-141. https://doi.org/10.1177/20494637221139472
Maffei, A., Haley, M., & Fontanini, A. (2012). Neural processing of gustatory information in insular circuits. *Current Opinion in Neurobiology*, *22*(4), 709-716. https://doi.org/https://doi.org/10.1016/j.conb.2012.04.001
Magerl, W., & Treede, R. D. (1996). Heat-evoked vasodilatation in human hairy skin: axon reflexes due to low-level activity of nociceptive afferents. *The Journal of Physiology*, *497*(3), 837-848. https://doi.org/https://doi.org/10.1113/jphysiol.1996.sp021814
Mathew, J., Perez, T. M., Adhia, D. B., De Ridder, D., & Mani, R. (2024). Is There a Difference in EEG Characteristics in Acute, Chronic, and Experimentally Induced Musculoskeletal Pain States? a Systematic Review. *Clinical EEG and Neuroscience*, *55*(1), 101-120. https://doi.org/10.1177/15500594221138292
May, E. S., Tiemann, L., Gil Ávila, C., Bott, F. S., Hohn, V., Gross, J., & Ploner, M. (2024 Preprint). Assessing the predictive value of peak alpha frequency for the sensitivity to pain. *bioRxiv*, 2024.2006.2027.600974. https://doi.org/10.1101/2024.06.27.600974
Mayhew, S. D., Hylands-White, N., Porcaro, C., Derbyshire, S. W. G., & Bagshaw, A. P. (2013). Intrinsic variability in the human response to pain is assembled from multiple, dynamic brain processes. *NeuroImage*, *75*, 68-78. https://doi.org/10.1016/j.neuroimage.2013.02.028
McGrath, P. A. (1994). Psychological aspects of pain perception. *Archives of Oral Biology*, *39*, S55-S62. https://doi.org/https://doi.org/10.1016/0003-9969(94)90189-9
Meigen, T., & Bach, M. (1999). On the statistical significance of electrophysiological steady-state responses. *Documenta Ophthalmologica*, *98*(3), 207-232. https://doi.org/10.1023/A:1002097208337
Mesulam, M.-M., & Mufson, E. J. (1985). The insula of Reil in man and monkey: architectonics, connectivity, and function. In *Association and auditory cortices* (pp. 179-226). Springer.
Millard, S. K., Speis, D. B., Skippen, P., Chiang, A. K. I., Chang, W.-J., Lin, A. J., Furman, A. J., Mazaheri, A., Seminowicz, D. A., & Schabrun, S. M. (2024). Can non-invasive brain stimulation modulate peak alpha frequency in the human brain? A systematic review and meta-analysis. *European Journal of Neuroscience*, *60*(3), 4182-4200. https://doi.org/https://doi.org/10.1111/ejn.16424

Milton, A., Rowland, A., Stothart, G., Clatworthy, P., Pennington, C. M., & Kazanina, N. (2020). Fast Periodic Visual Stimulation indexes preserved semantic memory in healthy ageing. *Scientific Reports*, *10*(1), 13159. https://doi.org/10.1038/s41598-020-69929-5
Miniussi, C., & Thut, G. (2010). Combining TMS and EEG Offers New Prospects in Cognitive Neuroscience. *Brain Topography*, *22*(4), 249-256. https://doi.org/10.1007/s10548-009-0083-8
Miron, D., Duncan, G. H., & Bushnell, C. M. (1989). Effects of attention on the intensity and unpleasantness of thermal pain. *Pain*, *39*(3), 345-352. https://doi.org/10.1016/0304-3959(89)90048-1
Miyazaki, M., Shibasaki, H., Kanda, M., Xu, X., Shindo, K., Honda, M., Ikeda, A., Nagamine, T., Kaji, R., & Kimura, J. (1994). Generator Mechanism of Pain-Related Evoked Potentials Following CO2 Laser Stimulation of the Hand: Scalp Topography and Effect of Predictive Warning Signal. *Journal of Clinical Neurophysiology*, *11*(2), 242-254. https://journals.lww.com/clinicalneurophys/fulltext/1994/03000/generator_mechanism_of_pain_related_evoked.10.aspx
Modares-Haghighi, P., Boostani, R., Nami, M., & Sanei, S. (2021). Quantification of pain severity using EEG-based functional connectivity. *Biomedical Signal Processing and Control*, *69*, 102840. https://doi.org/https://doi.org/10.1016/j.bspc.2021.102840
Moisset, X., de Andrade, D. C., & Bouhassira, D. (2016). From pulses to pain relief: an update on the mechanisms of rTMS-induced analgesic effects. *European Journal of Pain*, *20*(5), 689-700. https://doi.org/https://doi.org/10.1002/ejp.811
Momi, D., Ozdemir, R. A., Tadayon, E., Boucher, P., Di Domenico, A., Fasolo, M., Shafi, M. M., Pascual-Leone, A., & Santarnecchi, E. (2022). Phase-dependent local brain states determine the impact of image-guided transcranial magnetic stimulation on motor network electroencephalographic synchronization. *The Journal of Physiology*, *600*(6), 1455-1471. https://doi.org/https://doi.org/10.1113/JP282393
Morawetz, C., Bode, S., Derntl, B., & Heekeren, H. R. (2017). The effect of strategies, goals and stimulus material on the neural mechanisms of emotion regulation: A meta-analysis of fMRI studies. *Neuroscience & Biobehavioral Reviews*, *72*, 111-128. https://doi.org/https://doi.org/10.1016/j.neubiorev.2016.11.014
Mørch, C. D., Frahm, K. S., Coghill, R. C., Arendt-Nielsen, L., & Andersen, O. K. (2015). Distinct temporal filtering mechanisms are engaged during dynamic increases and decreases of noxious stimulus intensity. *Pain*, *156*(10), 1906-1912. https://doi.org/10.1097/j.pain.0000000000000250
Morel, A., Gallay, M. N., Baechler, A., Wyss, M., & Gallay, D. S. (2013). The human insula: Architectonic organization and postmortem MRI registration. *Neuroscience*, *236*, 117-135. https://doi.org/https://doi.org/10.1016/j.neuroscience.2012.12.076
Moungou, A., Thonnard, J.-L., & Mouraux, A. (2016). EEG frequency tagging to explore the cortical activity related to the tactile exploration of natural textures. *Scientific Reports*, *6*(1), 20738. https://doi.org/10.1038/srep20738
Mouraux, A., Diukova, A., Lee, M. C., Wise, R. G., & Iannetti, G. D. (2011). A multisensory investigation of the functional significance of the "pain matrix". *NeuroImage*, *54*(3), 2237-2249. https://doi.org/https://doi.org/10.1016/j.neuroimage.2010.09.084
Mouraux, A., Guerit, J. M., & Plaghki, L. (2003). Non-phase locked electroencephalogram (EEG) responses to CO2 laser skin stimulations may reflect central interactions between A partial partial differential- and C-fibre afferent volleys. *Clin Neurophysiol*, *114*(4), 710-722. https://doi.org/10.1016/s1388-2457(03)00027-0
Mouraux, A., & Iannetti, G. D. (2008). Across-trial averaging of event-related EEG responses and beyond. *Magnetic Resonance Imaging*, *26*(7), 1041-1054. https://doi.org/https://doi.org/10.1016/j.mri.2008.01.011
Mouraux, A., & Iannetti, G. D. (2009). Nociceptive Laser-Evoked Brain Potentials Do Not Reflect Nociceptive-Specific Neural Activity. *Journal of Neurophysiology*, *101*(6), 3258-3269. https://doi.org/10.1152/jn.91181.2008
Mouraux, A., & Iannetti, G. D. (2018). The search for pain biomarkers in the human brain. *Brain*, *141*(12), 3290-3307. https://doi.org/10.1093/brain/awy281

Mouraux, A., Iannetti, G. D., Colon, E., Nozaradan, S., Legrain, V., & Plaghki, L. (2011). Nociceptive Steady-State Evoked Potentials Elicited by Rapid Periodic Thermal Stimulation of Cutaneous Nociceptors. *The Journal of Neuroscience*, *31*(16), 6079-6087. https://doi.org/10.1523/jneurosci.3977-10.2011

Mulders, D., de Bodt, C., Lejeune, N., Courtin, A., Liberati, G., Verleysen, M., & Mouraux, A. (2020). Dynamics of the perception and EEG signals triggered by tonic warm and cool stimulation. *PLOS ONE*, *15*(4), e0231698. https://doi.org/10.1371/journal.pone.0231698

Nahas, Z., M.D., Charlotte C. Teneback, B.S. „ Andy Kozel, M.D. „ Andrew M. Speer, M.D. „ Cart DeBrux, M.D. „ Monica Molloy, R.N., M.S.N. „ Laurie Stallings, Pharm.D. „ Kenneth M. Spicer, M.D. „ George Arana, M.D. „ Daryl E. Bohning, Ph.D. „ S. Craig Risch, M.D. , and, & Mark S. George, M.D. (2001). Brain Effects of TMS Delivered Over Prefrontal Cortex in Depressed Adults. *The Journal of Neuropsychiatry and Clinical Neurosciences*, *13*(4), 459-470. https://doi.org/10.1176/jnp.13.4.459

Naidich, T. P., Kang, E., Fatterpekar, G. M., Delman, B. N., Gultekin, S. H., Wolfe, D., Ortiz, O., Yousry, I., Weismann, M., & Yousry, T. A. (2004). The Insula: Anatomic Study and MR Imaging Display at 1.5 T. *American Journal of Neuroradiology*, *25*(2), 222-232. https://www.ajnr.org/content/ajnr/25/2/222.full.pdf

Namkung, H., Kim, S.-H., & Sawa, A. (2017). The Insula: An Underestimated Brain Area in Clinical Neuroscience, Psychiatry, and Neurology. *Trends in Neurosciences*, *40*(4), 200-207. https://doi.org/10.1016/j.tins.2017.02.002

Nelson, A. J., Staines, W. R., Graham, S. J., & McIlroy, W. E. (2004). Activation in SI and SII: the influence of vibrotactile amplitude during passive and task-relevant stimulation. *Cognitive Brain Research*, *19*(2), 174-184. https://doi.org/https://doi.org/10.1016/j.cogbrainres.2003.11.013

Nickel, M. M., May, E. S., Tiemann, L., Schmidt, P., Postorino, M., Ta Dinh, S., Gross, J., & Ploner, M. (2017). Brain oscillations differentially encode noxious stimulus intensity and pain intensity. *NeuroImage*, *148*, 141-147. https://doi.org/https://doi.org/10.1016/j.neuroimage.2017.01.011

Nickel, M. M., Ta Dinh, S., May, E. S., Tiemann, L., Hohn, V. D., Gross, J., & Ploner, M. (2020). Neural oscillations and connectivity characterizing the state of tonic experimental pain in humans. *Human Brain Mapping*, *41*(1), 17-29. https://doi.org/https://doi.org/10.1002/hbm.24784

Nickel, M. M., Tiemann, L., Hohn, V. D., May, E. S., Gil Ávila, C., Eippert, F., & Ploner, M. (2022). Temporal–spectral signaling of sensory information and expectations in the cerebral processing of pain. *Proceedings of the National Academy of Sciences*, *119*(1), e2116616119. https://doi.org/doi:10.1073/pnas.2116616119

Nieuwenhuys, R. (2012). Chapter 7 - The insular cortex: A review. In M. A. Hofman & D. Falk (Eds.), *Progress in brain research* (Vol. 195, pp. 123-163). Elsevier. https://doi.org/https://doi.org/10.1016/B978-0-444-53860-4.00007-6

Nir, R.-R., Sinai, A., Moont, R., Harari, E., & Yarnitsky, D. (2012). Tonic pain and continuous EEG: Prediction of subjective pain perception by alpha-1 power during stimulation and at rest. *Clinical Neurophysiology*, *123*(3), 605-612. https://doi.org/https://doi.org/10.1016/j.clinph.2011.08.006

Norcia, A. M., Appelbaum, L. G., Ales, J. M., Cottereau, B. R., & Rossion, B. (2015). The steady-state visual evoked potential in vision research: A review. *Journal of Vision*, *15*(6), 4-4. https://doi.org/10.1167/15.6.4

Nosek, B. A., Spies, J. R., & Motyl, M. (2012). Scientific Utopia:II. Restructuring Incentives and Practices to Promote Truth Over Publishability. *Perspectives on Psychological Science*, *7*(6), 615-631. https://doi.org/10.1177/1745691612459058

Nozaradan, S. (2014). Exploring how musical rhythm entrains brain activity with electroencephalogram frequency-tagging. *Philosophical Transactions of the Royal Society B: Biological Sciences*, *369*(1658), 20130393. https://doi.org/doi:10.1098/rstb.2013.0393

Nozaradan, S., Peretz, I., Missal, M., & Mouraux, A. (2011). Tagging the Neuronal Entrainment to Beat and Meter. *The Journal of Neuroscience*, *31*(28), 10234-10240. https://doi.org/10.1523/jneurosci.0411-11.2011
Ohara, S., Crone, N. E., Weiss, N., Kim, J. H., & Lenz, F. A. (2008). Analysis of synchrony demonstrates that the presence of "pain networks" prior to a noxious stimulus can enable the perception of pain in response to that stimulus. *Experimental Brain Research*, *185*(2), 353-358. https://doi.org/10.1007/s00221-008-1284-1
Ohara, S., Crone, N. E., Weiss, N., Vogel, H., Treede, R.-D., & Lenz, F. A. (2004). Attention to pain is processed at multiple cortical sites in man. *Experimental Brain Research*, *156*(4), 513-517. https://doi.org/10.1007/s00221-004-1885-2
Ostrowsky, K., Magnin, M., Ryvlin, P., Isnard, J., Guenot, M., & Mauguière, F. (2002). Representation of Pain and Somatic Sensation in the Human Insula: a Study of Responses to Direct Electrical Cortical Stimulation. *Cerebral Cortex*, *12*(4), 376-385. https://doi.org/10.1093/cercor/12.4.376
Owen, D. G., Clarke, C. F., Ganapathy, S., Prato, F. S., & St. Lawrence, K. S. (2010). Using perfusion MRI to measure the dynamic changes in neural activation associated with tonic muscular pain. *PAIN®*, *148*(3), 375-386. https://doi.org/https://doi.org/10.1016/j.pain.2009.10.003
Palva, S., & Palva, J. M. (2007). New vistas for alpha-frequency band oscillations. *Trends in Neurosciences*, *30*(4), 150-158. https://doi.org/10.1016/j.tins.2007.02.001
Pantev, C., Roberts, L. E., Elbert, T., Ro β , B., & Wienbruch, C. (1996). Tonotopic organization of the sources of human auditory steady-state responses. *Hearing Research*, *101*(1), 62-74. https://doi.org/https://doi.org/10.1016/S0378-5955(96)00133-5
Paulus, M. P., & Stein, M. B. (2006). An Insular View of Anxiety. *Biological Psychiatry*, *60*(4), 383-387. https://doi.org/https://doi.org/10.1016/j.biopsych.2006.03.042
Peciña, M., & Zubieta, J. K. (2015). Over a decade of neuroimaging studies of placebo analgesia in humans: what is next? *Molecular Psychiatry*, *20*(4), 415-415. https://doi.org/10.1038/mp.2015.33
Peng, W., Hu, L., Zhang, Z., & Hu, Y. (2014). Changes of Spontaneous Oscillatory Activity to Tonic Heat Pain. *PLOS ONE*, *9*(3), e91052. https://doi.org/10.1371/journal.pone.0091052
Peng, W., & Tang, D. (2016). Pain Related Cortical Oscillations: Methodological Advances and Potential Applications [Review]. *Frontiers in Computational Neuroscience*, *10*(9). https://doi.org/10.3389/fncom.2016.00009
Pernet, C., Garrido, M. I., Gramfort, A., Maurits, N., Michel, C. M., Pang, E., Salmelin, R., Schoffelen, J. M., Valdes-Sosa, P. A., & Puce, A. (2020). Issues and recommendations from the OHBM COBIDAS MEEG committee for reproducible EEG and MEG research. *Nature Neuroscience*, *23*(12), 1473-1483. https://doi.org/10.1038/s41593-020-00709-0
Perugini, M., Gallucci, M., & Costantini, G. (2014). Safeguard Power as a Protection Against Imprecise Power Estimates. *Perspectives on Psychological Science*, *9*(3), 319-332. https://doi.org/10.1177/1745691614528519
Petrovic, P., Kalso, E., Petersson, K. M., & Ingvar, M. (2002). Placebo and Opioid Analgesia--Imaging a Shared Neuronal Network. *Science*, *295*(5560), 1737-1740. https://doi.org/doi:10.1126/science.1067176
Petrovic, P., Petersson, K. M., Ghatan, P. H., Stone-Elander, S., & Ingvar, M. (2000). Pain-related cerebral activation is altered by a distracting cognitive task. *Pain*, *85*(1), 19-30. https://doi.org/https://doi.org/10.1016/S0304-3959(99)00232-8
Peyron, R., Laurent, B., & García-Larrea, L. (2000). Functional imaging of brain responses to pain. A review and meta-analysis (2000). *Neurophysiologie Clinique/Clinical Neurophysiology*, *30*(5), 263-288. https://doi.org/https://doi.org/10.1016/S0987-7053(00)00227-6
Pfurtscheller, G. (1981). Central beta rhythm during sensorimotor activities in man. *Electroencephalography and clinical neurophysiology*, *51*(3), 253-264. https://doi.org/https://doi.org/10.1016/0013-4694(81)90139-5
Pfurtscheller, G. (1992). Event-related synchronization (ERS): an electrophysiological correlate of cortical areas at rest. *Electroencephalography and clinical*

neurophysiology, *83*(1), 62-69. https://doi.org/https://doi.org/10.1016/0013-4694(92)90133-3
Pfurtscheller, G. (2003). Induced Oscillations in the Alpha Band: Functional Meaning. *Epilepsia*, *44*(s12), 2-8. https://doi.org/https://doi.org/10.1111/j.0013-9580.2003.12001.x
Pfurtscheller, G., & Lopes da Silva, F. H. (1999). Event-related EEG/MEG synchronization and desynchronization: basic principles. *Clinical Neurophysiology*, *110*(11), 1842-1857. https://doi.org/https://doi.org/10.1016/S1388-2457(99)00141-8
Pfurtscheller, G., Stancák, A., & Neuper, C. (1996). Post-movement beta synchronization. A correlate of an idling motor area? *Electroencephalography and clinical neurophysiology*, *98*(4), 281-293. https://doi.org/https://doi.org/10.1016/0013-4694(95)00258-8
Plaghki, L., Delisle, D., & Godfraind, J. M. (1994). Heterotopic nociceptive conditioning stimuli and mental task modulate differently the perception and physiological correlates of short CO2 laser stimuli. *Pain*, *57*(2), 181-192. https://doi.org/https://doi.org/10.1016/0304-3959(94)90222-4
Ploner, M., Bingel, U., & Wiech, K. (2015). Towards a taxonomy of pain modulations. *Trends in Cognitive Sciences*, *19*(4), 180-182. https://doi.org/https://doi.org/10.1016/j.tics.2015.02.007
Ploner, M., Gross, J., Timmermann, L., Pollok, B., & Schnitzler, A. (2006). Oscillatory activity reflects the excitability of the human somatosensory system. *NeuroImage*, *32*(3), 1231-1236. https://doi.org/https://doi.org/10.1016/j.neuroimage.2006.06.004
Ploner, M., Gross, J., Timmermann, L., Pollok, B., & Schnitzler, A. (2006). Pain suppresses spontaneous brain rhythms. *Cereb Cortex*, *16*(4), 537-540. https://doi.org/10.1093/cercor/bhj001
Ploner, M., Lee, M. C., Wiech, K., Bingel, U., & Tracey, I. (2010). Prestimulus functional connectivity determines pain perception in humans. *Proceedings of the National Academy of Sciences*, *107*(1), 355-360. https://doi.org/doi:10.1073/pnas.0906186106
Ploner, M., Sorg, C., & Gross, J. (2017). Brain Rhythms of Pain. *Trends in Cognitive Sciences*, *21*(2), 100-110. https://doi.org/https://doi.org/10.1016/j.tics.2016.12.001
Qiu, Y., Inui, K., Wang, X., Nguyen, B. T., Tran, T. D., & Kakigi, R. (2004). Effects of distraction on magnetoencephalographic responses ascending through C-fibers in humans. *Clinical Neurophysiology*, *115*(3), 636-646. https://doi.org/https://doi.org/10.1016/j.clinph.2003.10.017
Qiu, Y., Inui, K., Wang, X., Tran, T. D., & Kakigi, R. (2002). Effects of attention, distraction and sleep on CO2 laser evoked potentials related to C-fibers in humans. *Clinical Neurophysiology*, *113*(10), 1579-1585. https://doi.org/https://doi.org/10.1016/S1388-2457(02)00216-X
Quiton, R. L., & Greenspan, J. D. (2008). Across- and within-session variability of ratings of painful contact heat stimuli. *PAIN®*, *137*(2), 245-256. https://doi.org/https://doi.org/10.1016/j.pain.2007.08.034
R Core Team. (2023). *R: A Language and Environment for Statistical Computing*. In https://www.R-project.org/
Raja, S. N., Carr, D. B., Cohen, M., Finnerup, N. B., Flor, H., Gibson, S., Keefe, F. J., Mogil, J. S., Ringkamp, M., Sluka, K. A., Song, X.-J., Stevens, B., Sullivan, M. D., Tutelman, P. R., Ushida, T., & Vader, K. (2020). The revised International Association for the Study of Pain definition of pain: concepts, challenges, and compromises. *Pain*, *161*(9), 1976-1982. https://doi.org/10.1097/j.pain.0000000000001939
Ramantani, G., Maillard, L., & Koessler, L. (2016). Correlation of invasive EEG and scalp EEG. *Seizure*, *41*, 196-200. https://doi.org/https://doi.org/10.1016/j.seizure.2016.05.018
Rao, R. P. N., & Ballard, D. H. (1999). Predictive coding in the visual cortex: a functional interpretation of some extra-classical receptive-field effects. *Nature Neuroscience*, *2*(1), 79-87. https://doi.org/10.1038/4580
Regan, D. (1989). Human brain electrophysiology. *Evoked potentials and evoked magnetic fields in science and medicine*.

Retter, T. L., & Rossion, B. (2016). Uncovering the neural magnitude and spatio-temporal dynamics of natural image categorization in a fast visual stream. *Neuropsychologia*, *91*, 9-28. https://doi.org/https://doi.org/10.1016/j.neuropsychologia.2016.07.028
Retter, T. L., Rossion, B., & Schiltz, C. (2021). Harmonic Amplitude Summation for Frequency-tagging Analysis. *Journal of Cognitive Neuroscience*, *33*(11), 2372-2393. https://doi.org/10.1162/jocn_a_01763
Ridderinkhof, K. R., Ullsperger, M., Crone, E. A., & Nieuwenhuis, S. (2004). The Role of the Medial Frontal Cortex in Cognitive Control. *Science*, *306*(5695), 443-447. https://doi.org/doi:10.1126/science.1100301
Ridding, M. C., & Ziemann, U. (2010). Determinants of the induction of cortical plasticity by non-invasive brain stimulation in healthy subjects. *The Journal of Physiology*, *588*(13), 2291-2304. https://doi.org/https://doi.org/10.1113/jphysiol.2010.190314
Rinne, T., Särkkä, A., Degerman, A., Schröger, E., & Alho, K. (2006). Two separate mechanisms underlie auditory change detection and involuntary control of attention. *Brain Research*, *1077*(1), 135-143. https://doi.org/https://doi.org/10.1016/j.brainres.2006.01.043
Roa Romero, Y., Straube, T., Nitsch, A., Miltner, W. H. R., & Weiss, T. (2013). Interaction between stimulus intensity and perceptual load in the attentional control of pain. *PAIN®*, *154*(1), 135-140. https://doi.org/https://doi.org/10.1016/j.pain.2012.10.003
Rodriguez, E., George, N., Lachaux, J.-P., Martinerie, J., Renault, B., & Varela, F. J. (1999). Perception's shadow: long-distance synchronization of human brain activity. *Nature*, *397*(6718), 430-433. https://doi.org/10.1038/17120
Rogasch, N. C., & Fitzgerald, P. B. (2013). Assessing cortical network properties using TMS–EEG. *Human Brain Mapping*, *34*(7), 1652-1669. https://doi.org/https://doi.org/10.1002/hbm.22016
Rohel, A., Bouffard, J., Patricio, P., Mavromatis, N., Billot, M., Roy, J.-S., Bouyer, L., Mercier, C., & Masse-Alarie, H. (2021). The effect of experimental pain on the excitability of the corticospinal tract in humans: A systematic review and meta-analysis. *European Journal of Pain*, *25*(6), 1209-1226. https://doi.org/https://doi.org/10.1002/ejp.1746
Rolls, E. T., Huang, C.-C., Lin, C.-P., Feng, J., & Joliot, M. (2020). Automated anatomical labelling atlas 3. *NeuroImage*, *206*, 116189. https://doi.org/https://doi.org/10.1016/j.neuroimage.2019.116189
Rossion, B. (2014). Understanding individual face discrimination by means of fast periodic visual stimulation. *Experimental Brain Research*, *232*(6), 1599-1621. https://doi.org/10.1007/s00221-014-3934-9
Rossion, B., Prieto, E. A., Boremanse, A., Kuefner, D., & Van Belle, G. (2012). A steady-state visual evoked potential approach to individual face perception: Effect of inversion, contrast-reversal and temporal dynamics. *NeuroImage*, *63*(3), 1585-1600. https://doi.org/https://doi.org/10.1016/j.neuroimage.2012.08.033
Rossion, B., Retter, T. L., & Liu-Shuang, J. (2020). Understanding human individuation of unfamiliar faces with oddball fast periodic visual stimulation and electroencephalography. *European Journal of Neuroscience*, *52*(10), 4283-4344. https://doi.org/https://doi.org/10.1111/ejn.14865
Rossion, B., Torfs, K., Jacques, C., & Liu-Shuang, J. (2015). Fast periodic presentation of natural images reveals a robust face-selective electrophysiological response in the human brain. *Journal of Vision*, *15*(1), 18-18. https://doi.org/10.1167/15.1.18
Russo, J. F., & Sheth, S. A. (2015). Deep brain stimulation of the dorsal anterior cingulate cortex for the treatment of chronic neuropathic pain. *Neurosurgical focus*, *38 6*, E11.
Rustamov, N., Sharma, L., Chiang, S. N., Burk, C., Haroutounian, S., & Leuthardt, E. C. (2021). Spatial and Frequency-specific Electrophysiological Signatures of Tonic Pain Recovery in Humans. *Neuroscience*, *465*, 23-37. https://doi.org/https://doi.org/10.1016/j.neuroscience.2021.04.008
Saper, C. B. (2007). VISCERAL SENSATION AND VISCERAL SENSORY DISORDERS. *CONTINUUM: Lifelong Learning in Neurology*, *13*(6), 204-214. https://doi.org/10.1212/01.Con.0000299972.43513.28

Sarnthein, J., & Jeanmonod, D. (2008). High thalamocortical theta coherence in patients with neurogenic pain. *NeuroImage*, *39*(4), 1910-1917. https://doi.org/https://doi.org/10.1016/j.neuroimage.2007.10.019
Sarnthein, J., Stern, J., Aufenberg, C., Rousson, V., & Jeanmonod, D. (2005). Increased EEG power and slowed dominant frequency in patients with neurogenic pain. *Brain*, *129*(1), 55-64. https://doi.org/10.1093/brain/awh631
Sauseng, P., Klimesch, W., Stadler, W., Schabus, M., Doppelmayr, M., Hanslmayr, S., Gruber, W. R., & Birbaumer, N. (2005). A shift of visual spatial attention is selectively associated with human EEG alpha activity. *European Journal of Neuroscience*, *22*(11), 2917-2926. https://doi.org/https://doi.org/10.1111/j.1460-9568.2005.04482.x
Schepers, R. J., & Ringkamp, M. (2010). Thermoreceptors and thermosensitive afferents. *Neuroscience & Biobehavioral Reviews*, *34*(2), 177-184. https://doi.org/https://doi.org/10.1016/j.neubiorev.2009.10.003
Schlereth, T., Baumgärtner, U., Magerl, W., Stoeter, P., & Treede, R.-D. (2003). Left-hemisphere dominance in early nociceptive processing in the human parasylvian cortex. *NeuroImage*, *20*(1), 441-454. https://doi.org/https://doi.org/10.1016/S1053-8119(03)00345-8
Schmidt, R., Schmelz, M., Ringkamp, M., Handwerker, H. O., & Torebjörk, H. E. (1997). Innervation Territories of Mechanically Activated C Nociceptor Units in Human Skin. *Journal of Neurophysiology*, *78*(5), 2641-2648. https://doi.org/10.1152/jn.1997.78.5.2641
Schnitzler, A., & Gross, J. (2005). Normal and pathological oscillatory communication in the brain. *Nature Reviews Neuroscience*, *6*(4), 285-296. https://doi.org/10.1038/nrn1650
Schnitzler, A., & Ploner, M. (2000). Neurophysiology and functional neuroanatomy of pain perception. *J Clin Neurophysiol*, *17*(6), 592-603. https://doi.org/10.1097/00004691-200011000-00005
Schoffelen, J.-M., & Gross, J. (2009). Source connectivity analysis with MEG and EEG. *Human Brain Mapping*, *30*(6), 1857-1865. https://doi.org/https://doi.org/10.1002/hbm.20745
Schroeder, C. E., & Lakatos, P. (2009). Low-frequency neuronal oscillations as instruments of sensory selection. *Trends in Neurosciences*, *32*(1), 9-18. https://doi.org/10.1016/j.tins.2008.09.012
Schulz, E., May, E. S., Postorino, M., Tiemann, L., Nickel, M. M., Witkovsky, V., Schmidt, P., Gross, J., & Ploner, M. (2015). Prefrontal gamma oscillations encode tonic pain in humans [Article]. *Cerebral Cortex*, *25*(11), 4407-4414. https://doi.org/10.1093/cercor/bhv043
Schulz, E., Stankewitz, A., Witkovský, V., Winkler, A. M., & Tracey, I. (2019). Strategy-dependent modulation of cortical pain circuits for the attenuation of pain. *Cortex*, *113*, 255-266. https://doi.org/10.1016/j.cortex.2018.12.014
Schulz, E., Tiemann, L., Schuster, T., Gross, J., & Ploner, M. (2011). Neurophysiological Coding of Traits and States in the Perception of Pain. *Cerebral Cortex*, *21*(10), 2408-2414. https://doi.org/10.1093/cercor/bhr027
Sears, S. M., & Hewett, S. J. (2021). Influence of glutamate and GABA transport on brain excitatory/inhibitory balance. *Experimental Biology and Medicine*, *246*(9), 1069-1083. https://doi.org/10.1177/1535370221989263
Segerdahl, A. R., Mezue, M., Okell, T. W., Farrar, J. T., & Tracey, I. (2015). The dorsal posterior insula is not an island in pain but subserves a fundamental role - Response to: "Evidence against pain specificity in the dorsal posterior insula" by Davis et al. *F1000Res*, *4*, 1207. https://doi.org/10.12688/f1000research.7287.1
Segerdahl, A. R., Mezue, M., Okell, T. W., Farrar, J. T., & Tracey, I. (2015). The dorsal posterior insula subserves a fundamental role in human pain. *Nature Neuroscience*, *18*(4), 499-500. https://doi.org/10.1038/nn.3969
Seminowicz, D. A., & Davis, K. D. (2006). Interactions of Pain Intensity and Cognitive Load: The Brain Stays on Task. *Cerebral Cortex*, *17*(6), 1412-1422. https://doi.org/10.1093/cercor/bhl052
Shao, S., Shen, K., Yu, K., Wilder-Smith, E. P. V., & Li, X. (2012). Frequency-domain EEG source analysis for acute tonic cold pain perception. *Clinical Neurophysiology*, *123*(10), 2042-2049. https://doi.org/https://doi.org/10.1016/j.clinph.2012.02.084

Sharvit, G., Corradi-Dell'Acqua, C., & Vuilleumier, P. (2018). Modality-specific effects of aversive expectancy in the anterior insula and medial prefrontal cortex. *Pain*, *159*(8), 1529-1542. https://doi.org/10.1097/j.pain.0000000000001237
Shi, C.-J., & Cassell, M. D. (1998). Cascade projections from somatosensory cortex to the rat basolateral amygdala via the parietal insular cortex. *Journal of Comparative Neurology*, *399*(4), 469-491. https://doi.org/https://doi.org/10.1002/(SICI)1096-9861(19981005)399:4<469::AID-CNE3>3.0.CO;2-#
Shipp, S. (2004). The brain circuitry of attention. *Trends in Cognitive Sciences*, *8*(5), 223-230. https://doi.org/https://doi.org/10.1016/j.tics.2004.03.004
Shura, R. D., Hurley, R. A., & Taber, K. H. (2014). Insular Cortex: Structural and Functional Neuroanatomy. *The Journal of Neuropsychiatry and Clinical Neurosciences*, *26*(4), iv-282. https://doi.org/10.1176/appi.neuropsych.260401
Sieving, P. A., Arnold, E. B., Jamison, J., Liepa, A., & Coats, C. (1998). Submicrovolt flicker electroretinogram: cycle-by-cycle recording of multiple harmonics with statistical estimation of measurement uncertainty. *Investigative Ophthalmology & Visual Science*, *39*(8), 1462-1469.
Silvestrini, N., & Corradi-Dell'Acqua, C. (2023). Distraction and cognitive control independently impact parietal and prefrontal response to pain. *Social Cognitive and Affective Neuroscience*, *18*(1). https://doi.org/10.1093/scan/nsad018
Simmons, J. P., Nelson, L. D., & Simonsohn, U. (2011). False-Positive Psychology:Undisclosed Flexibility in Data Collection and Analysis Allows Presenting Anything as Significant. *Psychological Science*, *22*(11), 1359-1366. https://doi.org/10.1177/0956797611417632
Singer, T., Critchley, H. D., & Preuschoff, K. (2009). A common role of insula in feelings, empathy and uncertainty. *Trends in Cognitive Sciences*, *13*(8), 334-340. https://doi.org/10.1016/j.tics.2009.05.001
Singer, T., Seymour, B., O'Doherty, J., Kaube, H., Dolan, R. J., & Frith, C. D. (2004). Empathy for Pain Involves the Affective but not Sensory Components of Pain. *Science*, *303*(5661), 1157-1162. https://doi.org/doi:10.1126/science.1093535
Singer, W. (1999). Neuronal Synchrony: A Versatile Code for the Definition of Relations? *Neuron*, *24*(1), 49-65. https://doi.org/10.1016/S0896-6273(00)80821-1
Sokhadze, E. M., Casanova, M. F., Casanova, E. L., Lamina, E., Kelly, D. P., & Khachidze, I. (2017). Event-related potentials (ERP) in cognitive neuroscience research and applications. *NeuroRegulation*, *4*(1), 14-14.
Sörös, P., Marmurek, J., Tam, F., Baker, N., Staines, W. R., & Graham, S. J. (2007). Functional MRI of working memory and selective attention in vibrotactile frequency discrimination. *BMC Neuroscience*, *8*(1), 48. https://doi.org/10.1186/1471-2202-8-48
Spratling, M. W. (2017). A review of predictive coding algorithms. *Brain and Cognition*, *112*, 92-97. https://doi.org/https://doi.org/10.1016/j.bandc.2015.11.003
Srinivasan, R., Russell, D. P., Edelman, G. M., & Tononi, G. (1999). Increased Synchronization of Neuromagnetic Responses during Conscious Perception. *The Journal of Neuroscience*, *19*(13), 5435-5448. https://doi.org/10.1523/jneurosci.19-13-05435.1999
Stancak, A., & Fallon, N. (2013). Emotional modulation of experimental pain: a source imaging study of laser evoked potentials [Original Research]. *Frontiers in human neuroscience*, *7*. https://doi.org/10.3389/fnhum.2013.00552
Stephani, C., Fernandez-Baca Vaca, G., Maciunas, R., Koubeissi, M., & Lüders, H. O. (2011). Functional neuroanatomy of the insular lobe. *Brain Structure and Function*, *216*(2), 137-149. https://doi.org/10.1007/s00429-010-0296-3
Strube, A., Horing, B., Rose, M., & Büchel, C. (2023). Agency affects pain inference through prior shift as opposed to likelihood precision modulation in a Bayesian pain model. *Neuron*, *111*(7), 1136-1151.e1137. https://doi.org/10.1016/j.neuron.2023.01.002
Strube, A., Rose, M., Fazeli, S., & Büchel, C. (2021a). Alpha-to-beta- and gamma-band activity reflect predictive coding in affective visual processing. *Scientific Reports*, *11*(1), 23492. https://doi.org/10.1038/s41598-021-02939-z
Strube, A., Rose, M., Fazeli, S., & Büchel, C. (2021b). The temporal and spectral characteristics of expectations and prediction errors in pain and thermoception. *eLife*, *10*, e62809. https://doi.org/10.7554/eLife.62809

Thomaidou, M. A., Blythe, J. S., Houtman, S. J., Veldhuijzen, D. S., van Laarhoven, A. I. M., & Evers, A. W. M. (2021). Temporal structure of brain oscillations predicts learned nocebo responses to pain. *Scientific Reports*, *11*(1), 9807. https://doi.org/10.1038/s41598-021-89368-0

Tiemann, L., May, E. S., Postorino, M., Schulz, E., Nickel, M. M., Bingel, U., & Ploner, M. (2015). Differential neurophysiological correlates of bottom-up and top-down modulations of pain. *Pain*, *156*(2). https://journals.lww.com/pain/Fulltext/2015/02000/Differential_neurophysiological_correlates_of.13.aspx

Tillman, D. B., Treede, R. D., Meyer, R. A., & Campbell, J. N. (1995). Response of C fibre nociceptors in the anaesthetized monkey to heat stimuli: correlation with pain threshold in humans. *The Journal of Physiology*, *485*(3), 767-774. https://doi.org/https://doi.org/10.1113/jphysiol.1995.sp020767

Torta, D. M., Legrain, V., Mouraux, A., & Valentini, E. (2017). Attention to pain! A neurocognitive perspective on attentional modulation of pain in neuroimaging studies. *Cortex*, *89*, 120-134. https://doi.org/https://doi.org/10.1016/j.cortex.2017.01.010

Tracey, I., & Mantyh, P. W. (2007). The Cerebral Signature for Pain Perception and Its Modulation. *Neuron*, *55*(3), 377-391. https://doi.org/https://doi.org/10.1016/j.neuron.2007.07.012

Tracey, I., Ploghaus, A., Gati, J. S., Clare, S., Smith, S., Menon, R. S., & Matthews, P. M. (2002). Imaging Attentional Modulation of Pain in the Periaqueductal Gray in Humans. *The Journal of Neuroscience*, *22*(7), 2748. https://doi.org/10.1523/JNEUROSCI.22-07-02748.2002

Treede, R.-D. (2003). Neurophysiological studies of painpathways in peripheral and central nervous systemdisorders. *Journal of Neurology*, *250*(10), 1152-1161. https://doi.org/10.1007/s00415-003-0237-7

Treede, R.-D., Kenshalo, D. R., Gracely, R. H., & Jones, A. K. P. (1999). The cortical representation of pain. *Pain*, *79*(2), 105-111. https://doi.org/https://doi.org/10.1016/S0304-3959(98)00184-5

Treede, R. D., Meyer, R. A., & Campbell, J. N. (1990). Comparison of heat and mechanical receptive fields of cutaneous C-fiber nociceptors in monkey. *Journal of Neurophysiology*, *64*(5), 1502-1513. https://doi.org/10.1152/jn.1990.64.5.1502

Uddin, L. Q., Kinnison, J., Pessoa, L., & Anderson, M. L. (2014). Beyond the Tripartite Cognition–Emotion–Interoception Model of the Human Insular Cortex. *Journal of Cognitive Neuroscience*, *26*(1), 16-27. https://doi.org/10.1162/jocn_a_00462

Valentini, E., Halder, S., McInnerney, D., Cooke, J., Gyimes, I. L., & Romei, V. (2022). Assessing the specificity of the relationship between brain alpha oscillations and tonic pain. *NeuroImage*, *255*, 119143. https://doi.org/https://doi.org/10.1016/j.neuroimage.2022.119143

Valentini, E., Shindy, A., Witkovsky, V., Stankewitz, A., & Schulz, E. (2023). Interindividual variability and individual stability of pain- and touch-related neuronal gamma oscillations. *Journal of Neurophysiology*, *129*(6), 1400-1413. https://doi.org/10.1152/jn.00530.2021

Valet, M., Sprenger, T., Boecker, H., Willoch, F., Rummeny, E., Conrad, B., Erhard, P., & Tolle, T. R. (2004). Distraction modulates connectivity of the cingulo-frontal cortex and the midbrain during pain—an fMRI analysis. *Pain*, *109*(3), 399-408. https://doi.org/https://doi.org/10.1016/j.pain.2004.02.033

Varela, F., Lachaux, J.-P., Rodriguez, E., & Martinerie, J. (2001). The brainweb: Phase synchronization and large-scale integration. *Nature Reviews Neuroscience*, *2*(4), 229-239. https://doi.org/10.1038/35067550

Veldhuijzen, D. S., Kenemans, J. L., de Bruin, C. M., Olivier, B., & Volkerts, E. R. (2006). Pain and Attention: Attentional Disruption or Distraction? *The Journal of Pain*, *7*(1), 11-20. https://doi.org/https://doi.org/10.1016/j.jpain.2005.06.003

von Economo, C. (1927). *Zellaufbau der Großhirnrinde des Menschen: 10 Vorlesungen*. Springer.

von Stein, A., Chiang, C., & König, P. (2000). Top-down processing mediated by interareal synchronization. *Proceedings of the National Academy of Sciences*, *97*(26), 14748-14753. https://doi.org/doi:10.1073/pnas.97.26.14748
Wager, T. D., Atlas, L. Y., Lindquist, M. A., Roy, M., Woo, C.-W., & Kross, E. (2013). An fMRI-Based Neurologic Signature of Physical Pain. *New England Journal of Medicine*, *368*(15), 1388-1397. https://doi.org/10.1056/NEJMoa1204471
Wager, T. D., Matre, D., & Casey, K. L. (2006). Placebo effects in laser-evoked pain potentials. *Brain, Behavior, and Immunity*, *20*(3), 219-230. https://doi.org/https://doi.org/10.1016/j.bbi.2006.01.007
Walton, K. D., Dubois, M., & Llinás, R. R. (2010). Abnormal thalamocortical activity in patients with Complex Regional Pain Syndrome (CRPS) Type I. *Pain*, *150*(1), 41-51. https://doi.org/https://doi.org/10.1016/j.pain.2010.02.023
Wang, H., Guo, Y., Tu, Y., Peng, W., Lu, X., Bi, Y., Iannetti, G. D., & Hu, L. (2022). Neural processes responsible for the translation of sustained nociceptive inputs into subjective pain experience. *Cerebral Cortex*, *33*(3), 634-650. https://doi.org/10.1093/cercor/bhac090
Wang, Q., Zhu, J.-J., Wang, L., Kan, Y.-P., Liu, Y.-M., Wu, Y.-J., Gu, X., Yi, X., Lin, Z.-J., Wang, Q., Lu, J.-F., Jiang, Q., Li, Y., Liu, M.-G., Xu, N.-J., Zhu, M. X., Wang, L.-Y., Zhang, S., Li, W.-G., & Xu, T.-L. (2022). Insular cortical circuits as an executive gateway to decipher threat or extinction memory via distinct subcortical pathways. *Nature Communications*, *13*(1), 5540. https://doi.org/10.1038/s41467-022-33241-9
Wiech, K. (2016). Deconstructing the sensation of pain: The influence of cognitive processes on pain perception. *Science*, *354*(6312), 584-587. https://doi.org/doi:10.1126/science.aaf8934
Wiech, K., Jbabdi, S., Lin, C. S., Andersson, J., & Tracey, I. (2014). Differential structural and resting state connectivity between insular subdivisions and other pain-related brain regions. *Pain*, *155*(10), 2047-2055. https://doi.org/10.1016/j.pain.2014.07.009
Wiech, K., Lin, C.-s., Brodersen, K. H., Bingel, U., Ploner, M., & Tracey, I. (2010). Anterior Insula Integrates Information about Salience into Perceptual Decisions about Pain. *The Journal of Neuroscience*, *30*(48), 16324-16331. https://doi.org/10.1523/jneurosci.2087-10.2010
Wiech, K., Ploner, M., & Tracey, I. (2008). Neurocognitive aspects of pain perception. *Trends in Cognitive Sciences*, *12*(8), 306-313. https://doi.org/https://doi.org/10.1016/j.tics.2008.05.005
Wiech, K., Seymour, B., Kalisch, R., Enno Stephan, K., Koltzenburg, M., Driver, J., & Dolan, R. J. (2005). Modulation of pain processing in hyperalgesia by cognitive demand. *NeuroImage*, *27*(1), 59-69. https://doi.org/https://doi.org/10.1016/j.neuroimage.2005.03.044
Wiethoff, S., Hamada, M., & Rothwell, J. C. (2014). Variability in Response to Transcranial Direct Current Stimulation of the Motor Cortex. *Brain Stimulation*, *7*(3), 468-475. https://doi.org/https://doi.org/10.1016/j.brs.2014.02.003
Womelsdorf, T., Schoffelen, J.-M., Oostenveld, R., Singer, W., Desimone, R., Engel, A. K., & Fries, P. (2007). Modulation of Neuronal Interactions Through Neuronal Synchronization. *Science*, *316*(5831), 1609-1612. https://doi.org/doi:10.1126/science.1139597
Wooten, M., Weng, H.-J., Hartke, T. V., Borzan, J., Klein, A. H., Turnquist, B., Dong, X., Meyer, R. A., & Ringkamp, M. (2014). Three functionally distinct classes of C-fibre nociceptors in primates. *Nature Communications*, *5*(1), 4122. https://doi.org/10.1038/ncomms5122
Yamasaki, H., Kakigi, R., Watanabe, S., & Naka, D. (1999). Effects of distraction on pain perception: magneto- and electro-encephalographic studies. *Cognitive Brain Research*, *8*(1), 73-76. https://doi.org/https://doi.org/10.1016/S0926-6410(99)00003-8
Yantis, S. (2008). The Neural Basis of Selective Attention: Cortical Sources and Targets of Attentional Modulation. *Current Directions in Psychological Science*, *17*(2), 86-90. https://doi.org/10.1111/j.1467-8721.2008.00554.x
Yarnitsky, D., Simone, D. A., Dotson, R. M., Cline, M. A., & Ochoa, J. L. (1992). Single C nociceptor responses and psychophysical parameters of evoked pain: effect of rate

of rise of heat stimuli in humans. *The Journal of Physiology*, *450*(1), 581-592. https://doi.org/https://doi.org/10.1113/jphysiol.1992.sp019144
Yarnitsky, D., Sprecher, E., Zaslansky, R., & Hemli, J. A. (1995). Heat pain thresholds: normative data and repeatability. *Pain*, *60*(3), 329-332. https://doi.org/https://doi.org/10.1016/0304-3959(94)00132-X
Yordanova, J., Kolev, V., & Polich, J. (2001). P300 and alpha event-related desynchronization (ERD). *Psychophysiology*, *38*(1), 143-152. https://doi.org/10.1111/1469-8986.3810143
Yue, L., Iannetti, G. D., & Hu, L. (2020). The Neural Origin of Nociceptive-Induced Gamma-Band Oscillations. *The Journal of Neuroscience*, *40*(17), 3478-3490. https://doi.org/10.1523/jneurosci.0255-20.2020
Zewdie, E., & Kirton, A. (2016). Chapter 1 - TMS Basics: Single and Paired Pulse Neurophysiology. In A. Kirton & D. L. Gilbert (Eds.), *Pediatric Brain Stimulation* (pp. 3-22). Academic Press. https://doi.org/https://doi.org/10.1016/B978-0-12-802001-2.00001-1
Zhang, R., Deng, H., & Xiao, X. (2024). The Insular Cortex: An Interface Between Sensation, Emotion and Cognition. *Neuroscience Bulletin*. https://doi.org/10.1007/s12264-024-01211-4
Zhang, Z. G., Hu, L., Hung, Y. S., Mouraux, A., & Iannetti, G. D. (2012). Gamma-Band Oscillations in the Primary Somatosensory Cortex—A Direct and Obligatory Correlate of Subjective Pain Intensity. *The Journal of Neuroscience*, *32*(22), 7429-7438. https://doi.org/10.1523/jneurosci.5877-11.2012
Zhou, H., Melloni, L., Poeppel, D., & Ding, N. (2016). Interpretations of Frequency Domain Analyses of Neural Entrainment: Periodicity, Fundamental Frequency, and Harmonics [Hypothesis and Theory]. *Frontiers in human neuroscience*, *10*. https://doi.org/10.3389/fnhum.2016.00274
Zoefel, B., ten Oever, S., & Sack, A. T. (2018). The Involvement of Endogenous Neural Oscillations in the Processing of Rhythmic Input: More Than a Regular Repetition of Evoked Neural Responses [Review]. *Frontiers in Neuroscience*, *12*. https://doi.org/10.3389/fnins.2018.00095
Zrenner, C., Belardinelli, P., Müller-Dahlhaus, F., & Ziemann, U. (2016). Closed-Loop Neuroscience and Non-Invasive Brain Stimulation: A Tale of Two Loops [Perspective]. *Frontiers in Cellular Neuroscience*, *10*. https://doi.org/10.3389/fncel.2016.00092
Zrenner, C., Desideri, D., Belardinelli, P., & Ziemann, U. (2018). Real-time EEG-defined excitability states determine efficacy of TMS-induced plasticity in human motor cortex. *Brain Stimulation*, *11*(2), 374-389. https://doi.org/10.1016/j.brs.2017.11.016